



UNITED STATES
NUCLEAR REGULATORY COMMISSION

WASHINGTON, D.C. 20555-0001

March 13, 1997

MEMORANDUM TO: John H. Austin, Chief
Performance Assessment and HLW
Integration Branch, DWM
Office of Nuclear Material Safety and Safeguards

Michael J. Bell, Chief
Engineering and Geosciences Branch, DWM
Office of Nuclear Material Safety and Safeguards

FROM: Christiana H. Lui *Christiana H. Lui*
Performance Assessment and Integration Section
Performance Assessment and HLW
Integration Branch, DWM
Office of Nuclear Material Safety and Safeguards

Philip S. Justus *Philip S. Justus*
Geosciences and Hydrology Review Section
Engineering and Geosciences Branch, DWM
Office of Nuclear Material Safety and Safeguards

Abou-Bakr K. Ibrahim *A. K. Ibrahim*
Geosciences and Hydrology Review Section
Engineering and Geosciences Branch, DWM
Office of Nuclear Material Safety and Safeguards

SUBJECT: TRIP REPORT FOR PROBABILISTIC SEISMIC HAZARD ANALYSIS -
SEISMIC SOURCE CHARACTERIZATION WORKSHOP #4, GROUND MOTION
WORKSHOP #2, SALT LAKE CITY, UTAH, JANUARY 6-10, 1997

DOE held its fourth workshop on seismic source characterization (SSC) and second workshop on ground motion (GM) for the proposed high-level waste repository at Yucca Mountain (YM), Nevada, on January 6-8, and 8-10, 1997, respectively. The results of these SSC and GM workshops will form the bases of the probabilistic seismic hazard analysis (PSHA) being conducted by DOE. A formal expert judgment process is being followed to obtain the needed inputs. The goal of the PSHA is to provide the annual probability with which various levels of vibratory ground motion and fault displacement may be exceeded at the YM site. The results of the PSHA will be used as a basis for developing seismic design inputs and in assessing the pre-closure and post-closure performance of the YM site and facilities.

97-03

CONTACTS: C. Lui, PAHL
415-6200
P. Justus, ENGB
415-6745
A. Ibrahim, ENGB
415-6651

280078

*NIH 16%
102.8
WMM-11*

NRC FILE CENTER COPY

9704010133 970313
PDR WASTE
WM-11 PDR

— Part 2

The objectives of this fourth SSC workshop were: (1) to present and discuss additional information and important interpretations to source characterization; (2) to provide an opportunity for the various three-member expert teams to present their preliminary interpretations regarding key SSC issues to the entire group for discussion; and (3) to train the expert teams on probability, uncertainty and elicitation. The objectives of the second GM workshop were: (1) to present available models for characterizing ground motions and to discuss their applicability for the proposed YM site; (2) to provide the experts an opportunity to participate in a preliminary GM modeling exercise; (3) to discuss and clarify the scope of GM assessment; and (4) to train the experts on probability, uncertainty and elicitation. Philip Justus, Abou-Bakr Ibrahim and Christiana Lui attended these workshops as observers from NRC. John Stamatakos and David Ferrill from the CNWRA also attended these workshops.

The first day (half-day) of the SSC workshop was devoted to presentations of additional information and important interpretations. Five key issues, namely tectonic models, potential seismic sources, maximum magnitudes, earthquake recurrence, and fault displacement methodology, were the focus of the second day and the first half of the third day. For each of these issues, two of the six expert teams presented their preliminary interpretation to the whole group for discussion. The potential significance of moment-magnitude and displacements on secondary faults in consideration of seismic and fault displacement hazards was raised during the group discussion. Kevin Coppersmith also briefly went over the subsequent steps, including elicitation interview, hazard calculations using the elicited judgments, feedback workshop and finalizing elicited judgments, in completing this expert elicitation process. He reminded participants that thermal- and construction-induced seismic sources were not in the scope of this workshop. They would be considered at a later date. The SSC meeting agenda and list of attendees are included as Attachment 1 and Attachment 2, respectively. Attachment 3 contains reprints of all technical presentations as enumerated in the SSC workshop agenda, and other relevant technical articles that were available to the staff during the workshop.

A joint training session was held for the SSC and GM experts in the afternoon on January 8, 1997, by the normative expert, Peter Morris. He went over some basic concepts in probability, the use of probability and decision tree to express uncertainty, types of motivational and cognitive biases in formulating subjective judgments, and provided some hands-on exercises. A copy of this training material can be found in Attachment 4.

The GM experts last met in April 1995, and were brought up-to-date by Norm Abrahamson. Relevant data and models were presented to the experts for discussion and consideration. The scope of the GM assessments was also discussed and clarified. John Anderson, one of the seven GM experts, discussed the Dinar earthquake in Turkey which had a normal faulting mechanism in an extensional regime comparable to that of YM. Paul Spaudich from the U.S. Geological Survey (USGS), summarized the data collected from different extensional regimes around the world. At the end of this GM workshop, the experts participated in a modeling exercise where they provided estimates of median GM for a magnitude 6.5 event at 10 km. The purposes of this exercise

were: (1) to ensure that the experts were clear of the assessment process; and (2) to explain to the experts the form in which their input should be provided for seismic hazard calculations. The result of this exercise showed a large variability in the median GM estimates. The GM meeting agenda and list of attendees are included as Attachment 5 and Attachment 6, respectively. Attachment 7 contains reprints of all technical presentations as enumerated in the GM workshop agenda, and other relevant technical articles that were available to the NRC staff during the workshop. The biosketches for the GM experts can be found in Attachment 8.

During the feedback sessions at the end of each day, NRC and CNWRA provided technical input to the group as appropriate. Staff commented on the need to account for triggering in determination of earthquake recurrence rates, and uncertainties of fault zone width in meeting DOE's current commitment to set back from Type I faults. The staff also asked if the earthquake data collected from the different extensional regime areas have comparable stress drop since stress drop is related to acceleration.

DOE and NRC also met to discuss issues related to the implementation of an expert judgment elicitation process outside the main workshop. Issues discussed were: (1) the need to demonstrate the robustness of the aggregated SSC result with regard to the composition of the expert teams; (2) the possibility of observing the actual elicitation interviews; (3) the need to allocate sufficient time so that the experts can provide the required assessments without compromising the quality of their assessments; (4) the use of "logic tree" in expressing and quantifying uncertainty; (5) if there is a real need to distinguish the various types of uncertainties, i.e., model vs. parameter and aleatory vs. epistemic, especially when the experts are not comfortable with this uncertainty characterization framework; and (6) the possibility of a combined SSC and GM feedback workshop to facilitate the interface between these two panels and to ensure consistency in the scope of the assessments. Tim Sullivan, Carl Stepp, Abou-Bakr Ibrahim, Philip Justus and Christiana Lui were present during this informal discussion.

Revision 1 of the PSHA project plan was distributed during the workshop and is included as Attachment 9. The workshop summaries which were prepared by the USGS for DOE can be found in Attachment 10.

The next set of SSC and GM workshops will be held at Salt Lake City, Utah, on April 14-18, 1997. The main goal of these workshops will be to provide feedback to the experts on their assessments after their preliminary assessments have been aggregated and propagated through the PSHA models by the Calculations Team. The final experts' assessments are due by early June 1997. The final PSHA report is due to DOE from its contractor by the end of August 1997.

Attachments: As stated

are: (1) to ensure that the experts are clear of the assessment process; and (2) to explain to the experts the form in which their input should be provided for seismic hazard calculations. The result of this exercise showed a large variability in the median GM estimates. The GM meeting agenda and list of attendees are included as Attachment 5 and Attachment 6, respectively. Attachment 7 contains reprints of all technical presentations as enumerated in the GM workshop agenda, and other relevant technical articles that were available to the NRC staff during the workshop. The biosketches for the GM experts can be found in Attachment 8.

During the feedback sessions at the end of each day, NRC and CNWRA provided technical input to the group as appropriate. Staff commented on accounting for triggering in determination of earthquake recurrence rates, and uncertainties of fault zone width in meeting DOE's current commitment to set back from Type I faults. The staff also asked if the earthquake data collected from the different extensional regime areas have comparable stress drop since stress drop is related to acceleration.

DOE and NRC also met to discuss issues related to the implementation of an expert judgment elicitation process outside the main workshop. Issues discussed were: (1) the need to demonstrate the robustness of the aggregated SSC result with regard to the composition of the expert teams; (2) the possibility of observing the actual elicitation interviews; (3) the need to allocate sufficient time so that the experts can provide the required assessments without compromising the quality of their assessments; (4) the use of "logic tree" in expressing and quantifying uncertainty; (5) if there is a real need to distinguish the various types of uncertainties, i.e., model vs. parameter and aleatory vs. epistemic, especially when the experts are not comfortable with this uncertainty characterization framework; and (6) the possibility of a combined SSC and GM feedback workshop to facilitate the interface between these two panels, to ensure consistency in the scope of the assessments. Tim Sullivan, Carl Stepp, Abou-Bakr Ibrahim, Philip Justus and Christiana Lui were present during this informal discussion.

Revision 1 of the PSHA project plan was distributed during the workshop and is included as Attachment 9. The workshop summaries which were prepared by the USGS for DOE can be found in Attachment 10.

The next set of SSC and GM workshops will be held at Salt Lake City, Utah, on April 14-18, 1997. The main goal of these workshops will be to provide feedback to the experts on their assessments after their preliminary assessments have been aggregated and propagated through the PSHA models by the Calculations Team. The final experts' assessments are due by early June 1997. The final PSHA report is due to DOE from its contractor by the end of August 1997.

DISTRIBUTION: w/o att*

Central File NMSS r/f* DWM r/f* PAHL r/f CNWRA* PSobel*
 JThoma* JKotra* SWastler* NEisenberg* MLee*

Please note: if you need to refer to the attachments please refer to PAHL r/f.

OFC	PAHL* <i>[initials]</i>	ENGB* <i>[initials]</i>	ENGB* <i>[initials]</i>	ENGB* <i>[initials]</i>	PAHL* <i>[initials]</i>
NAME	CLui/wd	PJustus	Abrahim	Brooks	KMcConnell
DATE	3/12/97 H	3/12/97	3/12/97	3/12/97	3/13/97

OFFICIAL RECORD COPY

In small Box on "DATE:" line enter: M = E-Mail Distribution Copy H = Hard Copy

PDR : YES X NO Category: Proprietary or CF Only X
 ACNW: YES X NO
 IG : YES NO X Delete file after distribution: Yes X No

were: (1) to ensure that the experts were clear of the assessment process; and (2) to explain to the experts the form in which their input should be provided for seismic hazard calculations. The result of this exercise showed a large variability in the median GM estimates. The GM meeting agenda and list of attendees are included as Attachment 5 and Attachment 6, respectively. Attachment 7 contains reprints of all technical presentations as enumerated in the GM workshop agenda, and other relevant technical articles that were available to the NRC staff during the workshop. The biosketches for the GM experts can be found in Attachment 8.

During the feedback sessions at the end of each day, NRC and CNWRA provided technical input to the group as appropriate. Staff commented on the need to account for triggering in determination of earthquake recurrence rates, and uncertainties of fault zone width in meeting DOE's current commitment to set back from Type I faults. The staff also asked if the earthquake data collected from the different extensional regime areas have comparable stress drop since stress drop is related to acceleration.

DOE and NRC also met to discuss issues related to the implementation of an expert judgment elicitation process outside the main workshop. Issues discussed were: (1) the need to demonstrate the robustness of the aggregated SSC result with regard to the composition of the expert teams; (2) the possibility of observing the actual elicitation interviews; (3) the need to allocate sufficient time so that the experts can provide the required assessments without compromising the quality of their assessments; (4) the use of "logic tree" in expressing and quantifying uncertainty; (5) if there is a real need to distinguish the various types of uncertainties, i.e., model vs. parameter and aleatory vs. epistemic, especially when the experts are not comfortable with this uncertainty characterization framework; and (6) the possibility of a combined SSC and GM feedback workshop to facilitate the interface between these two panels and to ensure consistency in the scope of the assessments. Tim Sullivan, Carl Stepp, Abou-Bakr Ibrahim, Philip Justus and Christiana Lui were present during this informal discussion.

Revision 1 of the PSHA project plan was distributed during the workshop and is included as Attachment 9. The workshop summaries which were prepared by the USGS for DOE can be found in Attachment 10.

The next set of SSC and GM workshops will be held at Salt Lake City, Utah, on April 14-18, 1997. The main goal of these workshops will be to provide feedback to the experts on their assessments after their preliminary assessments have been aggregated and propagated through the PSHA models by the Calculations Team. The final experts' assessments are due by early June 1997. The final PSHA report is due to DOE from its contractor by the end of August 1997.

DISTRIBUTION: w/o att*
 Central File NMSS r/f* DWM r/f* PAHL r/f CNWRA* PSobel*
 JThoma* JKotra* Swastler* NEisenberg* MLee*
 Please note: if you need to refer to the attachments please refer to PAHL r/f.
 * See previous concurrence:

OFC	PAHL*		ENGB*		ENGB*		ENGB*		PAHL*	
NAME	CLui/wd		PJustus		AIbrahim		DBrooks		KMcConnell	
DATE	3/12/97		3/12/97		3/12/97		3/12/97		/ /97	

OFFICIAL RECORD COPY

In small Box on "DATE:" line enter: M = E-Mail Distribution Copy H = Hard Copy
 PDR : YES X NO Category: Proprietary or CF Only X
 ACNW: YES X NO
 IG : YES NO X Delete file after distribution: Yes X No

FINAL AGENDA
SEISMIC SOURCE CHARACTERIZATION
PRELIMINARY INTERPETATIONS WORKSHOP
JANUARY 6-8, 1997
WASATCH ROOM, DOUBLETREE HOTEL
SALT LAKE CITY, UTAH

PURPOSE OF WORKSHOP

- To provide an opportunity for the expert teams to present and discuss their preliminary interpretations regarding key issues in seismic source characterization
- To train the expert teams on the process of elicitation and uncertainty characterization
- To present and discuss additional information and interpretations of importance to source characterization

APPROACH

- For each of the five key issues assigned, two teams will present their interpretations; all of the teams will discuss the issue and will be prepared with summary slides
- Focus on understanding the interpretations, their technical bases, consistency with data, and expression of uncertainty
- Each team should feel that they understand the interpretations of others and should be prepared to re-examine their thinking in light of what they hear
- The goal is for interpretations given at the elicitation interviews to be well-reasoned, technically-supported, and complete.

MONDAY, JANUARY 6, 1997

1:00-1:15	Introduction and Purpose (K. Coppersmith)
1:15-2:00	The Sundance Fault (C. Potter)
2:00-2:30	Hydrologic and Geochemical Considerations Relating to Evaluation of Faulting at Yucca Mountain (J. Stuckless)
2:30-3:15	Geophysical Interpretation of Yucca Mountain and Vicinity (E. Majer)
3:15-3:30	Break
3:30-4:15	Yucca Mountain Faults in a Regional Context (D. O'Leary)
4:15-5:00	Subhorizontal Detachments and Seismicity (B. Wernicke)
5:00-5:30	Precarious Rocks and Their Implications to Prehistorical Seismicity (J. Brune, J. Whitney)
5:30-5:45	Comments from Observers
5:45	Adjourn for Dinner

Attachment 1

102.8

TUESDAY, JANUARY 7, 1997

8:00 Continental breakfast in Wasatch #4
8:30-8:35 Introduction to Key Issues (K. Coppersmith)
8:35-10:30 **Issue #1: Tectonic Models**
8:35-9:05 Presentation of Team Interpretation (Ake, Slemmons, McCalpin)
9:05-9:35 Presentation of Team Interpretation (Smith, dePolo, Menges)
9:35-10:15 Discussion of Issue #1 (All Teams)
10:15-10:30 **Break**
10:30-12:30 **Issue #2: Potential Seismic Sources**
10:30-11:00 Presentation of Team Interpretation (Doser, Fridrich, Swan)
11:00-11:30 Presentation of Team Interpretation (Rogers, Young, Anderson)
11:30-12:30 Discussion of Issue #2 (All Teams)
12:30-1:30 **Lunch (on your own)**
1:30-3:15 **Issue #3: Maximum Magnitudes**
1:30-2:00 Presentation of Team Interpretation (Ake, Slemmons, McCalpin)
2:00-2:30 Presentation of Team Interpretation (Smith, dePolo, Menges)
2:30-3:15 Discussion of Issue #3 (All Teams)
3:15-3:30 **Break**
3:30-5:30 **Issue #4: Earthquake Recurrence**
3:30-4:00 Presentation of Team Interpretation (Doser, Fridrich, Swan)
4:00-4:30 Presentation of Team Interpretation (Rogers, Yount, Anderson)
4:30-5:30 Discussion of Issue #4 (All Teams)
5:30-5:45 Comments from Observers

WEDNESDAY, JANUARY 8, 1997

8:00 Continental Breakfast in Wasatch #4
8:30-10:30 **Issue #5: Fault Displacement Methodology**
8:30-9:00 Presentation of Team Interpretation (Arabasz, Anderson, Ramelli)
9:00-9:30 Presentation of Team Interpretation (Smith, Bruhn, Knuepfer)
9:30-10:30 Discussion of Issue #5 (All Teams)
10:30-10:45 **Break**
10:45-11:30 Additional Guidance on Fault Displacement Hazard (Fault Displacement Working Group)
11:30-12:00 General Discussion
12:00-1:00 **Lunch**
1:00-3:00 Elicitation Training (P. Morris)
3:00-3:15 Break
3:15-4:30 Elicitation Training (Continued)
4:30-4:45 Where We Go From Here (K. Coppersmith)
4:45-5:00 Comments from Observers
5:00 **Adjourn**

**YUCCA MOUNTAIN SEISMIC SOURCE CHARACTERIZATION
WORKSHOP #4 - PRELIMINARY INTERPRETATIONS**

**Registration List
JANUARY 6 TO 8, 1997**

Name	Signature	Affiliation
30. Parizek, Richard	DID NOT COME	Technical Review Board
31. Parks, Bruce	<i>Bruce Parks</i>	USGS
32. Penn, Sue	<i>Sue Penn</i>	WCFS
33. Perman, Roseanne	<i>Roseanne Perman</i>	Geomatrix
34. Pezzopane, Silvio	<i>Silvio Pezzopane</i>	USGS
35. Pomeroy, Paul	<i>Paul W. Pomeroy</i>	Advisory Committee on Nuclear Waste
36. Potter, Chris	<i>Chris Potter</i>	USGS
37. Quittmeyer, Richard	<i>R.C. Quittmeyer</i>	WCFS
38. Ramelli, Alan	<i>Alan Ramelli</i>	UNR
39. Reiter, Leon	<i>Leon Reiter</i>	NWTRB
40. Rogers, Al	<i>Al Rogers</i>	EQE International
41. Savy, Jean	<i>Jean Savy</i>	Lawrence Livermore National Laboratory
42. Schwartz, David	<i>David Schwartz</i>	USGS
43. Sheaffer, Patricia	<i>Patricia Sheaffer</i>	USGS
44. Slemmons, Burt	<i>Burt Slemmons</i>	WCFS
45. Smith, Ken	<i>Ken Smith</i>	UNR
46. Smith, Robert	<i>Robert Smith</i>	UU
47. Soeder, Daniel	DID NOT COME	USGS
48. Stamatakis, John	<i>John Stamatakis</i>	CNWRA
49. Stepp, Carl	<i>Carl Stepp</i>	WCFS
50. Stuckless, John	<i>John Stuckless</i>	USGS
51. Sullivan, Tim	<i>Tim Sullivan</i>	DOE
52. Swan, Bert	<i>Bert Swan</i>	Geomatrix
53. Toro, Gabe	<i>Gabe Toro</i>	Risk Engineering
54. Wernicke, Brian	<i>Brian Wernicke</i>	Cal Tech
55. Whitney, John	<i>John Whitney</i>	USGS
56. Wong, Ivan	<i>Ivan Wong</i>	WCFS
57. Youngs, Robert	<i>Robert Youngs</i>	Geomatrix
58. Yount, Jim	<i>Jim Yount</i>	UNR
59. DILLSON, DAVID	<i>David Dillson</i>	NEVADA NWPO
60.		

**YUCCA MOUNTAIN SEISMIC SOURCE CHARACTERIZATION
WORKSHOP #4 - PRELIMINARY INTERPRETATIONS**

Registration List

JANUARY 6 TO 8, 1997

Name	Signature	Affiliation
1. Abrahamson, Norm	<i>Did NOT come</i>	Consultant
2. Ake, Jon	<i>[Handwritten Signature]</i>	U.S. Bureau of Reclamation (USBR)
3. Allen, Clarence	<i>Clarence Allen</i>	Nuclear Waste Technical Review Board (NWTRB)
4. Anderson, Ernie	<i>Ernie Anderson</i>	U.S. Geological Survey (USGS)
5. Anderson, Larry	<i>Larry Anderson</i>	USBR
6. Arabasz, Walter	<i>Walter Arabasz</i>	University of Utah (UU)
7. Bell, John	<i>John Bell</i>	UNR
8. Bruhn, Ron	<i>Ron Bruhn</i>	UU
9. Brune, James	<i>James Brune</i>	UNR
10. Chaney, Tom	<i>Tom Chaney</i>	USGS
11. Coppersmith, Kevin	<i>Kevin Coppersmith</i>	Geomatrix
12. Cornell, Allin	<i>Allin Cornell</i>	Consultant
13. dePolo, Craig	<i>Craig dePolo</i>	UNR
14. Doser, Diane	<i>Diane Doser</i>	University of Texas, El Paso
15. Ferrill, David	<i>David Ferrill</i>	CNWRA
16. Fridrich, Chris	<i>Chris Fridrich</i>	USGS
17. Hanks, Tom	<i>Tom Hanks</i>	USGS
18. Ibrahim, Bakr	<i>Bakr Ibrahim</i>	U.S. Nuclear Regulatory Commission (NRC)
19. Justus, Phil	<i>Phil S. Justus</i>	NRC
20. King, Jerry	<i>Jerry King</i>	M&O/SAIC
21. Knuepfer, Peter	<i>Peter D. Knuepfer</i>	State University of New York at Binghamton
22. Lui, Christiana	<i>Christiana Lui</i>	NRC
23. Majer, Ernie	<i>Ernie Majer</i>	Lawrence Berkeley Labs
24. McCalpin, Jim	<i>Jim McCalpin</i>	GEO-HAZ Consulting, Inc.
25. McGuire, Robin	<i>Robin McGuire</i>	Risk Engineering
26. Menges, Chris	<i>Chris Menges</i>	USGS
27. Morris, Peter	<i>Peter Morris</i>	Applied Decision Analysis, Inc.
28. O'Leary, Dennis	<i>Dennis O'Leary</i>	USGS
29. Olig, Susan	<i>Susan Olig</i>	Woodward-Clyde Federal Services (WCFS)

INTRODUCTION AND PURPOSE

PRELIMINARY INTERPRETATIONS WORKSHOP SEISMIC SOURCE CHARACTERIZATION YUCCA MOUNTAIN SEISMIC HAZARD ANALYSIS

**JANUARY 6-8, 1996
SALT LAKE CITY, UTAH**

PRELIMINARY INTERPRETATIONS WORKSHOP

PURPOSE OF WORKSHOP

- **Opportunity for teams to present and discuss preliminary interpretations regarding key issues to source characterization**
- **To present and discuss additional information/interpretations**
- **To train teams on the process of elicitation and uncertainty characterization**

APPROACH

- **For each of five key issues, two teams will present their interpretations to get the discussion going**
- **Discussion will focus on: 1) understanding interpretations, 2) technical bases, 3) consistency with data, and 4) expressions of uncertainty**
- **Be prepared to defend, challenge, re-examine your thinking**
- **It is more important to discuss all issues in detail, have your questions answered; than to have polished presentations**

OVERALL GOAL

To prepare for the elicitations, such that the interpretations are well-reasoned, technically-supported, and complete

KEY ISSUES TO ADDRESS

1. *What tectonic models are appropriate to explain observations in the Yucca Mountain region?*
 - What are their relative credibilities?
2. *What the potential seismic sources in the Yucca Mountain region?*
 - What are their geometries?
 - What are the uncertainties?
3. *What are the maximum magnitudes associated with these potential seismic sources?*
 - What approaches are appropriate?
 - What parameters are used?
4. *What recurrence rates (frequency-magnitudes) are appropriate for each source?*
 - What approaches are used?
 - What parameters are used?
5. *What is your approach to assessing the potential for displacement within the site area?*
 - Locations of displacement
 - Size and frequency of displacement

PRESENTATION OF EACH TECHNICAL ISSUE

- **Present preliminary evaluations of each issue**
- **Defend alternatives selected and those rejected**
- **Summarize consistency of alternatives with available data**
- **Discuss your uncertainties**
- **Ask questions that will help you formulate your ideas for the elicitation**

The Sundance Fault

Presenter: Christopher Potter, USGS

Sundance Fault: Spengler et al., 1994
(USGS OFR 94-49; based on 1:240-scale
mapping by Braun et al.)

- Sundance is a NW-striking “fault system” within the potential repository block. Unlike the north-striking, west-side-down Ghost Dance, displacement on Sundance is east-side-down and dextral.
- “Sundance flt. system” is at least 274 m. wide. The “most conspicuous through-going feature” is termed the “Sundance fault.”
- Sundance fault offsets the Ghost Dance fault in a dextral sense by at least 52 m in the Split Wash area. Smaller offsets of the Ghost Dance fault also exist within the Ghost Dance fault system.
- Sundance Flt. may extend over a distance of at least 3 km.

Braun et al., 1996: Geologic Map along the Ghost Dance Fault -- 1:480-scale Geologic Map (Administrative Report to DOE)

- Initial purpose: Fracture mapping in support of unsaturated-zone hydrologic modeling.
- Mapped at 1:240 scale (1"=20'); compiled at 1:480 scale.
- Survey control: "Permanent" stakes define a grid with 200' spacing, keyed to NV State Coordinate System.
- Multiple criteria for recognition of internal contacts in the Tiva Canyon Tuff; map units based on Scott and Bonk (1984).
- Plotted contacts and structures planimetrically, relative to survey stakes; did not use a topographic base in the field.
- Identified numerous previously unrecognized minor faults.
- Ghost Dance fault "system:" 366 m wide; contains several continuous ancillary faults.

Sundance Fault: Potter et al., 1995 (1:2400-scale
map; administrative report to DOE)

APPROACH / METHODS

- Potter et al. mapped a 4-km-long, 565-m-wide northwest-trending swath (NW of Little Prow to south flank of Antler Ridge) along “Sundance trend” at a scale of 1:2400, using a topographic base.
- Potter et al. also used the same surveyed control grid employed by Braun et al., where the two maps overlap.
- Map units are based on Buesch et al. (1996), and include several zones in the crystal-rich (upper) member of Tiva Canyon Tuff that were not mapped by Braun et al.

Sundance Fault: Potter et al., 1995 (1:2400-scale map; administrative report to DOE)

RESULTS

- The Sundance fault zone has a limited extent (~750 m long).
- The Sundance fault zone does not offset the Ghost Dance; the Ghost Dance fault projects straight across Split Wash beneath Quaternary cover.
- The Ghost Dance fault steps to the right in two places. In neither case does the Ghost Dance appear to be offset by a younger fault.
- Tertiary faulting in the Tiva Canyon Tuff in the "central block" of Yucca Mountain was quite heterogeneous. Individual faults are laterally and vertically discontinuous.

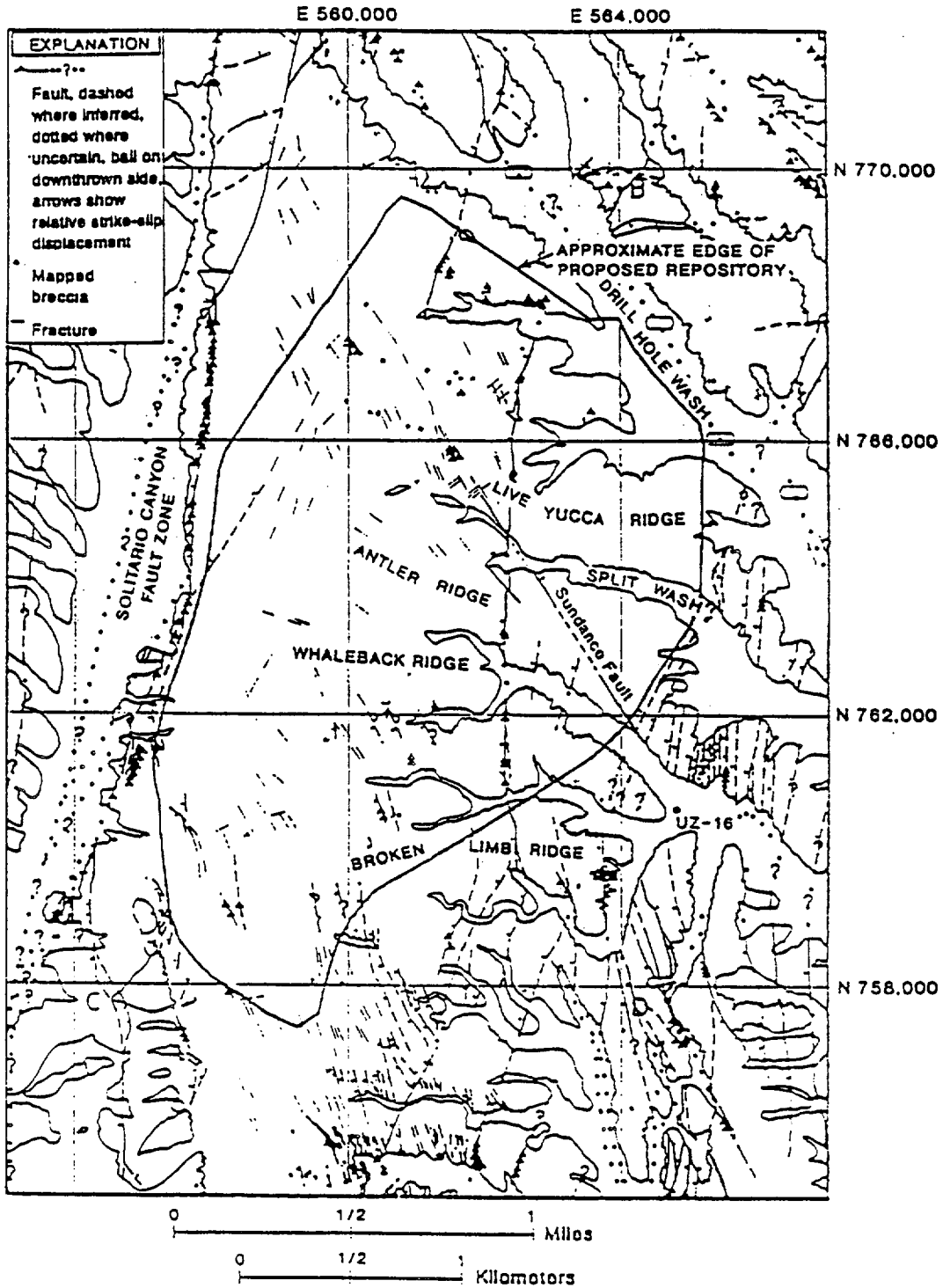
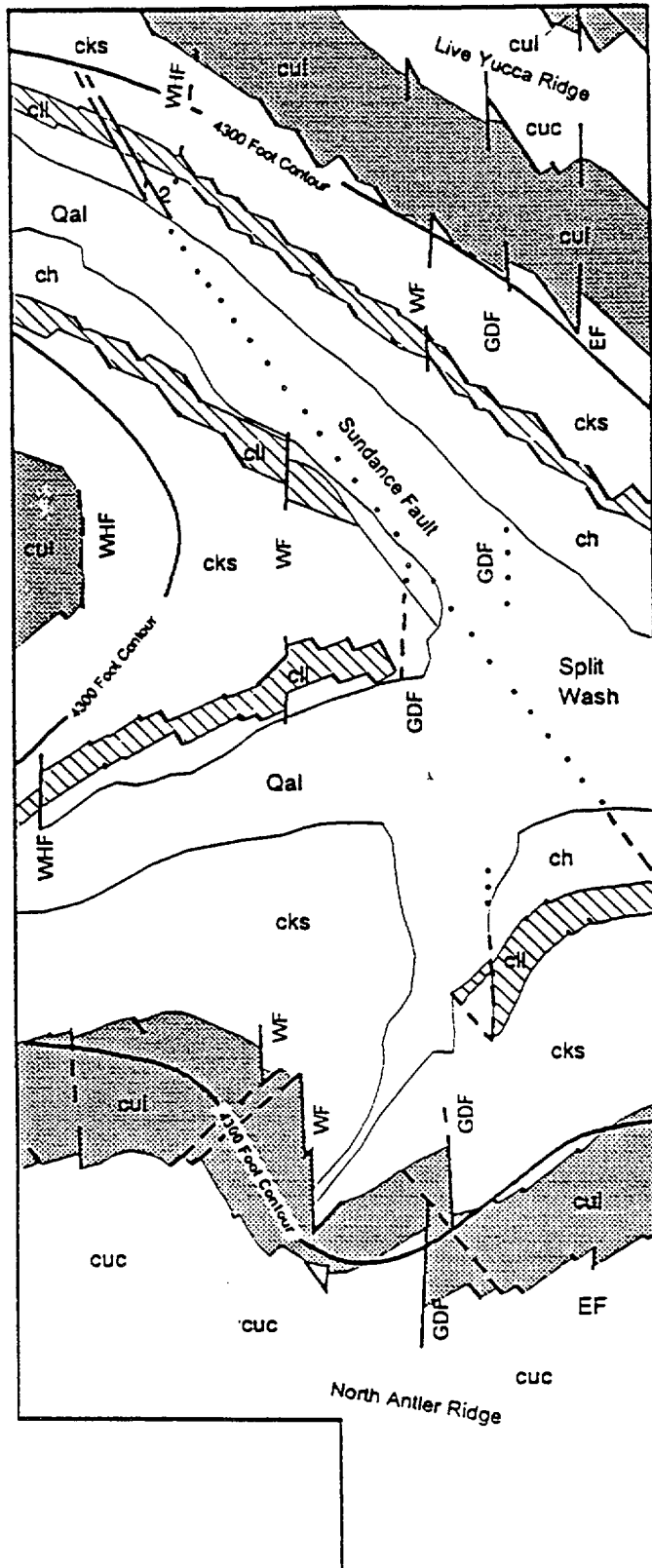


Figure 5.--Map of Yucca Mountain showing the location of the Sundance Fault relative to structural features mapped by Scott and Bonk (1984), and location of USW UZ-16 drill hole.

FROM SPENGLER + OTHERS,
1994.



EXPLANATION

UNITS OF TIVA CANYON TUFF

- Qal alluvium
- cuc upper cliff
- cul upper lithophysal
- cks clinkstone
- cll lower lithophysal
- ch hackly
- Contact
- Fault, dashed where inferred; dotted where concealed; arrow indicates rake of slickensides
- WHF West Hinge fault
- WF West fault
- GDF Ghost Dance fault
- EF East fault

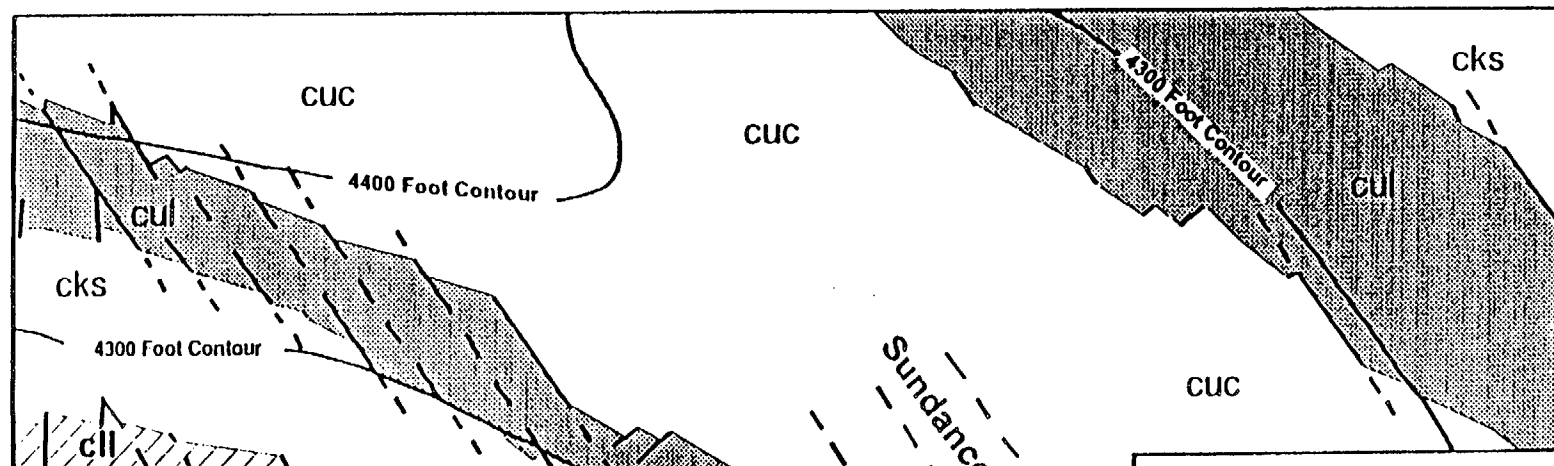


0 100 200 Feet
 0 30 60 Meters

Mapped during 1993 at a scale of 1 inch equals 20 feet

FROM SPENGLER + OTHERS, 1994

Figure 3.—Generalized geologic map of the Split Wash area showing offset of lithostratigraphic units along the Ghost Dance fault and Sundance fault systems.



- - - Contact
 - - - Fault, dashed where inferred

Mapped during 1993 at a scale of 1 inch equals 20 feet

UNITS OF TIVA CANYON TUFF
 cuc upper cliff
 cul upper lithophysal
 cks clinkstone
 cll lower lithophysal

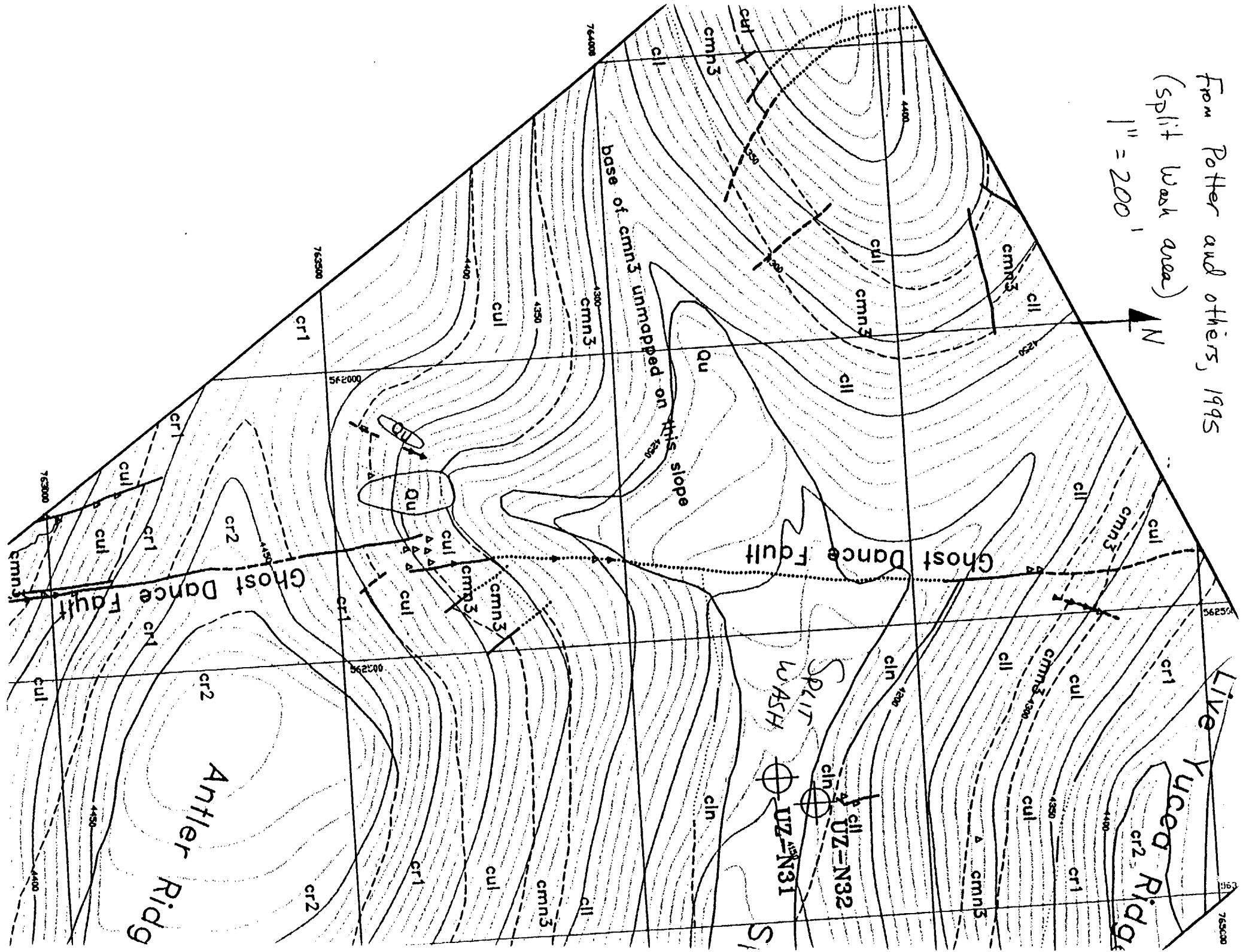
N
 0 100 200 Feet
 0 30 60 Meters

Figure 4.--Generalized geologic map of the eastern part of Antler Ridge showing offset of lithostratigraphic units along the Sundance fault.

FROM SPENGLER + OTHERS,
 1994

From Potter and others, 1995
(Split Wash area)

1" = 200'



BROCHER AND OTHERS

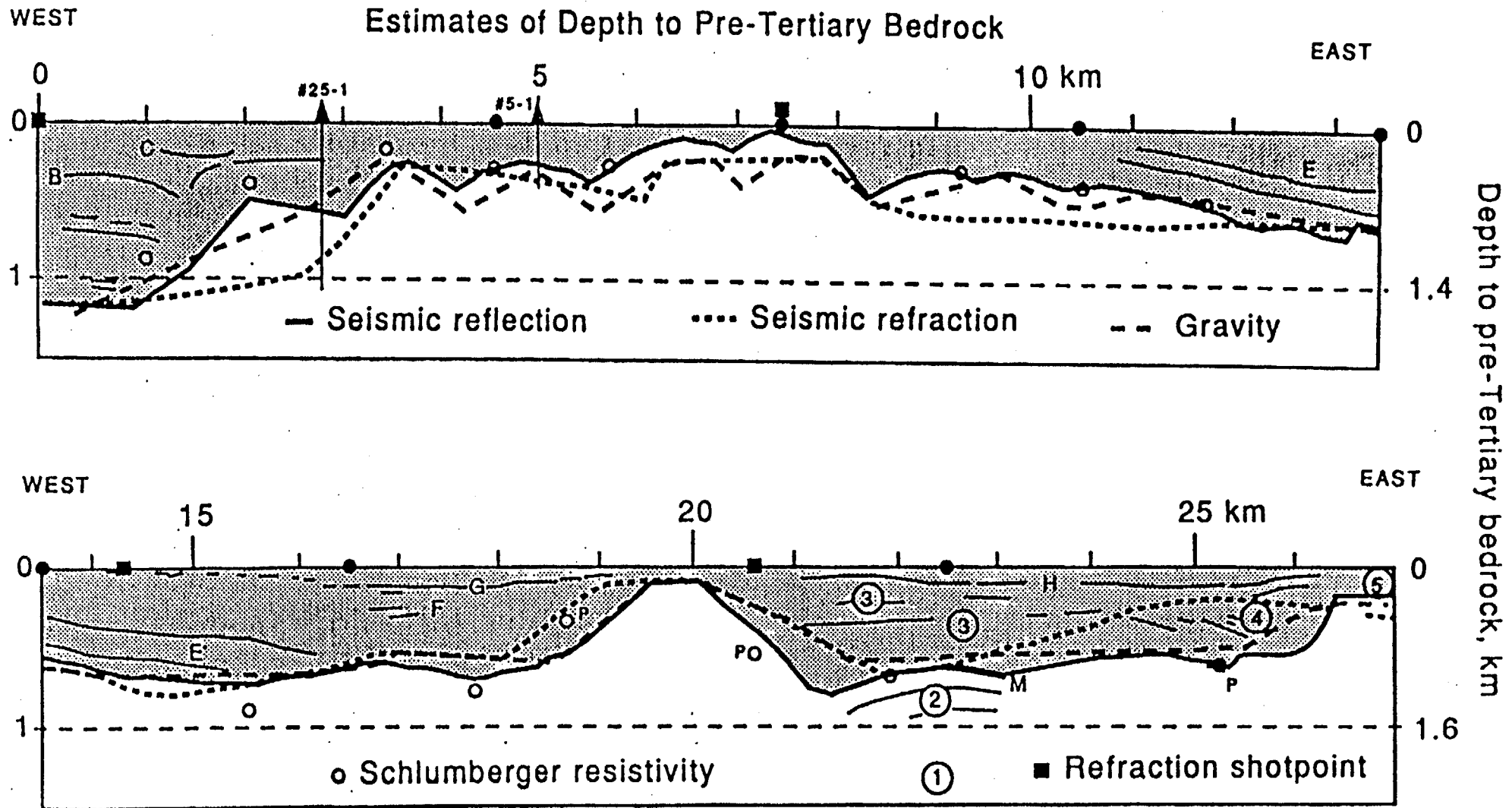
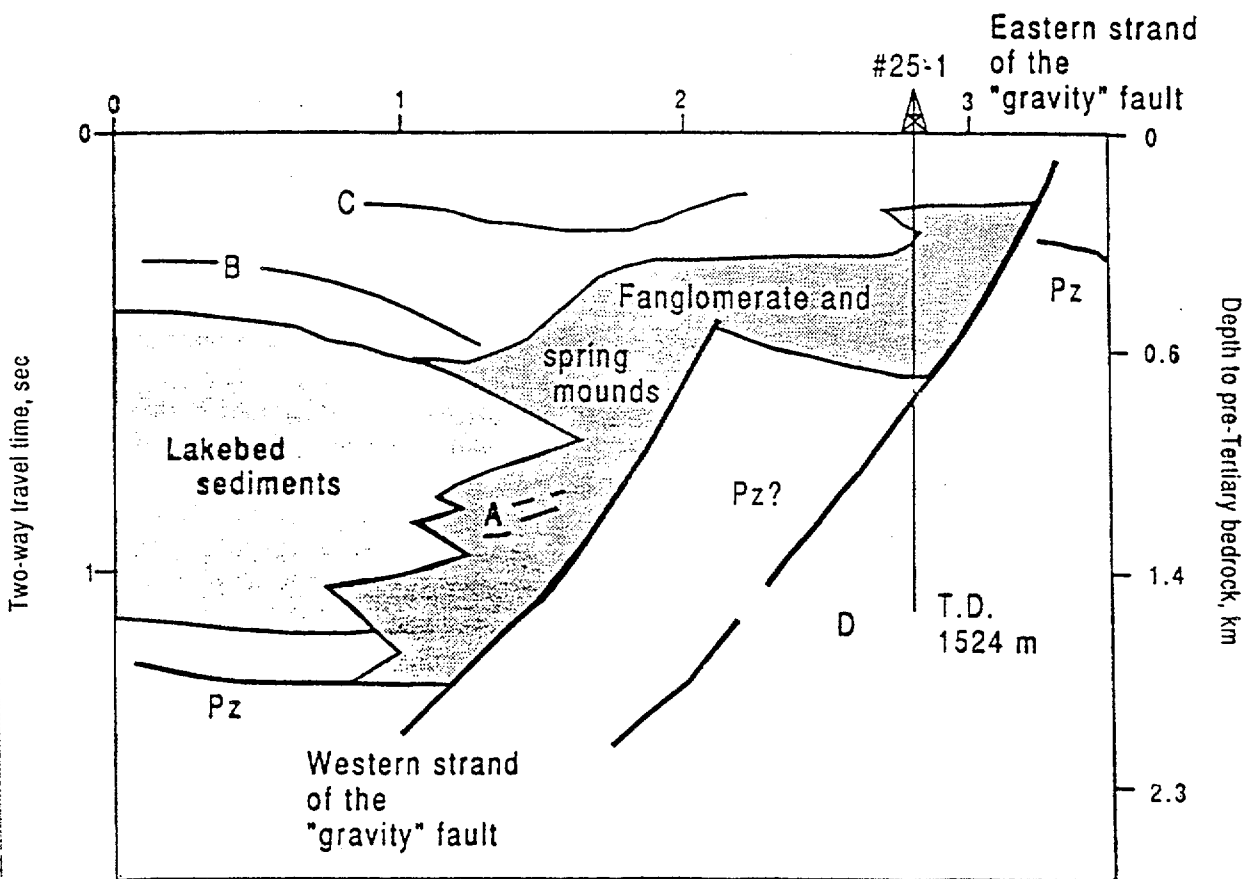
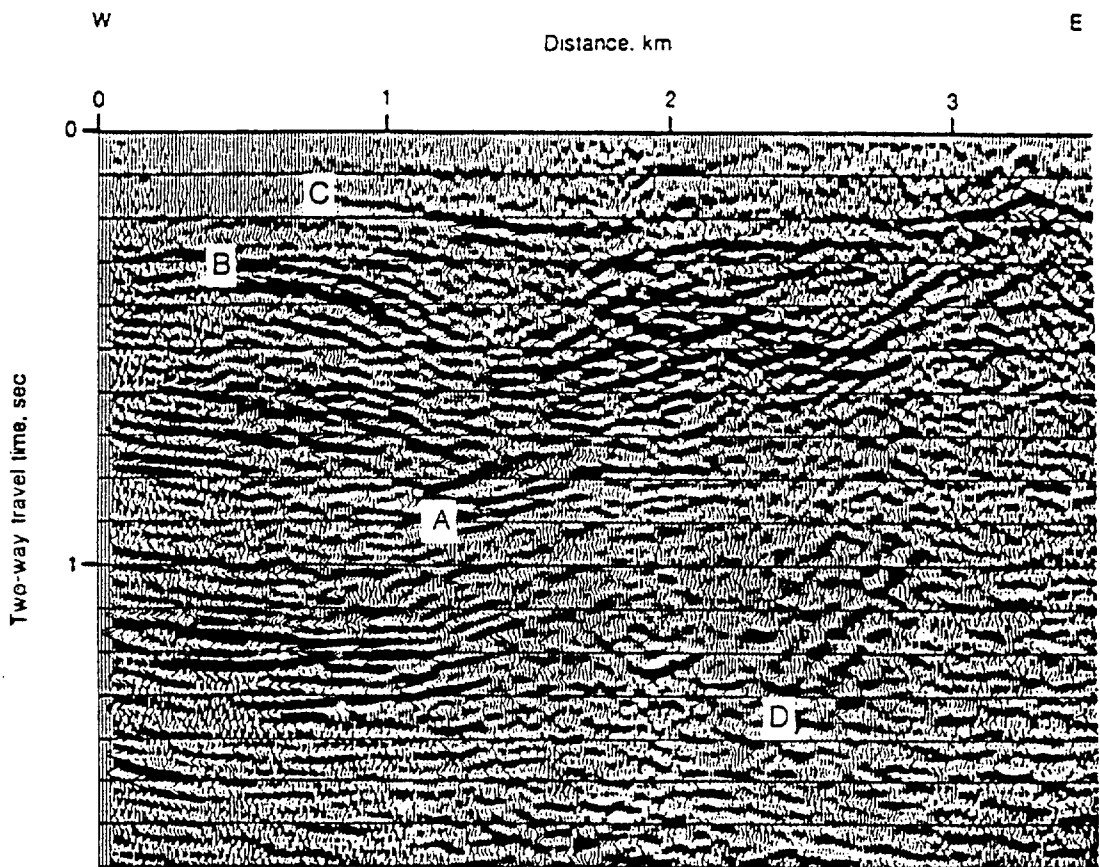


Figure 4. Comparison of estimates for the depth to the pre-Tertiary bedrock along line AV-1 derived from gravity, seismic reflection and refraction, and resistivity measurements. Velocity-depth model (W. D. Mooney, 1988, written commun.) and density-depth model (Brocher and others, 1990) were converted to two-way traveltimes assuming vertical incidence. Two-way traveltimes for resistivity depths were derived from the stacking velocities for line AV-1. The filled squares are the locations of refraction shotpoints used by W. D. Mooney (1988, written commun.). The circles indicate locations of the resistivity measurements, a P next to a circle indicates that this measurement was projected up to a kilometer onto line AV-1 (Greenhaus and Zablocki, 1982). Filled circles are the locations of the explosion sources used for the lower-crustal reflection profile shown in Figure 3. Some of the reflections within the Tertiary basin fill (shaded) are indicated for comparison with Figures 3 and 5-10. Locations of Schlumberger wildcat holes #25-1 and #5-1 (Harris and others, 1992) are projected onto the line.



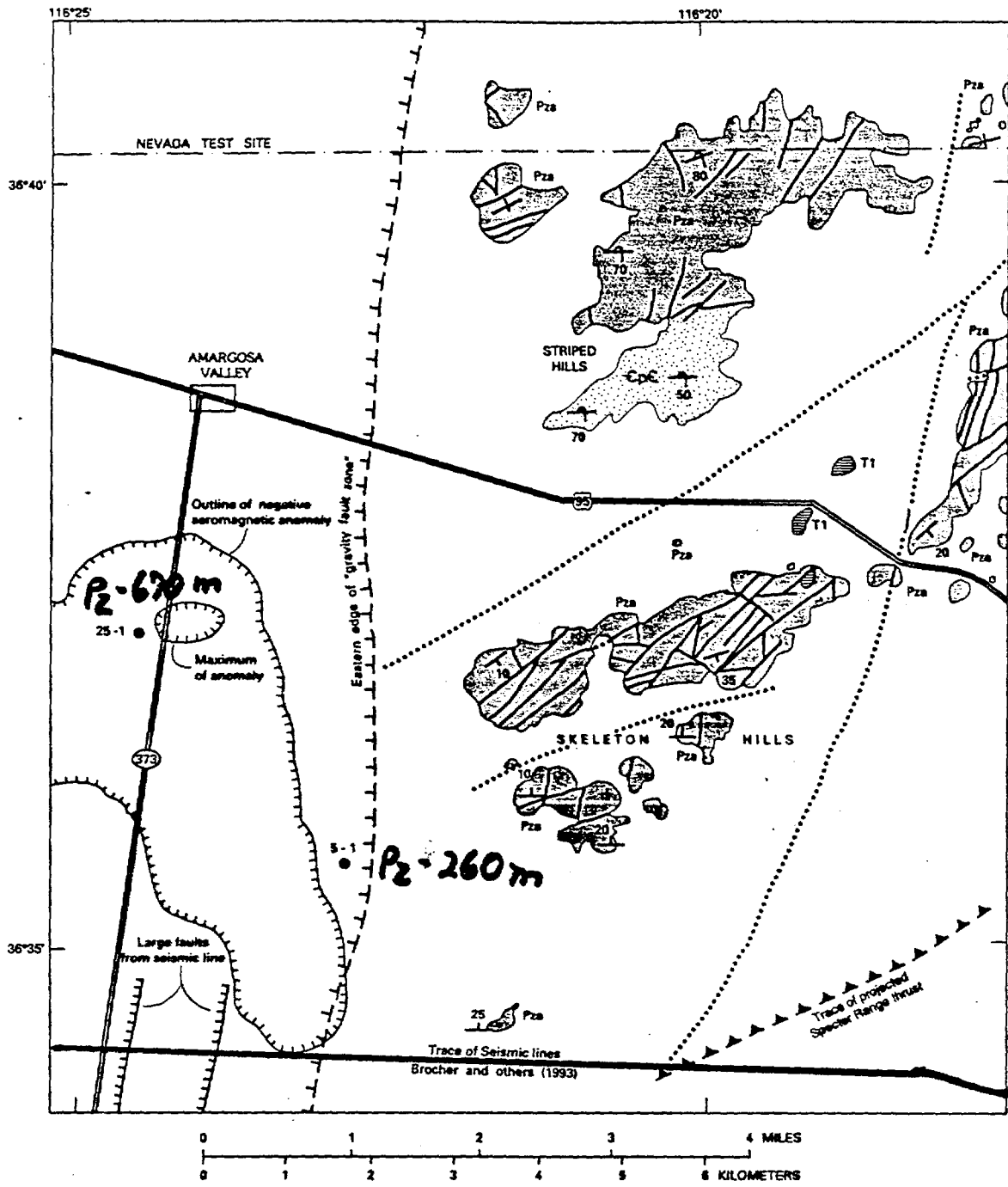
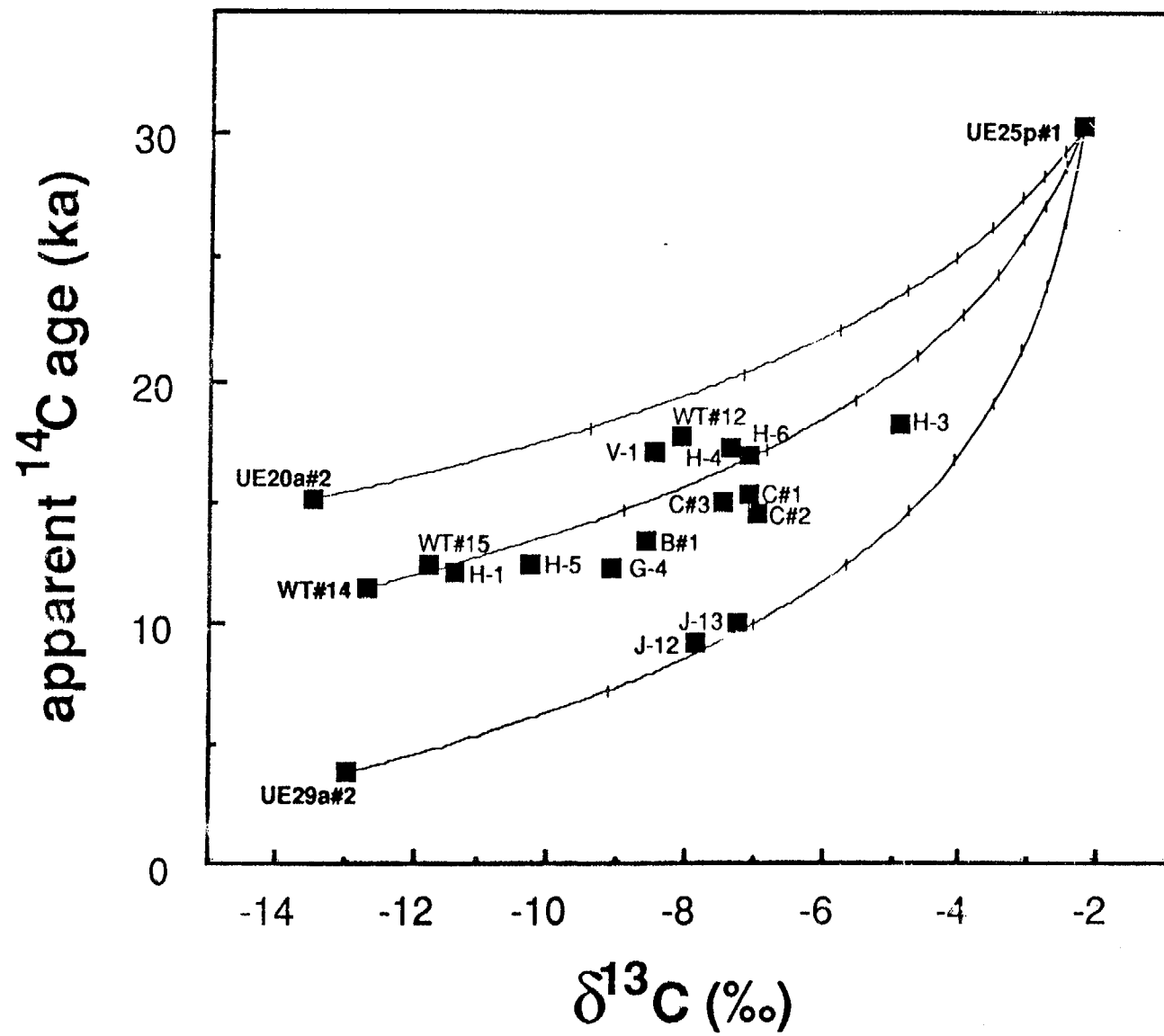
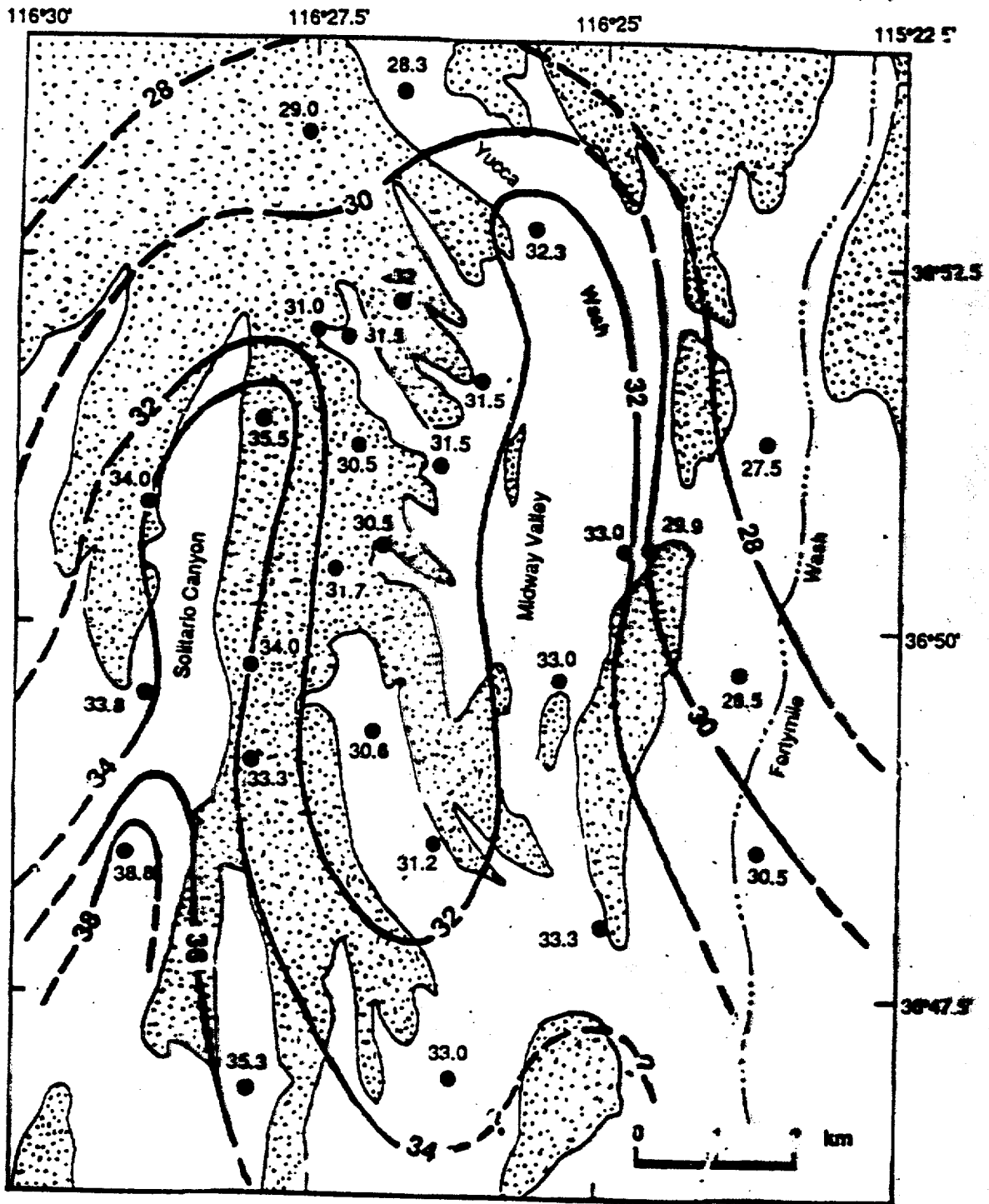


Figure 1. Map of area around drill holes Felderhoff Federal 25-1 and 5-1.



Temperature (°C) at Water Table



(Data from Sass et al., 1988, USGS-OFR-87-649)

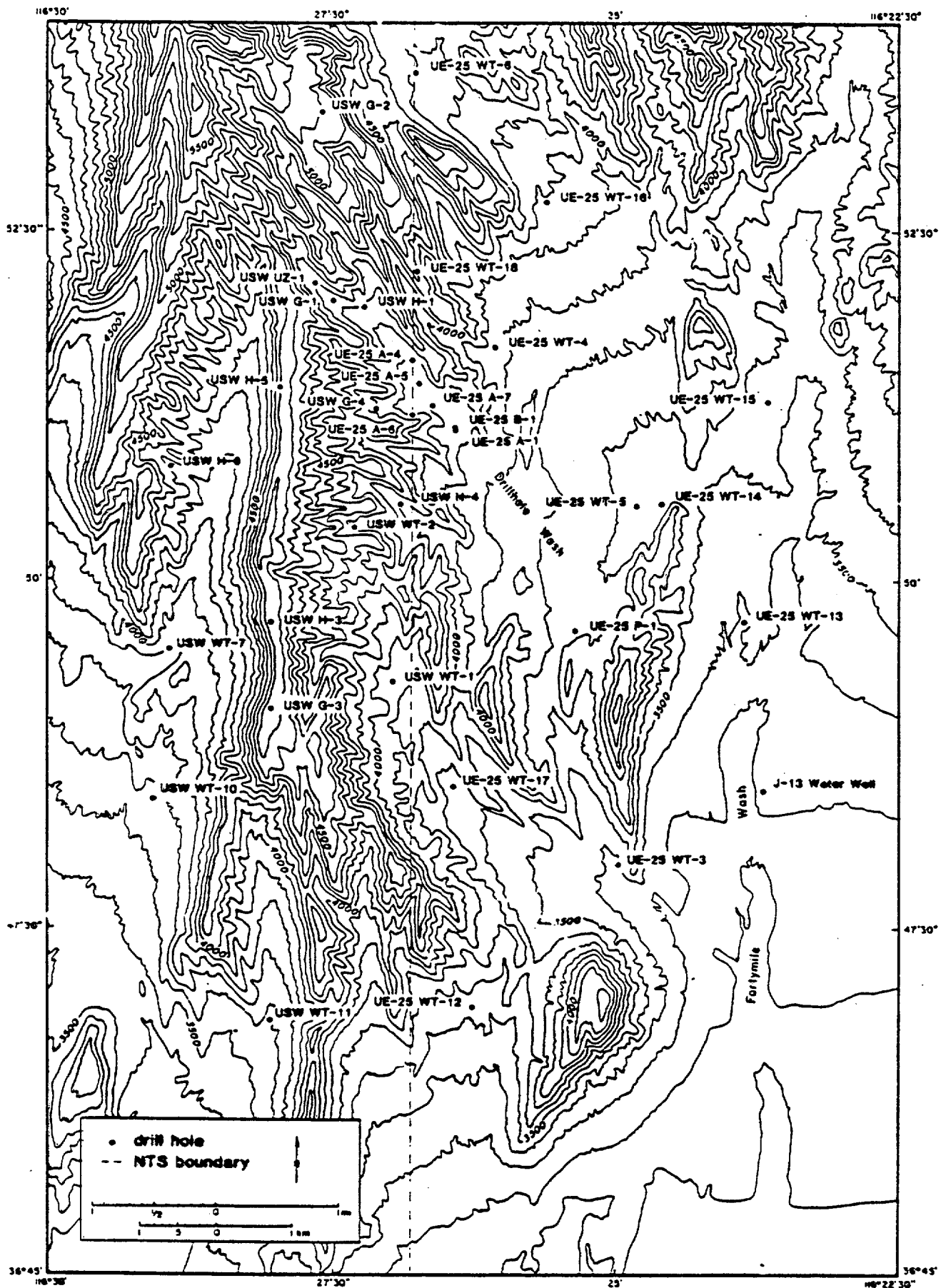


Figure 2. Map showing locations of wells studied (see index, Figure 1).
Contour interval, 100 ft.

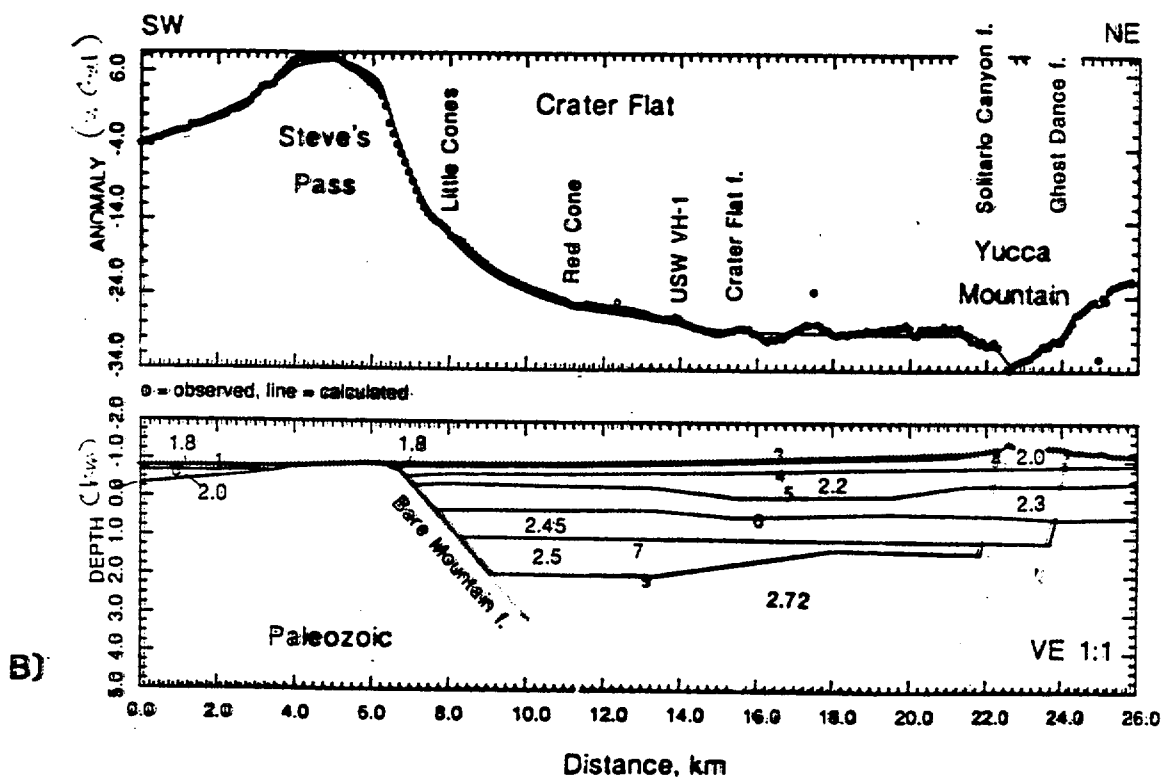
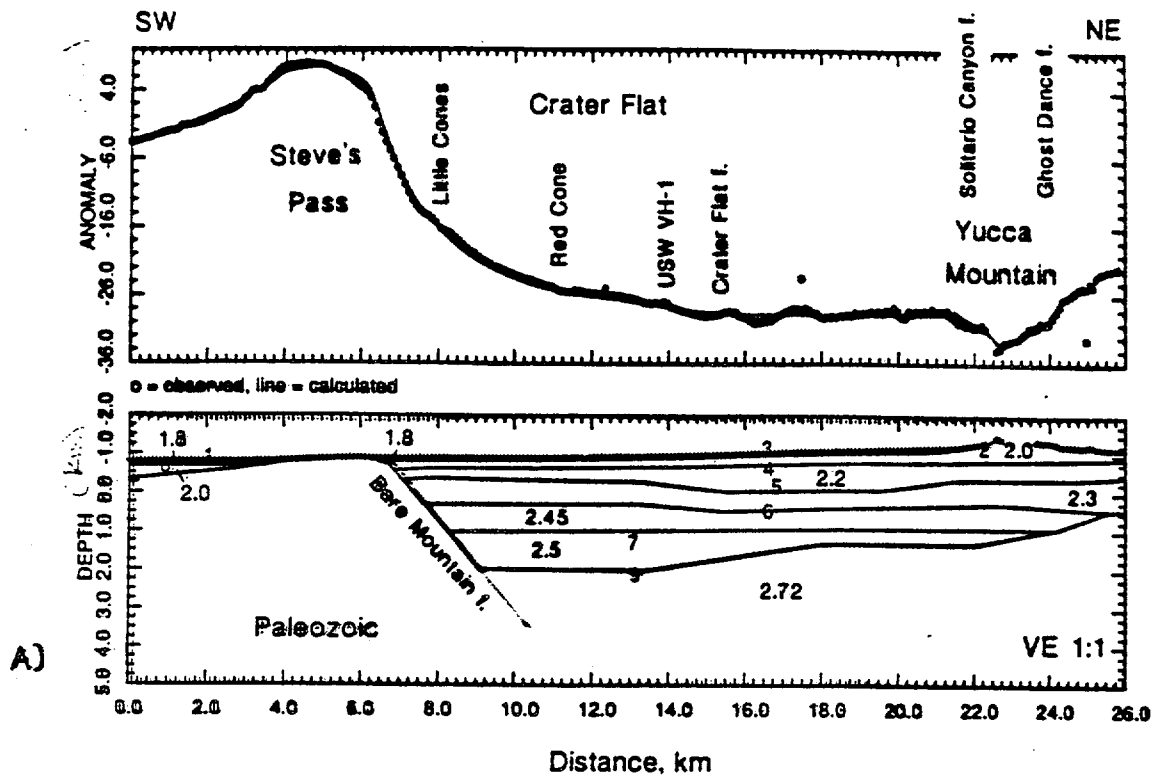


Figure 19. Isostatic gravity anomaly model for Line 2. The start of the seismic line (St. 101) is at model km 0, the end of the seismic line (St. 1133) is at km 26. Models include: (A) a single step in the top of Paleozoic basement beneath Yucca Mountain, and (B) two steps in top of Paleozoic basement beneath Yucca Mountain. Layer densities are given in g/cm^3 . Zero elevation on the depth model corresponds to sea level. Geographic and borehole features are given for reference; fault is abbreviated as "f".

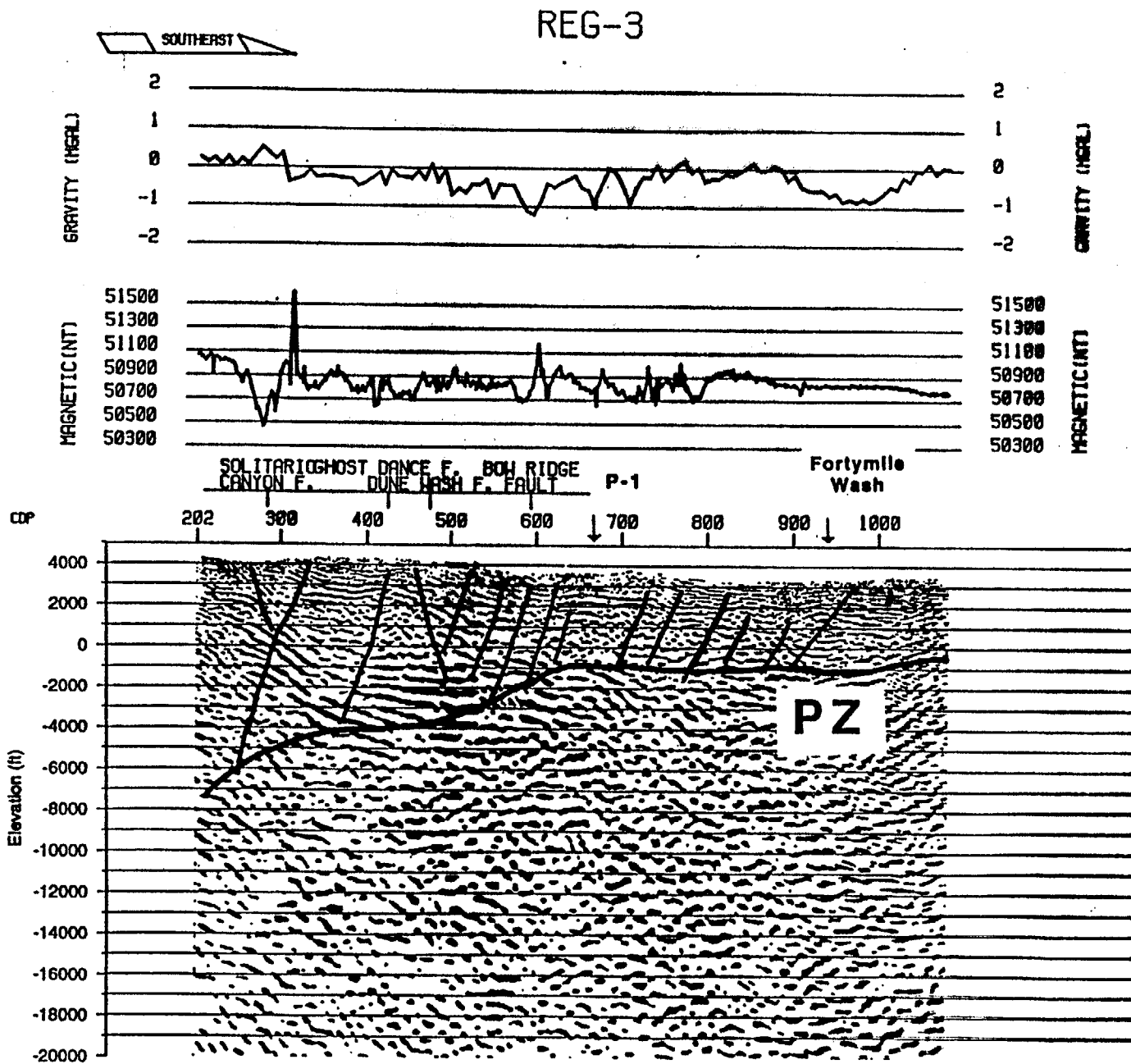


Figure 87b. Interpreted regional seismic line REG-3 with residual gravity and total magnetics.

from LRL Milestone report OBOSM: Synthesis of borehole and surface geophysical studies at Yucca Mountain,
 Nevada, Vol. 1: Surface Geophysics, August 1996

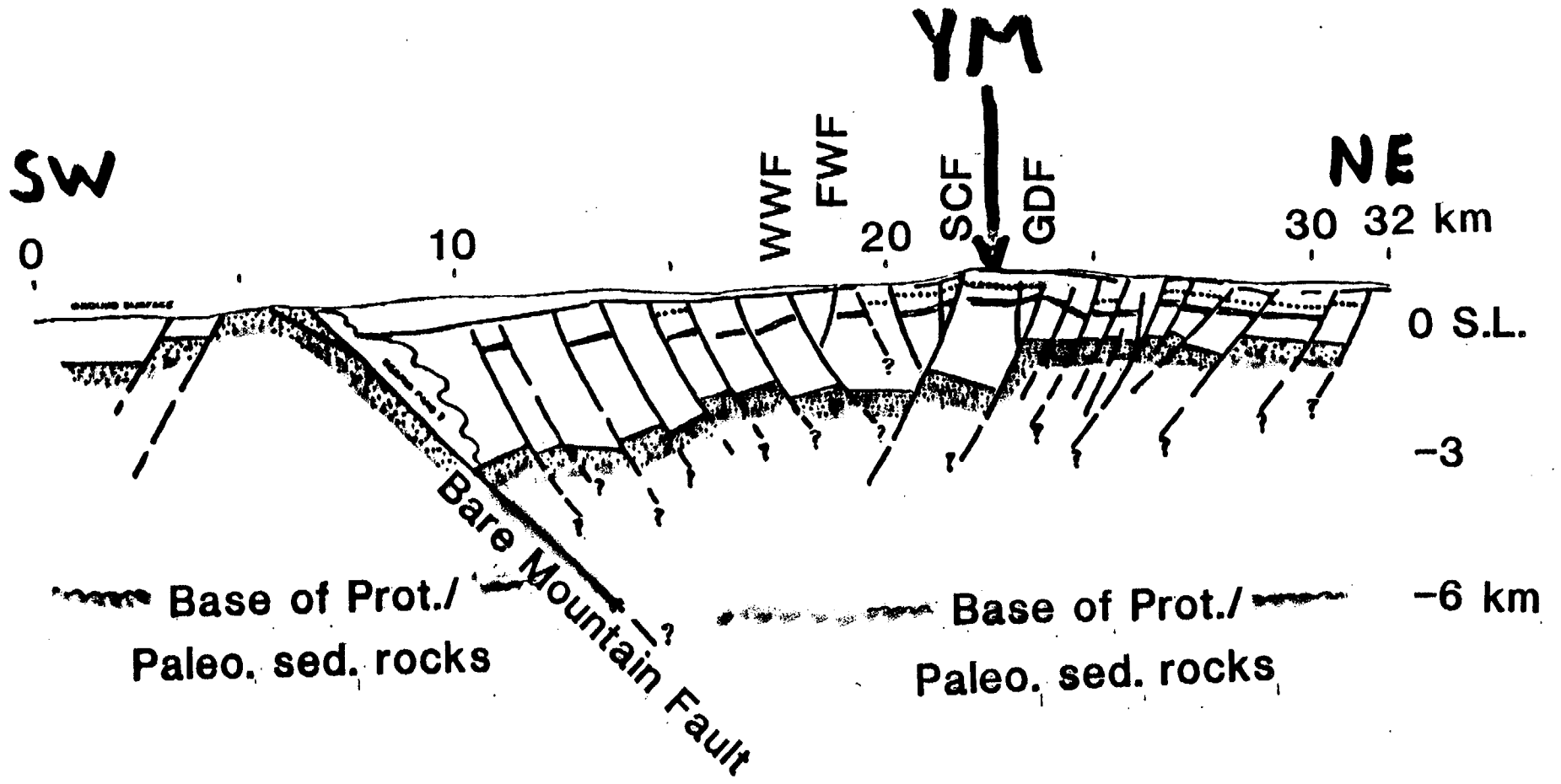


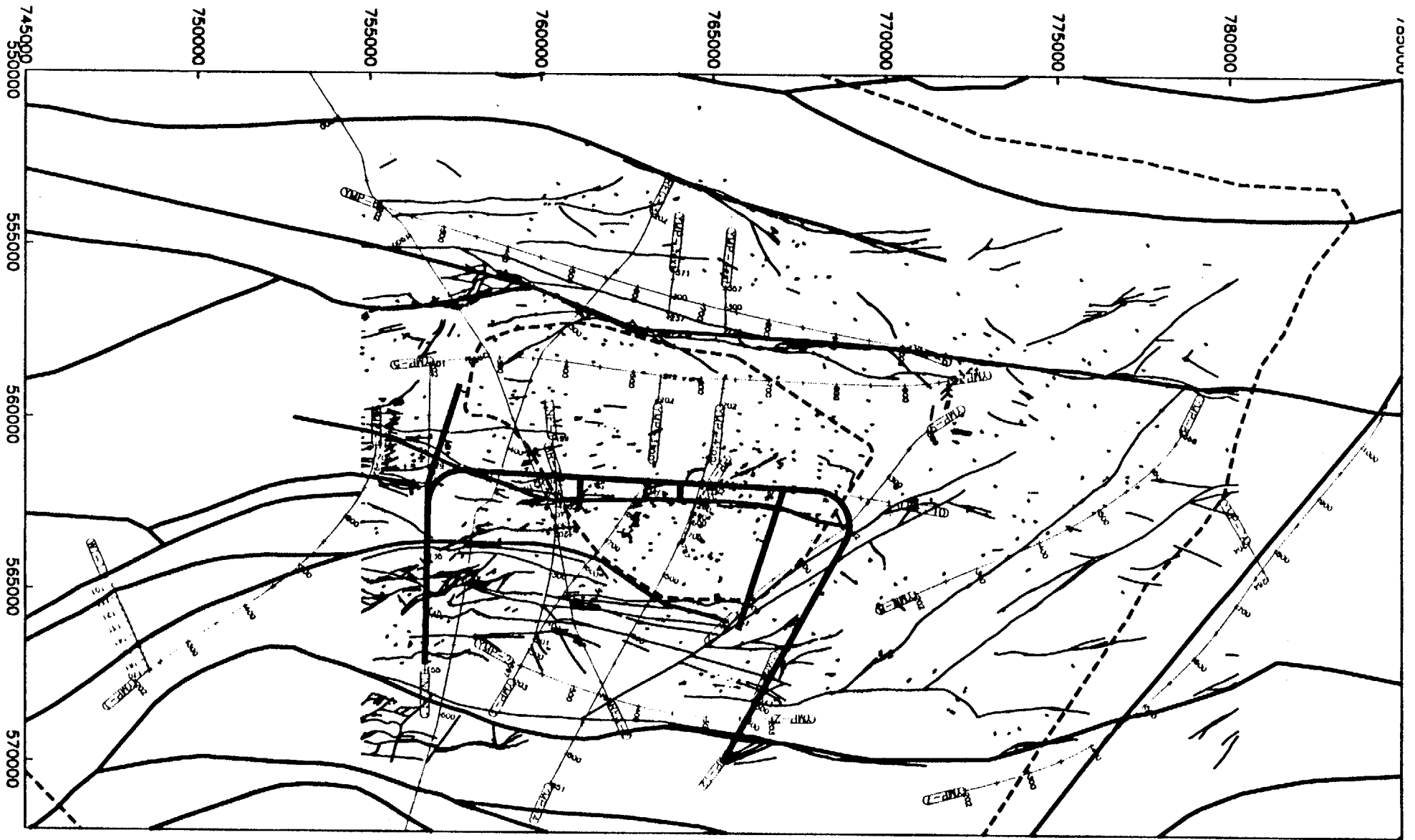
TABLE 5. SEISMIC LINE INFORMATION

Line	Date	Station Spacing (m)	Last Source Station	Last Sensor Station	Total Length (km)	First CDP			Last CDP		
						Station	East	North	Station	East	North
YMP-1	1995 Jan 31-Feb 2	12	363	365	3.18	202	567725	748189	715	560831	755179
YMP-2	1994 Dec 14-17	12	286	310	2.52	203	568667	766721	597	567071	759184
YMP-3	1995 Aug 5-8	6	464	476	2.25	203	567574	759195	918	561752	763114
YMP-3Ext	1995 Sept 18	6	179	196	0.57	237	557048	763687	371	555739	763846
YMP-3Top	1995 Aug 14	6	136	137	0.22	202	559432	763400	272	558749	763486
YMP-4	1994 Dec 21-22, 1995 Jan 12-14	12	436	436	4.03	276	560373	765034	851	570588	760272
YMP-4Ext	1995 Sept 17	6	167	192	0.57	228	557445	765347	357	556179	765352
YMP-4Top	1995 Aug 15	6	142	143	0.25	202	559583	765203	283	558796	765325
YMP-5	1995 Jan 25-29	12	485	490	4.68	202	558367	756861	964	558851	771811
YMP-6	1995 Feb 8-13	12	506	524	5.09	202	553879	755327	1011	557878	770714
YMP-7	1995 Jan 17-20	12	562	562	5.54	202	570705	772318	1072	559457	784568
YMP-7a	1995 Feb 7	12	131	132	0.38	204	563495	780526	264	564522	781107
YMP-8	1995 Jan 15-17	12	338	338	2.86	202	565026	770877	668	560354	778606
YMP-9	1995 Jan 14-15	12	196	196	1.15	202	563115	768874	389	560299	771228
YMP-12	1995 Jan 21-22	3	248	301	0.60	202	569564	765512	543	568079	766288
YMP-13a	1995 Feb 3-4	1	232	232	0.13	187	562456	760699	342	562169	760633
YMP-13b						383	562269	760629	463	562257	760759
YMP-14a	1995 Feb 5-6	1	241	241	0.24	181	562187	760727	346	562496	760745
YMP-14b						393	562405	760800	481	562391	760657
HR-1	1995 Aug 19-20	2	400	400	0.60	202	561881	764920	787	563577	764104
HR-2	1995 Aug 21-22	2	354	350	0.38	317	562991	760802	723	561695	760505
LINE-1	1993 Oct 25-27	12	153	260	1.91	201	566403	759791	499	560612	760338
LINE-2	1993 Oct 27-28	12	99	230	1.55	221	563154	768788	423	565610	765675
RV-1	1995 Sept 8-15	6	883	952	5.11	202	661231	723869	1822	666146	708883
REG-2 (Regional)	1994 Nov	25	1092	1133	25.8	202	498572	717172	2266	568200	762022
REG-3 (Regional)	1994 Nov	25	333	541	11.0	202	554070	763232	1082	588040	753893

E. Majek

TABLE 1. GEOPHYSICAL DATA COLLECTED

Line	Seismic	Gravity	Magnetics	Vertical Seismic Profile (VSP) Well	Magneto-tellurics (MT)
YMP-1	X	X	X		
YMP-2	X	X	X	RF-4, RF-7a	
YMP-3	X	X	X	SD-12, UZ-16	X
YMP-3ext	X	X			
YMP-3top	X				
YMP-4	X	X	X		
YMP-4ext	X	X			
YMP-4top	X				
YMP-5	X	X	X		
YMP-6	X	X	X		
YMP-7	X		X		
YMP-7a	X	X	X		
YMP-8	X	X	X	G-2	
YMP-9	X	X	X		
LINE-10		X	X		
LINE-11		X			
YMP-12	X	X	X		
YMP-13a	X				
YMP-13b	X				
YMP-14a	X				
YMP-14b	X				
HR-1	X				
HR-2	X				
LINE-1	X			WT-2	
LINE-2	X			G-4, NRG-6	
WT-17		X			
RV-1	X	X			
RV-2		X			
REG-2 (Regional)	X	X	X		
REG-3 (Regional)	X	X	X		



BLUE Lines - Geophysical Data; RED Lines - Faults from geologic model [Zelinski & Clayton, 1996];
BLACK Lines - Faults from Day et al. (1996); and GREEN Lines are ESF and repository boundaries.

Entire Aeromagnetic Dataset - Merged and Gridded

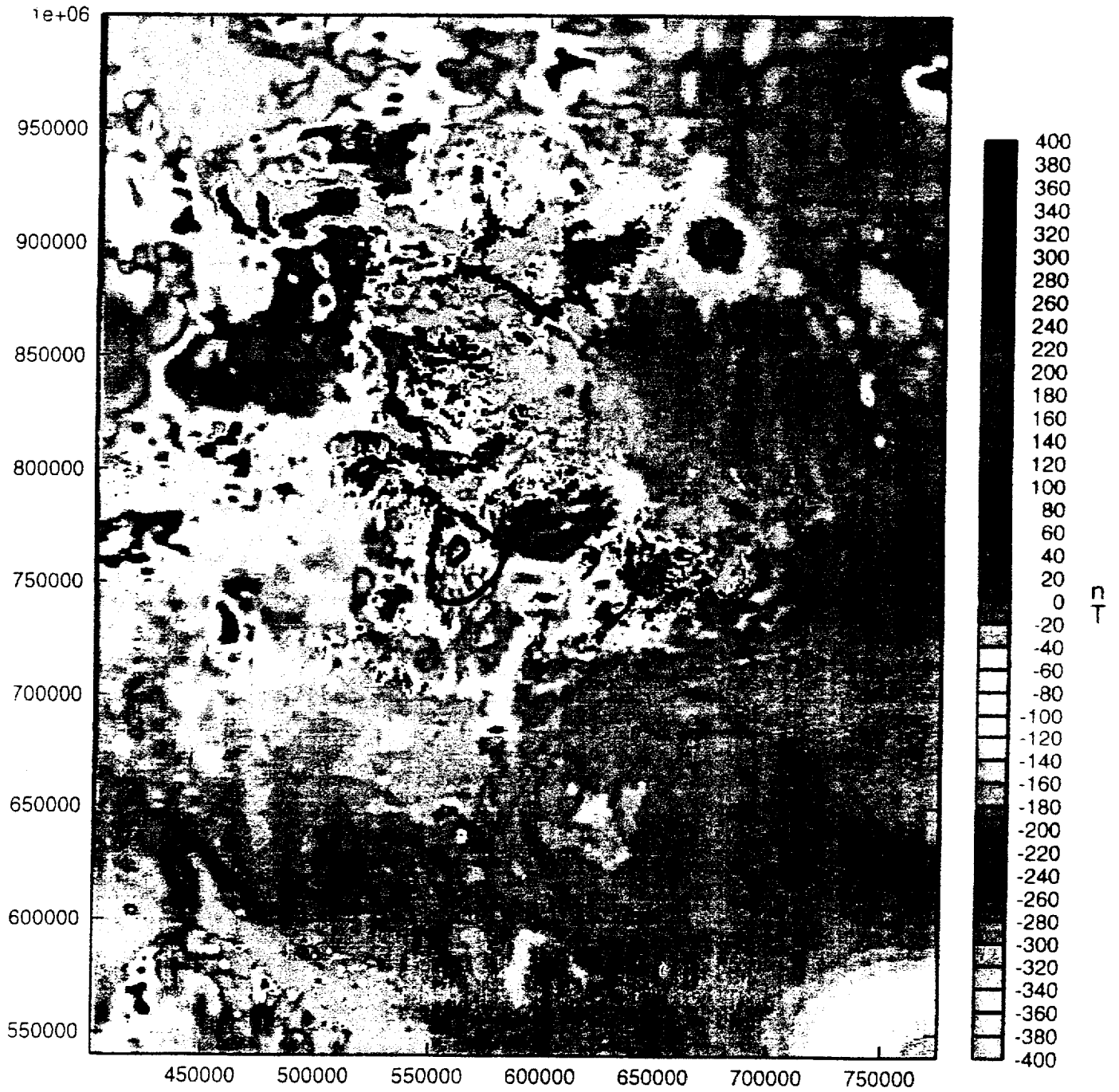


Figure 1. The entire aeromagnetic dataset of the Yucca Mountain Region. The outer black line is the conceptual boundary and the inner black line is the repository boundary. Coordinates are in Nevada State Plane feet.

Aeromagnetic Data - Merged and Gridded

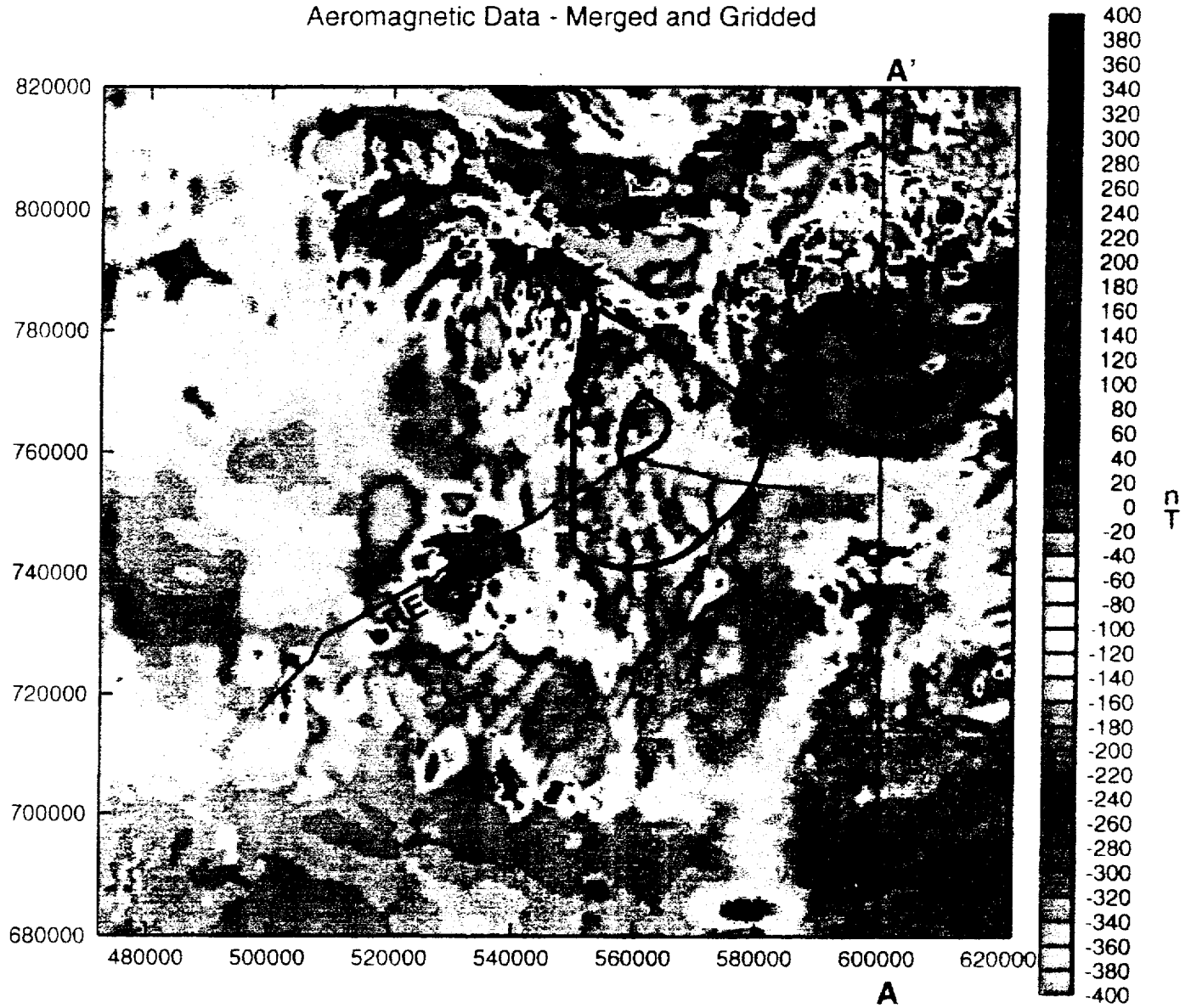


Figure 3. The location of the two profiles: REG-2 & 3 and A-A'. Both profiles cross broader magnetic anomalies to which depth estimates are made. Coordinates are in Nevada State Plane feet

Aeromagnetic Data - Upward Continued

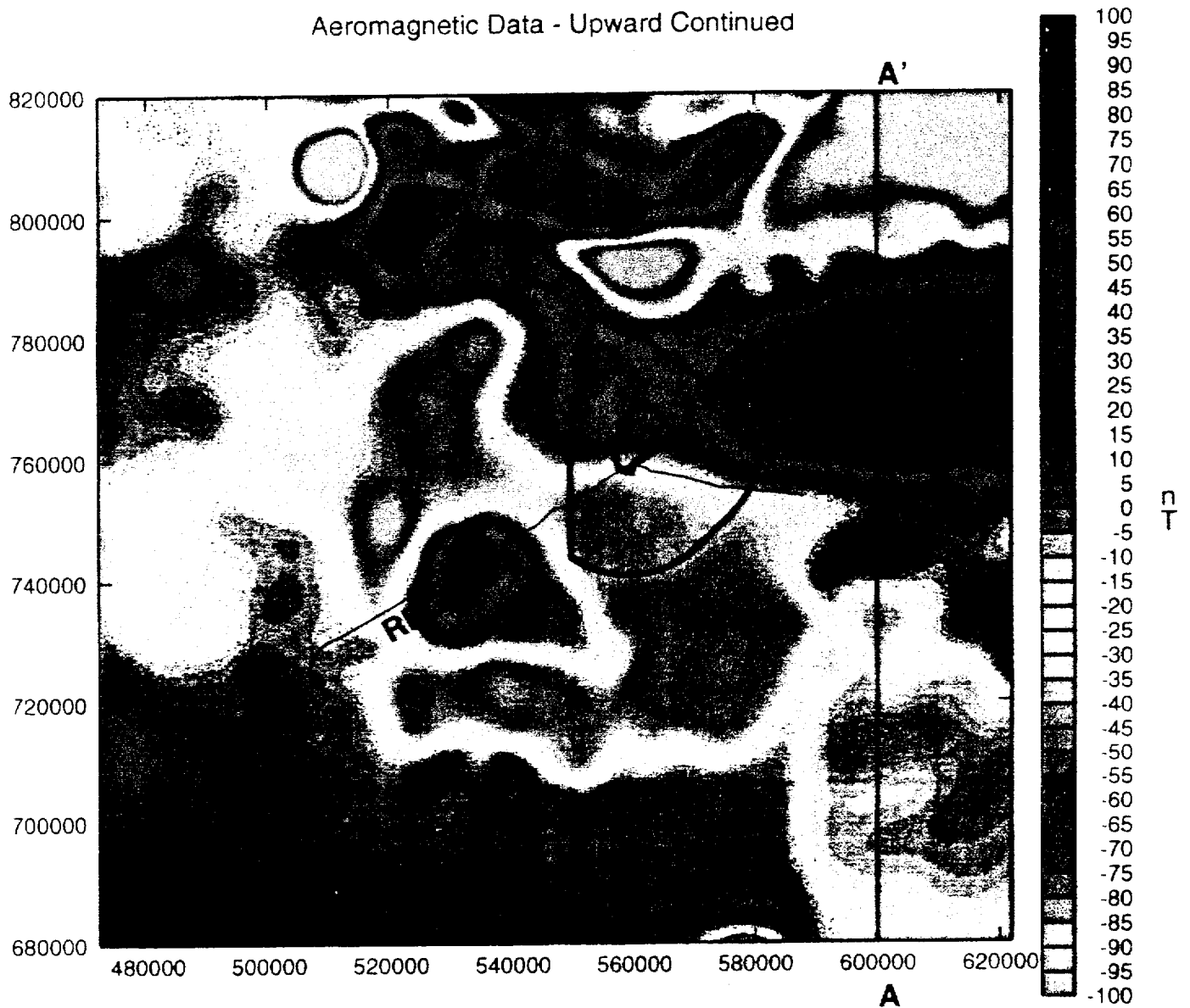


Figure 4. The upward continuation of the magnetic field in Figure 3 to 5000 feet above topography. This was done to eliminate high frequency signals. Coordinates are in Nevada State Plane feet.

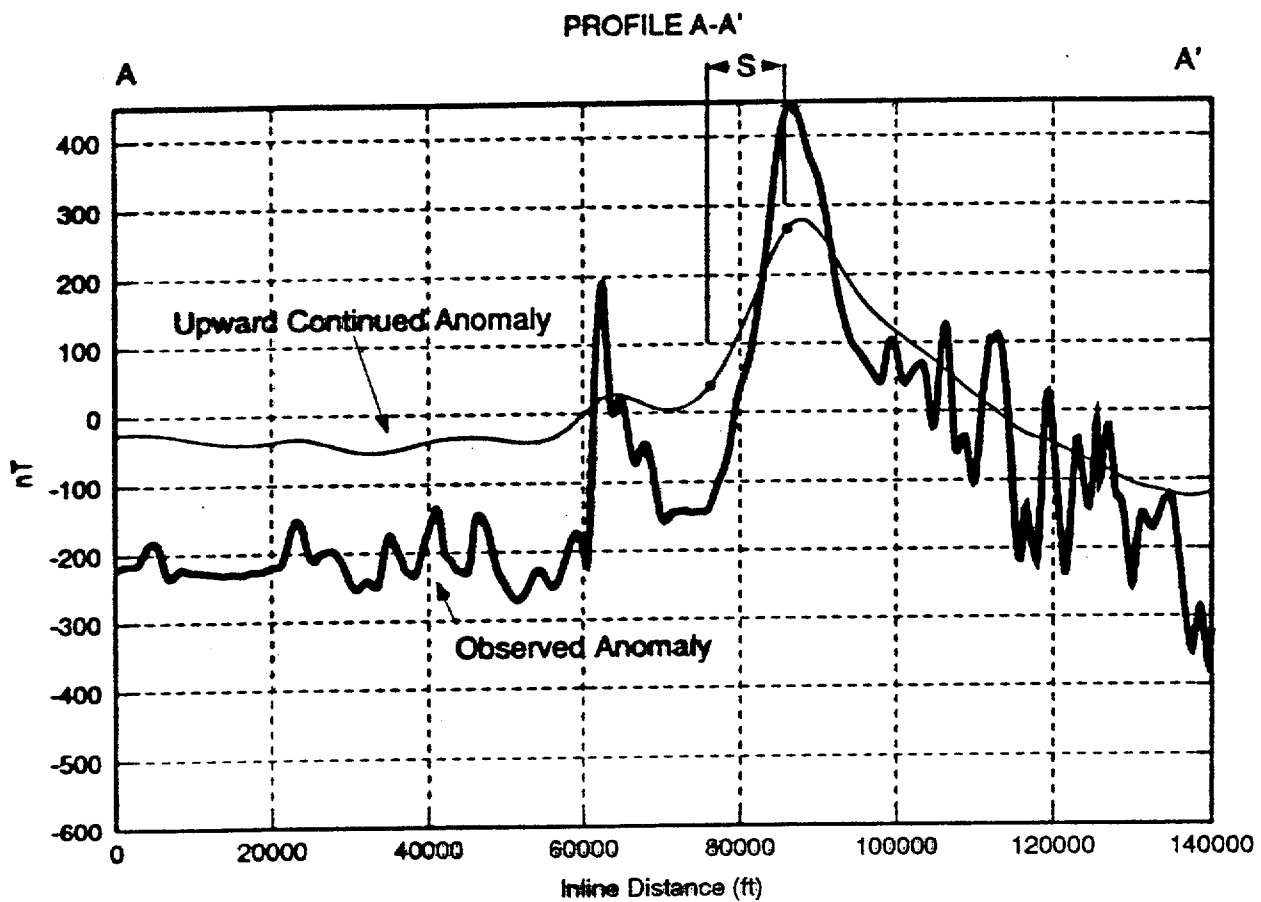


Figure 6. The magnetic anomalies along Profile A-A'. The half-slope width, S, can be used to estimate the depth of the magnetic body.

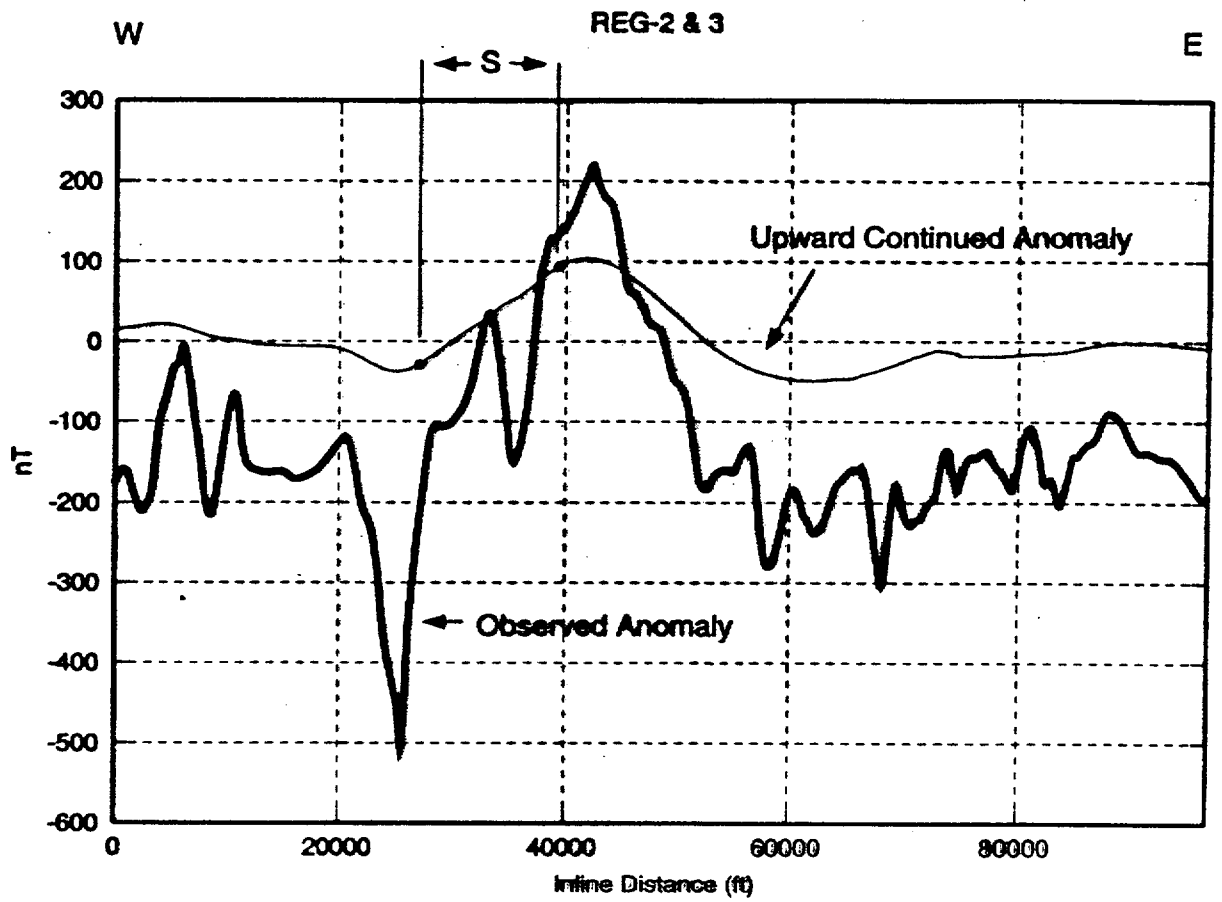


Figure 5. The magnetic anomalies along Profile REG-2 & 3. The half-slope width, S , can be used to estimate the depth of the magnetic body.

Enlarged Aeromagnetic Data with Fault Overlay



Figure 2. An enlarged section of Figure 1, with faults from Sawyer et al. (1995) overlain as white lines. Coordinates are in Nevada State Plane feet.

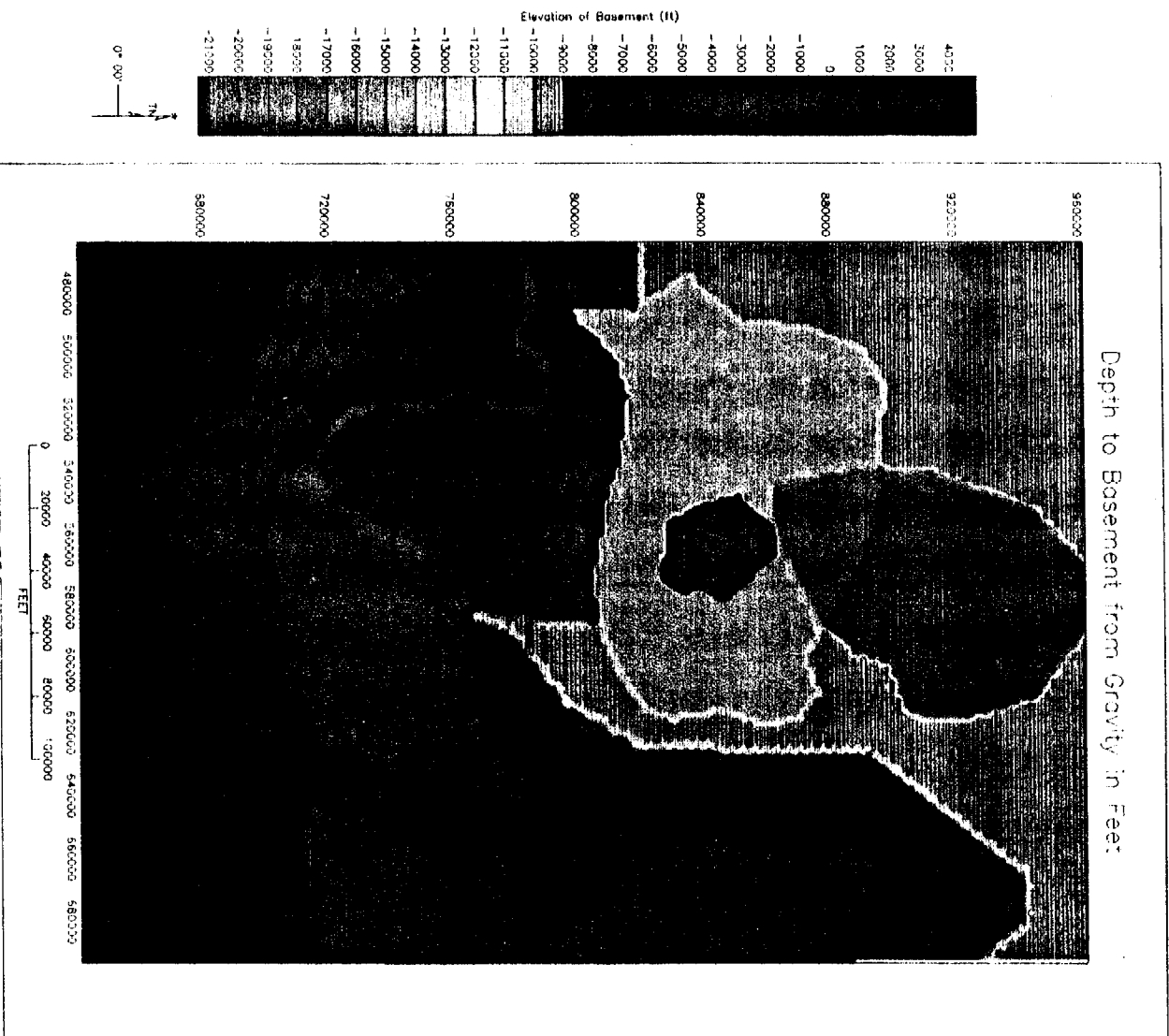


Figure 85A. Plan view of basement structure derived from gravity data. Elevation is given in feet.

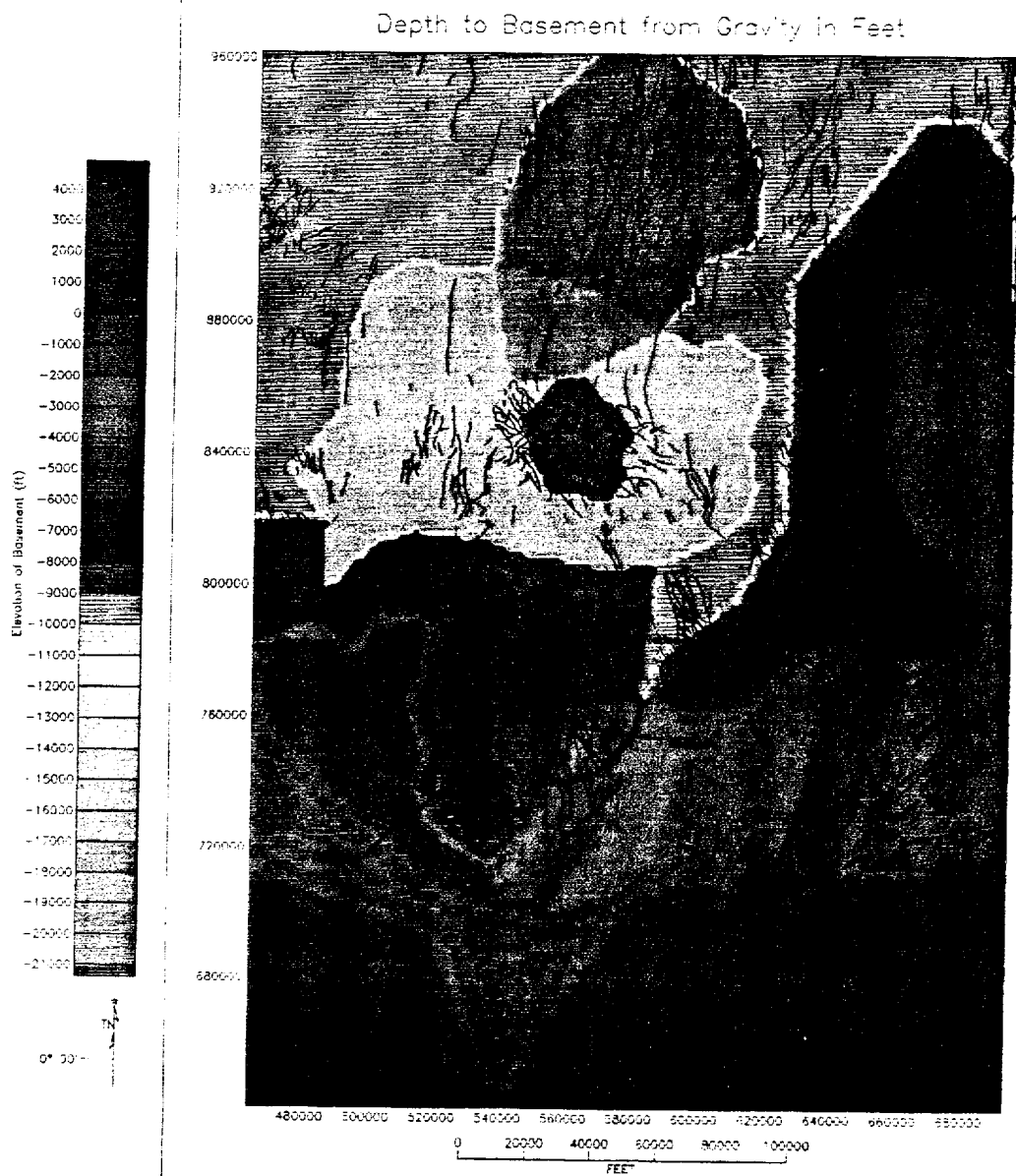


Figure 101. Plan view of basement structure derived from gravity data. Elevation is given in feet. Dark areas are paleozoic outcrops, the black lines are faults (geologic data are from Sawyer et al. 1995). The black dots in the Rock Valley area are epicenter locations of aftershocks from the Little Skull Mountain earthquake.

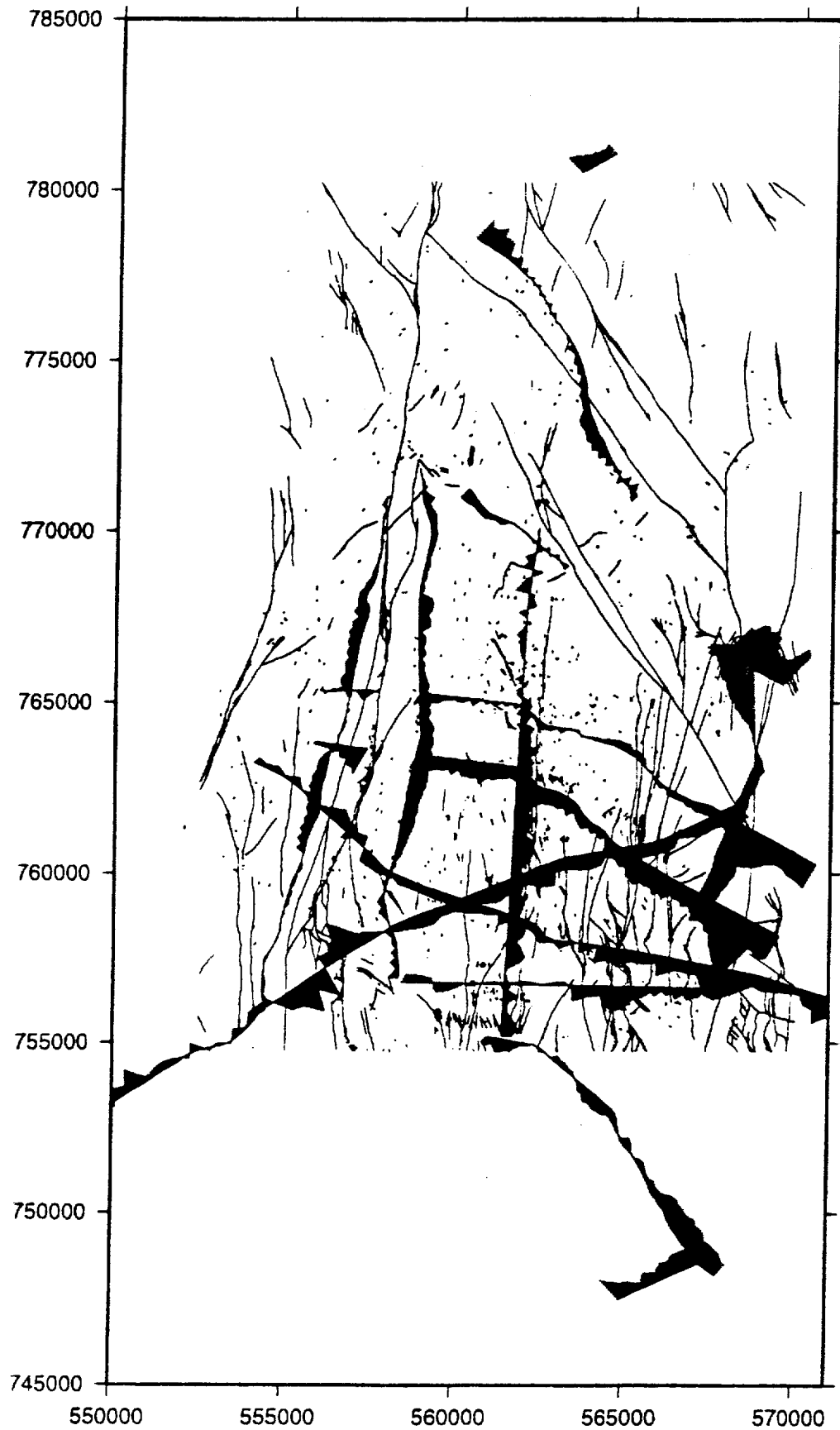


Figure 100. Repository residual gravity lines shown as wiggle lines along track where one inch equals 5 mGals. The red areas are negative values and the blue areas are positive values. Faults from Day et al. (1996).

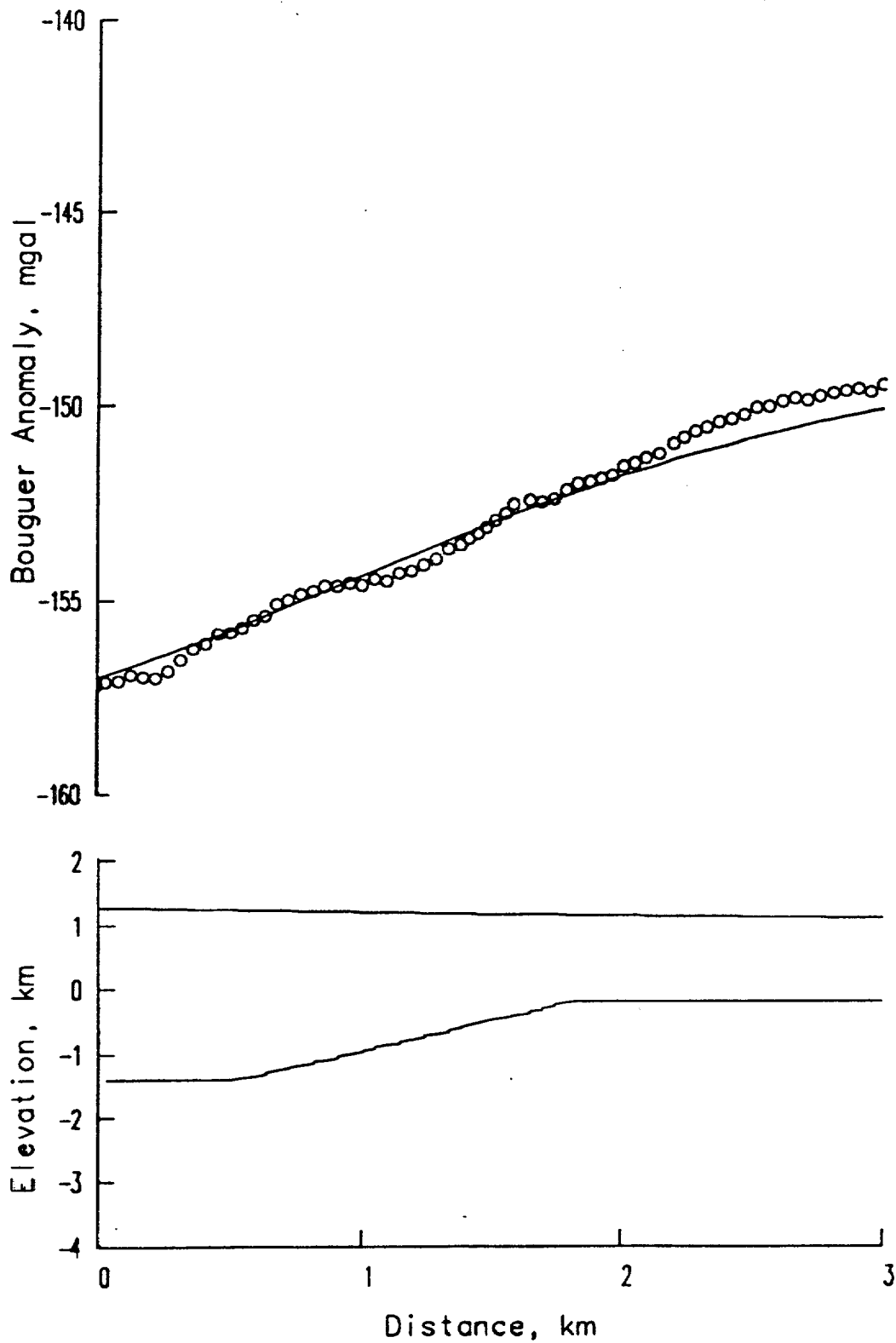


Figure 72. Cross section along repository line YMP-1. The lower panel shows the surface elevation and the contact between sedimentary rocks and the underlying basement rocks: The upper panel shows the Bouguer gravity anomalies, with the circles being the observed data and the continuous curve connecting the values calculated from the regional density model. This line runs from northwest to southeast, with northwest being on the left.

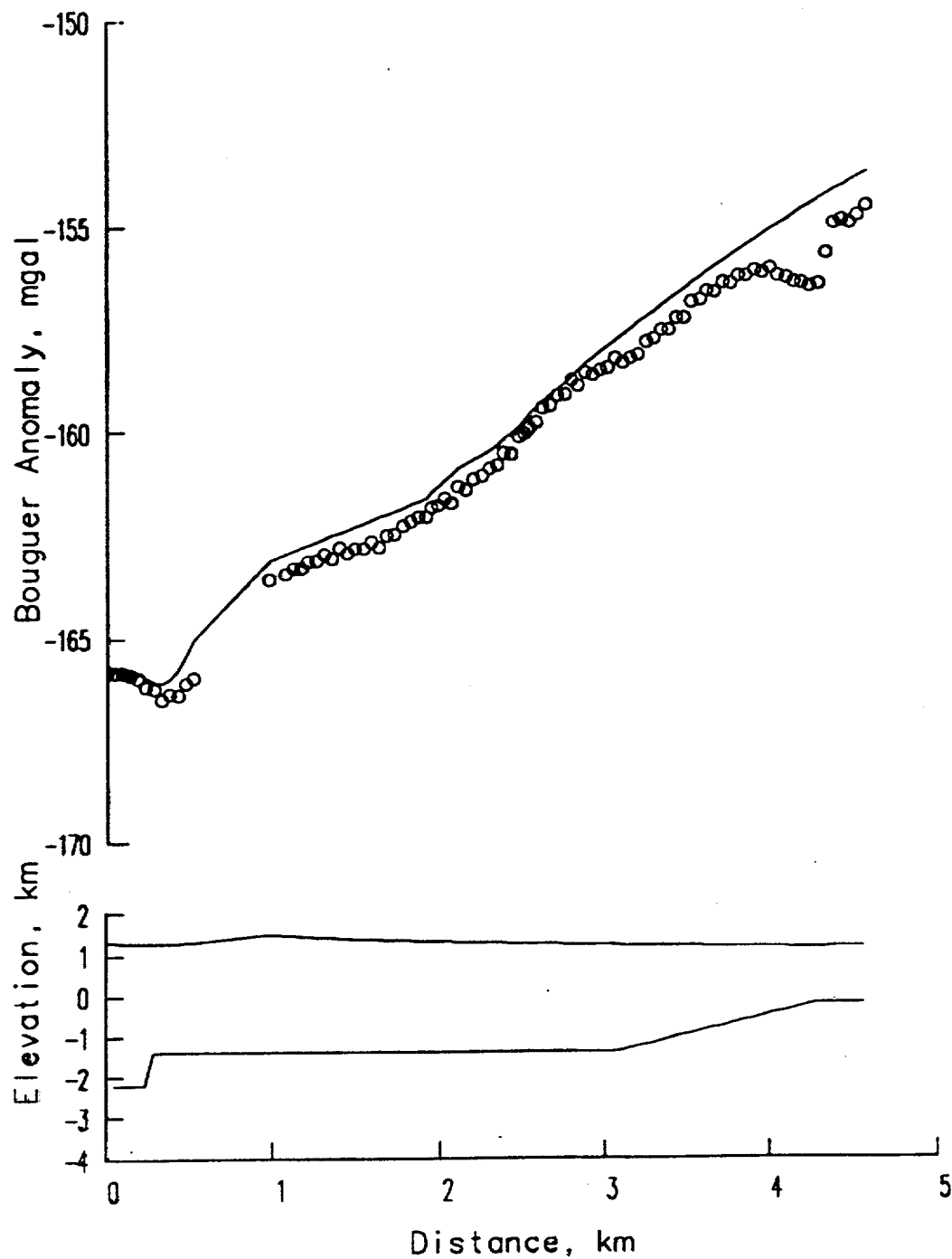


Figure 75. Cross section along repository line YMP-3. The lower panel shows the surface elevation and the contact between sedimentary rocks and the underlying basement rocks. The upper panel shows the Bouguer gravity anomalies, with the circles being the observed data and the continuous curve connecting the values calculated from the regional density model. This line runs from west to east, with west being on the left.

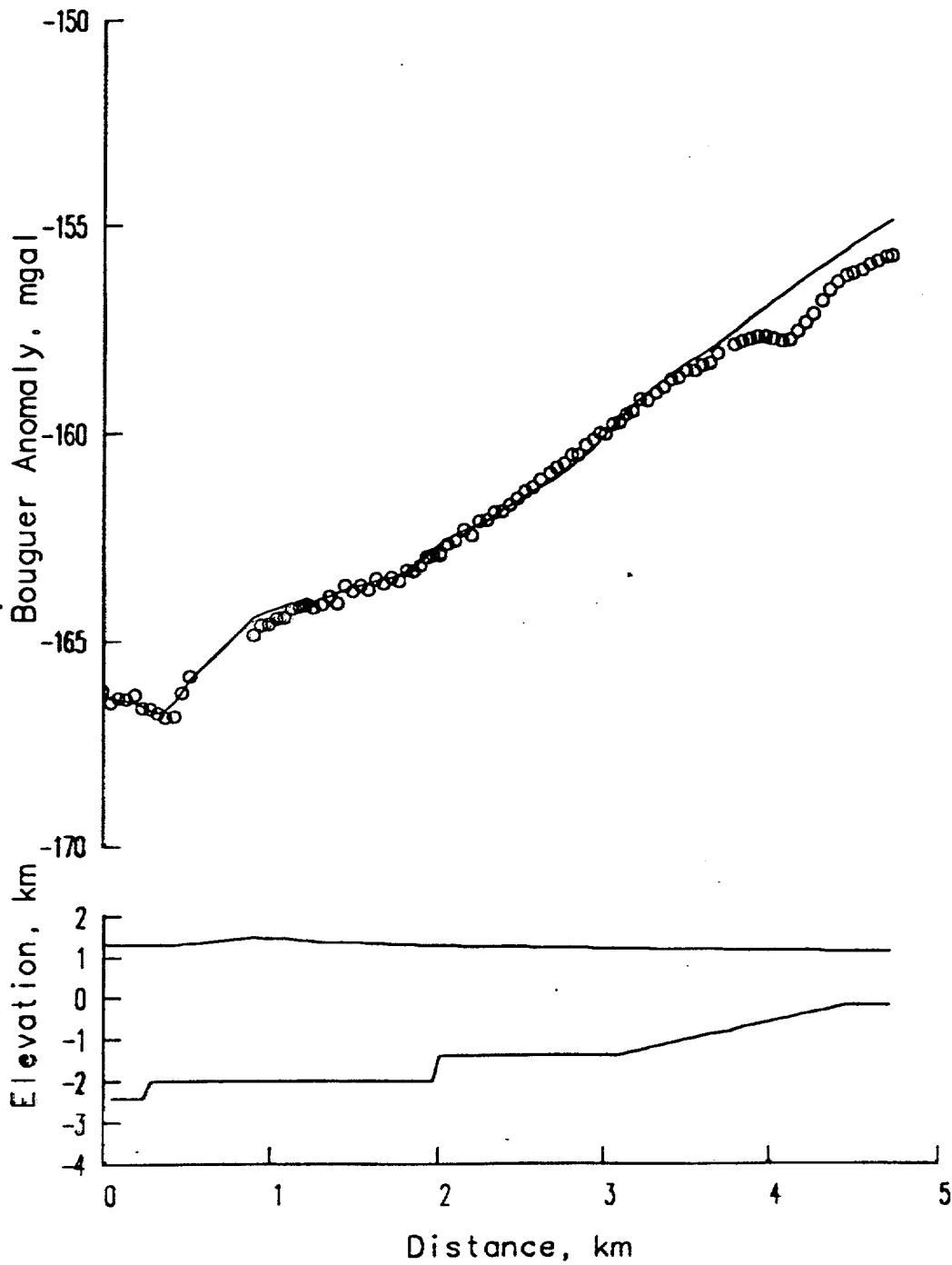


Figure 76. Cross section along repository line YMP-4. The lower panel shows the surface elevation and the contact between sedimentary rocks and the underlying basement rocks. The upper panel shows the Bouguer gravity anomalies, with the circles being the observed data and the continuous curve connecting the values calculated from the regional density model. This line runs from west to east, with west being on the left.

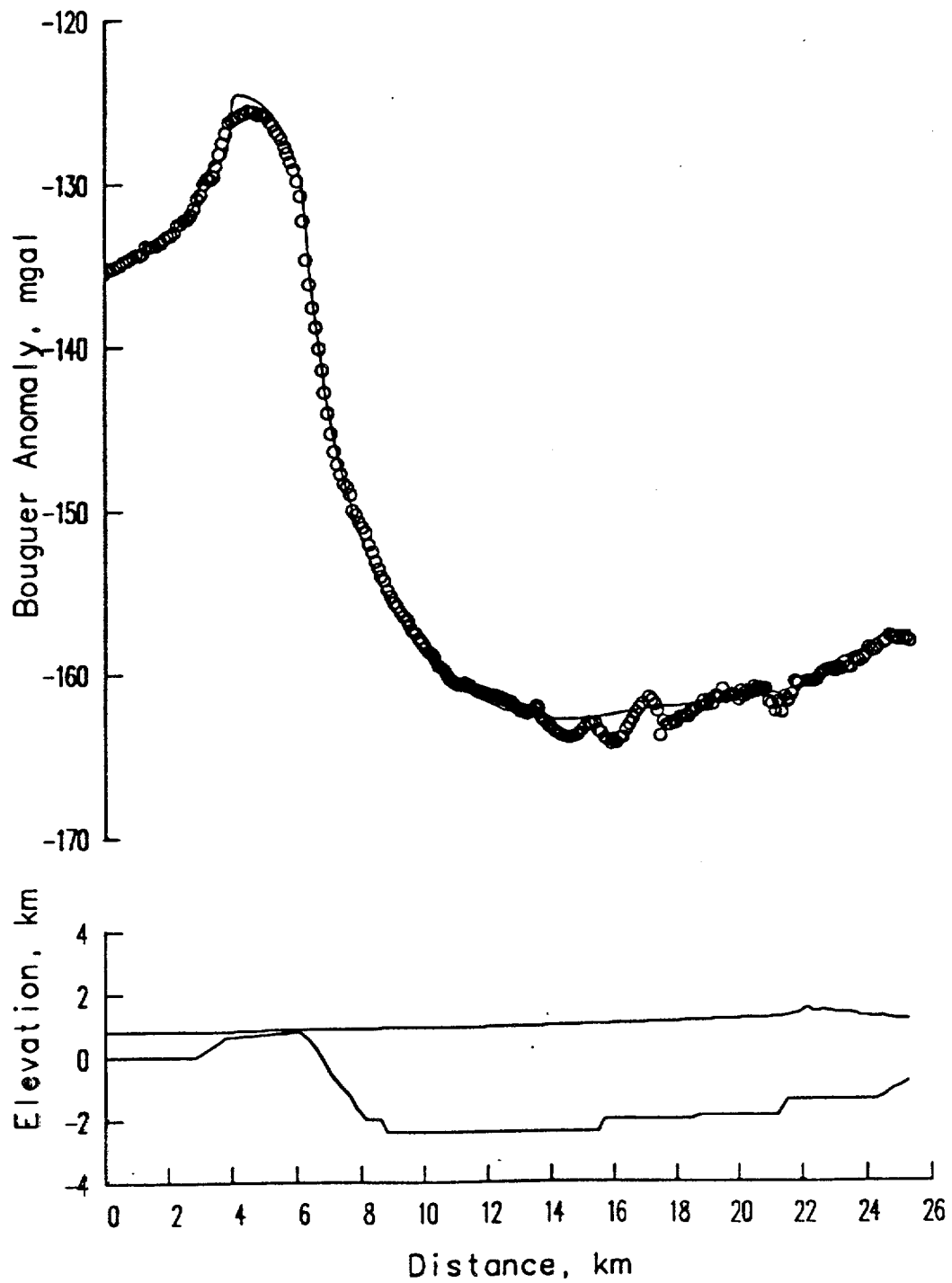


Figure 68. Cross section along regional line REG-2. The lower panel shows the surface elevation and the contact between sedimentary rocks and the underlying basement rocks. The upper panel shows the Bouguer gravity anomalies, with the circles being the observed data and the continuous curve connecting the values calculated from the regional density model. This line runs from west to east, with west being on the left.

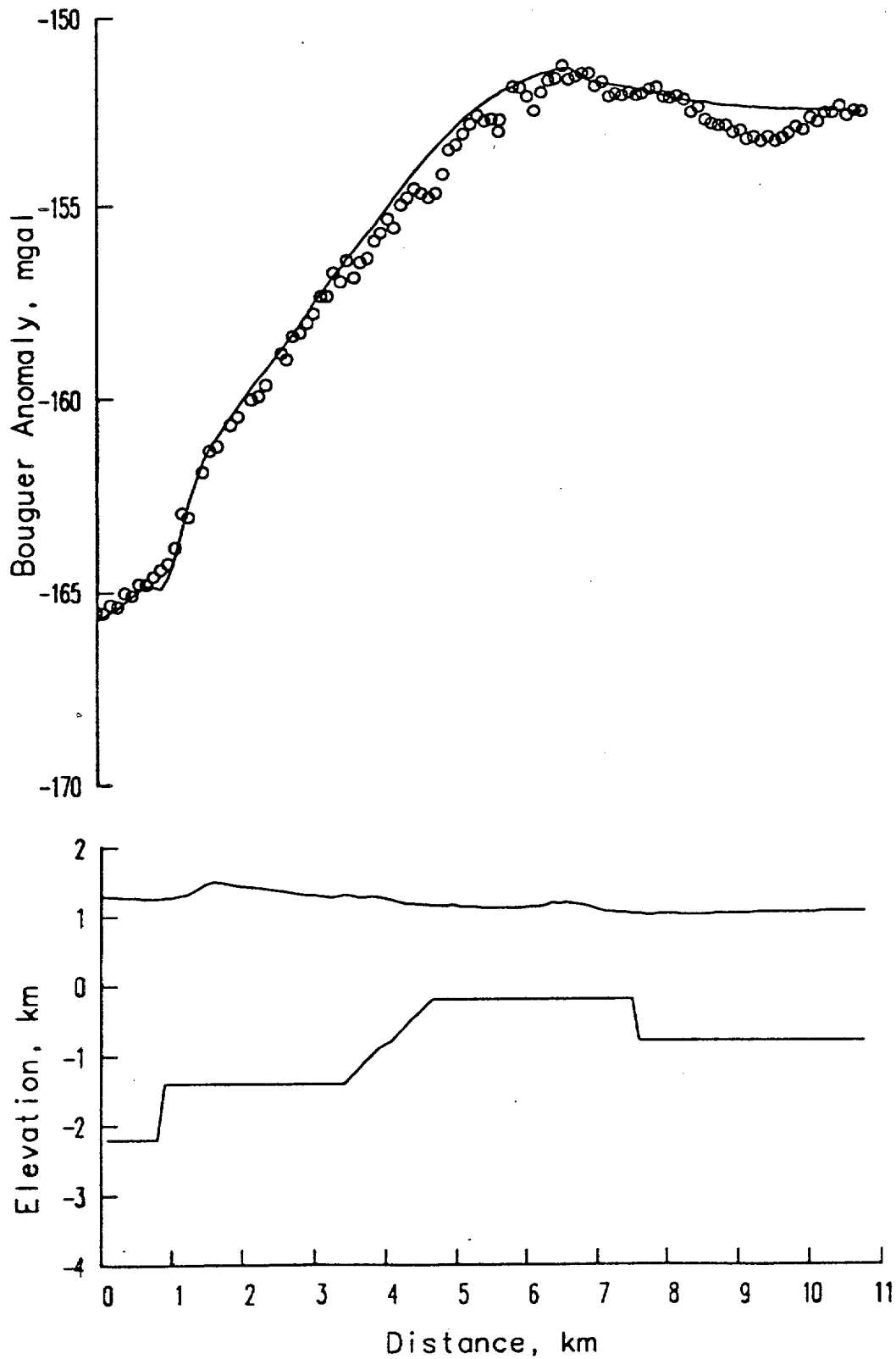


Figure 69. Cross section along regional line REG-3. The lower panel shows the surface elevation and the contact between sedimentary rocks and the underlying basement rocks. The upper panel shows the Bouguer gravity anomalies, with the circles being the observed data and the continuous curve connecting the values calculated from the regional density model. This line runs from west to east, with west being on the left.

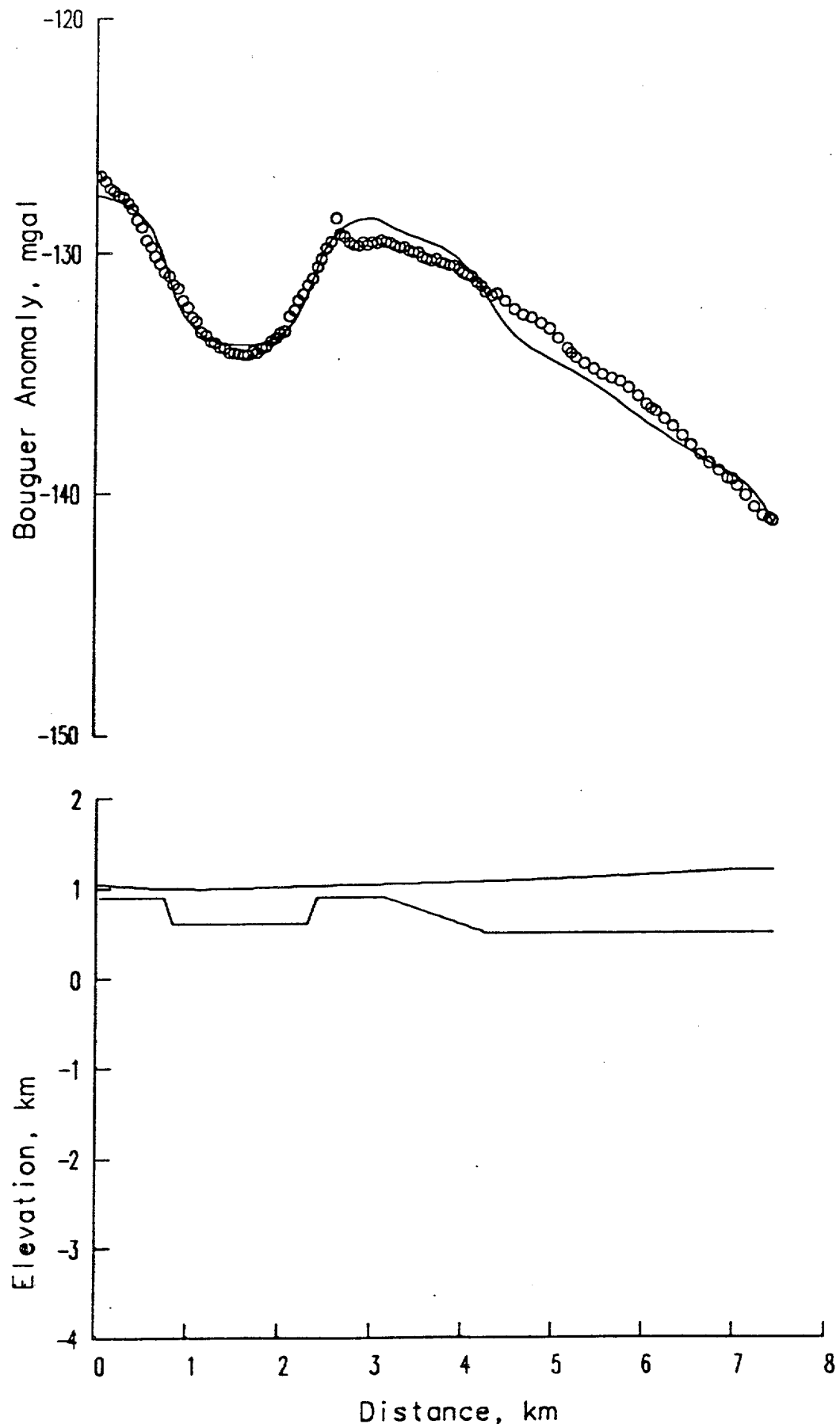


Figure 70. Cross section along regional line RV-2. The lower panel shows the surface elevation and the contact between sedimentary rocks and the underlying basement rocks. The upper panel shows the Bouguer gravity anomalies, with the circles being the observed data and the continuous curve connecting the values calculated from the regional density model. This line runs from south to north, with south being on the left.

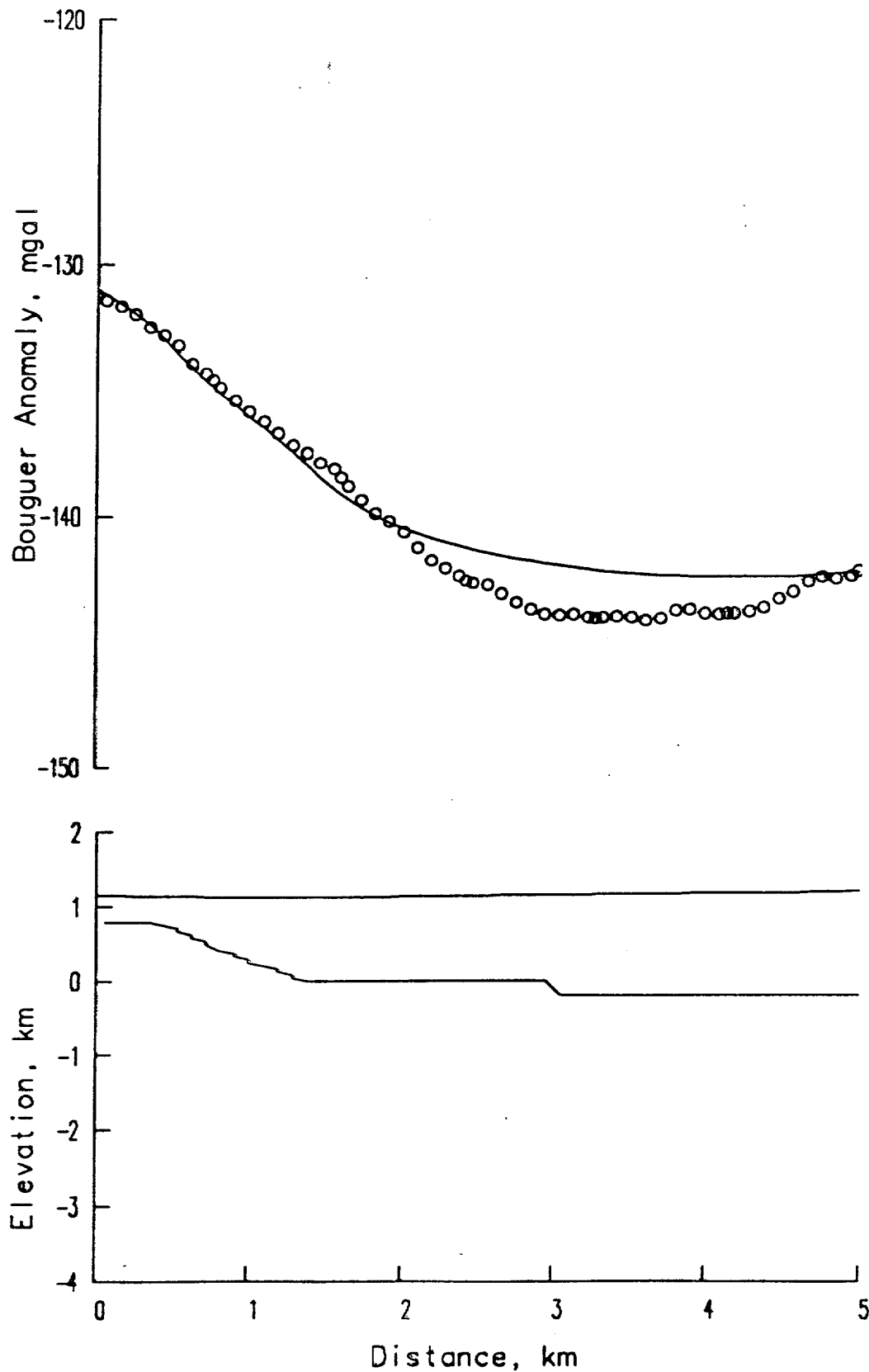


Figure 71. Cross section along regional line RV-1. The lower panel shows the surface elevation and the contact between sedimentary rocks and the underlying basement rocks. The upper panel shows the Bouguer gravity anomalies, with the circles being the observed data and the continuous curve connecting the values calculated from the regional density model. This line runs from south to north, with south being on the left.

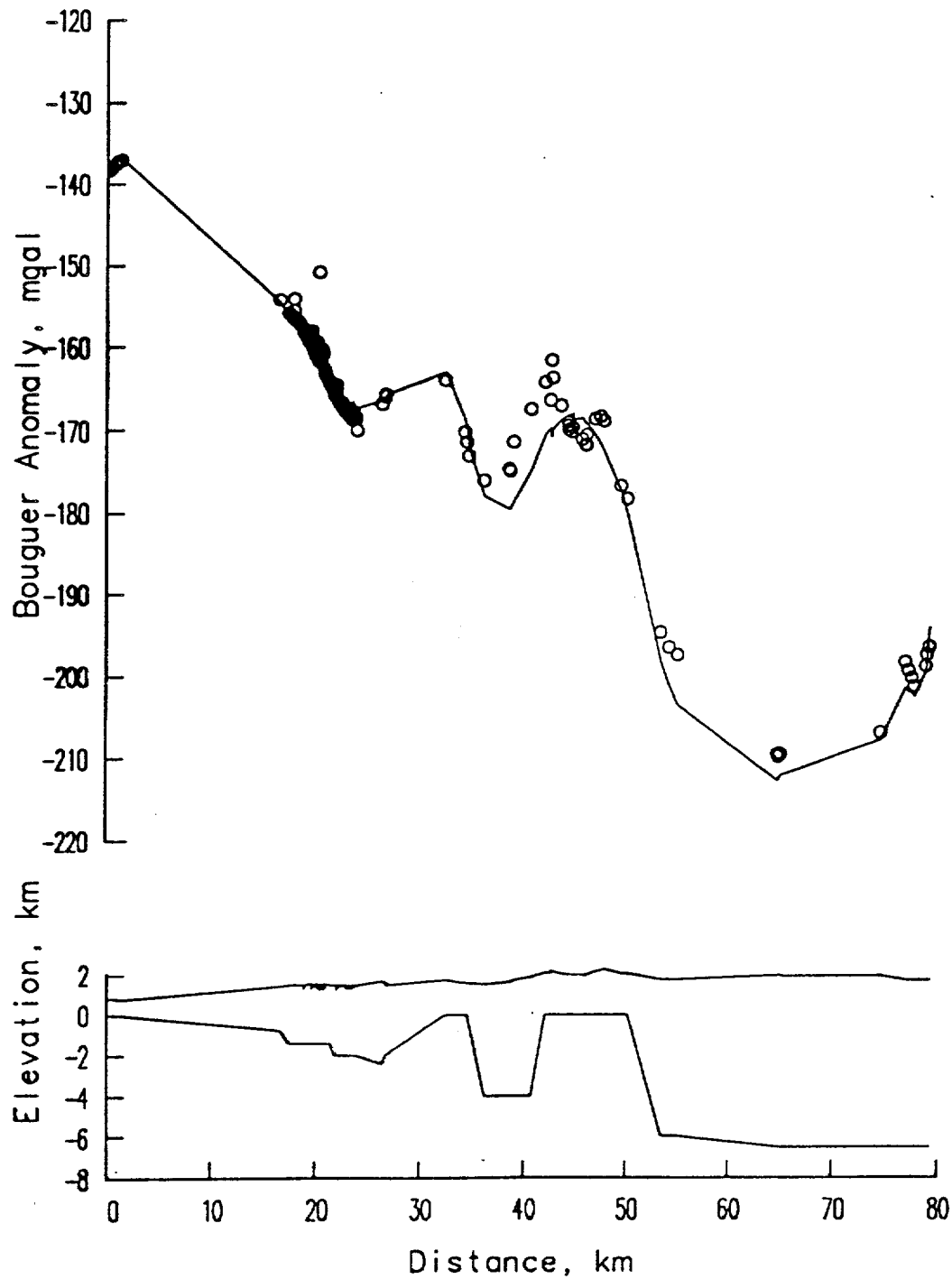


Figure 66. Cross section along the longitude line -116.46 degrees. The lower panel shows the surface elevation and the contact between sedimentary rocks and the underlying basement rocks. The upper panel shows the Bouguer gravity anomalies, with the circles being the observed data and the continuous curve connecting the values calculated from the regional density model. This line runs from south to north, with south being on the left.

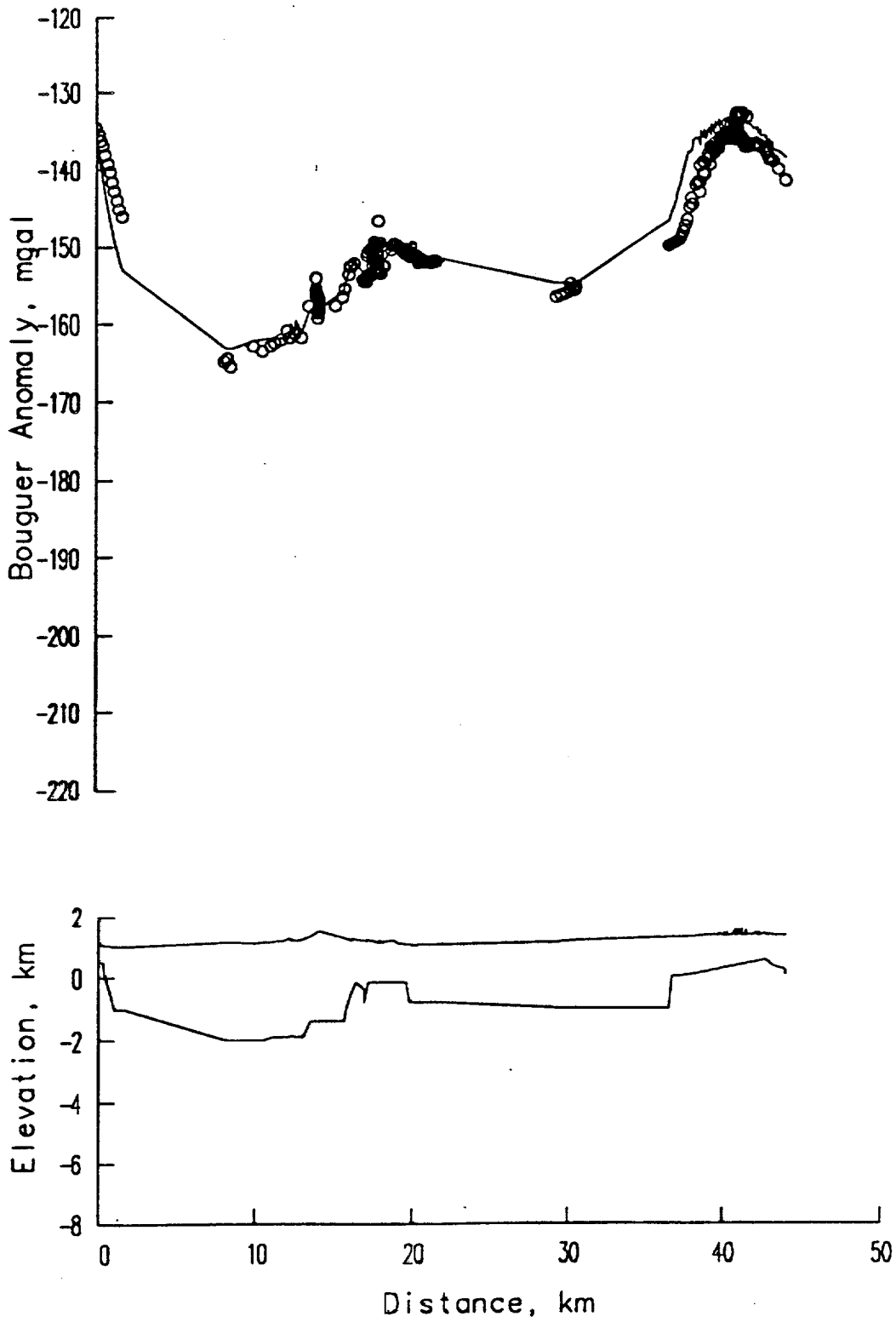


Figure 67. Cross section along the latitude line 36.82 degrees. The lower panel shows the surface elevation and the contact between sedimentary rocks and the underlying basement rocks. The upper panel shows the Bouguer gravity anomalies, with the circles being the observed data and the continuous curve connecting the values calculated from the regional density model. This line runs from west to east, with west being on the left.

TIME	VRHS										
0	3699	0	3699	0	3699	0	3699	0	3699	0	3699
121	4215	240	4835	240	4835	240	4835	240	4835	240	4835
480	5882	480	5882	1800	6874	1800	6874	1800	6874	1800	6874
838	7886	838	7886	1900	11872	1900	11872	1900	11872	1900	11872
1999	11872	1999	11872								

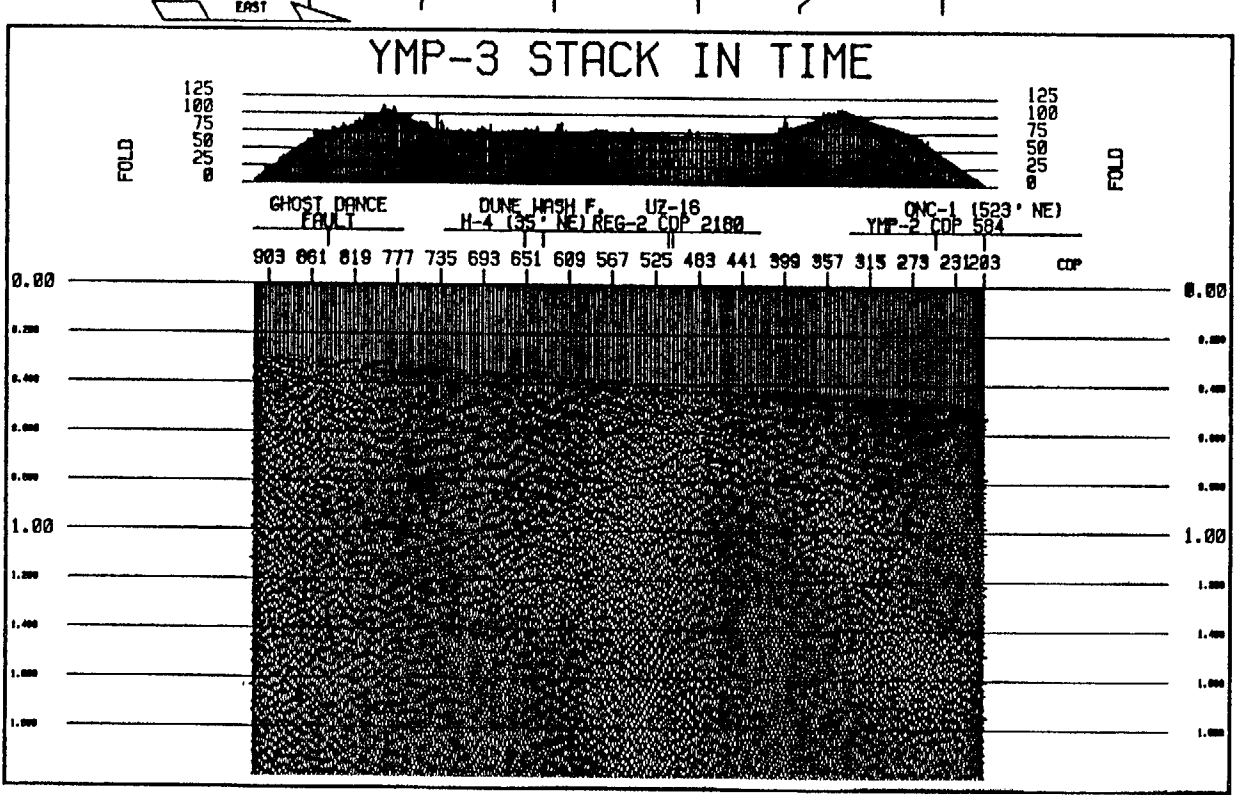
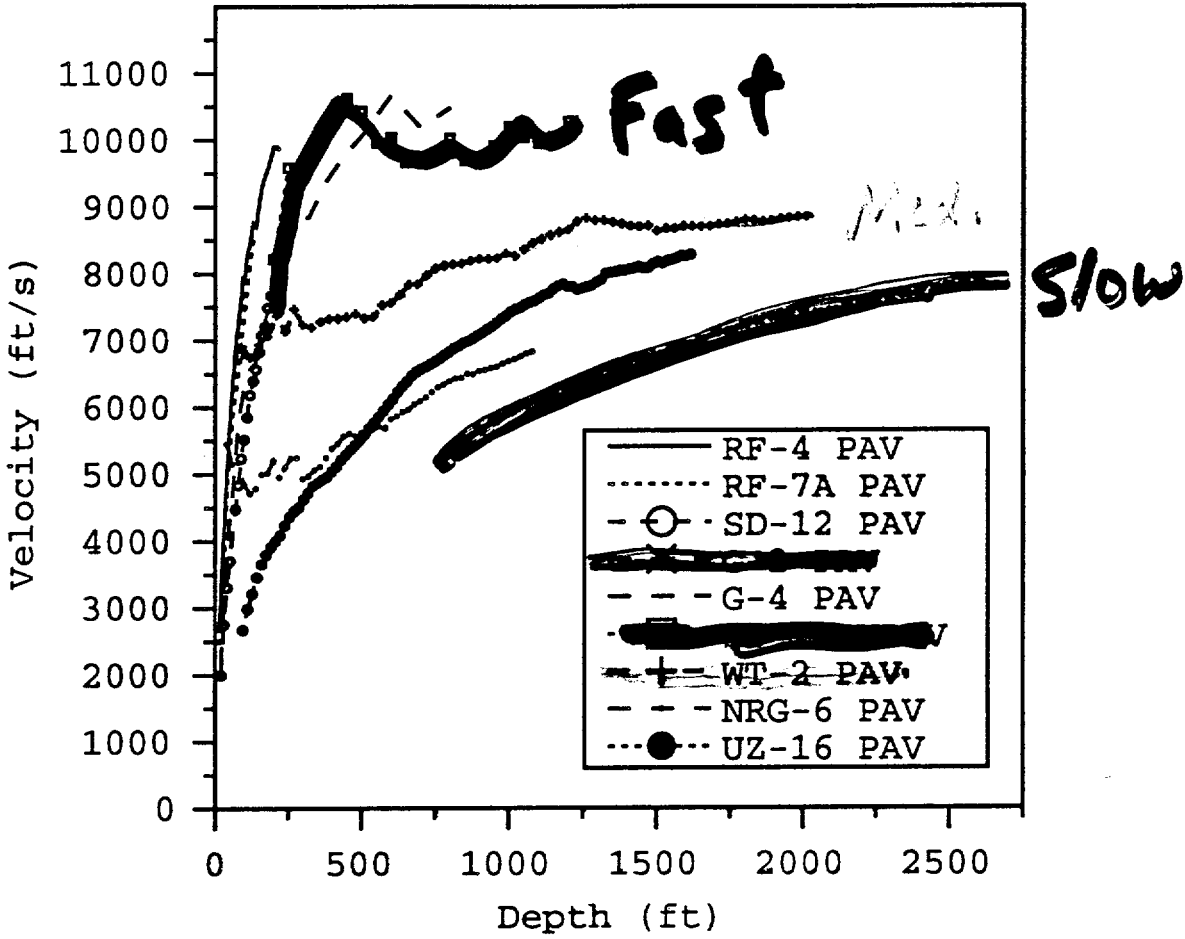


Figure 15a. YMP-3 stack in time with stacking velocities shown at top.

YMP - LBNL
P-Wave Seismic Velocity
Average Velocity from VSP



WT-2 VSP TWO-WAY TIME REFLECTIVITY

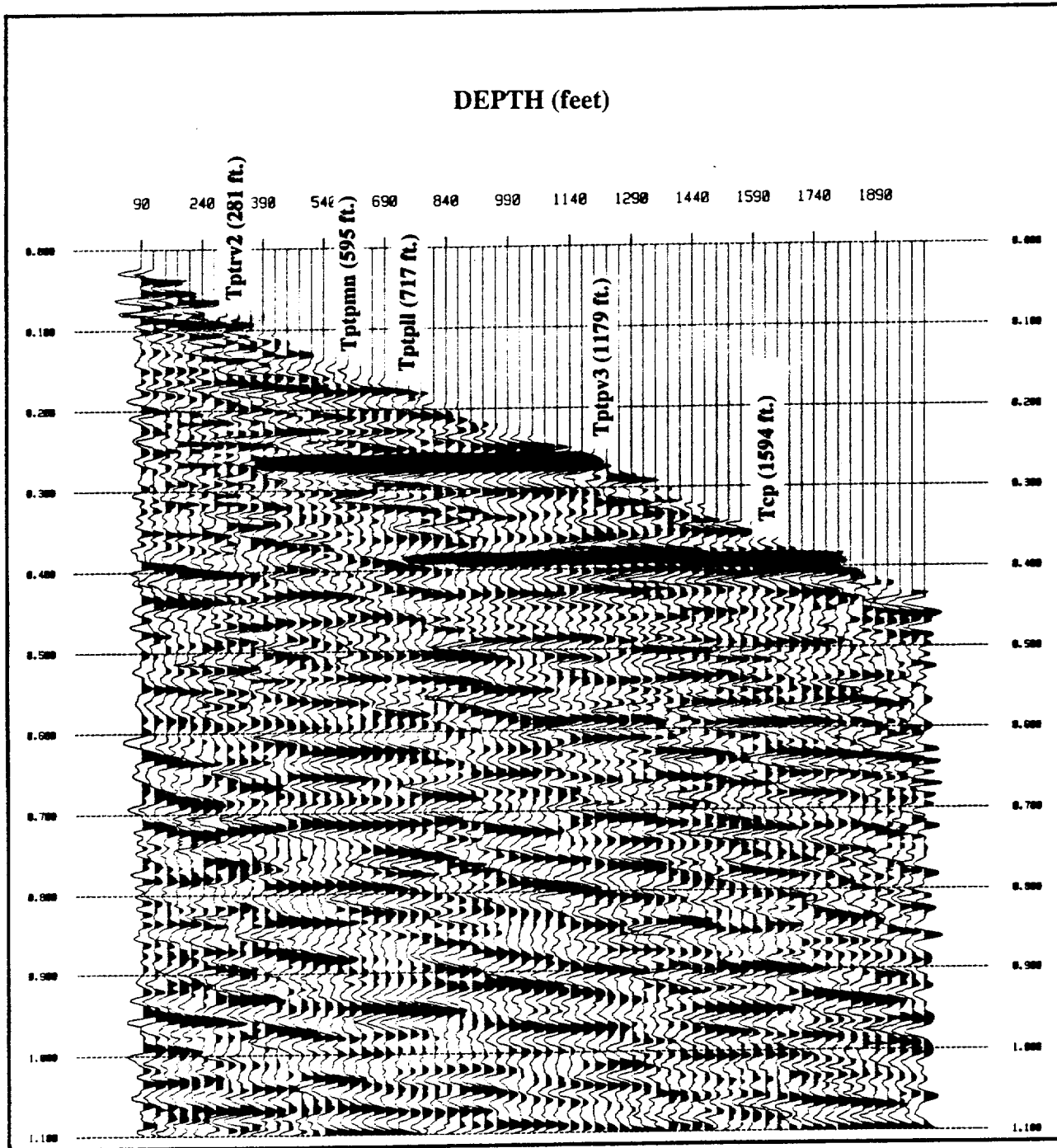


Figure 34a. Two way travel time as observed in WT-2 (one way times two) with the observed lithology marked on the VSP data. The data were not available to correlate the depths to the Tcb horizon, therefore for reference the Tcp was marked on the VSP profile.

UZ-16 VSP TWO-WAY TIME REFLECTIVITY

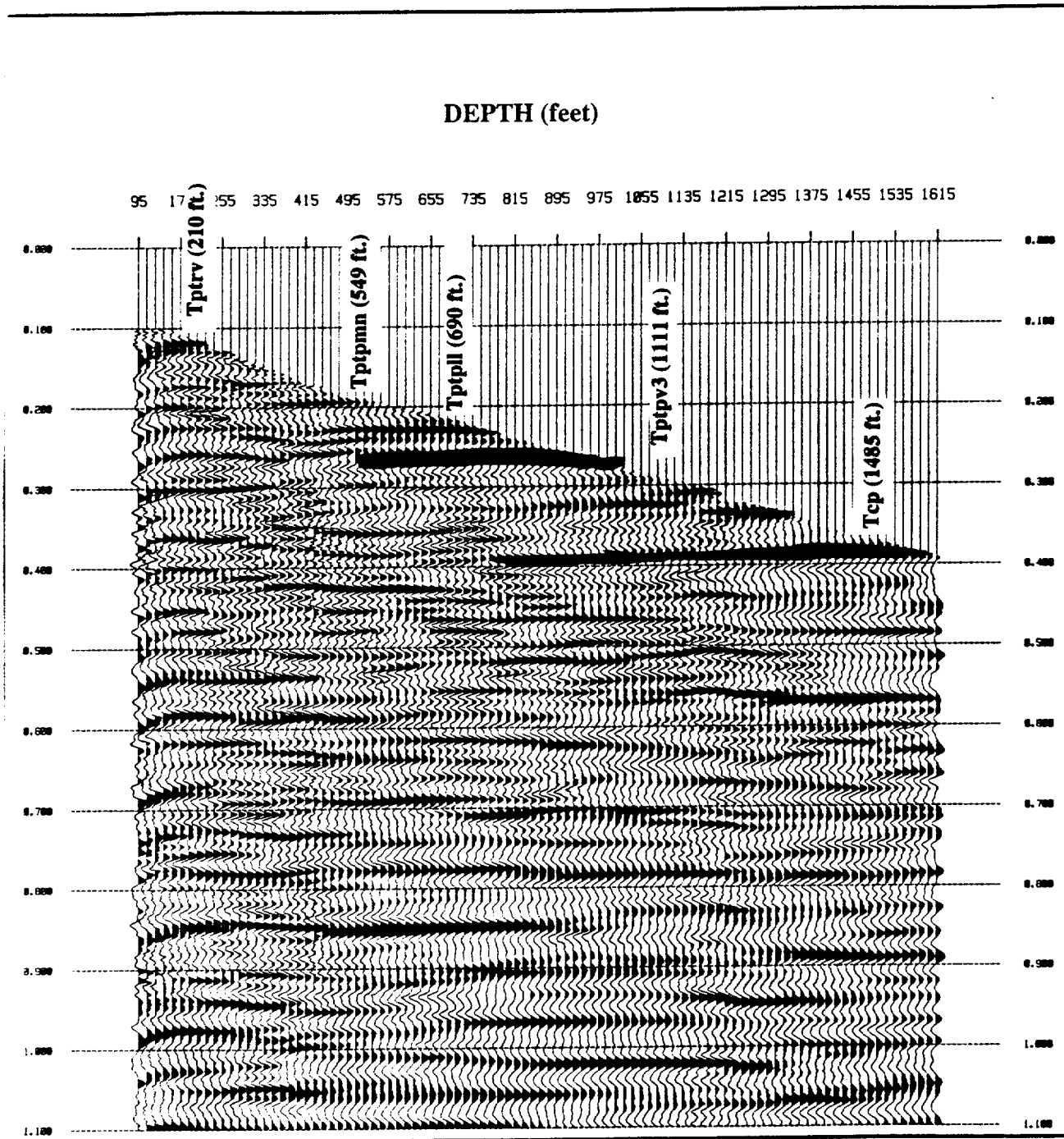


Figure 34b. Two way travel time as observed in UZ-16 (one way times two) with the observed lithology marked on the VSP data. The data were not available to correlate the depths to the Tcb horizon, therefore for reference the Tcb was marked on the VSP profile.

UZ16: Total porosity from log data

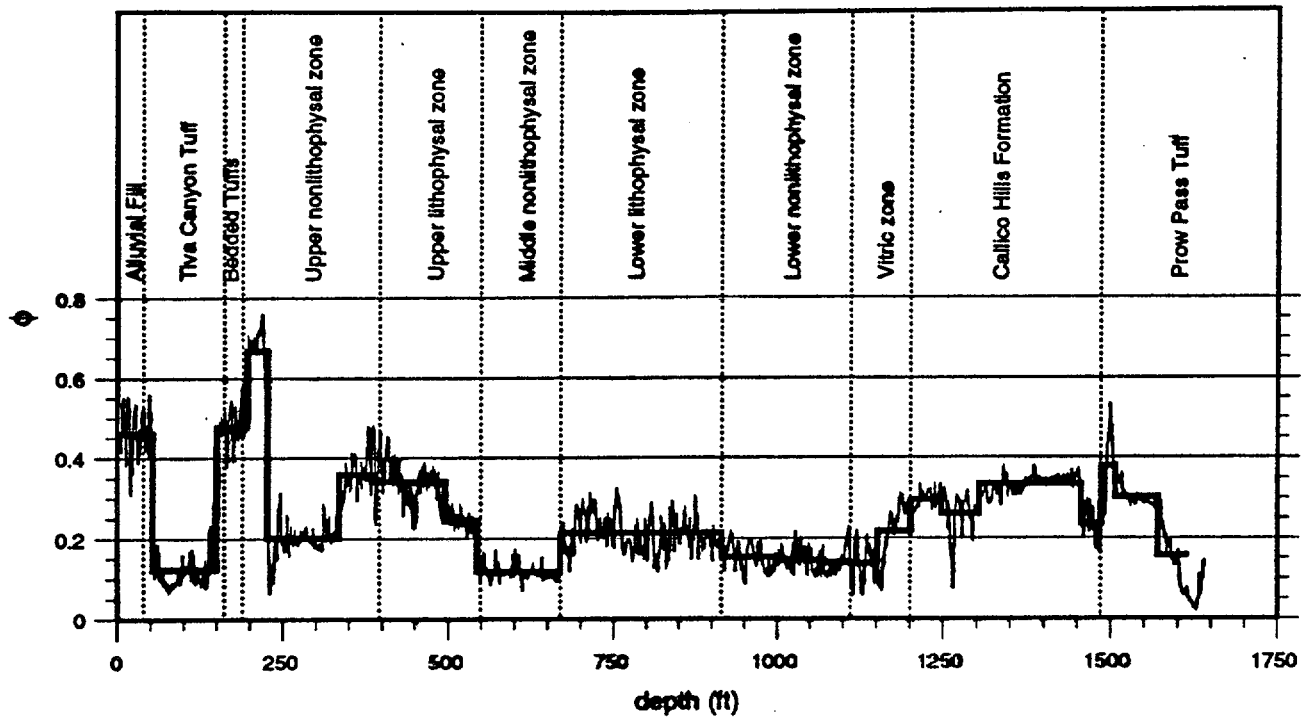


Fig. 4a Total porosity from the well log data in UZ 16.

UZ16: Total water saturation from log data

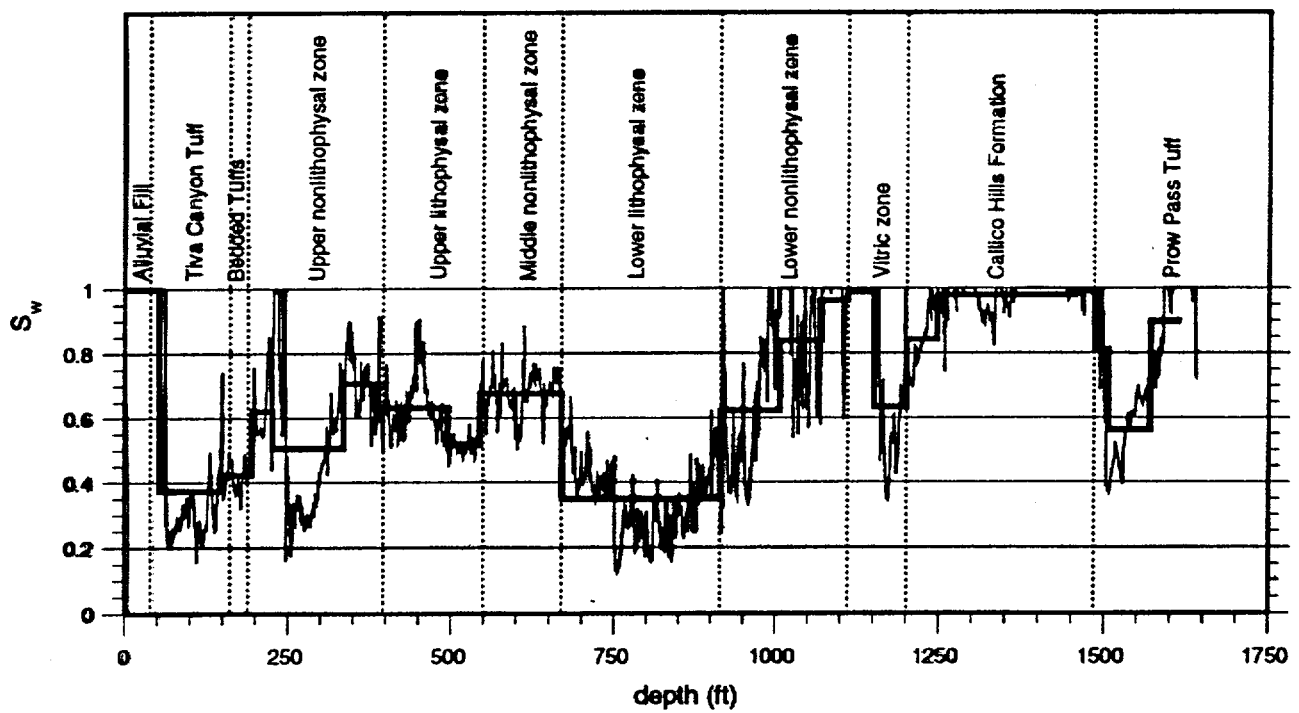


Fig. 4b Total water saturation from the well log data in UZ 16.

UZ16: Synthetic velocity profile with corrected porosities

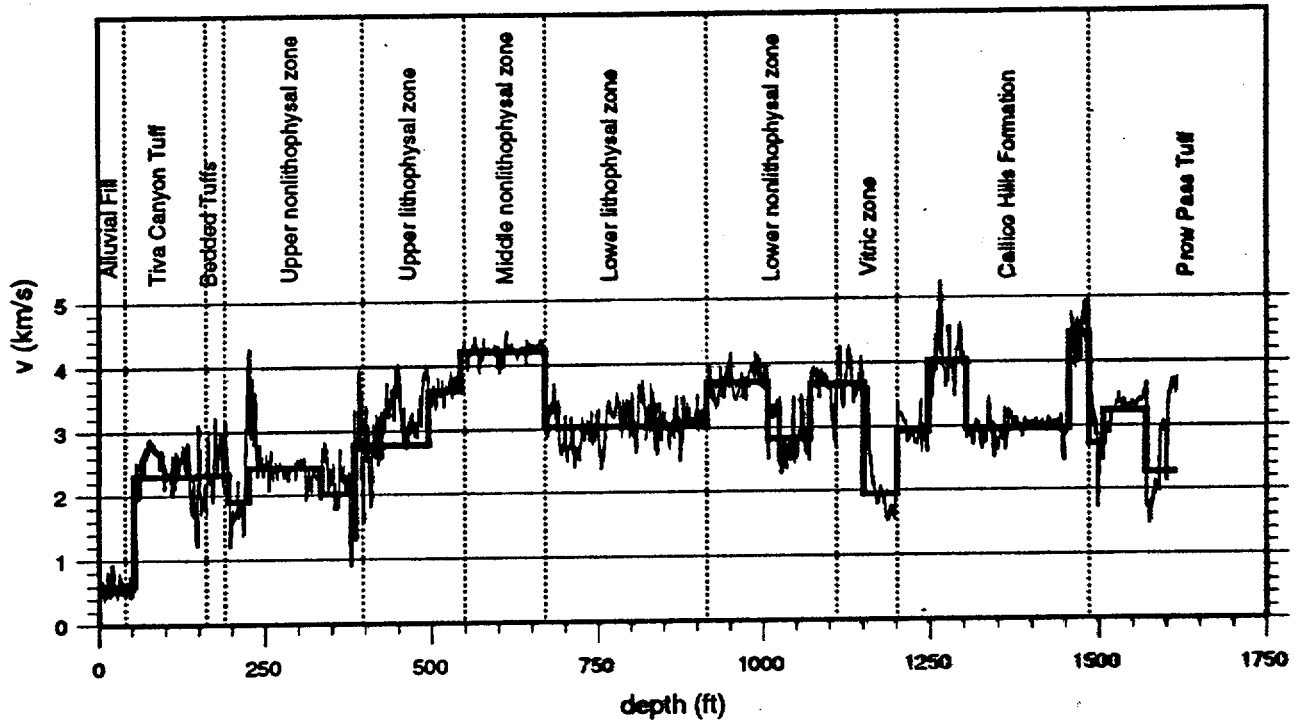


Fig. 8 Velocity profile computed with the corrected porosity values in the bedded tuffs and at the top of the Prow Pass Tuff.

UZ16: Bulk density from log data

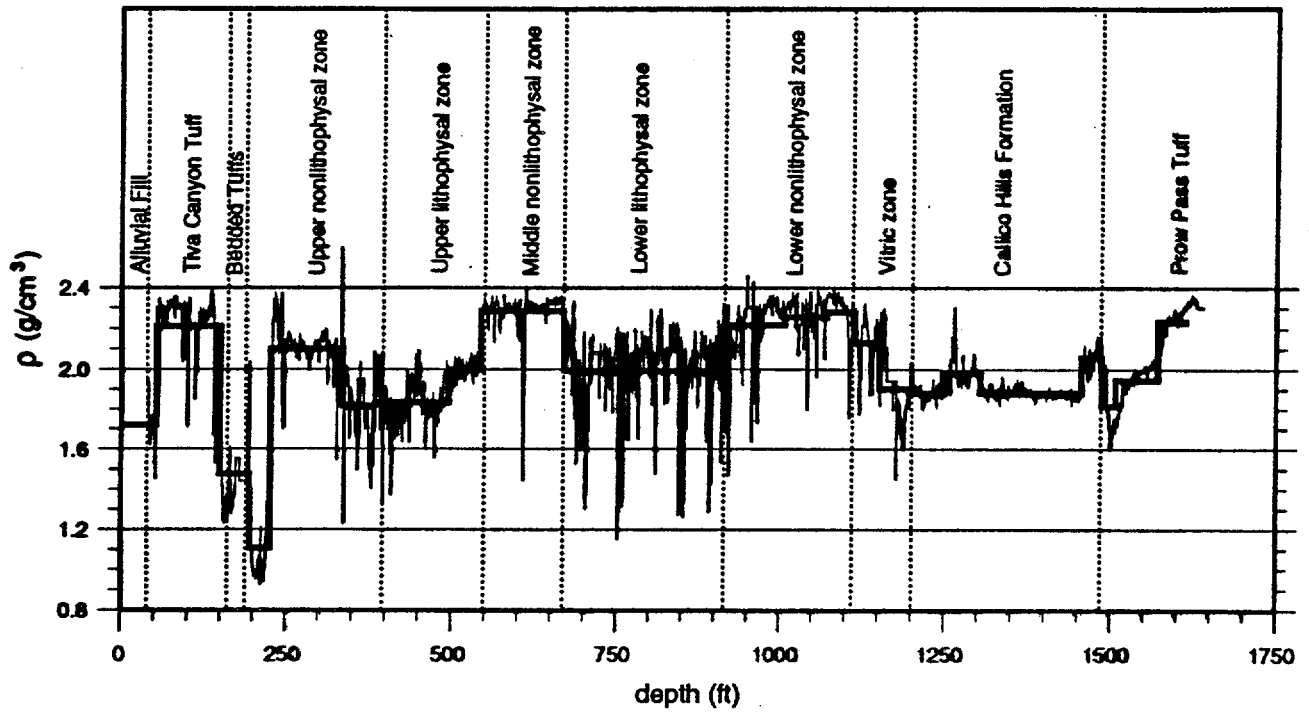


Fig. 4c Bulk density from the well log data in UZ 16.

UZ16: Interval velocities derived from VSP data

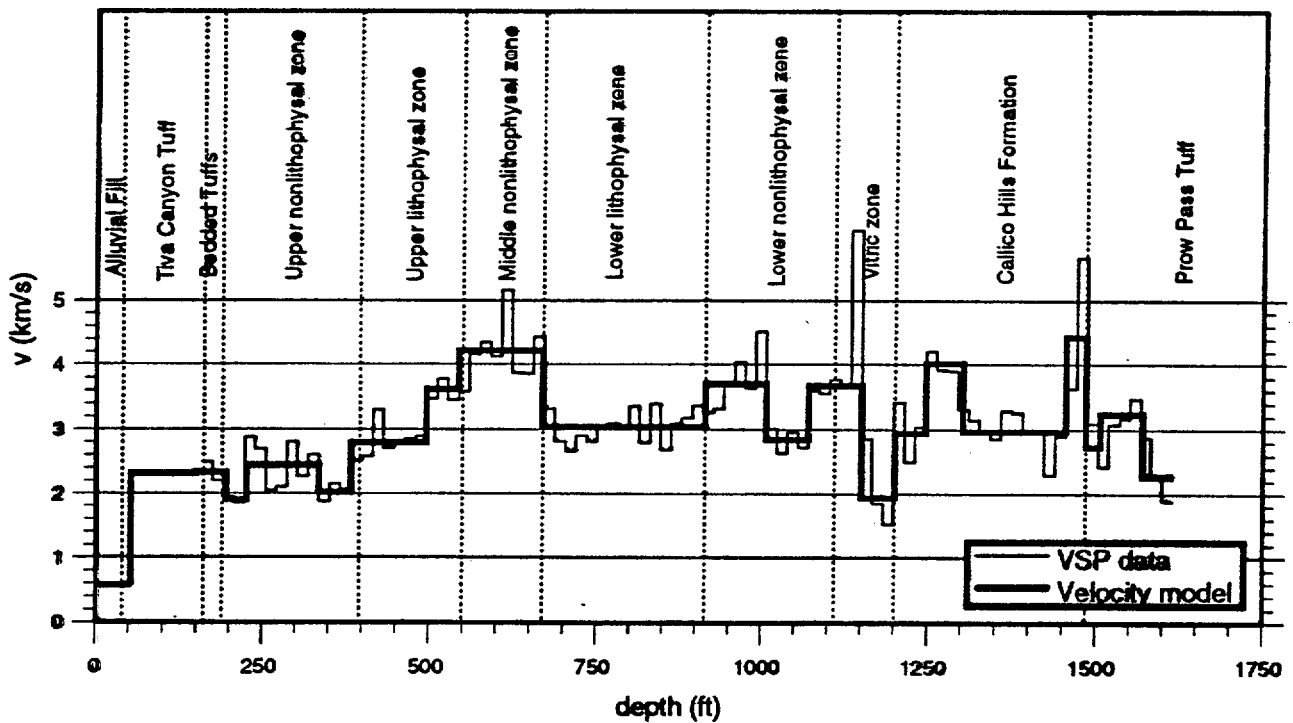


Fig. 5 Interval velocities derived from the VSP data in UZ 16.

UZ16: Reflected P-wave with the original log data

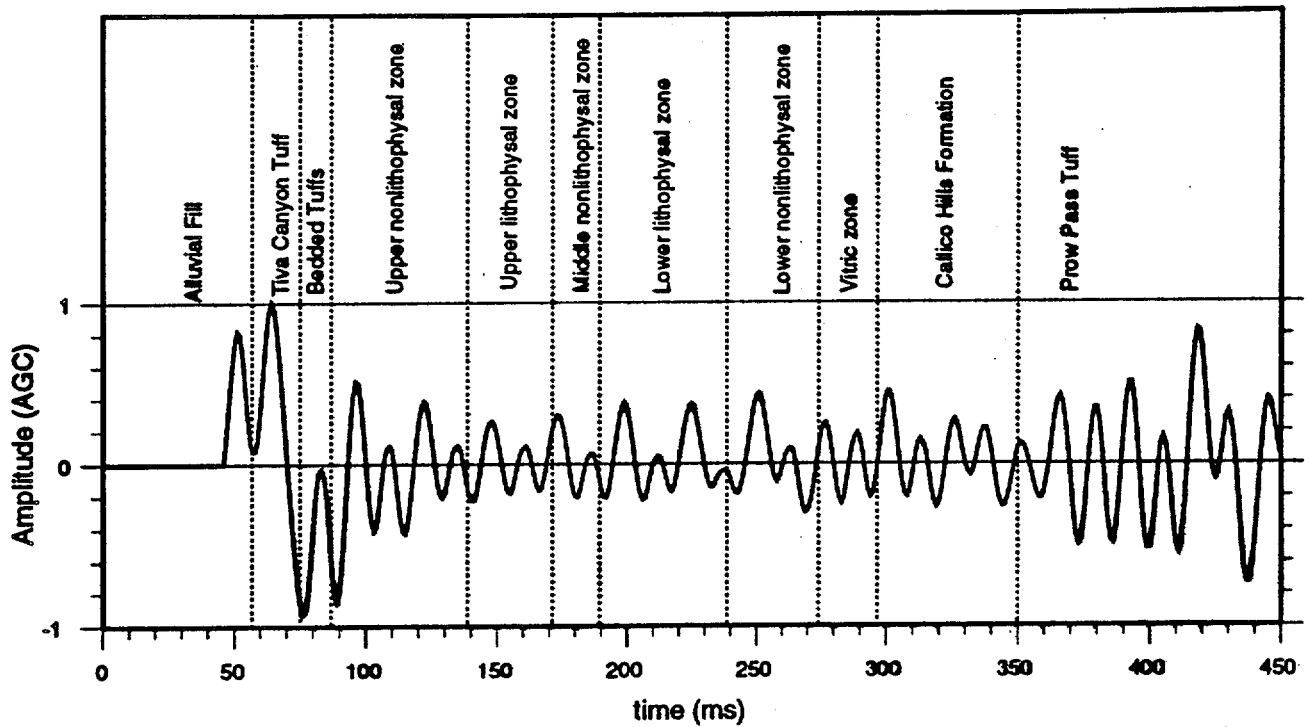


Fig. 7a Reflected P-wave computed with the original data including the low velocity layers but without any velocity variation within the layers.

UZ16: Reflected P-wave with the original log data

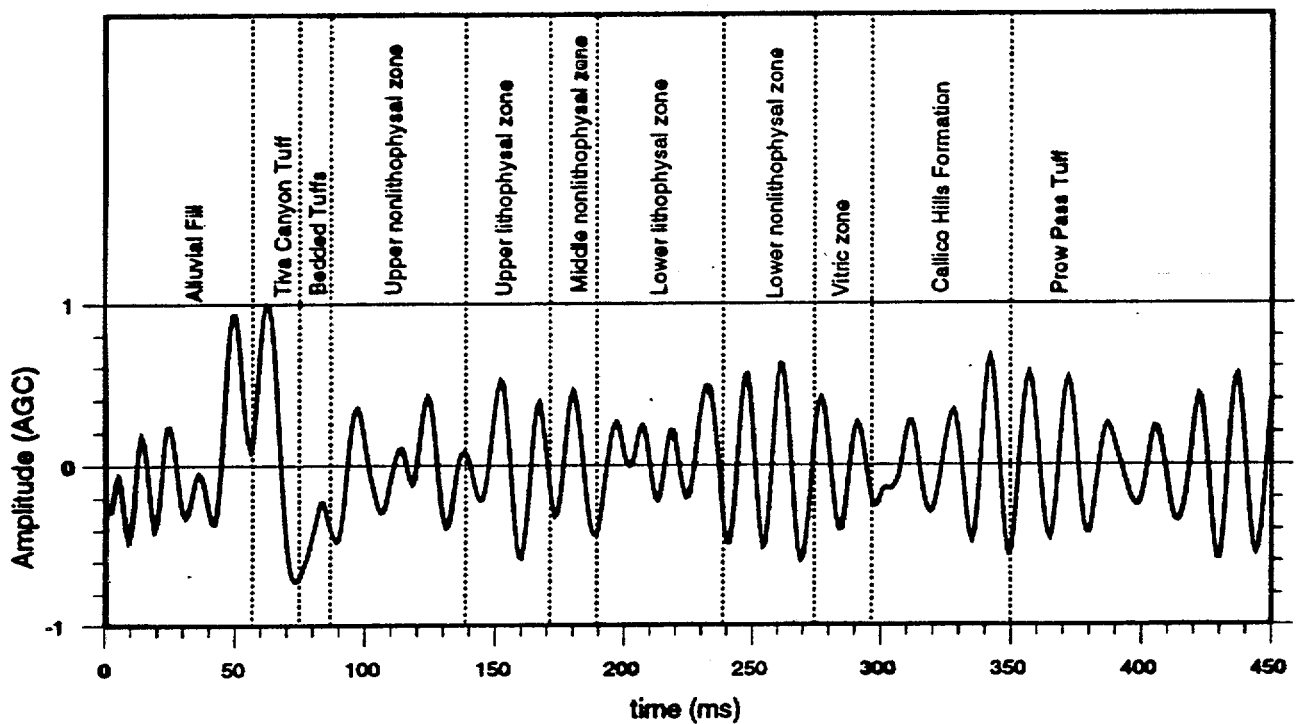


Fig. 7b The same model as in Figure 4a, but it includes the velocity variation within the layers.

UZ16: Reflected P-wave with the corrected porosities

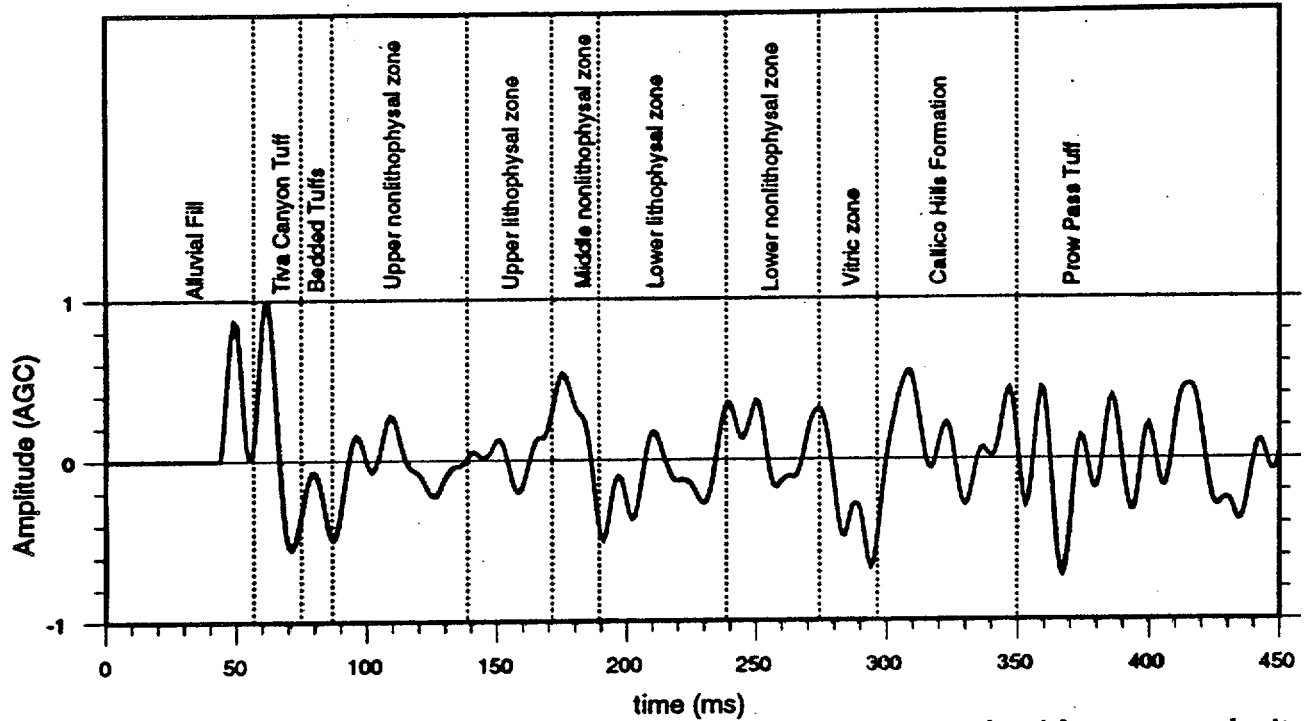


Fig. 9a Reflected P-wave computed with the corrected porosities and without any velocity variation within the layers.

UZ16: Reflected P-wave with the corrected porosities

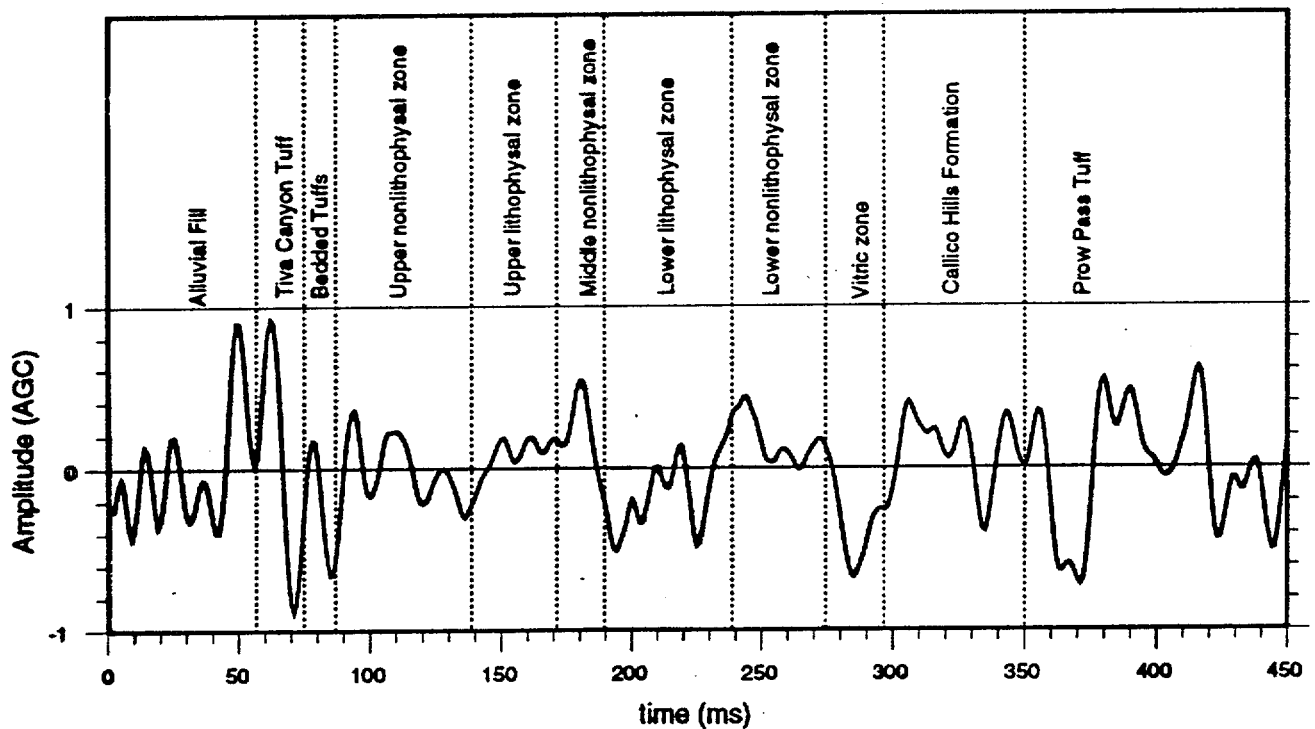


Fig. 9b The same model as in Figure 6a, but it includes the velocity variation within the layers.

Basement Models

Seismic

— Brocher (USGS)

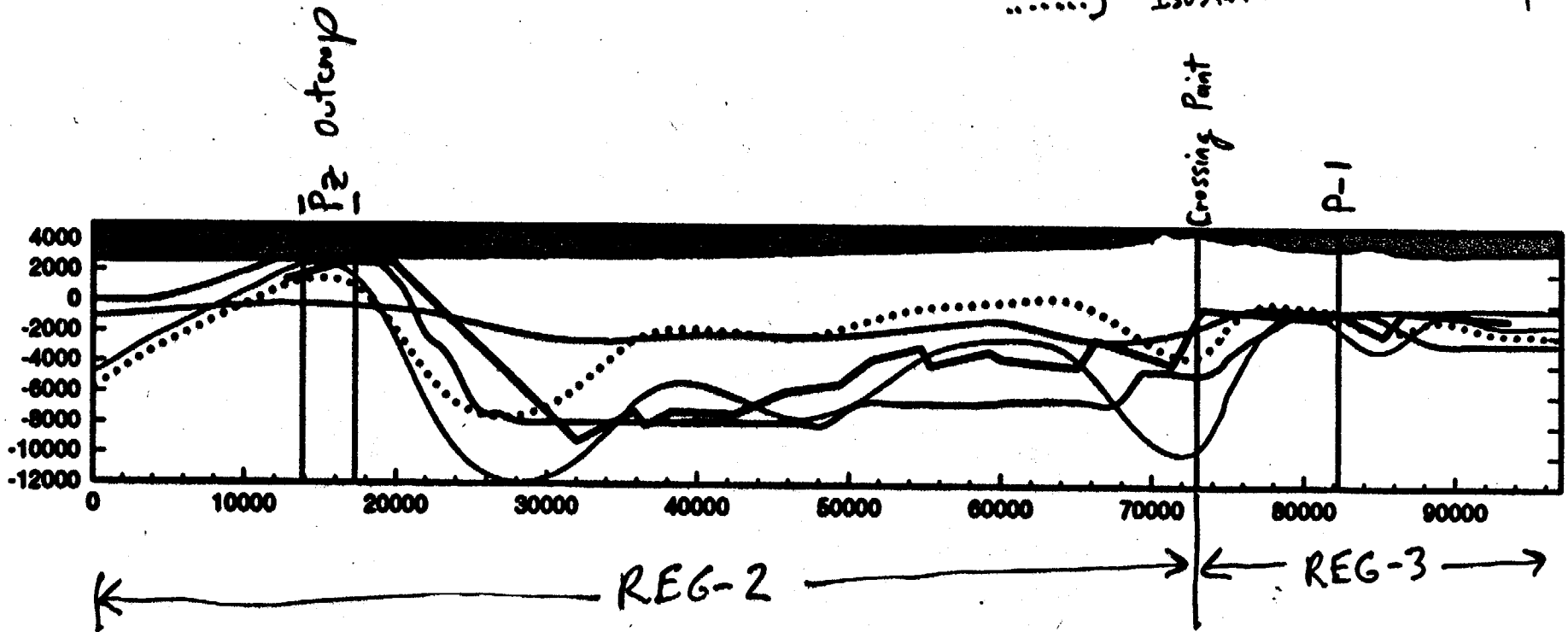
Gravity

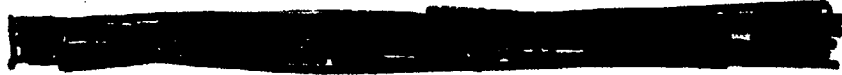
— LBNL

— Penck (USGS)

— } Earthfield Models

..... } Isostatic + Residual Gravity





PRELIMINARY INTERPRETATIONS WORKSHOP
SEISMIC SOURCE CHARACTERIZATION
YUCCA MOUNTAIN SEISMIC HAZARD ANALYSIS

JANUARY 6-8, 1996
SALT LAKE CITY, UTAH

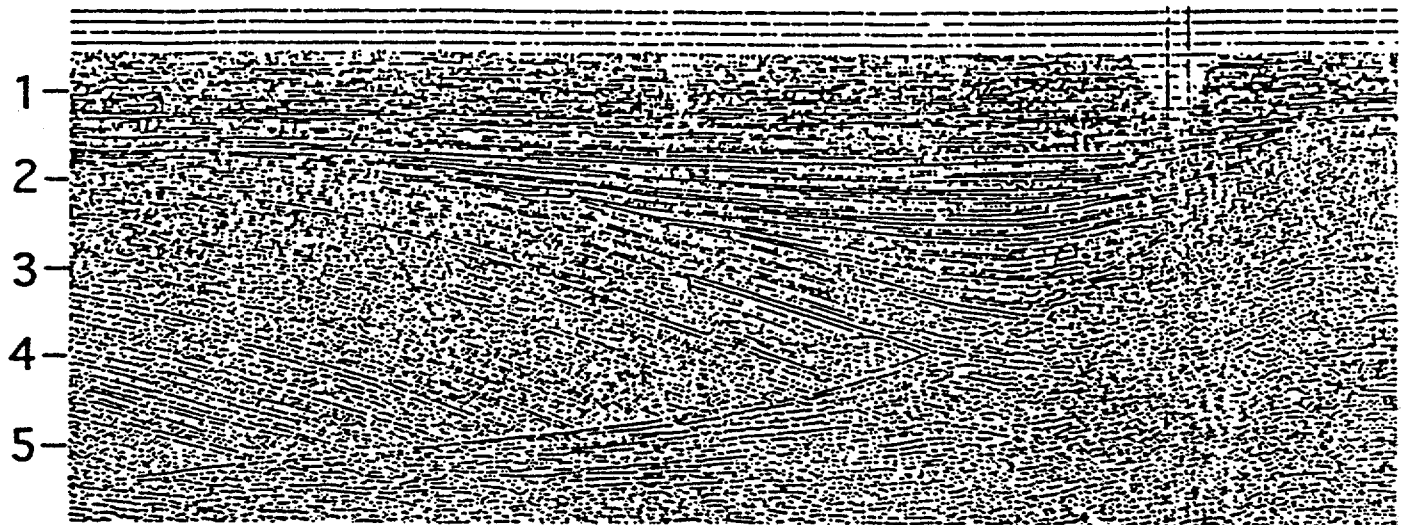
LOW-ANGLE NORMAL FAULTS
AND SEISMICITY: A REVIEW

+

SOUTHERN GREAT BASIN GPS

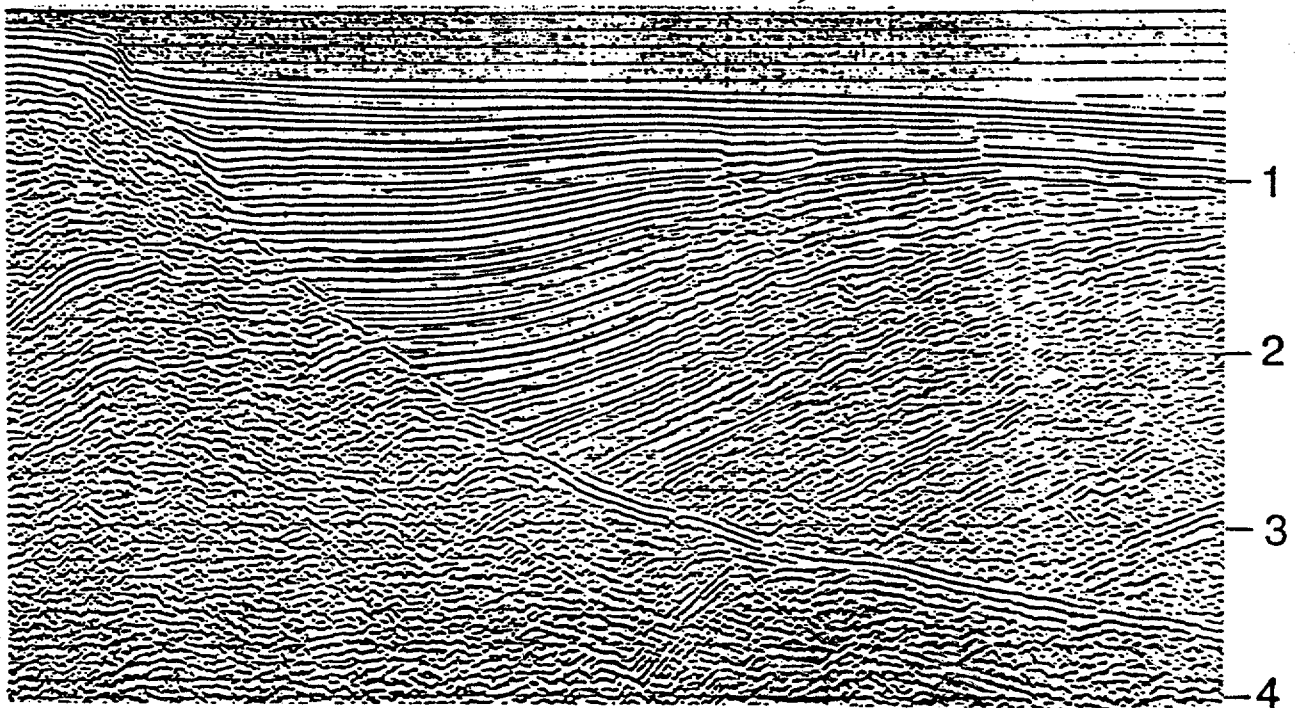
Presenter: B. Wernicke

a)



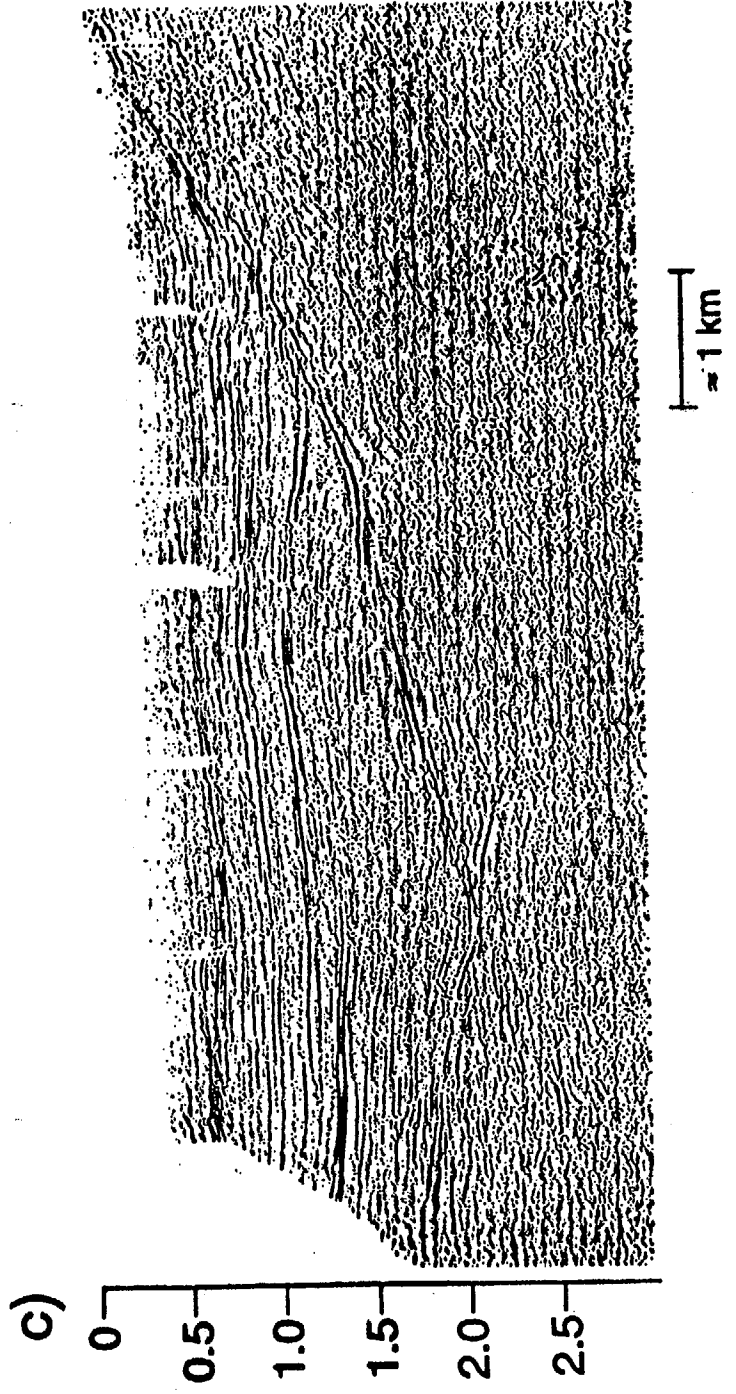
≈ 2 km

b)

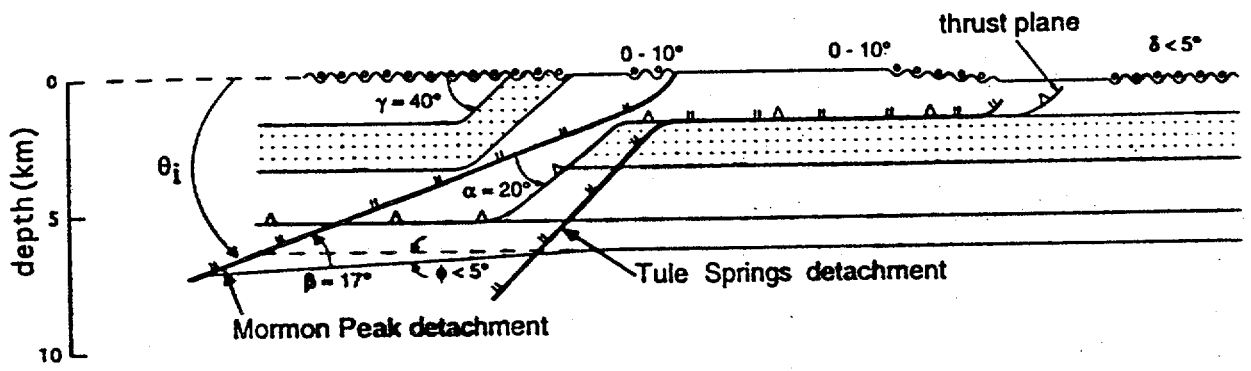


≈ 2 km

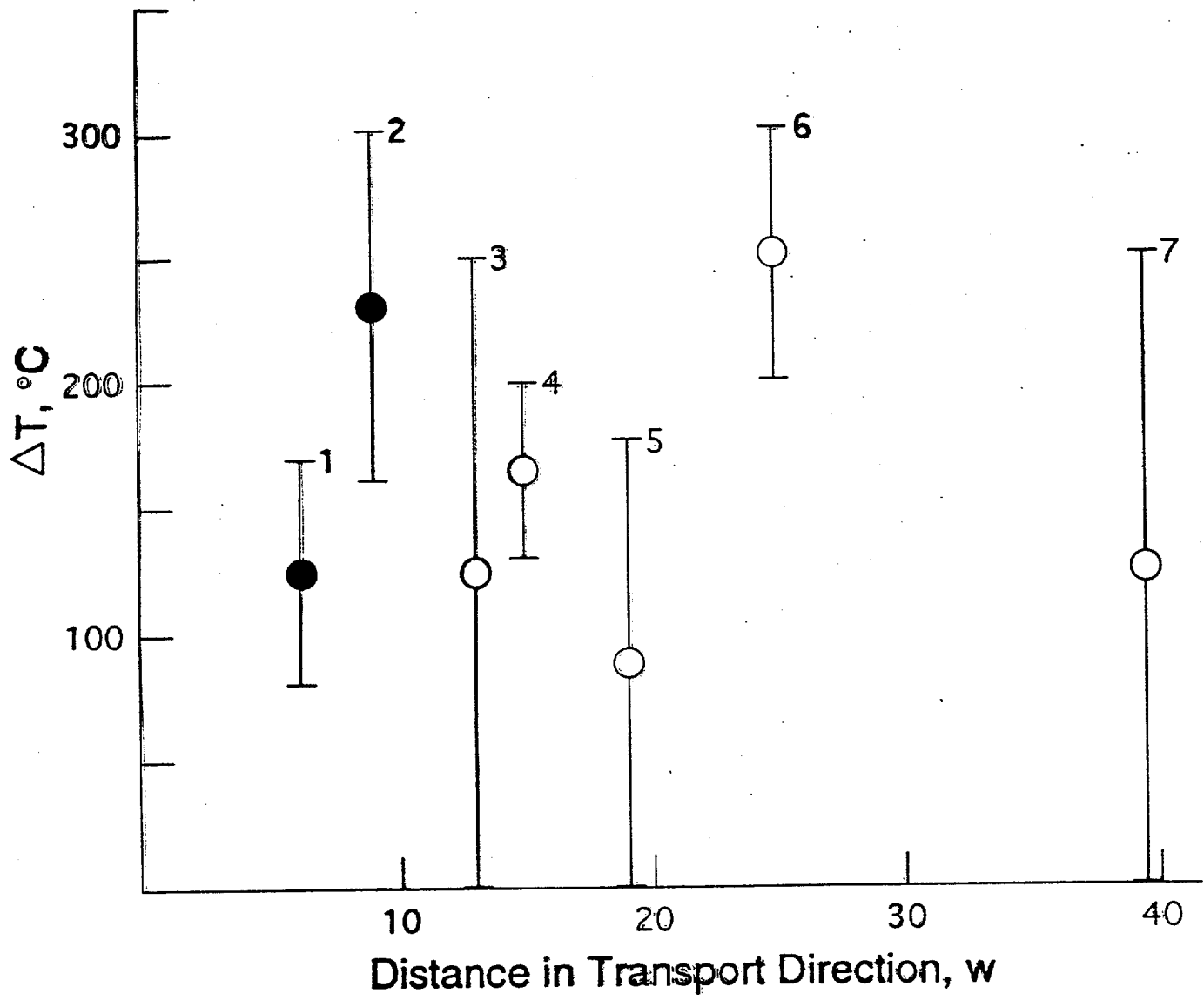
Wernicke, Figure 7



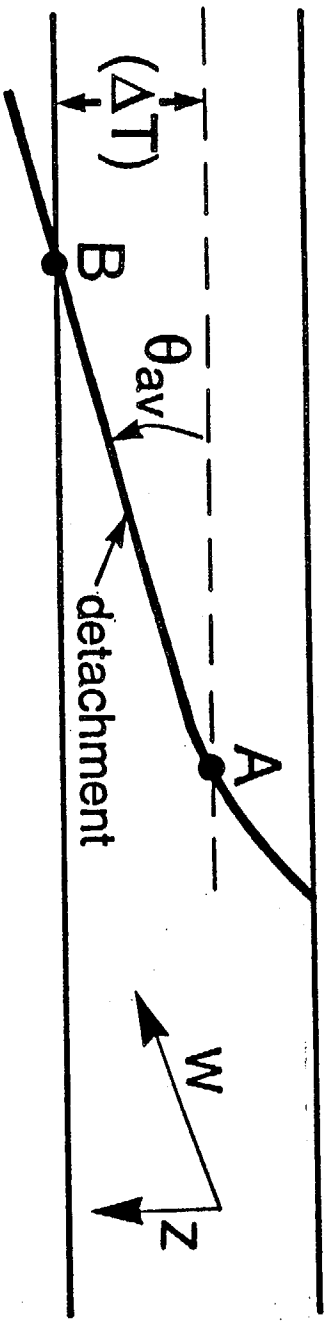
Wernicke, Figure 7



Wernicke, Figure 3

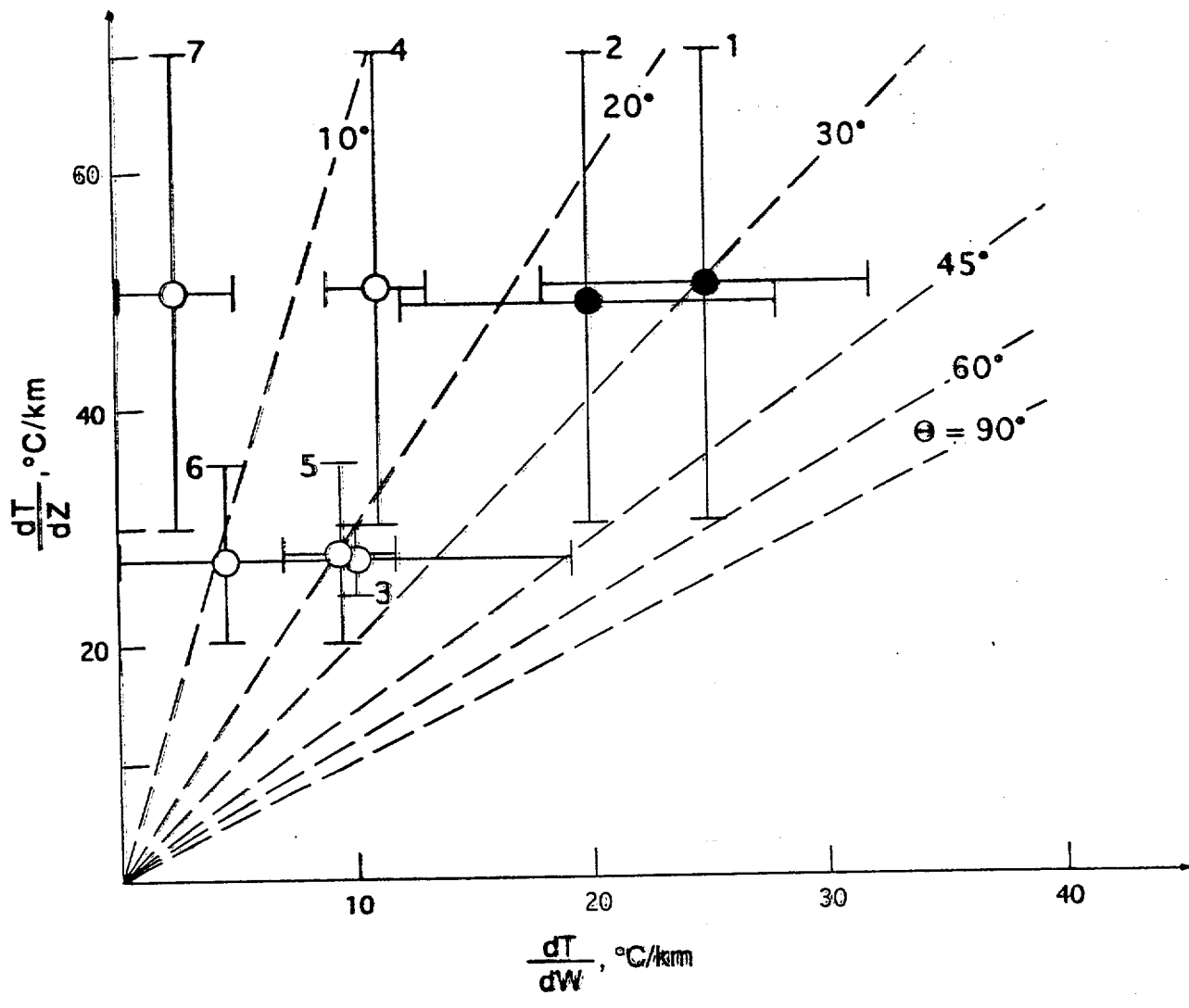


Wernicke, Figure 4

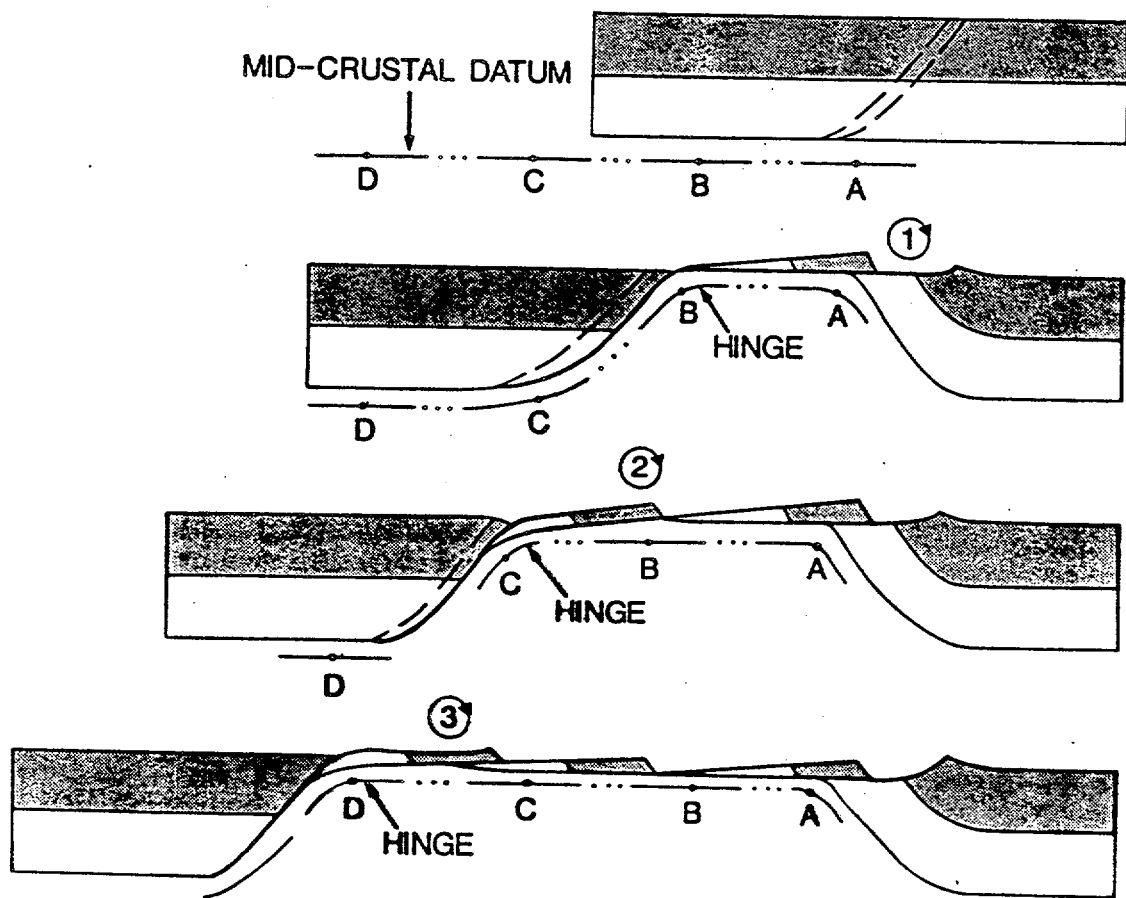


$$\theta_{av} = \sin^{-1} \frac{dT/dw}{dT/dz}$$

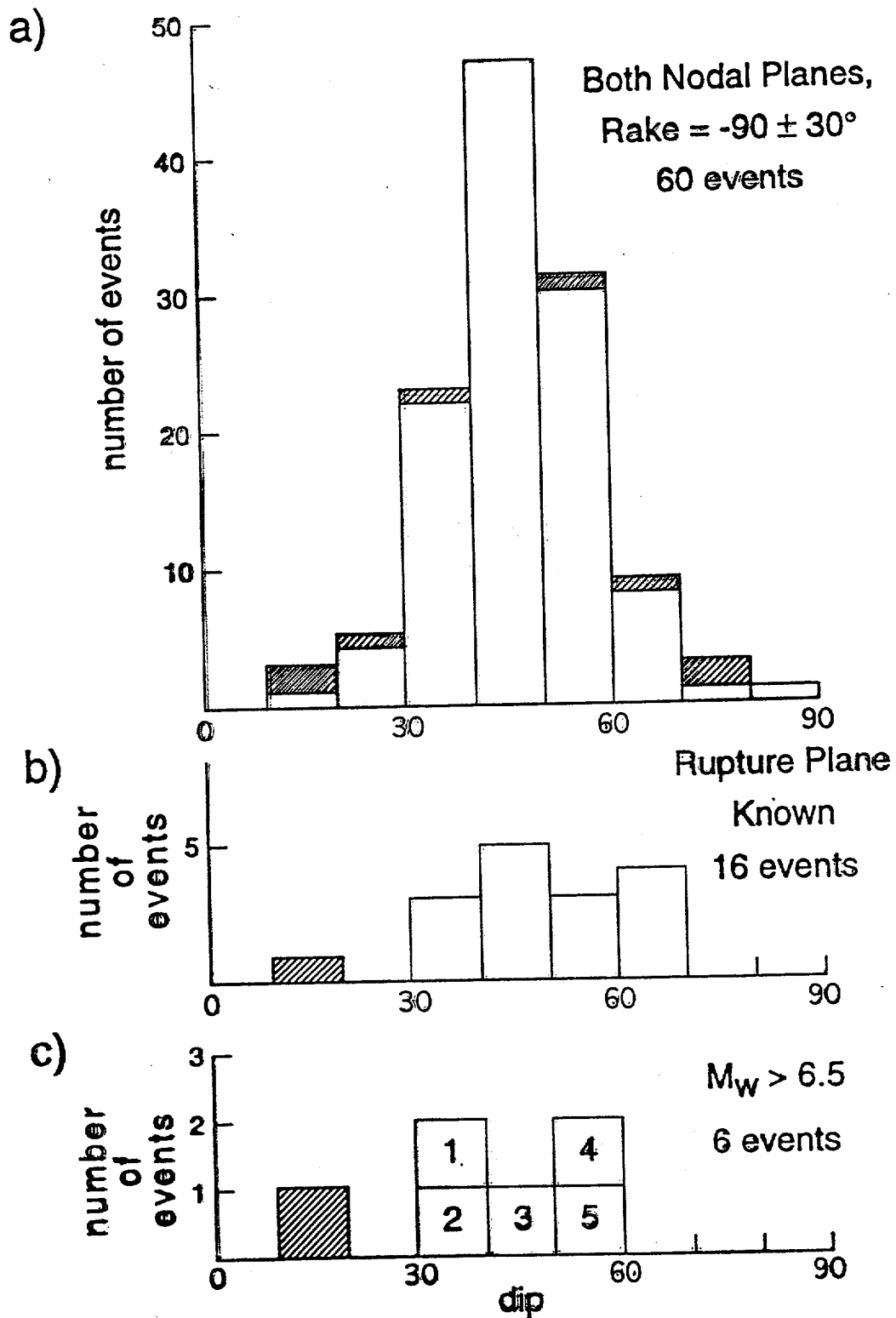
Wernicke, Figure 5



Wernicke, Figure 6



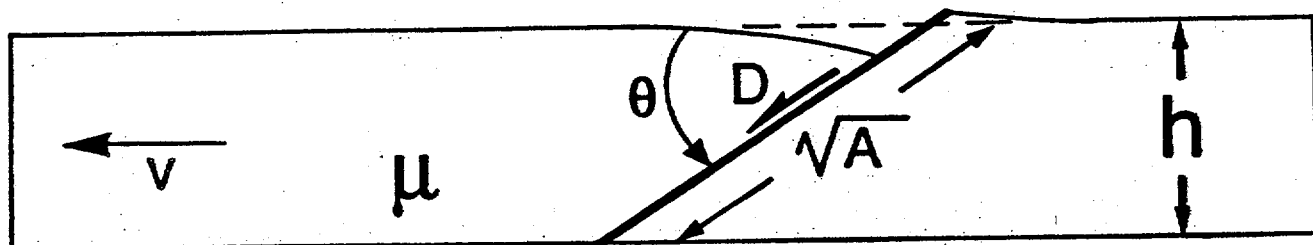
Wernicke, Figure 9



Wernicke, Figure 8

* insensitive to θ ?

- θ - dip of fault
- D - coseismic slip
- A - area of fault plane
- * μ - rigidity modulus
- * $\Delta\sigma$ - stress drop
- * h - thickness of seismogenic crust
- * v - spreading velocity



I. Shallow faults absorb more strain:

$$\Delta\sigma \propto \mu \frac{D}{\sqrt{A}}; \quad \sqrt{A} = \frac{h}{\sin\theta}; \quad \therefore D \propto \frac{1}{\sin\theta} \quad (1)$$

II. Shallow faults more efficient:

$$v = D \cos\theta R'; \quad \therefore D \propto \frac{1}{R' \cos\theta} \Rightarrow R' \propto \tan\theta \quad (3)$$

III. Fewer shallow faults per unit strike distance:

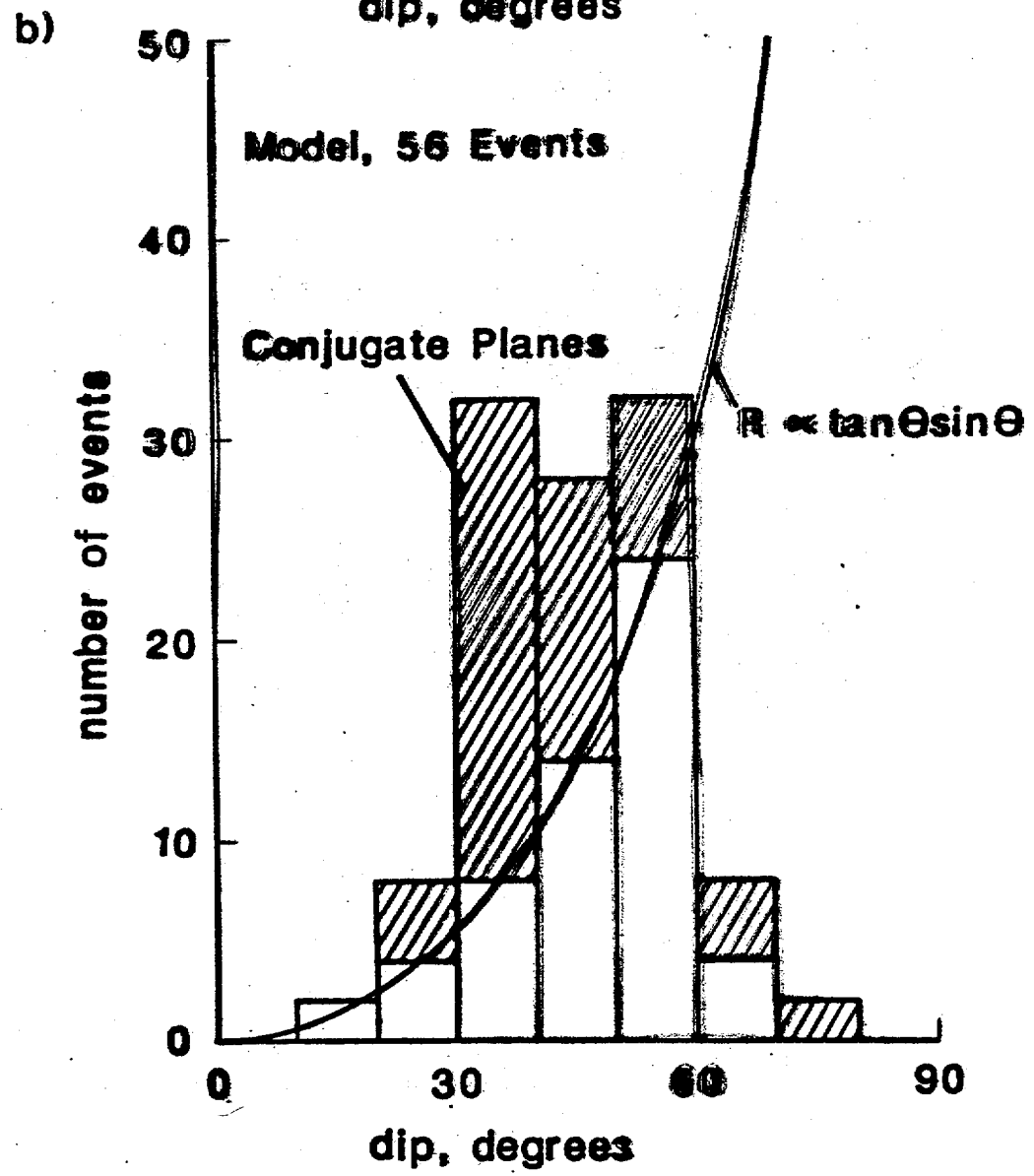
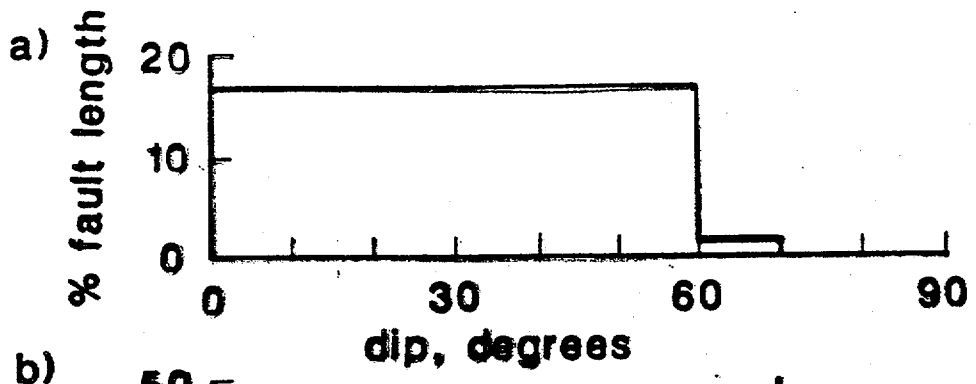
$$\frac{1}{\sqrt{A}} = \frac{\text{faults}}{\text{unit fault length}}, \quad R' = \frac{\text{events}}{\text{time} \cdot \text{fault}}; \quad \frac{R'}{\sqrt{A}} \propto R \sin\theta \quad (4)$$

$$(3) \div (4) \Rightarrow \boxed{R \propto \tan\theta \sin\theta}$$

e.g. 15° -fault rift has ~28 times ~~less~~ events per unit time than 60° -fault rift.

$$\text{Since } M_0 = \mu AD, \quad M_0 \propto \frac{1}{\sin^3\theta}$$

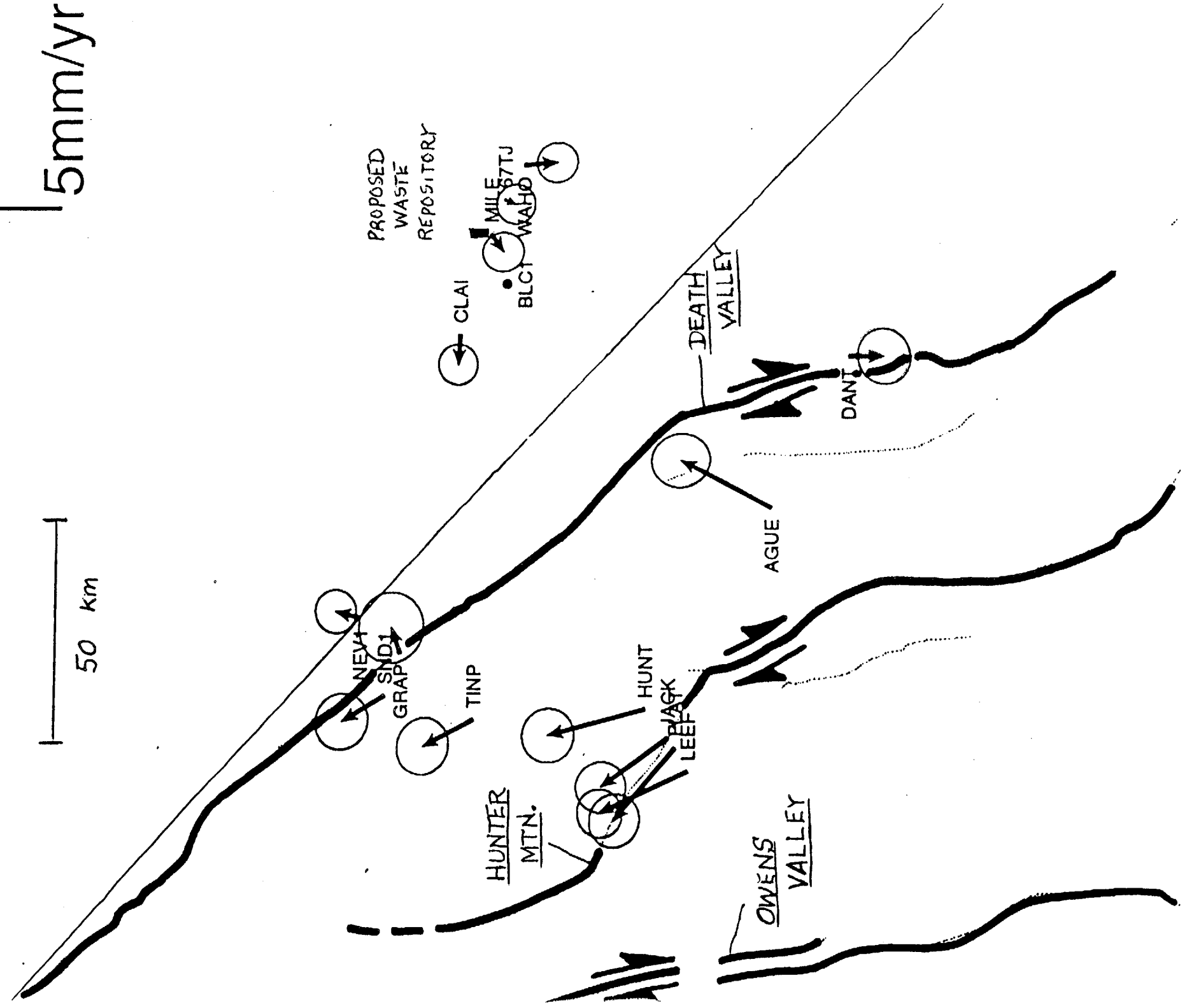
If 50° fault \rightarrow M6-M7, 15° fault \rightarrow M7-M8.



Wernicke, Figure 11

5mm/yr
↑

50 km



PROPOSED
WASTE
REPOSITORY

CLAI

MILE 57TJ
BLCT WAHO

DEATH
VALLEY

DANTE

AGUE

NEVT
SND1
GRAP

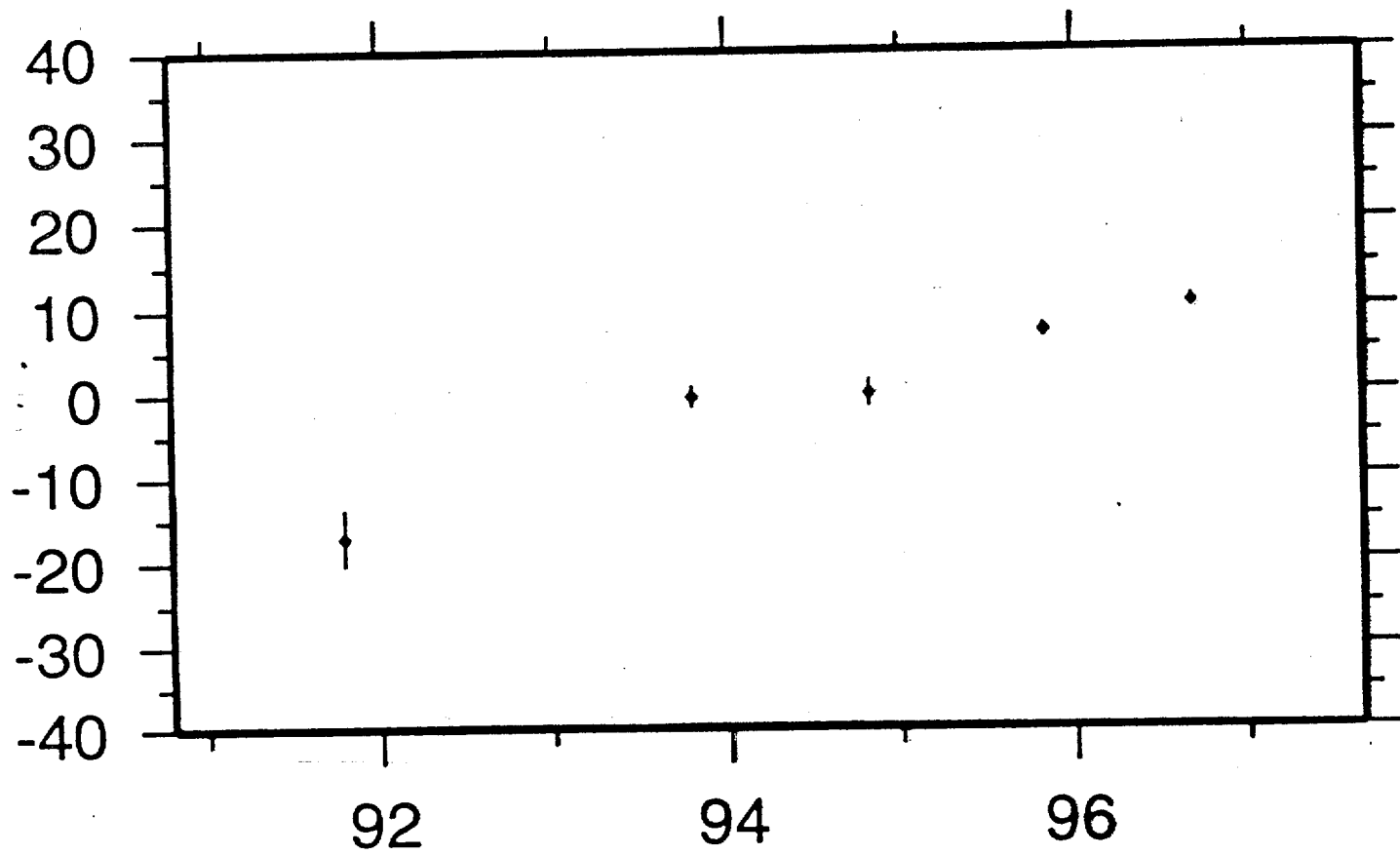
TINP

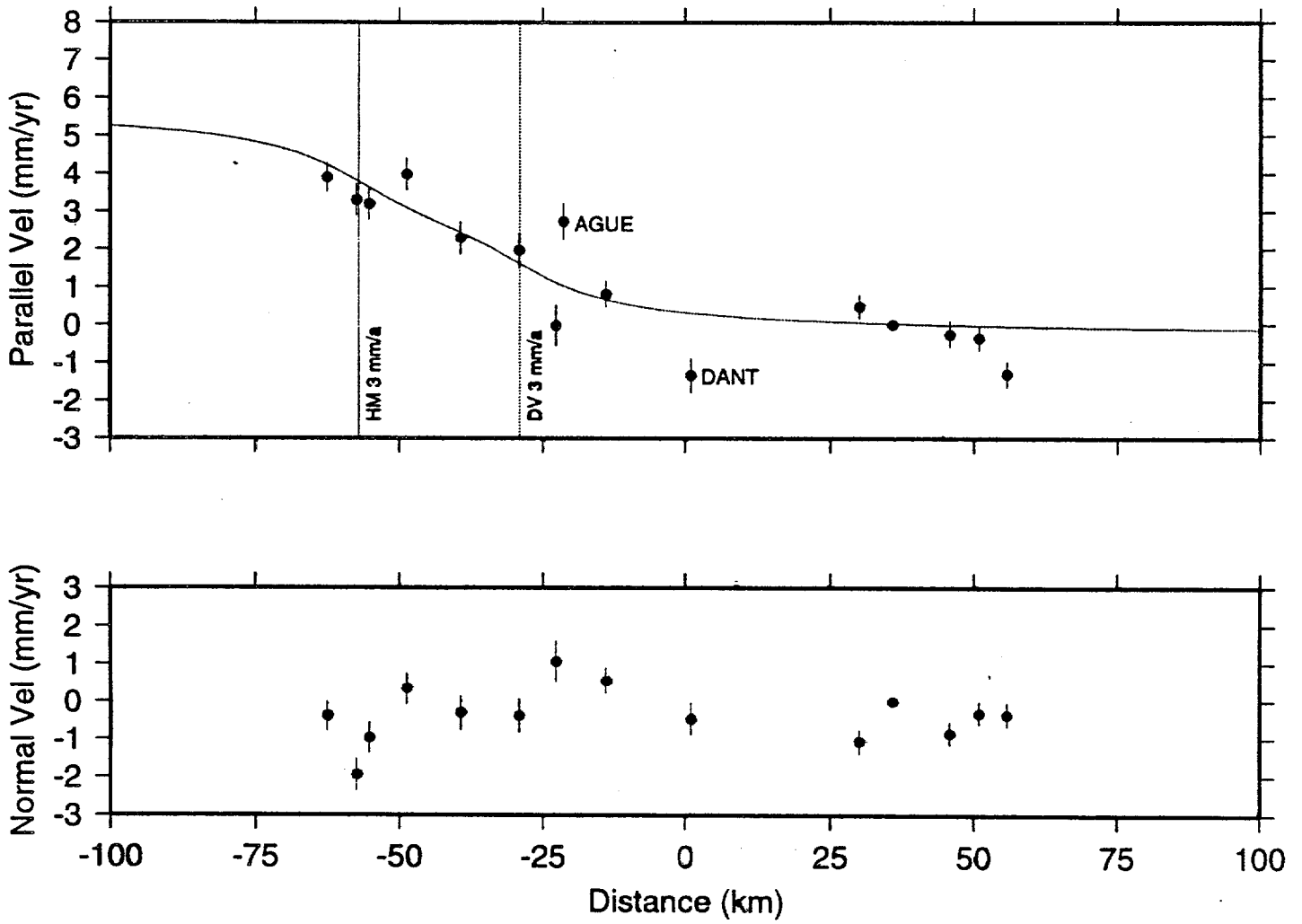
HUNTER
MTN.

HUNT
BLACK
LEEFE

OWENS
VALLEY

MILE to LEEF_GPS Solution N + -37899.941 m





**Screw Dislocation Velocity Model:
Death Valley/Furnace Creek and Hunter Mountain Faults**

Yucca Mountain faults in a regional context

D. O'Leary USGS

"Yucca Mountain faults" comprise the faults that cut Yucca Mountain. Aside from their location, what is the nature of these faults that allows them to be discriminated within a "regional context"? Each fault could be characterized and described individually, but it is more analytically convenient to classify them and by this means to compare them with faults apart from Yucca Mountain.

FAULT POPULATIONS

1. Block bounding faults (BBFs) There are at least three BBFs, so designated because they form the structural margins of tilted blocks about 5 km across (including the "repository block"). These faults include the Paintbrush Canyon-Stagecoach Road fault (nominally a single structure), the Solitario Canyon fault, and the Windy Wash fault. They vary in structure along strike from simple planar features to complex multi-strand zonal faults having numerous splays and jogs. Cumulative throw on each BBF of up to a few hundred m is expressed as major topographic relief. The great continuity, linearity, scissors offset, and large cumulative throw (normal, down to west, facing collapsed or "rolled over" hanging walls) suggests that these faults have seismotectonic significance. Relatively warm water in wells in Solitario Canyon and Midway Valley implies that the Solitario Canyon fault and the Paintbrush Canyon fault, at least, penetrate the Paleozoic substrate and its deep confined aquifer. Whether any or all of these faults penetrate to the base of the seismogenic crust is uncertain. The most likely candidate for deep penetration is the Paintbrush Canyon-Stagecoach Road fault, as this follows the isostatic gravity gradient along the east side of Crater Flat basin, suggesting that it is a crustal-scale break.
2. Intrablock faults Chiefly small, discontinuous, normal faults that form graben, splays, bridging faults, footwall collapse structures, layer-confined faults, and minor oblique or strike slip faults, etc.; commonly associated with much fracturing or brecciation. Among these are the Ghost Dance, Sun Dance, Iron Ridge and Fatigue Wash faults. Although faults of this population are of varied origin and could be subdivided in smaller populations, they are perhaps all consequent to movement of the block bounding faults and the blocks themselves, and reflect various intrablock or local strain failures that probably (in some cases) date back to the consolidation phase of tuff emplacement. It is questionable whether many of these faults penetrate deeply the Pz substrate; most are probably confined to the volcanic carapace.
3. Oblique faults Chiefly northwest-striking dextral faults having minor offset and mostly located near the northern end of the mountain (e.g. Pagany Wash and Sever Wash faults). These appear to be minor lateral adjustments to mountain-wide extension involving relatively late movement on the BBFs. They are probably confined to the volcanic carapace. Because they are aligned near to the azimuth of the block dip slopes, they have guided erosion and have relatively prominent topographic expressions.
4. Radial faults A fringe of faults that extends radially out from the caldera complex into Crater Flat. These faults generally reflect west-directed extension but are dominated by a caldera-centered stress field; most likely these faults are confined to the volcanic carapace.

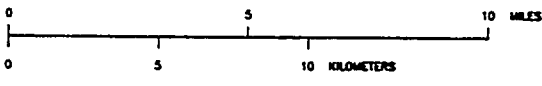
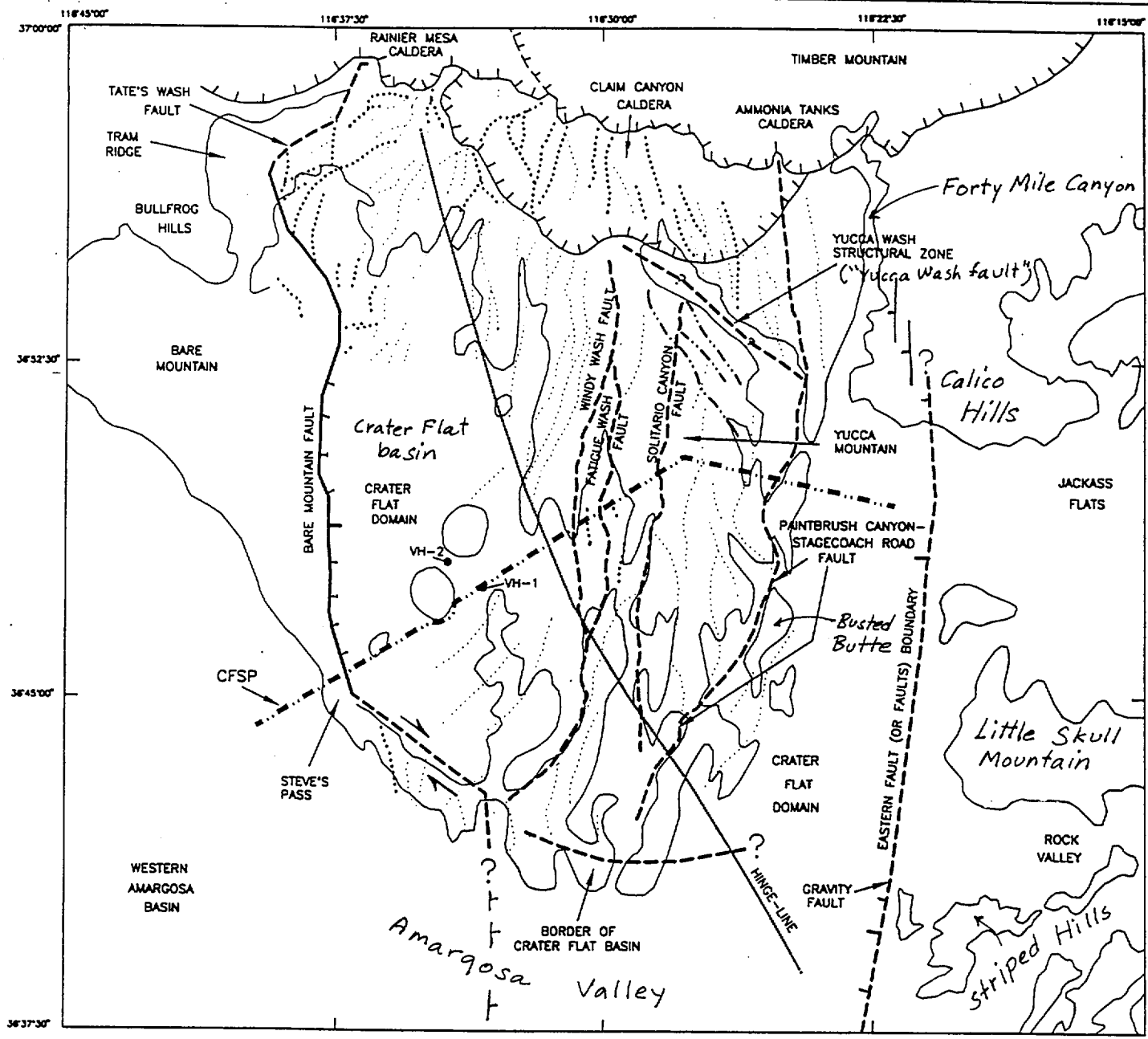
FAULT HISTORY

All the faults at Yucca Mountain clearly have their origin and development tied to events that post-date deposition of the Topopah Spring Tuff. there are two main components to this history:

1. A dominant, early, *local west-directed extensional component* tied to evolution of the southwest Nevada volcanic field and the evolution of Crater Flat basin. Major extension occurred between 12.7 Ma and 11.6 Ma, with least compressive stress oriented N60°W. This resulted in an angular unconformity between the Paintbrush Group and the 11.7 Ma rhyolite of Fluorspar Canyon and the 11.6 Ma Rainier Mesa Tuff. Block tilting of between 10°-40° occurred in the interval.
2. A subordinate, later component of *vertical axis clockwise rotation* probably tied to dextral shear external to Crater Flat basin. From 11.6 Ma to 11.45 Ma slip changed from normal to steep oblique (sinistral on northeast-striking faults, dextral on north-striking faults); as much as 30° rotation occurred, increasing to the south, along with continued tilting of blocks of Timber Mountain Group tuffs. A NNW-trending "hingeline" can be drawn across Yucca Mountain. North of the line rotations are less than 20°; south of the line rotations are greater than 20°. Imposition of dextral shear occurred as much as 1 Ma following a majority of basinal extension and subsidence. Was this simply an effect of local Crater Flat basin widening to the south, or does it reflect an imposed Walker Lane shear external to the basin? Regional paleomagnetic studies by Hudson suggest the latter. Local enclaves of Miocene clockwise vertical axis rotation are found elsewhere within the tectonic setting - the deformation style is not unique to Yucca Mountain.

CONCLUSIONS

- Different styles of normal and oblique faulting resulted in complex extension of the volcanic carapace during and shortly after the period of caldera volcanism. All the faults at Yucca Mountain are kinematically related to this process in the post 12.7 Ma period. The process of extension has greatly decelerated with time but rates of faulting have not decreased uniformly among the different fault populations.
- West-directed extension at Yucca Mountain involved two processes: subsidence and extension of Crater Flat basin, and imposition of dextral shear. The first process is intimately associated with local volcanism, the second with regional "Walker Lane" deformation. Both processes appear to have roughly paced the history of caldera evolution in late Neogene time implying that primary deformation involved a hot, weak, thin crust. Activation of the ancient faults in the present environment is feeble and sporadic.



EXPLANATION	
	Regional faults, dashed where inferred, tick on hanging wall
	Caldera margin
	Right-slip faults
	East dipping normal faults
	West dipping normal faults
	Bedrock / alluvium contact
	VH-2 ● Boreholes and descriptors
	CFSP Crater Flat seismic profile track

Figure 8.6. The Crater Flat domain and its inferred bounding structures.

ASSOCIATIONS AND BOUNDING FEATURES

Yucca Mountain is a typical Walker Lane tectonic feature in that it is the exposed part of a *structurally isolated tectonic enclave* that manifests a strain history and a structural pattern distinct from that of surrounding terrane. In other words it is a *tectonic domain*. How is this domain (the Crater Flat domain) isolated from adjacent domains?

Lateral boundaries

1. Bare Mountain fault The faulted and extended tuffs of Yucca Mountain descend beneath the alluvium of Crater Flat and are clearly bounded to the west by the Bare Mountain fault (BMF). The BMF is a major range-front or down to basin fault as indicated by a 50 mgal gravity gradient and an elevated footwall represented by Bare Mountain. The BMF appears to have functioned as a complex tear fault: complex because geophysical data indicate it consists of more than one fault slice - perhaps a group of step faults arrayed as much as 3 km outboard of the present day range front, but buried by alluvial fans; a tear fault because it shows a component of dextral slip that increases to the south, but the fault frays out or otherwise changes in structural style and displacement at either end of Crater Flat basin.
2. The Claim Canyon caldera rim The extended fault pattern of Yucca Mountain dies out among the northward converging radial faults that fringe the south side of the caldera complex. The pronounced tilted block morphology associated with the BBFs is abruptly terminated against Yucca Wash. This fact, along with the WNW-directed rectilinearity of the wash, suggests a controlling structure ("Yucca Wash fault" of various workers). However, field work indicates no through-going fault in Yucca Wash, and the main faults at Yucca Mountain extend north of Yucca Wash, more or less maintaining their strikes. Yucca Wash may represent a minor wedge-like opening along which the entire volcanic carapace has pulled away from the more massive caldera rim assemblage to the north.
3. Structure in Jackass Flats As a stratigraphic assemblage, the volcanic carapace of Yucca Mountain extends far to the east of Jackass Flats. A domain boundary must be present somewhere in Jackass Flats, however, to isolate the Yucca Mountain extension from the east-west strikes expressed in the Striped Hills and Little Skull Mountain. An obvious candidate structure is the alluvium-covered gravity fault. North of Little Skull Mountain the presence of a domain boundary is problematic. The required boundary may be represented by a zone of north-striking, west side down faults across the western flank of the Calico Hills dome; the dome itself (taken as an arrested pre-eruptive volcanic edifice) may have distorted or obliterated any better defined domain-bounding fault zone. There is no geological evidence for structural control of Forty Mile Wash or Forty Mile Canyon. In the narrowest, most conservative sense of a "bounding fault" the Paintbrush Canyon fault could represent the major bounding structure for the fault pattern exposed across Yucca Mountain, as down to the east structure is implied by the depression of Jackass Flats east of Busted Butte.
4. Southern end of Crater Flat basin The aeromagnetic anomaly patterns show that the outcrops (dissected north-dipping cuestas) along the southern end of crater Flat mark the southern end of the extended Yucca Mountain carapace, hence the southern margin of the Crater Flat domain. This terminus also coincides essentially with the southern margin of Crater Flat basin. Stream erosion along the scarp front accounts for the removal of volcanic strata to the south, but whether or not the cuesta scarp is also fault controlled is presently unknown. The problem is relevant to the tectonic setting because the isostatic gravity gradient indicates that the BMF continues south as a relatively minor fault that bounds the west side of Amargosa Valley, and that this fault forms a southeast-striking jog along the southern end of the Crater Flat basin. Kinematics requires that this jog have a dextral shear component. Aligned outcrop boundaries and contacts suggest that the inferred fault is expressed as a zone of en-echelon, distributed shear segments that more or less coincide with the orientation of block boundaries defined by degree of paleomagnetically defined block rotation. Dextral shear is in accord with clockwise vertical axis rotation to the north.

117°

116° 37°

36° 30'

Mid Valley
CP Hills

Calico Hills

Jackass Flats

Little Skull Mt.

10km

Bare Mountain

Amarqosa Valley

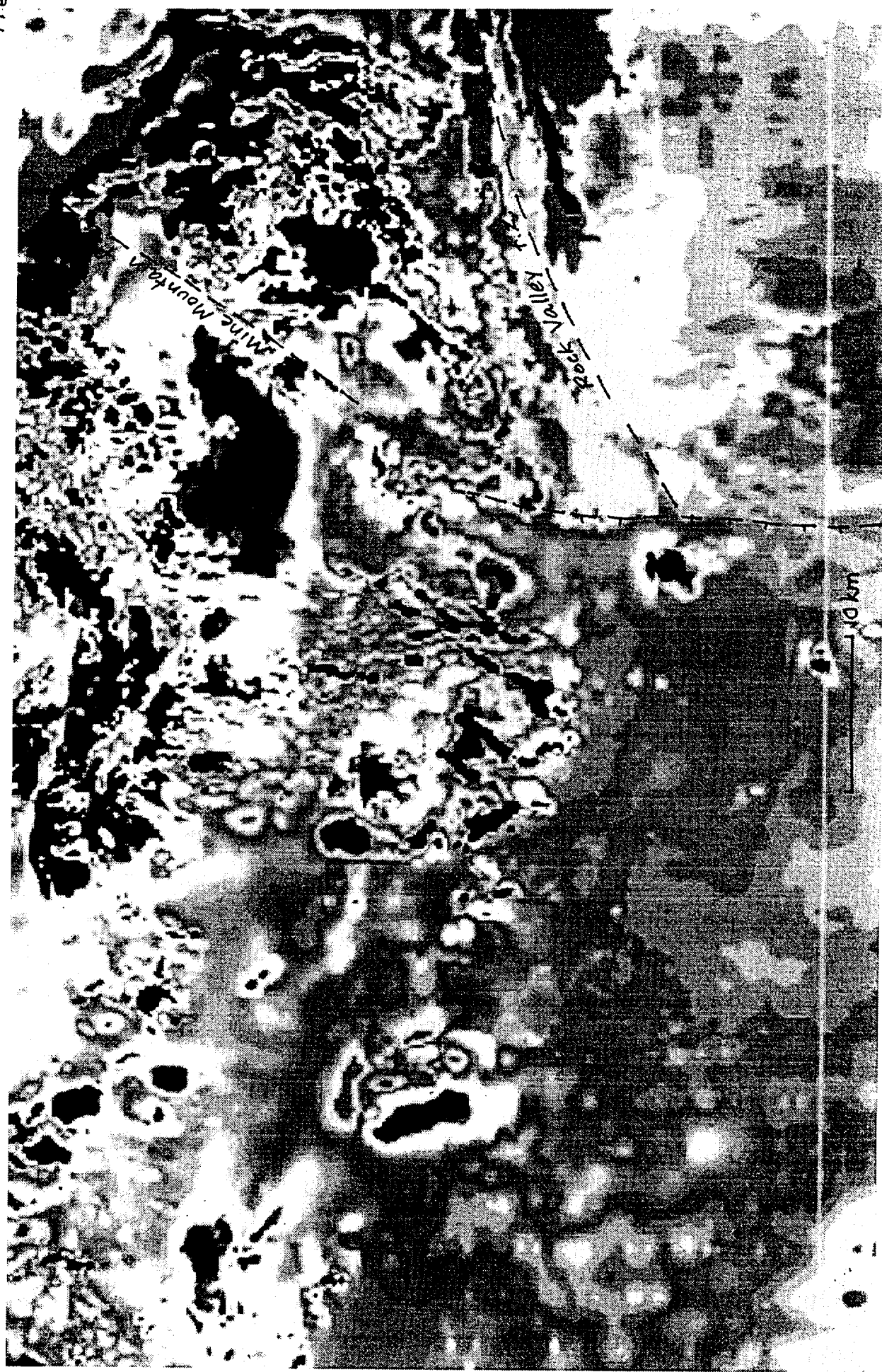
Amarqosa trough

Death Valley

Isostatic gravity map of the Beatty 1°x30' quadrangle

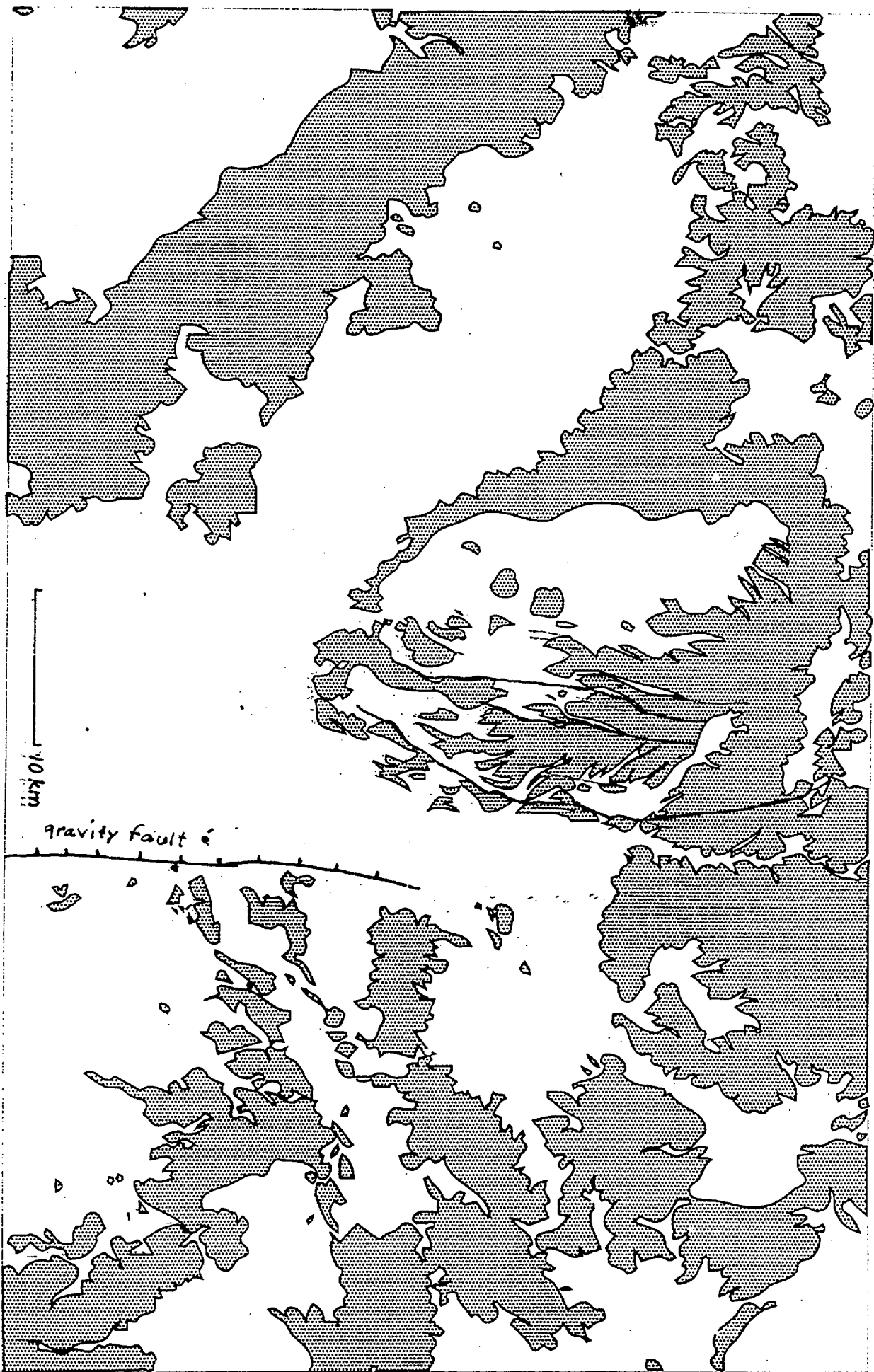
117°

116° 37'



-36° 30'

Aeromagnetic map of the Beatty 1° x 30' map



Bedrock overlay of the Beatty 10 x 30' quadrangle





Windy Wash
Left

Stagnant Rd
Left

"gravity"
fault

"hinge line"

Bare Mt
fault



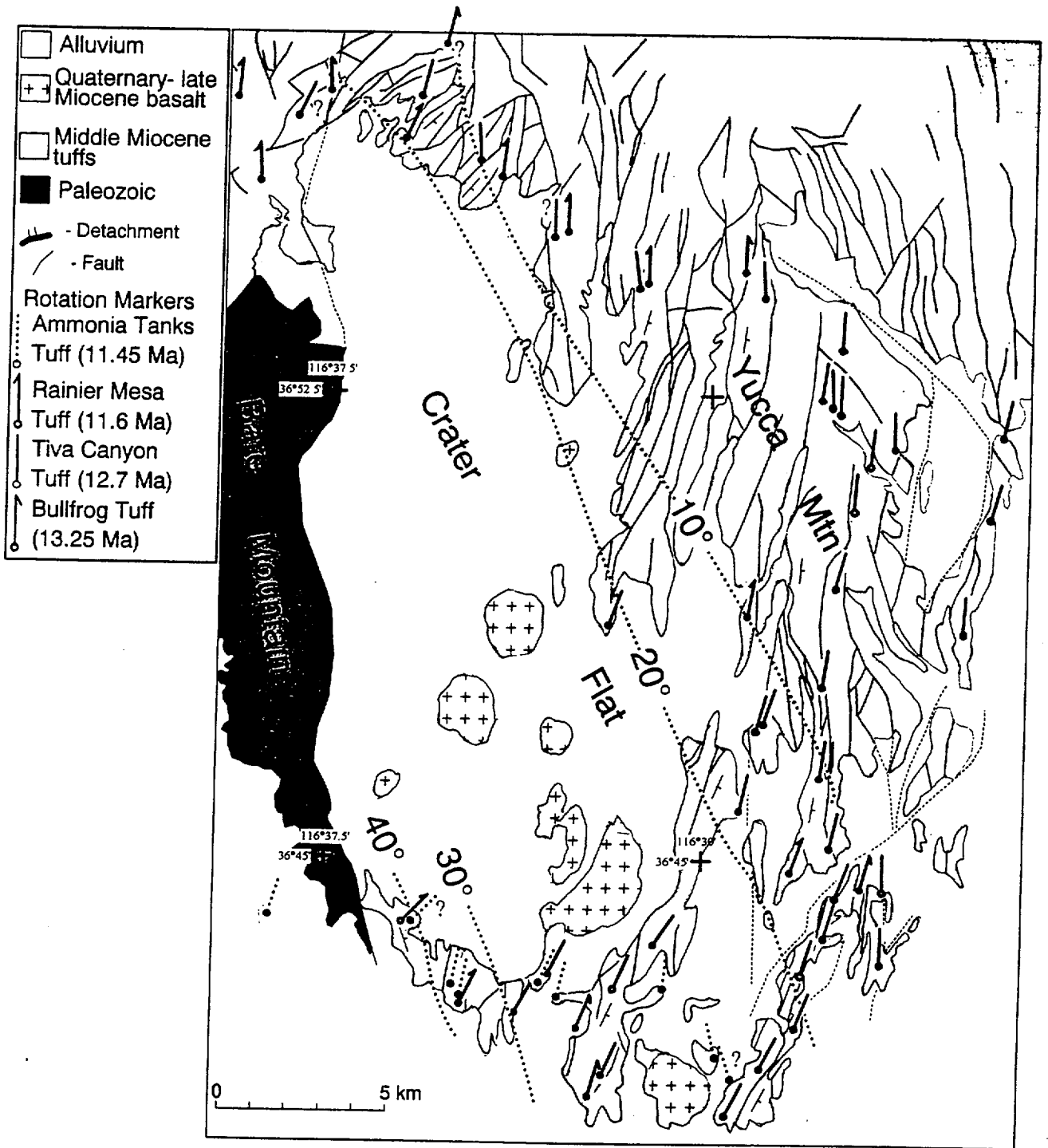


Figure 9.

from Scott Minor, Hudson, and Fridrich, 1996; USGS Open File 96 -
(in press)

Vertical boundaries

Whatever may be said about the uncertainties of the USGS seismic reflection profile that extends across Crater Flat and Yucca Mountain, certain key structural facts are confirmed:

1. Crater Flat basin is a westward-deepening asymmetric trough.
2. Yucca Mountain is the emergent part of a 1.5 to 3 km thick broken volcanic carapace that caps a structurally complex infrastructure which does not mimic the upper surface profile of the carapace.
3. The lack of prominent coherent reflections at depth indicates absence of extensive fault planes that dip at angles of less than 30° (listric or detachment faults).

By analogy with contacts elsewhere in the region, the Miocene volcanic /Paleozoic contact is a fundamentally *erosional* contact locally dominated by *structural relief*. The fact that large offsets at this contact beneath Yucca Mountain are not clearly correlatable with the BBFs suggests that if the BBFs are though-the-brittle-crust faults they are *not* inherited from the infrastructure but instead represent a post-12.7 Ma generation of faults. It is therefore important to appreciate that the faults observable at Yucca Mountain may represent only a subset of seismogenic faults that exist below the Pz contact, despite the evidence for repeated Pleistocene movement in the Yucca Mountain faults which alone might suggest that these faults are the only or even the most important seismogenic faults at the mountain.

CONCLUSIONS

Whatever tectonic model explains faulting at Yucca Mountain must account for: 1. the tectonic isolation of Yucca Mountain within the domain boundaries described above, 2. The exclusive association of extension with Crater Flat basin, 3. The kinematic history of the domain bounding structures as an essential component of the tectonic history of Yucca mountain itself, 4. the apparent structural “detachment “ of the volcanic carapace from the subjacent infrastructure.

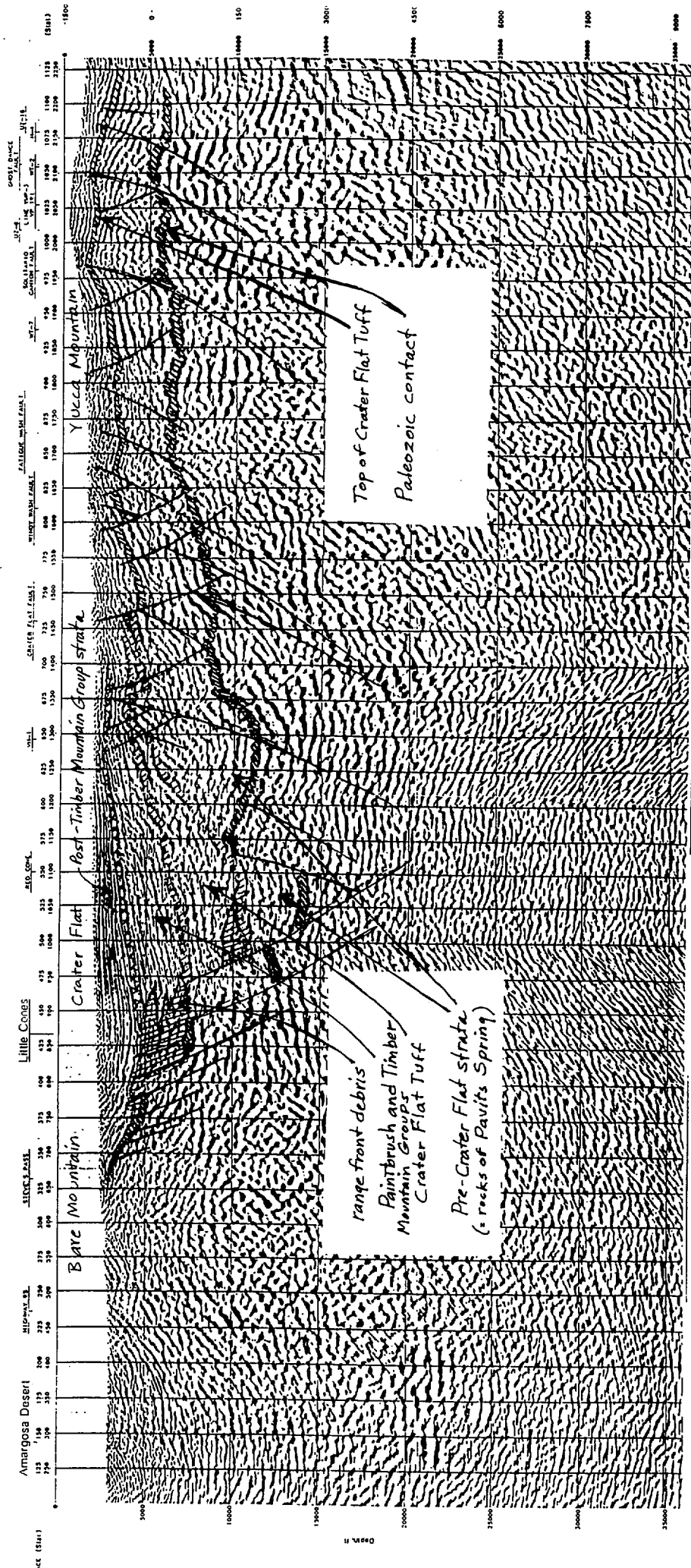


Figure 8.11. Western segment of Crater Flat seismic reflection profile (Brocher and others, 1966). See figure 8.6 for location. Interpretations shown here are for this report. Subvertical solid lines indicate faults.

STRUCTURAL ISOLATION

Although the Crater Flat domain is structurally isolated, it is not unique. The following comparisons are described.

1. Pahute Mesa Will Carr pointed out that the characteristic fault pattern at Yucca Mountain is replicated in similar rocks at Pahute Mesa north of the caldera complex. It would seem that the caldera complex punctuates a larger "protoYucca Mountain" fault zone. But the Yucca Mountain faults are coeval with and postdate the caldera complex, hence, the fault pattern north and south of the caldera complex suggests the influence of deep-seated trough or basin-centered extension active during or after the eruptive episode. If these faults are inherited, they are inherited in the sense that they manifest post-12.7 Ma reactivation of broadly trough-centered extension within basins or "holes" proximal to the caldera complex. Individual pre-12.7 Ma faults may not be instrumental in effecting surface offsets.
2. Mid Valley Mid Valley, located 40 km northeast of Yucca Mountain, is a local basin flanked to the north by Shoshone Mountain and to the east by the CP Hills. The southern, north-sloping flank of the valley is a half-scale version of Yucca Mountain. Here, the slope that culminates to the south at Lookout Peak is mantled by Timber Mountain tuffs and Paintbrush tuffs cut in blocks rotated down to the west, the same style of deformation present at Yucca Mountain. The tuffs rest unconformably on a substrate of rock of the Wahmonie Formation which does not seem to have the same structural configuration as the capping tuffs of the Yucca Mountain sequence. If the structure is decoupled, then the Yucca Mountain-style extension in Mid Valley may have some component of mass movement. In other respects, a crude analogy with Yucca Mountain is present, in which Mid Valley represents Crater Flat and the Mine Mountain fault zone represents the Bare Mountain fault. Unlike Yucca Mountain, however, the strike of the extended blocks at Mid Valley is at a high angle to the axis of subsidence.
3. Volcanic Tablelands The volcanic tablelands, a low plateau at the northern end of Owens Valley, raises the issue of distributed faulting over a weak layer (a different example of a quasi-decoupled volcanic carapace influenced by motion within or across an older substrate affected by extension and subsidence). The tablelands are built of about 150 m of Bishop Tuff on about 1 km of alluvium. The en echelon to subparallel series of blocks cut by down to the west extensional faults is taken here to model the earliest phase of the faulting style present at Yucca Mountain. The analogy implies that all the tableland faults are distributed, most are decoupled from the alluvial substrate, and although the extensional deformation is inherited from Owens Valley itself, the only true post-Bishop Tuff-age faults in the valley are confined to the tablelands.

CONCLUSIONS

The comparisons given above are meant to show that Yucca Mountain style extensional faulting is primarily associated with local basin subsidence and/or widening. The extension is essentially basin and range style (i.e. north-south striking normal faults) that are distributed over a substrate that may have a different stress history or a different material response to extension; although faults in the substrate have post-carapace age displacement, they are older faults and probably are not simple continuations to depth of the faults exposed at the surface. Some of the faulting in the carapace has aspects of mass movement, resembling in overall structure and form large, incipient slab slides. This suggests some degree of detachment from the substrate.

from W.V. Carr, 1990, GSA Memoir 176, Chpt. 13.

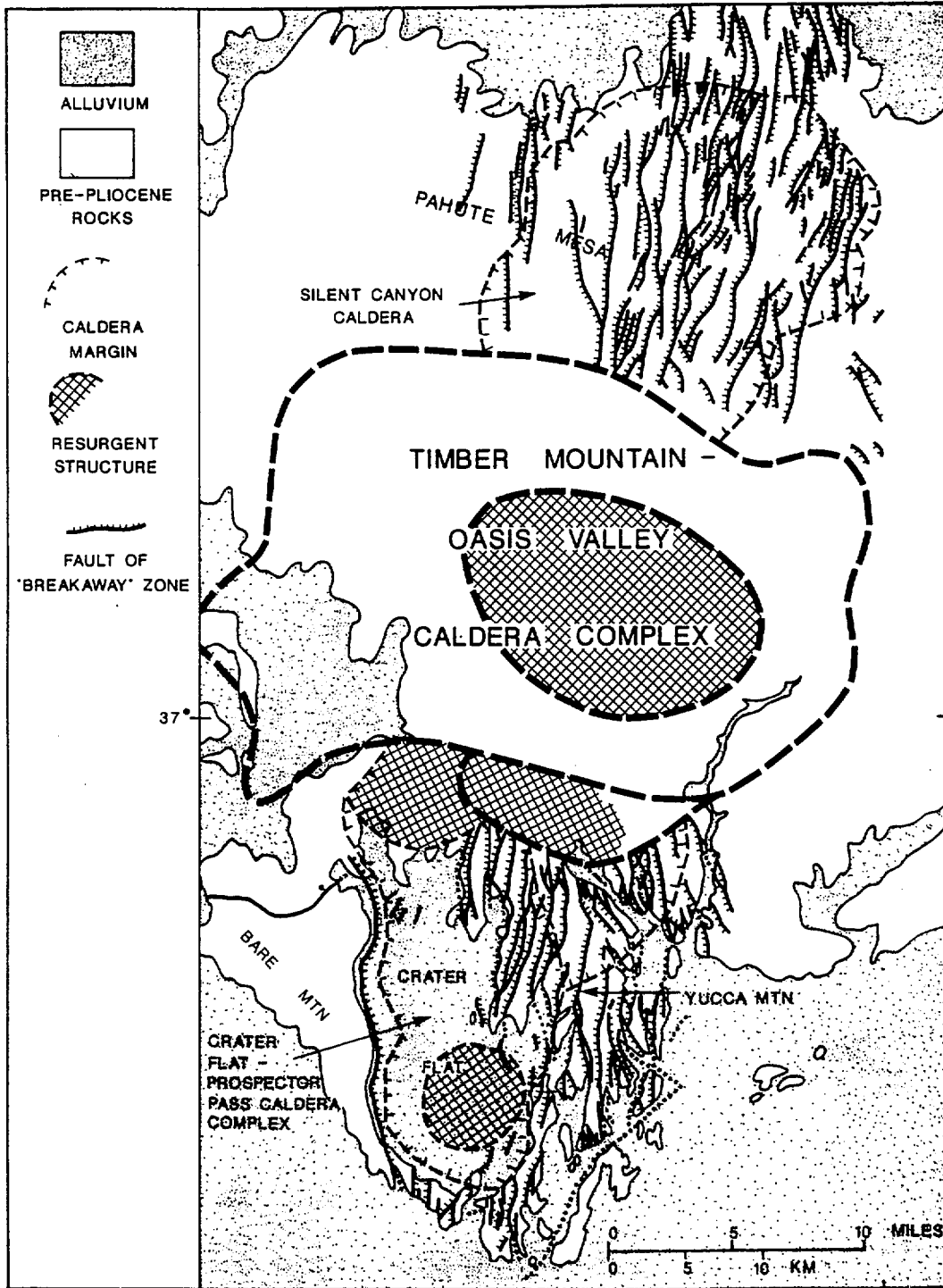
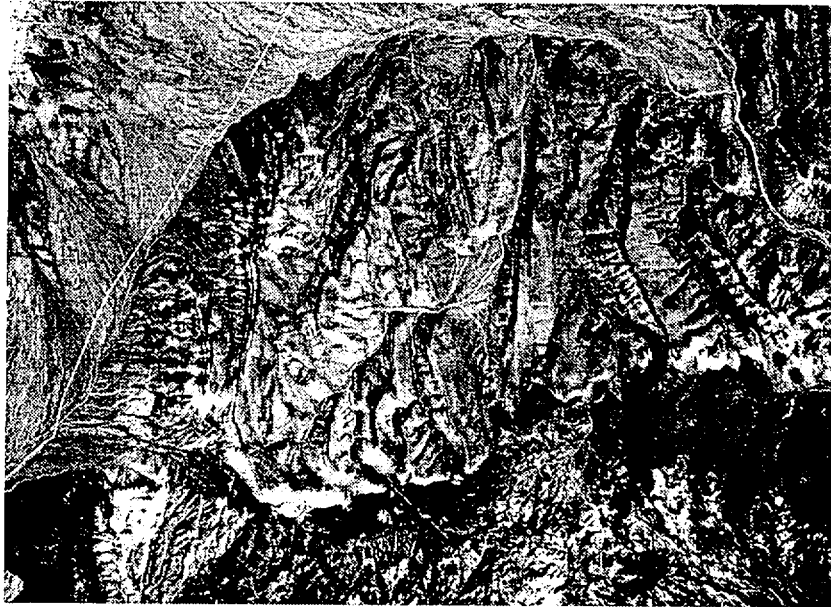
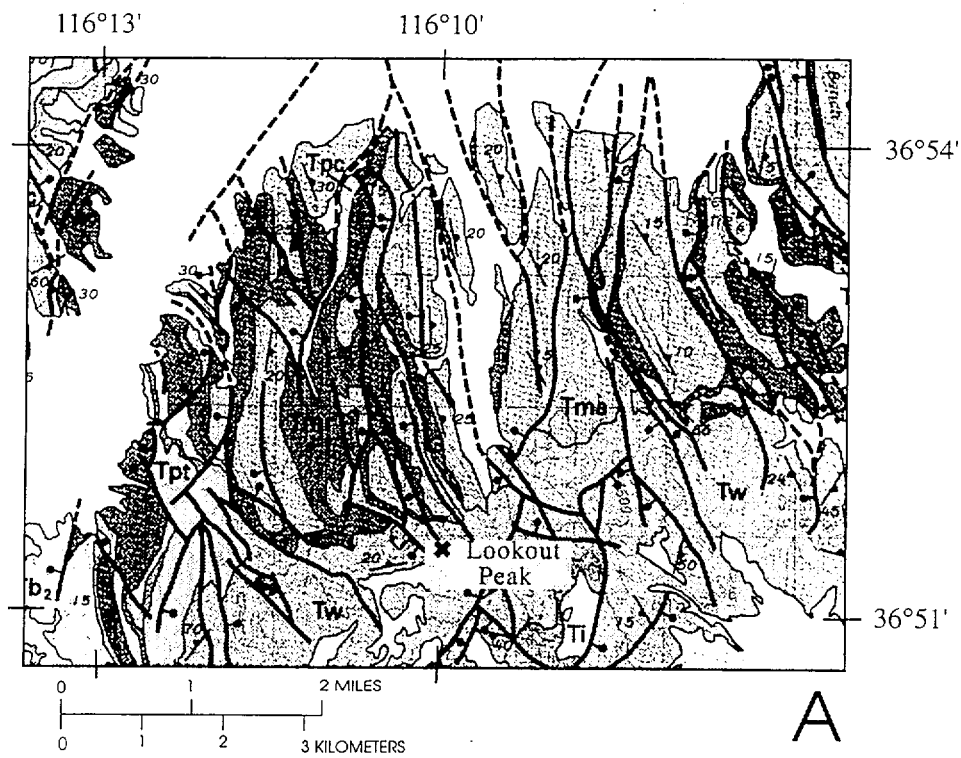


Figure 6. Fault system interpreted to be, in part, a "breakaway" zone along the eastern side of the Kawich-Greenwater Rift, showing the concentration of faults in the eastern part of the rift, within and adjacent to the Silent Canyon and Crater Flat-Prospector Pass calderas. Structure of resurgent domes is omitted, and faults outside the rift zone or within Timber Mountain caldera are not shown.



B

Figure 10. A. pattern of faults and unit contacts along the southern part of Mid Valley: Tw=Wahmonie Formation; Tpc, Tpt= Paintbrush Group; Tmr, Tma= Timber Mountain Group (from Frizzell and Shulters). B. aerial photograph shows physiography of same area.



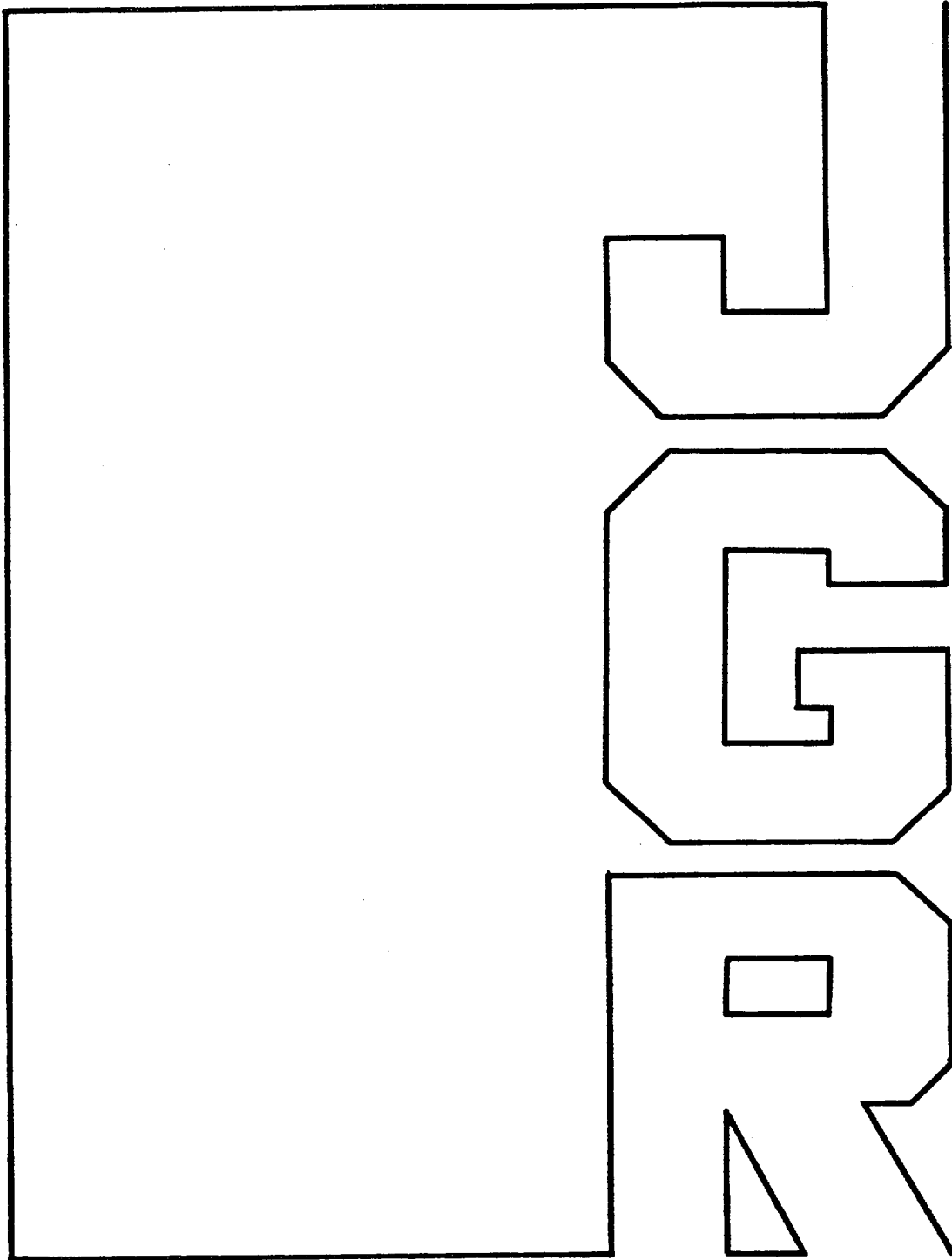
FIGURE 77. Aerial view of the southeast part of the Volcanic Tableland showing systems of an echelon faults. Fish Slough extends across the lower right corner of photograph.
Photo by Roland von Huene.

TECTONIC IMPLICATIONS

1. Presently, extension in the Walker Lane is confined to local deep holes and to domain boundaries. Many of the holes have the style of oblique pull-aparts or half graben. In a cooling, strengthening crust these holes may concentrate stress deeply enough to guide basalt intrusion. Crater Flat basin may have originated as a sector graben of the Claim Canyon caldera, formed initially as a tear within the more broadly extending Amargosa trough during the period of caldera activity.
2. Post-11.4 Ma extension in Crater Flat probably activates pre-caldera structures as well as post-12.7 Ma north-striking faults at Yucca Mountain and Pahute Mesa. However, much of the fault structure at Yucca Mountain is in the style of a complex slab slide; it suggests that the volcanic carapace has fragmented and partly slid into the widening/deepening Crater Flat basin, although this may be an early, no longer active feature of the mountain's history.
3. If Yucca Mountain faults are not antithetic to the Bare Mountain fault, the BMF and the BBFs could be tectonically linked to a common axial rift-like extension center aligned NNE within Crater Flat basin. This suggests that rare episodes of basaltic volcanism attend BBF fault activity, but not necessarily vice versa.
4. Seismogenic faults at Yucca Mountain are no longer than about 25 km - the length of Yucca Mountain in Crater Flat basin (except for the Paintbrush Canyon fault). Depth of most faults is confined to the volcanic carapace and some relatively small thickness of the infrastructure. The carapace probably rests directly on an unknown thickness of lower Tertiary strata different from the tuffs (i.e Titus Canyon/Pavits Spring strata) which may have acted as a weak layer (quasi detachment), especially toward the deeper part of the basin. Deep BBFs may transition into faults that are down to basin faults in the Paleozoic but have different attitudes and linkages (are more complex) than any seen at the surface.
5. The most tectonically significant faults in the Crater Flat domain may be the Bare Mountain fault and the Paintbrush Canyon-Stage Coach Road faults.

Low-angle normal faults and seismicity: A review

Brian Wernicke



Low-angle normal faults and seismicity: A review

Brian Wernicke

Division of Geological and Planetary Sciences, California Institute of Technology, Pasadena



Abstract. Although large, low-angle normal faults in the continental crust are widely recognized, doubts persist that they either initiate or slip at shallow dips ($<30^\circ$), because (1) global compilations of normal fault focal mechanisms show only a small fraction of events with either nodal plane dipping less than 30° and (2) Andersonian fault mechanics predict that normal faults dipping less than 30° cannot slip. Geological reconstructions, thermochronology, paleomagnetic studies, and seismic reflection profiles, mainly published in the last 5 years, reinforce the view that active low-angle normal faulting in the brittle crust is widespread, underscoring the paradox of the seismicity data. For dip-slip faults large enough to break the entire brittle layer during earthquakes ($M_w \sim 6.5$), consideration of their surface area and efficiency in accommodating extension as a function of dip θ suggests average recurrence intervals of earthquakes $R' \propto \tan \theta$, assuming stress drop, rigidity modulus, and thickness of the seismogenic layer do not vary systematically with dip. If the global distribution of fault dip, normalized to total fault length, is uniform, the global recurrence of earthquakes as a function of dip is shown to be $R \propto \tan \theta \sin \theta$. This relationship predicts that the frequency of earthquakes with nodal planes dipping between 30° and 60° will exceed those with planes shallower than 30° by a factor of 10, in good agreement with continental seismicity, assuming major normal faults dipping more than 60° are relatively uncommon. Revision of Andersonian fault mechanics to include rotation of the stress axes with depth, perhaps as a result of deep crustal shear against the brittle layer, would explain both the common occurrence of low-angle faults and the lack of large faults dipping more than 60° . If correct, this resolution of the paradox may indicate significant seismic hazard from large, low-angle normal faults.

Introduction

It is appropriate for the 75th anniversary of the American Geophysical Union that recognition be given to the 50th anniversary of a paper by Longwell [1945]. Although not the first description of such phenomena [e.g., Ransome *et al.*, 1910], the paper was remarkable in its documentation using maps, photographs, and cross sections of spectacularly exposed normal faults in the Las Vegas region, with displacements of 1–2 km and dips of 0 – 30° . In one large-scale exposure, since partly drowned beneath the waters of Lake Mead, a fault was observed to flatten downward, from about 30° to 5° over a cross-sectional depth of 600 m.

It is perhaps a measure of a theoretically based prejudice against low-angle normal faults that Longwell [1945] excluded regional crustal extension as a cause for faulting. He instead interpreted them to result from extension on the crests of large-scale compressional anticlines. Mechanical arguments for downward flattening (listric) normal faults date back at least to McGee [1883], but Hafner [1951], citing Longwell's [1945] observations, showed that certain loading conditions along the base of an elastic plate induce curvature of stress trajectories favorable for the formation of low-angle normal faults.

Despite both observation and theory, the assumption that the least principal stress direction is horizontal throughout an extending crust [e.g., Anderson, 1942] held sway for the suc-

ceeding three decades. Low-angle extensional structures, though documented by geological mapping studies, were interpreted as either peculiar thrust faults or surficial landsliding phenomena. Sliding and spreading of rootless, internally coherent, extended allochthons along faults dipping only a few degrees is well known. It includes cases where detachment occurs along incompetent horizons in sediments such as shale or salt, as developed over thousands of square kilometers in the northern Gulf of Mexico [Worrall and Snelson, 1989]. However, it also includes examples where the sliding occurs within competent horizons, as in the Ordovician dolostones along the Heart Mountain detachment [Pierce, 1957; Hauge, 1990]. These examples generally involve only the upper few kilometers of the crust and are not accompanied by coeval extension of the underlying continental basement. In contrast, fault systems in the Basin and Range, such as those described by Longwell [1945], clearly involve continental basement and are observed in some cases to cut structurally downward through 10 km or more of the crust.

Beginning with a handful of Basin and Range field studies [e.g., Anderson, 1971; Wright and Troxel, 1973; Proffett, 1977], it was not until the late 1970s that the numerous documented low-angle normal faults gained a measure of acceptance as a direct expression of large-magnitude continental extension. At about the same time, it was also realized that many metamorphic tectonites in the Basin and Range previously thought to be Mesozoic or Precambrian in age were actually Tertiary [e.g., Davis and Coney, 1979]. In many cases these rocks lay in the footwalls of regionally extensive low-angle normal faults or "detachments" that could be traced for several tens of kilometers parallel to their transport directions. By 1980, it was clear

Copyright 1995 by the American Geophysical Union.

Paper number 95JB01911.
0148-0227/95/95JB-01911\$05.00

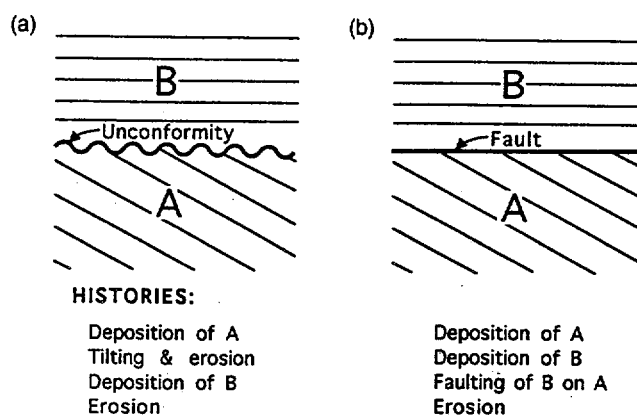


Figure 1. Contrast in geological history from interpreting a contact between older sedimentary sequence A and younger sequence B as (a) an unconformity and (b) a low-angle normal fault.

that numerous isolated exposures of detachments and their metamorphic substrate formed a nearly continuous belt from Sonora, Mexico, to southern British Columbia, referred to as the Cordilleran metamorphic core complexes [Crittenden *et al.*, 1980; Armstrong, 1982]. It was realized that the footwalls of many exposed detachments were not strongly metamorphosed in the Tertiary, raising the possibility that low-angle normal faults formed and were active entirely in shallow crust [e.g., Wernicke *et al.*, 1985; Spencer, 1985; Dokka, 1986; John, 1987].

These observations ran counter to Jackson and White's [1989] descriptive synthesis of some 56 earthquakes on active continental normal faults. They concluded that (*italics theirs*)

Among the most important observations that now influence the debate are . . . that large earthquakes do *not* occur on listric faults that flatten at shallow depths (as originally thought: e.g. McKenzie, 1978a, b), but on faults that are steep throughout the seismogenic upper crust . . .

Whether or not this conclusion is correct is a first-order problem in understanding the structure and dynamics of the lithosphere.

Geological Significance

The recognition of low-angle normal faults and the core complex tectonic association is now global and includes oceanic lithosphere as well as the continents [e.g., Mutter and Karson, 1992]. The significance of these structures for geology as a whole may be illustrated by considering an unexposed low-angle contact roughly parallel to overlying, younger sedimentary unit B but discordant to underlying sedimentary (or metamorphic) unit A (Figure 1). Prior to 1980, many geologists would have interpreted such a contact as either an unconformity or a thrust fault. The possibility of the contact being a normal fault may have been overlooked on the basis that known low-angle fault contacts were restricted to thrusts, which generally emplace older rocks on younger. The geologic histories for these two cases are of course markedly different (Figure 1). The Basin and Range provides numerous case histories of the problem, where contacts between Tertiary and underlying pre-Tertiary strata, in some cases with high angle between the contact and Tertiary strata, were interpreted as unconformities. For example, low-angle contacts mapped by Kennitzer [1937], Fritz [1968], and Dibblee [1970] as unconfor-

mities have since been documented to be low-angle normal faults (Davis *et al.* [1980], Gans *et al.* [1989], and Dokka [1986], respectively). Similarly, major low-angle fault systems interpreted as thrusts by Noble [1941], Misch [1960], and Drewes and Thorman [1978] are now widely regarded as normal faults related to Cenozoic extension (Wright and Troxel [1984], Miller *et al.* [1983], and Dickinson [1991], respectively). Reinterpretations currently underway in other mountain belts are similarly profound.

These Basin and Range field relations represented a class of geologic contact that had not been previously recognized as a fundamental tectonic element. Recognizing them as such is as basic to accurate historical inference in geology as, for example, the knowledge that rocks with igneous texture intrude their surroundings in a molten state.

Mechanical Significance

The fact that low-angle normal faults are not predicted by Andersonian theory is also fundamental to interpreting the stress state and physical constitution of the crust. In the 1980s, debate centered on the kinematics of generating the core-complex association. Most current models suggest asymmetrical denudation along large normal faults that transect the upper 15–20 km of the crust at low angle, accompanied by isostatic rebound and flexure of the unloaded footwall [e.g., Wernicke, 1981; Howard *et al.*, 1982; Allmendinger *et al.*, 1983; Spencer, 1984; Wernicke, 1985; Davis *et al.*, 1986; Wernicke, 1992]. Recently, controversy has centered on the initial dip and subsequent modification of these faults and the roles of footwall metamorphic tectonite and magmatism.

This paper addresses the question: Are brittle low-angle normal faults active while at low dip? A number of authors have expressed doubt that shallowly dipping normal faults are important features in the extending seismogenic crust, pointing to Andersonian theory and a lack of seismicity on such faults [e.g., Buck, 1988; King and Ellis, 1990]. A large body of literature has nonetheless focused on non-Andersonian explanations for active low-angle normal faulting [e.g., Xiao *et al.*, 1991; Forsyth, 1992; Axen, 1992; Parsons and Thompson, 1993]. If low-angle normal faults are indeed active in the seismogenic crust, why are there so few, if any earthquakes observed on them? Evidence summarized below, mostly published in the last 5 years, tends to reinforce this paradox. A simple mechanical model relating fault dip to earthquake recurrence is developed that may provide an explanation.

Observations of Low-Angle Normal Faults

Andersonian theory predicts that extension of the crust results in faults that initially dip 60° but provides no insight as to how such faults with large finite slip develop kinematically. For example, normal faults may rotate during and after their slip history, as in the case of a system of "domino-style" or "book-shelf" fault blocks [Wernicke and Burchfiel, 1982], in which case, dips lower than 60° are generally expected [e.g., Thatcher and Hill, 1991]. The key questions are whether a given fault in the seismogenic part of the crust was active at shallow dip, and whether the fault initiated at shallow dip. Low-angle normal faults present no conflict with Andersonian theory if, for example, they initiate at 60° and rotate down to 30° while active and are then further rotated to very low angle while inactive by a younger set of domino-style faults [Morton and Black, 1975; Proffett, 1977; Miller *et al.*, 1983]. Clearly, many low-angle normal faults, including most of those described by Longwell

[1945], cut upper crustal sedimentary layers at high angle and therefore probably had steep original dip.

A compilation of all well-determined focal mechanisms of normal fault earthquakes ($M_w > 5.2$, using moment-magnitude scale of Kanamori [1977]) in continents with nearly pure dip-slip movement (56 events) showed that most nodal planes dip between 30° and 60° [Jackson, 1987; Jackson and White, 1989]. A subset of those events where the fault plane is resolved by surface rupture (15 events) showed no faults with dip less than 30°. Based on this survey, many workers have stressed the uniformitarian interpretation ("the present is the key to the past") that all low-angle normal faults dipping less than 30° are rotated while inactive from dips greater than 30°, either by younger high-angle faults or by isostatic adjustment [e.g., Buck, 1988; Gans et al., 1989; King and Ellis, 1990].

Others argued that although such rotations may be common, initiation and slip on shallow (<15 km depth) normal faults are required by geological and geophysical data [e.g., Wernicke et al., 1985; John, 1987; Wernicke and Axen, 1988; Davis and Lister, 1988; Yin and Dunn, 1992; Scott and Lister, 1992; Dokka, 1993; Axen, 1993]. These data include geologic reconstructions and fault rocks associated with detachments, thermochronologic and paleomagnetic investigations of exposed detachment footwalls, and seismic reflection profiles.

Geologic Reconstructions

A direct approach to resolving whether normal faults either slip or initiate at low-angle is restoration of well-constrained geologic sections. In the U.S. Cordillera, some low-angle normal faults cut abruptly downward through 10 km or more of preextensional strata and crystalline basement (e.g., Mojave Mountains, Arizona [Howard and John, 1987]; Egan Range, Nevada [Gans et al., 1989]; South Virgin Mountains, Nevada [Fryxell et al., 1992]; and Priest Lake area, Idaho [Harms and Price, 1992]). These fault systems cut through uppermost crustal levels (<1 km) at their shallow ends. In other instances, however, the increase in footwall structural depth is small in comparison to exposed downdip length of the footwall. This seems especially true where detachment systems cut across wide (30–50 km) areas of deeper crustal rocks (~5–15 km paleodepth), as in most core complexes. Some examples include the Raft River Range, Utah [Compton et al., 1977; Malaveielle, 1987; Manning and Bartley, 1994]; the Ruby Mountains–East Humboldt Range area, Nevada [Mueller and Snoke, 1993]; the Black Mountains, California [Holm et al., 1992]; the Chemehuevi Mountains, California [John, 1987]; the Harcuvar and Buckskin Mountains, Arizona [Spencer and Reynolds, 1991]; the South Mountains, Arizona [Reynolds, 1985]; and the Catalina-Rincon Mountains, Arizona [Dickinson, 1991]. In some instances, however, faults transect even the upper 7–8 km of the crust at low average initial dip [e.g., Wernicke et al., 1985; Axen, 1993].

An example of the latter may be found in the Mormon Mountains–Tule Springs Hills area of southern Nevada [Wernicke et al., 1985; Axen et al., 1990; Axen, 1993]. Two Miocene detachments are superimposed on the frontal decollement thrust of the Cordilleran fold and thrust belt [e.g., Burchfiel et al., 1992], including the Mormon Peak detachment [Wernicke et al., 1985] (Figure 2) and the Tule Springs detachment [Axen, 1993]. The Mormon Peak detachment cuts downward from the hanging wall of the thrust into its footwall (Figure 2), such that the angles between the detachment and (1) the thrust ramp

and subparallel allochthonous strata and (2) the autochthonous strata below the thrust are defined within a few degrees (α and β , respectively, Figure 3). The angles between prerift Miocene volcanic and sedimentary strata and (1) strata in the thrust ramp and (2) autochthonous strata of the foreland just in front of the thrust plate are also well defined (γ and δ , respectively, Figure 3). Assuming west dipping allochthonous strata of the thrust ramp zone above and below the detachment were parallel, the dip of the detachment with respect to the prerift Miocene strata is

$$\theta_i = \gamma - \alpha \approx 20^\circ.$$

Thrust loading presumably would have deflected the autochthonous strata to westward dip ϕ relative to the undeformed foreland (Figure 3). For undisturbed thin-skinned foreland thrust belts worldwide and especially the Cordilleran belt, this deflection is generally no more than about 5° [e.g., Price, 1981; Royse et al., 1975; Allmendinger, 1992; Royse, 1993]. Assuming low ϕ ,

$$\theta_i < \beta + \phi + \delta < 27^\circ.$$

Therefore two independent observations, (1) the detachment's relations with the thrust ramp and overlying Tertiary and (2) its relations with the thrust autochthon and overlying Tertiary, both suggest an initial dip of the Mormon Peak detachment of about 20°–27° [Wernicke et al., 1985].

The initial dip of the Tule Springs detachment is also clearly defined [Axen, 1993] (Figure 3). The detachment runs subparallel to the thrust plane where it overrides autochthonous strata for a horizontal distance of at least 10 km. Thus the detachment initiated at the dip of the decollement thrust and the autochthonous strata prior to extension. In addition to this constraint, the unconformity between synrift strata and allochthonous strata is not markedly angular (Figure 3). Detailed consideration of these constraints, including reconstruction of the detachment's hanging wall, suggest an initial dip in the range 3°–15° [Axen, 1993].

The Mormon Mountains–Tule Springs Hills detachment system is among the best exposed upper crustal, low-angle normal fault systems in the world, but it is not clear how typical its low upper crustal initiation angles are compared with active slip at low angle on more deeply exhumed structures. The anisotropy of shallowly west dipping thrusts and bedding in the thin-skinned thrust belt may have somehow played a role in generating the low initial dips. Seismic reflection data to the north along the frontal Cordilleran thrust belt also suggest shallow crustal normal faults with low initial dips developed just west of the frontal thrusts [e.g., Bally et al., 1966; Royse et al., 1975; Allmendinger et al., 1983; Smith and Bruhn, 1984; Planke and Smith, 1991]. The Mormon Mountains–Tule Springs Hills area lies at a point where these extensional structures begin to cut southward well into the cratonic foreland of the thrust belt, thereby exhuming the frontal most thrusts from paleodepths of 7–8 km.

A second example of shallowly dipping normal faults in the uppermost crust occurs in the Whipple Mountains area of southeastern California and west central Arizona [Davis and Lister, 1988; Scott and Lister, 1992]. There, several large areas of hanging wall synrift strata (either flat-lying or cut by high-angle normal faults of opposing dips) are truncated from below by the very shallowly dipping Whipple-Buckskin detachment system. The depth to the active detachment system, con-

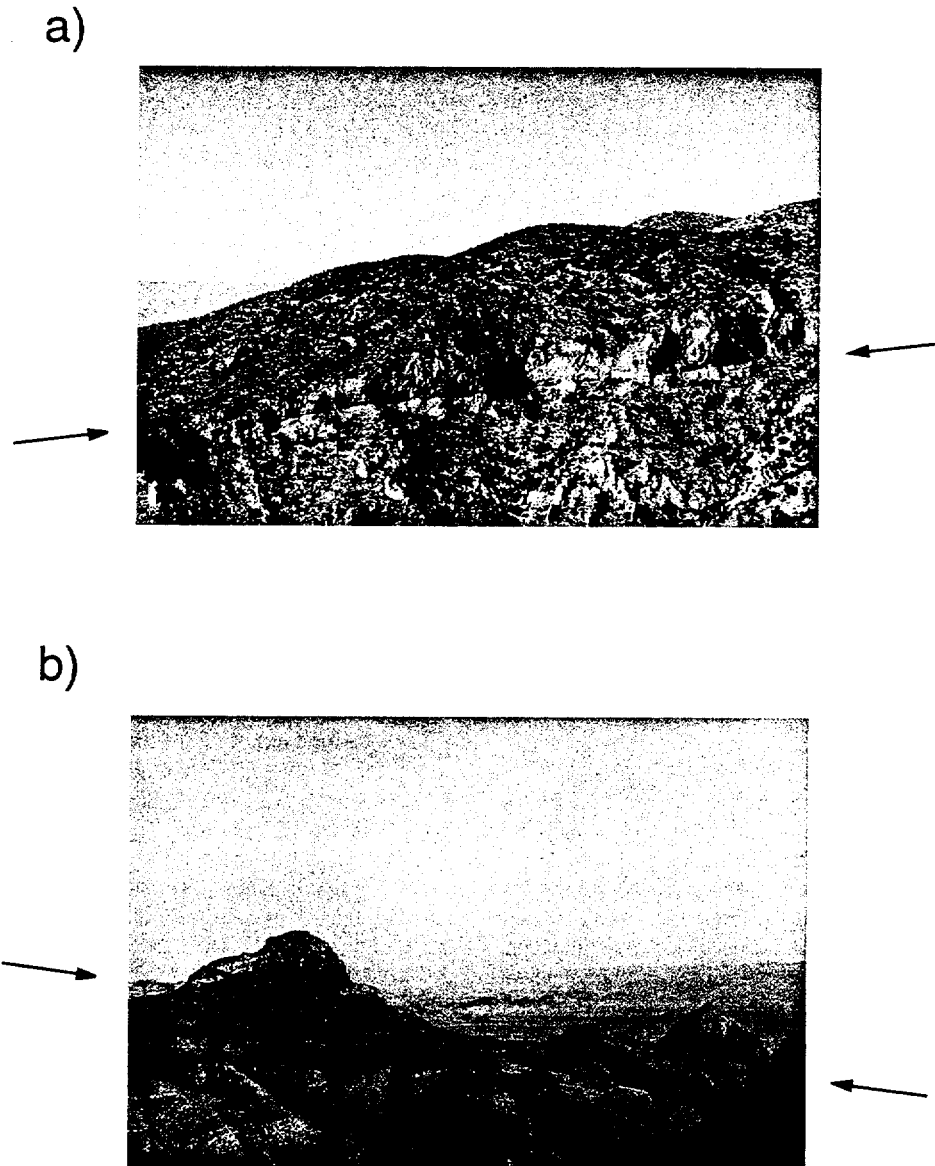


Figure 2. Photographs of Mormon Peak detachment, Nevada. (a) Looking north, western Mormon Mountains, fault (between arrows) emplaces Carboniferous strata over Cambrian. Cliff on right side is approximately 50 m high. (b) Looking south, western Mormon Mountains, detachment (planar topographic bench between arrows) cuts at about 5° across footwall Cambrian strata (light and dark banding, lower left). Hanging wall comprises three blocks of imbricately normal faulted Ordovician through Carboniferous strata, variably tilted to the left. There is approximately 600 m of relief from valley in foreground to high peak on left.

strained by the thickness of synextensional strata, was less than 2–3 km. These relations argue strongly for a low initial dip for the fault initially cutting through hanging wall strata, although it does not constrain the trajectory through the footwall, which likely had a more complex history [Davis and Lister, 1988]. In addition, the base of a large syntectonic landslide mass derived from the exposed footwall was deposited across the detachment system subparallel to the fault plane, offset some 10 km along it, and later cut by normal faults which are in turn cut by the detachment [Yin and Dunn, 1992].

Field geologic relations are fundamental to understanding detachment geometry and kinematics. Additional data, including thermochronology, paleomagnetic data, seismic reflection profiling, and seismicity, are required to test competing models for their evolution. In general, geologic reconstructions suggest

a biplanar or listric geometry for major normal faults, with highly variable depth of flattening ranging from less than 5 km to more than 10 km preextensional depth [e.g., Spencer and Reynolds, 1991; Wernicke, 1992], a conclusion largely reinforced by these additional data.

Thermochronologic Data

An important tool for addressing the original configuration of crustal-scale normal faults is the thermal history of their footwalls, especially where there are wide exposures in the transport direction of the fault. Published applications of this method include just a few examples, mainly in the central and southern Basin and Range, and so the results may be geographically biased. Generally, the time of footwall unroofing is

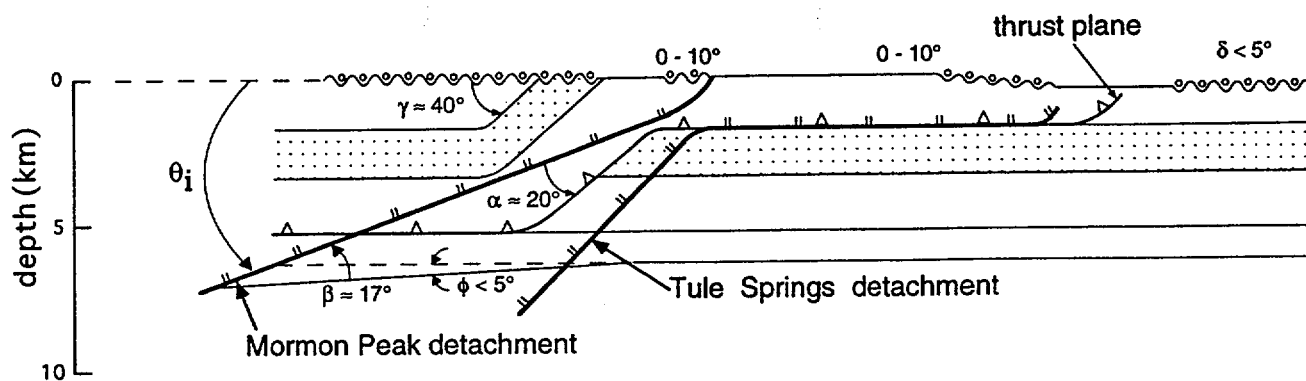


Figure 3. Reconstruction of Mormon Peak and Tule Springs detachments, slightly modified from *Axen et al.* [1990] and *Axen* [1993] for clarity. Thick lines with double ticks, detachments; line with teeth, thrust fault; wavy line with dots, sub-Tertiary unconformity; other thin lines, various stratigraphic contacts. See text for discussion.

clearly expressed by rapid cooling events between 400°C and 100°C. The ambient temperature of most footwalls (excluding cooling of synrift plutons) is usually well below the Ar retention temperature in hornblende (450–500°C) and close to that for retention in micas, or about 300–400°C [e.g., *Richard et al.*, 1990; *John and Foster*, 1993; *Holm and Dokka*, 1993; *Dokka*, 1993]. A pattern emerging from these studies in the Cordillera is that deeper portions of the footwall cool from these temperatures to less than 100°C (fission track annealing temperature in apatite) in a period of 1–10 m.y. [e.g., *Holm and Dokka*, 1993].

In most examples it is possible to establish the maximum variation in temperature across the exposed footwall immediately prior to the thermal perturbation caused by unroofing. Given the downdip temperature variation across the footwall prior to unroofing, the average dip of the fault can be determined for variable assumptions of the preextensional geothermal gradient. This technique has been employed for a number of extensional terrains in the Cordillera, where footwall strain, including elongation via detachment-related shearing or post-detachment normal faulting, and transient effects from syntectonic intrusions, may be taken into account. The paleothermal field gradient (preunroofing, downdip thermal gradient of the exposed footwall) between two points A and B with temperature difference ΔT is related to the paleogeothermal gradient by the average dip of the fault (Figure 4), which is

$$\theta = \sin^{-1} \frac{dT/dw}{dT/dz} \quad (1)$$

where dT/dz is the geothermal gradient just prior to unroofing and dT/dw is the measured field paleothermal gradient.

The overall range of field paleothermal gradient, with uncertainties, is 0–33°C/km, measured across downdip distances of 6–40 km (Figure 4). The two highest gradients are from the upper 5–10 km paleodepth (Piute and Harcuvar detachments, shown as solid symbols in Figure 5), while the other, deeper examples range from 0 to 19°C/km.

The ambient geothermal gradient in the Basin and Range prior to unroofing has been determined in several areas where the time-temperature history has been determined from rocks of independently estimated paleodepth. For eastcentral Nevada, the average geothermal gradient at 35 Ma was about 20°C/km in the upper 10 km of the crust prior to unroofing [*Dumitru et al.*, 1991]. In the Gold Butte area of southern Nevada, an apatite fission track study indicates a gradient of

about 25–30°C/km at 15 Ma in the upper 3–4 km of the crust [*Fitzgerald et al.*, 1991]. In the eastern Mojave Desert region, rather higher gradients at about 18 Ma of $50 \pm 20^\circ\text{C}/\text{km}$ for the Piute Mountains and a range of 30–50°C/km for the Chemehuevi Mountains have been suggested [*Foster et al.*, 1991; *John and Foster*, 1993]. In the Death Valley region, ambient temperatures at 10–15 km depth at 8–10 Ma were about 300–350°C, suggesting a range of 25–35°C/km [*Holm and Wernicke*, 1990; *Holm et al.*, 1992]. Possible gradients near or above 50°C/km in the eastern Mojave region are determined for a time near the end of a major magmatic episode and are probably relatively transient. Thus a range in gradients of 20–35°C/km would probably represent the average upper crustal paleogeothermal gradient in most areas of the Basin and Range since mid-Tertiary time, in agreement with the geotherms of *Lachenbruch and Sass* [1978], with magmatic and extensional strain locally raising it to 2 or perhaps 3 times that amount.

A plot of field paleothermal gradient determined from Figure 5 versus paleogeothermal gradient, contoured in initial dip according to equation (1), is shown in Figure 6. In these examples, fault rocks show evidence of brittle extensional faulting and cataclasis, but major bulk elongations of the entire footwall block, particularly in the brittle field, are unlikely. These data suggest that although some sections yield dips as high as 45°–60° at the extremes of their uncertainties, most of the data suggest initial dips of less than 30°. The two examples yielding the highest dips (SW Harquahala Mountains and Piute Range) involve relatively short transects across uppermost parts of the crust (Figure 6). The Gold Butte example may also have a high average dip (up to 45°), but it too involves uppermost crustal rocks in its shallow part (<5 km paleodepth) where the denuding fault originally dipped about 60° [*Fryxell et al.*, 1992; *Fitzgerald et al.*, 1991], and hence the fault probably flattened downward to its deepest exposures in order

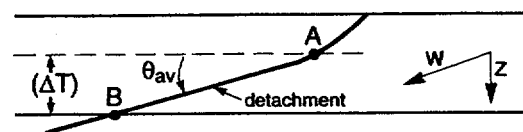


Figure 4. Diagram showing variables used to derive relationship between field paleothermal gradient, paleogeothermal gradient, and fault dip between points A and B (equation (1)). See text for discussion.

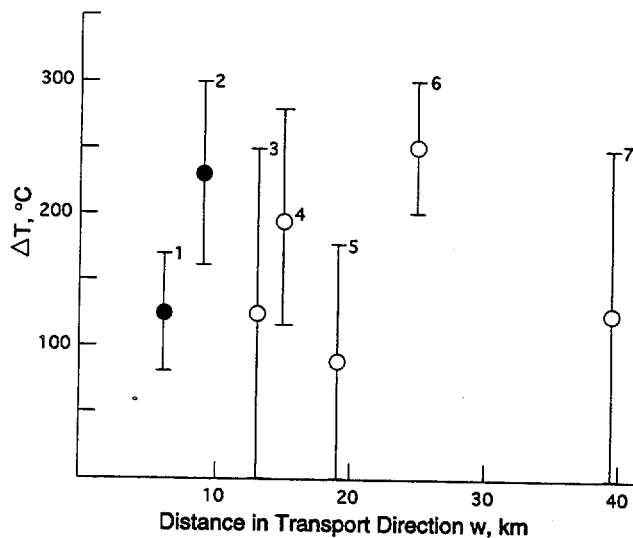


Figure 5. Maximum variation of paleotemperature in down-dip direction across footwalls of Cordilleran detachments, just prior to unroofing. Solid symbols indicate upper crustal sections only. Locations and sources: 1, Piute Mountains detachment, eastern Mojave Desert, California [Foster *et al.*, 1991]; 2, southwestern Harcuvar Mountains, west central Arizona [Richard *et al.*, 1990]; 3, Garden Wash detachment, South Virgin Mountains, Nevada [Fitzgerald *et al.*, 1991; Fryxell *et al.*, 1992; J. E. Fryxell, unpublished data 1994]; 4, Chemehuevi Mountains detachment, lower Colorado River trough, California [John and Foster, 1993]; 5, Newberry Mountains detachment, central Mojave Desert, California [Dokka, 1993]; 6, Amargosa detachment, Death Valley region, California [Holm and Wernicke, 1990; Holm *et al.*, 1992; Holm and Dokka, 1993]; 7, Buckskin-Rawhide detachment, lower Colorado River trough, Arizona [Richard *et al.*, 1990; Spencer and Reynolds, 1991].

to maintain even a high extreme of average dip at 45°. The remaining four examples, all from relatively wide, deep exposures, suggest average initial dips of 30° or less.

In summary, thermochronology that allows comparison of field paleothermal gradient with paleogeothermal gradient prior to unroofing is a useful means of constraining the initial configuration of large normal faults. In general, the field gradient is less than 1/2 the value of the paleogeothermal gradient, corresponding to initial fault dips of 30° or less (equation (1)). Faults where the initial dip may be significantly over 30° seem to be restricted to high crustal levels.

Paleomagnetic Data

Paleomagnetic studies are also a potentially useful method for determining the initial dip of normal faults. If pretilt or syntilt magnetizations can be identified, they provide quantitative estimates, at relatively high precision, of the original and syntectonic dip of the detachment. To date, only two such studies have been published for core complexes with wide downdip exposures of midcrustal rocks, including the South Mountains, Arizona [Livaccari *et al.*, 1993, 1995], and the Black Mountains, California [Holm *et al.*, 1993]. In both areas, largely undeformed intrusive rocks from the detachment footwalls span much of the history of ductile deformation and rapid unroofing.

The South Mountains footwall is exposed for approximately 20 km in the transport direction and is composed of Protero-

zoic basement intruded by four groups of intrusives, including two discrete plutons and two sets of younger dikes [Reynolds, 1985]. Superposition relations of the intrusive suite indicate unroofing and ductile shearing began shortly after intrusion of the older pluton [Reynolds, 1985]. The older dikes intruded late in the history of ductile deformation, while the younger dikes intruded during brittle deformation, late in the unroofing history [Livaccari *et al.*, 1993, 1995; Fitzgerald *et al.*, 1993]. Thermochronologic data indicate rapid cooling of footwall rocks between 22 and 17 Ma, from solidus temperatures in the oldest intrusion to 300°C between 22 and 20 Ma, then from 300°C to below 100°C from 20 to 17 Ma [Fitzgerald *et al.*, 1993].

Paleomagnetic data indicate concordance of high-coercivity, high unblocking temperature magnetizations with early Miocene expected directions for all four intrusive suites [Livaccari *et al.*, 1993, 1995]. These data suggest unroofing along a fault with initial dip of about 10°.

The Black Mountains example has a more complex history. In structurally deep portions of the detachment footwall, an 11.7 Ma mafic intrusive complex is locally ductilely deformed and folded along with Proterozoic country rocks [Asmerom *et al.*, 1990; Holm and Wernicke, 1990; Mancktelow and Pavlis, 1994]. It is intruded by silicic plutons and mafic to silicic dikes ranging in age from ~9 to 6.5 Ma which largely escaped ductile deformation [Holm *et al.*, 1992]. Rapid cooling and unroofing of the entire complex from over 300°C to less than 100°C occurred between ~8.5 and 6.0 Ma [Holm and Dokka, 1993].

High unblocking temperature, high-coercivity magnetizations from the younger group of intrusions may be restored to their Miocene expected directions by a 50°–80° counterclockwise rotation about a vertical axis, interpreted as deformation associated with postunroofing dextral-oblique shear on the Death Valley fault zone [Holm *et al.*, 1993; Mancktelow and Pavlis, 1994]. These plutons do not show a significant inclination anomaly. Subtracting the vertical axis rotation from the directions in the early mafic intrusion, an additional tilt of, in total, some 20°–40° is required to restore the mean direction from this intrusion into agreement with a Miocene expected direction [Holm *et al.*, 1993]. There is considerable between-

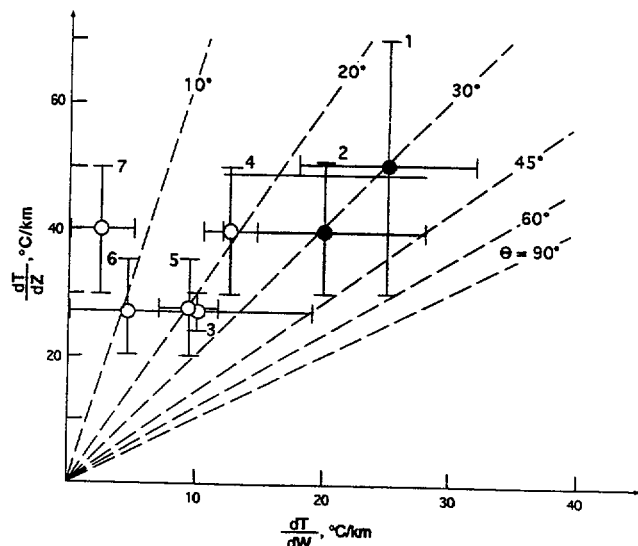


Figure 6. Plot of paleogeothermal gradient dT/dz versus field paleothermal gradient dT/dw for the seven detachments; solid symbols indicate upper crustal examples from Figure 5.

site dispersion (up to 90°) in high-temperature, high-coercivity magnetizations from the mafic complex, possibly resulting in part from postintrusive folding, and thus it is difficult to precisely determine the net tilt. However, since the oldest silicic plutons predate rapid cooling of the complex, little or no net tilt occurred during unroofing between 8.5 and 6.0 Ma. Thermochronologic data suggest rapid unroofing is time transgressive in a downdip direction, which may support the concept of a "rolling hinge" (discussed in more detail below) moving through the footwall rocks during denudation, and thus it is possible the detachment may have briefly had a steeper dip during unroofing [Holm and Dokka, 1993; Holm et al., 1993].

These two examples, while both suggesting little net tilt as a result of unroofing, also demonstrate the potential of the approach, especially for crystalline rocks that characterize many detachment footwalls. Contrasts in the overall history of the two examples, however, suggests many surprises lie ahead for paleomagnetic studies of detachment complexes.

Seismic Reflection Profiles

Interpretations of seismic reflection data have played a major role in developing an awareness of low-angle normal faults, particularly in the geophysical community [e.g., Bally et al., 1981; Wernicke and Burchfiel, 1982; Allmendinger et al., 1983; Smith and Bruhn, 1984]. Hundreds of profiles, most of them unpublished, from a broad spectrum of extensional environments show strong, shallowly dipping reflections from low-angle fault planes that bound asymmetric half graben, often projecting up to surface exposures of the faults. These data strongly suggest low-angle (<30°) normal faults are common features in the upper 15 km of the continental crust.

Because the data are usually proprietary, the exact location of the line, velocity control, and the possible effects of migration are often not presented in publications. Thus with much of the data, "sideswipe" of a steeper fault such that it appears to be low-angle, "pull-down" of the shallow part of the fault due to low-velocity basin fill, and steepening of the fault plane reflection upon migration are important caveats in evaluating whether any given fault is a low-angle normal fault. However, such data are normally acquired perpendicular or parallel to structural trends in the area, mitigating the problem of sideswipe. Pull-down is also not usually a major effect on fault dip. For a typical section, the shallow part of the normal fault is imaged downdip for at least 10 km, structural relief on the basin fill-bedrock contact in the hanging wall is less than 3 km, and basin fill velocity is on average greater than half that of bedrock (e.g., parameters for a typical basin in the Basin and Range [Smith et al., 1989]). Using these extremes for a 10-km segment of fault, the apparent dip on a time section is no more than 10°–12° less than the true dip. Migration of reflections also serves to steepen dips but at large scale with dips less than 30° the dip of a given reflection is not significantly increased.

Among the best documented images of shallow listric fault phenomena are from the northern Gulf of Mexico, where large-scale slumping of passive margin shelf strata toward the slope along a salt décollement is the underlying cause of faulting, rather than whole crust extension [e.g., Worrall and Snelson, 1989].

The most spectacular seismic image of a basement-involved, upper crustal low-angle normal fault (or for that matter, of any fault) is the Consortium for Continental Reflection Profiling (COCORP) and related profiles across the Sevier Desert de-

tachment in the Basin and Range province of west central Utah [Allmendinger et al., 1983]. This profile revealed a strong, continuous, multicyclic reflection that cuts from the surface, along a major range front, down to over 5 s two-way travel time (12–15 km depth) with an average dip of 12° to the west [Allmendinger et al., 1983, Figure 2]. As shown by a grid of industry profiles and well data along its shallow, eastern portion, Cenozoic half graben above the reflection are bounded by relatively steep faults that do not offset it [e.g., McDonald, 1976; Planke and Smith, 1991]. These data also show that the detachment covers an area of at least 7000 km².

The position of the reflection within the east directed Cordilleran thrust belt led to the early interpretation that the reflection was a thrust fault, reactivated as a Cenozoic extensional structure [e.g., McDonald, 1976]. The geometric similarity of the seismic profiles to exposed Cordilleran detachment systems led to the suggestion that the reflection was primarily a Cenozoic normal fault which may not have been a reactivated thrust, since many detachments do not appear to reactivate old thrusts [Wernicke, 1981; Anderson et al., 1983; Allmendinger et al., 1983; Wernicke et al., 1985; Allmendinger et al., 1986] (Figure 2).

This long-standing interpretation of well and reflection data has recently been challenged, primarily based on a comparison of microstructures from drill cuttings taken near the reflection with those of the Muddy Mountain thrust, a major décollement thrust fault in southern Nevada [Anders and Christie-Blick, 1994]. In two wells, the reflection is a contact between Tertiary sandstone and Paleozoic carbonate, while the Muddy Mountain thrust emplaces Paleozoic carbonate over Mesozoic sandstone. Along the Muddy Mountain thrust, microfracture density in cataclasites within a few meters of the fault is at least a factor of three higher than in surrounding rocks [Brock and Engelder, 1977]. The cuttings, however, revealed no evidence of dense microfracturing near the contact, which was therefore interpreted as an unconformity rather than a fault [Anders and Christie-Blick, 1994].

The difficulties in establishing any contact relation from well cuttings are considerable, since a given set of cuttings samples a 10-m interval. It is not known what is being sampled in the size fraction preserved as cuttings. For example, prefractured grains of the cataclasite may not survive pulverization by drilling. It is also possible that cataclasites on large detachments do not develop microfractures in the same way as thrusts or that thick cataclastic zones on detachments may be locally excised by faulting. Further tests, including analysis on cuttings recovered from known fault zones and on pulverized and unpulverized samples from surface-exposed low-angle normal faults, will be required to evaluate this technique. Other problematical aspects of their interpretations are discussed by Allmendinger and Royse [1995] and Otton [1995].

Interpretations of the Sevier Desert detachment notwithstanding, three examples, one from the Bohai Gulf in northern China, one from the Gulf of Oman, and one from the Basin and Range, are typical of profiles from areas of basement-involved continental extension (Figure 7) and include intracratonic rift, passive margin shelf, and orogenic "collapse" tectonic settings, respectively.

The Gulf of Bohai resides within the Sino-Korean craton, more than 500 km west of its boundary against the Pacific plate. The imaged fault (Figure 7a) and associated half graben is one of over 50 such basins known from the region [Zhang, 1994]. The fault plane is listric, with an apparent dip of about

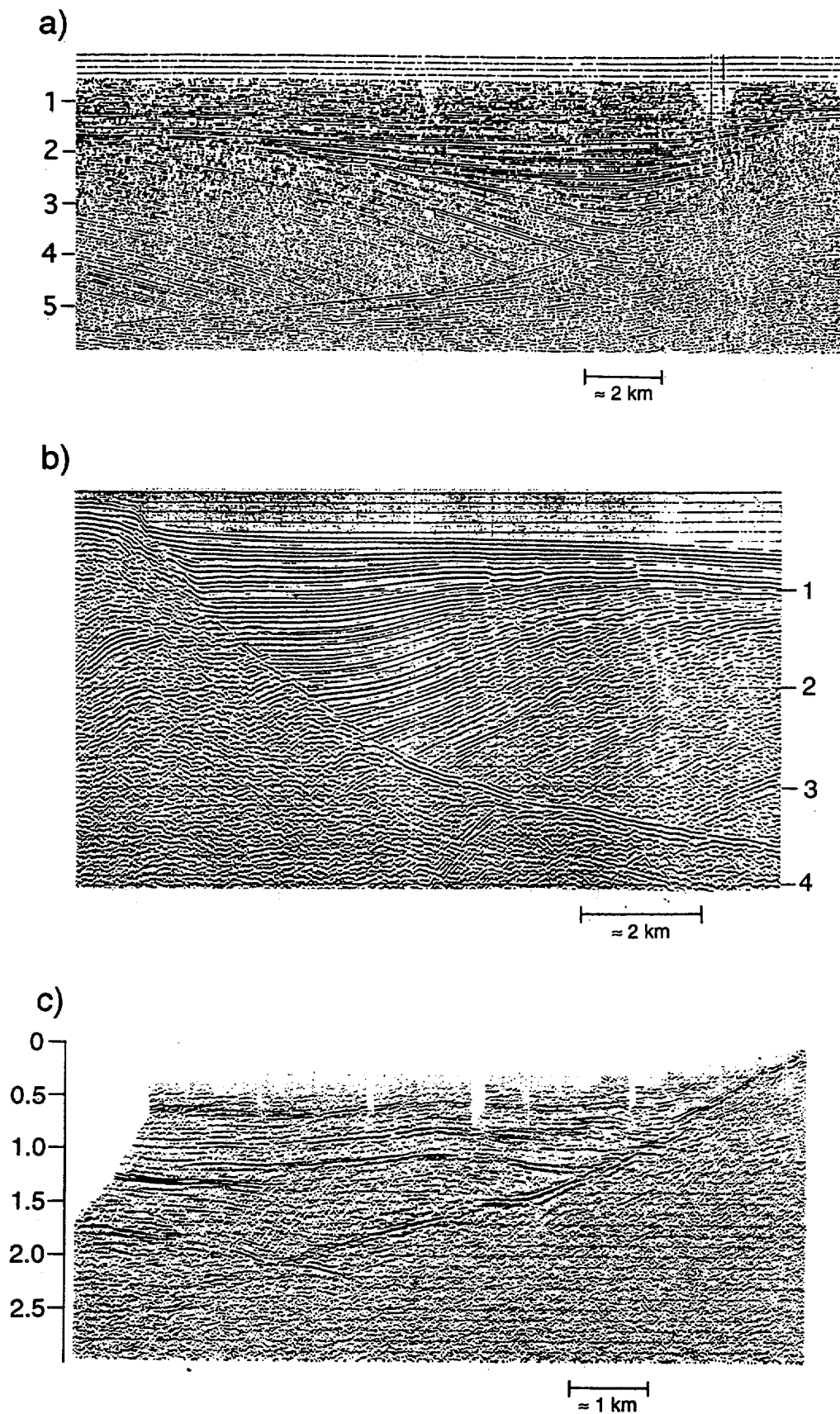


Figure 7. Seismic reflection profiles of low-angle normal faults. Vertical scales are all two-way travel times, in seconds. (a) Gulf of Bohai, east of Beijing, China, from Zhang [1994]; (b) Gulf of Oman, from Wernicke and Burchfiel [1982]; (c) Lamaille Valley, Nevada, from Smith *et al.* [1989]. See text for discussion.

35° near the surface, flattening downward to about 5° [Zhang, 1994]. Although the total depth of the section is not known, the fault is imaged down to a two-way travel time of 5.5 s, including a few hundred meters of water. At 3–5 km/s average velocity, this yields a depth range for the section of 9–15 km.

The Gulf of Oman example (Figure 7b) lies along the northeastern passive margin of the Arabian Peninsula. Following Late Cretaceous obduction of the Semail ophiolite, the Oman Mountains and bordering shelf region experienced basement-involved extension in Late Cretaceous and Tertiary time [e.g., Mann et al., 1990]. The imaged fault is conceivably associated with large-scale slumping toward the trench rather than basement-involved continental extension, perhaps analogous to the Gulf of Mexico. However, evidence for a protracted history of basement-involved extension nearby on land, and the absence of major evaporites or diapirism in the Gulf of Oman [e.g., Mann et al., 1990; White and Ross, 1979] suggest an analogy with Gulf of Mexico is inappropriate. The fault plane is clearly imaged to about 4 s two-way travel time or a probable depth range of 6–10 km.

The Basin and Range example (Figure 7c) is from the center of the province along the topographically sharp range front of the Ruby Mountains–East Humboldt Range core complex [Smith et al., 1989; Mueller and Snoke, 1993]. Hanging wall sediments are nonmarine Cenozoic basin fill, while footwall rocks are migmatitic gneisses of the core complex. Detailed velocity analysis for this example suggests the fault is a low-angle structure dipping about 10°–22° in the upper 4 km of the crust [Smith et al., 1989]. The fault projects toward a fault scarp in alluvium, suggesting activity in late Quaternary time. Numerous other examples of either young or once-active low-angle normal faults have been described from the Basin and Range based on combined subsurface and neotectonic data [e.g., Effimov and Pinezich, 1986; Burchfiel et al., 1987; Johnson and Loy, 1992; Bohannon et al., 1993].

It is difficult to argue that any of the above examples have been passively rotated (i.e., while inactive) from a steep dip. Hanging wall sediments and the topographic surface in all examples preclude significant tilting of the fault planes during their latest phases of movement, which would require unrealistic paleotopography and depositional slope. In all examples, however, it is difficult to constrain the initial dip of the fault. The apparent fault bed angle along the low-angle segments suggests relatively modest net rotations of about 20°–40°. However, because the faults are listric, these dips may be due to rollover of an independently deforming hanging wall block, rather than a measure of the rotation of the fault plane [e.g., Xiao et al., 1991].

It is emphasized that these three examples are not particularly unique. Images from basement-involved, upper crustal low-angle (0–30°) normal faults have been published from all three tectonic settings elsewhere (e.g., boundary faults of the Rio Grande rift [Russell and Snelson, 1990]; Outer Isles fault in the shelf region off Scotland [Brewer and Smythe, 1984]; the Slocan Lake fault in the Canadian Cordillera [Cook et al., 1992]). As in the case of the Sevier Desert detachment, a number of examples show fault plane reflections continuously traceable at shallow dip from near the surface to depths of 15–20 km [e.g., Brewer and Smythe, 1984; Cook et al., 1992]. It is also stressed that reflection data indicate there are a large number of normal faults with moderate to steep dips through the upper 10–15 km of the crust [e.g., Anderson et al., 1983; Okaya and Thompson, 1985; Brun et al., 1991].

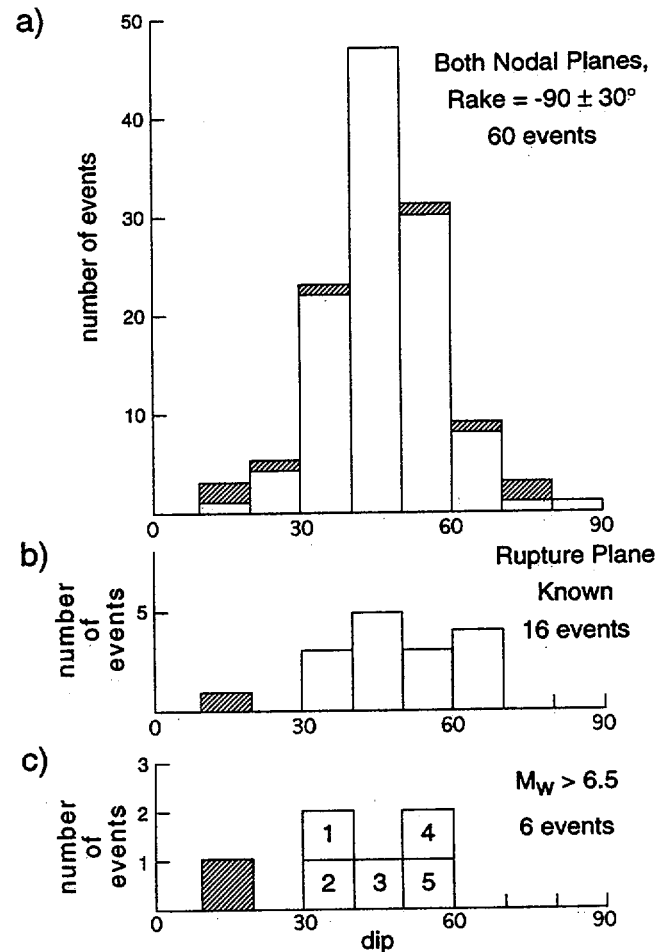


Figure 8. Frequency of earthquakes versus dip, cross-hatched events from Abers [1991]. (a) Both nodal planes, from Jackson and White [1989] and Abers [1991]; (b) events with known focal plane, including event 1 of Abers [1991]; (c) events larger than moment magnitude 6.5, from Doser and Smith [1989] (Basin and Range events), Jackson and White [1989], and Abers [1991], including 1, Aegean Sea, 1970; 2, Aegean Sea, 1969; 3, Hebgen Lake, 1959; 4, Borah Peak, 1983; and 5, Italy, 1980.

Seismicity

The weight of evidence from field geology, thermochronologic studies, paleomagnetic studies, and seismic reflection profiling suggests active slip of major normal faults dipping less than 30° and in some cases initiation of these faults at shallow dip, especially along their deeper parts. However, the majority of focal planes from a compilation of all normal fault earthquakes with a mechanism defined by detailed waveform modeling dip between 30° and 60° (Figure 8). Three of the eight shallowly dipping planes are from focal mechanism studies for events in 1982 and 1985 in the Woodlark-D'Entrecasteaux extensional province of Papua New Guinea [Abers, 1991], determined after Jackson and White's [1989] synthesis. Of four dip-slip events studied, two had nodal planes dipping about 15°–20°, and another two dipped about 30°. Although no surface rupture is known from these events, they are the only large earthquakes known to have occurred in a tectonic environment of Pliocene and Quaternary metamorphic core complexes [Hill et al., 1992; Baldwin et al., 1993]. The largest event, with $M_w =$

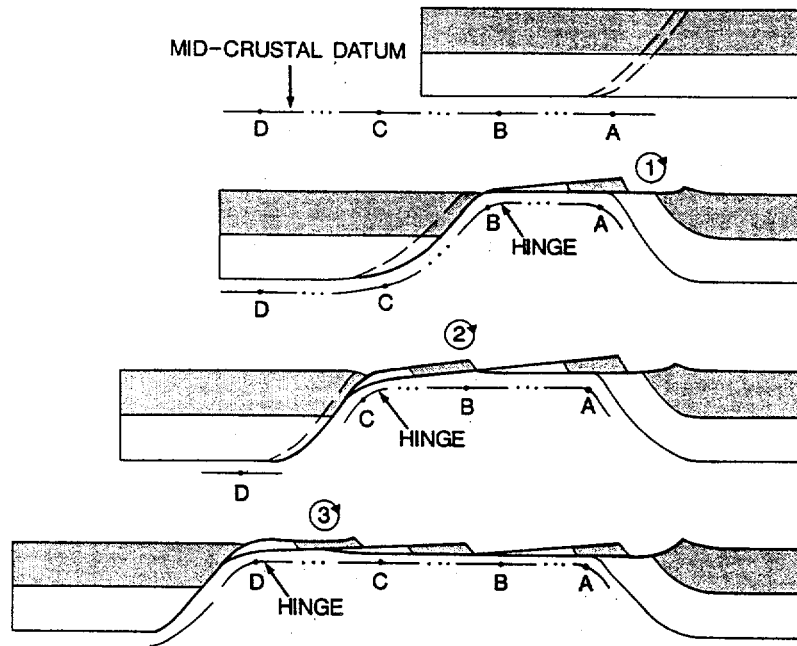


Figure 9. Rolling hinge model of detachment faulting [from Wernicke, 1992]. See text for discussion.

6.8, was positioned such that its shallow nodal plane projects into the young detachment described by Hill *et al.* [1992], and thus the shallow plane was suggested to be the more likely rupture plane [Abers, 1991].

The addition of the Papua New Guinea data to the earlier compilation (Figure 8a), even for those events in which the rupture plane is known (Figure 8b), nonetheless reveals a predominance of moderate to steeply inclined planes, as has been reported in a number of previous reviews [Jackson, 1987; Jackson and White, 1989; Doser and Smith, 1989].

As emphasized by Jackson [1987] and Jackson and White [1989], large normal fault earthquakes nucleate near the base of the seismogenic layer and cut most or all of the way through it. They also noted that the largest known normal fault ruptures have strike lengths of the same order as their dip lengths, with few exceeding about 20 km. Thus if we consider a 45° fault cutting a seismogenic layer 15 km thick, we expect a seismic moment [e.g., Scholz, 1990]

$$M_0 = \mu AD \approx 5 \times 10^{18} \text{ N m},$$

assuming an average fault slip D of 2 m, a roughly equant fault plane of area A , and a rigidity μ of about 6 GPa. This corresponds to a moment magnitude $M_w = \sim 6.5$.

In the compilation of Jackson and White [1989], which included 56 dip-slip normal events (rake within 30° of -90°), only a dozen or so of these are of $M_w \geq 6.5$, and these dominate the recorded moment release on normal fault earthquakes. Globally, there are only six normal dip-slip events with $M_w = 6.5$ or greater where the plane is resolved (Figure 8c), if the large event described by Abers [1991] is included. As can be seen in Figure 8c, nodal planes dipping 30°–60° are still most common, as in the larger sample that includes mostly small events. However, the Papua New Guinea event represents a much more substantial fraction of the sample for the large events, which is far more evenly distributed with respect to dip.

Discussion

Paradox of Seismicity and the Geologic Record

Many factors have been proposed to reconcile the predominance of moderately dipping planes defined by seismicity with the existence of low-angle normal faults. These include (1) "rolling hinge" or "flexural rotation" models, (2) a nonuniformitarian lack of active low-angle normal faults, (3) aseismic creep along low-angle faults, and (4) long recurrence intervals between earthquakes on low-angle faults (e.g., discussions by Jackson [1987], Buck [1988], Doser and Smith [1989], King and Ellis [1990], and Wernicke [1992]).

Rolling hinge models. Rolling hinge models suggest that isostatic unloading during and after slip induces short-wavelength flexure and tilting of the footwall [e.g., Buck, 1988; Wernicke and Axen, 1988; Hamilton, 1988], so that many ancient normal faults with subhorizontal dip may have been much steeper while active (Figure 9). For example, according to Buck's [1988] model, based on physical reasoning, all normal faults are essentially planar and project steeply through the brittle, seismogenic part of the crust with moderate to steep dip, terminating at the base of the brittle layer. Flexural rotation of the footwall produces a series of sequentially detached fault blocks, all of which are bounded by high-angle faults. The Andersonian theory and seismicity data are thereby resolved with the formation of subhorizontal detachments and core complexes, as the model does not require active slip on low-angle fault planes. A similar conclusion was reached by King and Ellis [1990].

In contrast, the model of Wernicke and Axen [1988], based on geological observations along the boundary between the Basin and Range province and Colorado Plateau [cf. King and Ellis, 1990] stresses a relationship between the dip of footwall bedding of normal faults and their initial dips. The footwalls of initially steep normal faults were deformed in abrupt short-wavelength flexures and large, subvertical fractures (e.g., the

northern Virgin Mountains, Nevada), while those with shallow initial dips resulted in broad footwall upwarps (e.g., western Mormon Mountains and Sevier Desert areas). Subsequent studies have documented both flexure and shear in a number of detachment footwalls, consistent with the concept of a rolling hinge [Bartley *et al.*, 1990; Manning and Bartley, 1994; Selverstone *et al.*, 1995].

Wernicke and Axen [1988, p. 851] concluded that the transient steepness of at least some ancient detachments in the brittle crust may ameliorate the paradox with focal mechanisms but that this does not reconcile the seismic data with those faults active at low dip in the brittle crust, such as the Sevier Desert, Mormon Peak, Whipple Mountains, and Panamint Valley detachments [cf. Johnson and Loy, 1992; Scott and Lister, 1992]. Given the evidence summarized above for active slip on low-angle normal faults, rolling hinge models that exclude shallow faulting seem not to provide a satisfactory explanation of the seismicity data.

Paucity of active low-angle normal faults. Another explanation is that none of the currently active zones of continental extension include low-angle normal faults. Since most examples of low-angle normal faults in the literature are ancient, as for phylum *Trilobita*, there may be no reason to suspect they are active at present. However, a number of examples, including those from Papua New Guinea [Hill *et al.*, 1992]; the Sevier Desert, Panamint Valley [Burchfiel *et al.*, 1987], and Lamoille Valley (Figure 7c) in the Basin and Range; and the Gulf of Oman (Figure 7a) appear to involve Quaternary deposits. Hence unlike the trilobites, examples from the most recent period of earth history do not appear to be particularly rare, and so their sudden disappearance would be rather fortuitous.

A subset of this explanation is that low-angle normal faults are favored in certain tectonic settings that are currently not active [e.g., Burchfiel *et al.*, 1992]. The examples discussed above (e.g., Figure 7), however, seem to occur in a variety of tectonic environments, including orogenic collapse, intracratonic rift, and passive margin settings, all of which are now active globally. Thus the nonuniformitarian hypothesis that shallowly dipping nodal planes are rare because low-angle normal faults are simply nowhere currently active does not seem particularly appealing.

Aseismic brittle creep. Another way to explain the seismicity is that low-angle normal faults tend to creep aseismically [e.g., Jackson, 1987; Doser and Smith, 1989]. This explanation has interesting implications for the physics of earthquake rupture, although it is at present not obvious what the cause might be.

The major effect would presumably be the brittle constitutive rheology of the fault zone. Such an effect would presumably be temperature dependent and therefore depth dependent. For example, a transition from stick-slip to stable frictional sliding with depth, hypothesized for the San Andreas fault zone [Tse and Rice, 1986] may in some way apply to normal faults, such that their flat segments are less prone to seismic slip than steeper segments in the upper crust. Such a rheological effect would have to apply to a wide variety of rock compositions, as detachments seem to be developed in every major rock type [e.g., Davis, 1980]. However, the observation that large events on steep faults penetrate to 10–15 km depth [Jackson and White, 1989], well below the range of depths discussed above for shallowly dipping normal faults, seems to argue against such an explanation.

Alternatively, it may be that either the low dip or the orien-

tation of stress axes favors creep for reasons currently unknown. However, thrust earthquakes display a wide range of dip, with low-angle thrusts responsible for the largest known earthquakes. The fact that both thrust and normal fault earthquakes occur argues against isolating stress orientation as cause of aseismic behavior.

Long recurrence intervals. Another potential solution to the problem might be longer recurrence intervals for shallow faults and perhaps due to the greater efficiency of low-angle faults in absorbing elastic strain that accommodates horizontal extension. Since larger fault planes would be able to accommodate more strain, low-angle faults might fail more rarely, and in larger events, than steeper ones, explaining the dearth of low-angle planes in global seismicity [Doser and Smith, 1989; Wernicke, 1992]. In addition, Forsyth [1992] suggests that finite slip on low-angle normal faults is favored by the fact that less energy, and hence less regional stress, is required for a given amount of extension in comparison with slip on high-angle faults. Geometrically, seismic slip on low-angle normal faults is more efficiently invested in accommodating horizontal extension than slip on high-angle faults, requiring fewer earthquakes.

One difficulty with this solution is that it does not explain why there are very few small- to moderate-sized earthquakes ($M_w < 6$) which would be expected if there are numerous active low-angle normal faults. The solution to this difficulty mainly depends on whether seismicity is clustered in time near infrequent mainshocks or occurs steadily through the interseismic interval. The former seems to be the most likely for large faults. For example, the two locked portions of the San Andreas fault, and perhaps the Cascadia subduction zone, are capable of generating large earthquakes, but most of the seismic moment release associated with them, including adjustments near the boundaries of coseismic slip, occurs within a few years of the mainshock, followed by long intervals where even microearthquakes are relatively uncommon.

In the next section, these concepts are integrated with some simple aspects of earthquake mechanics, providing a quantitative basis for empirical relations of earthquake frequency versus dip described by Jackson [1987], Doser and Smith [1989], Jackson and White [1989], and Thatcher and Hill [1991]. In general, this approach may offer a fairly simple resolution to the paradox.

Seismicity of Dip-Slip Faults

Model. Consider a hypothetical seismogenic layer of thickness h transected by a fault dipping θ (Figure 10). The average stress drop $\Delta\sigma$ on the fault is proportional to the average slip D and area of slip A [e.g., Scholz, 1990],

$$\Delta\sigma \propto \mu \frac{D}{\sqrt{A}}.$$

The area of slip, assuming it about equant, is related to fault dip by

$$\sqrt{A} = h/\sin \theta \quad (2)$$

which implies that for constant stress drop, layer thickness and rigidity modulus for a given earthquake,

$$D \propto 1/\sin \theta. \quad (3)$$

In other words, large, low-angle fault planes may accumulate more strain between earthquakes than small steep ones. For a

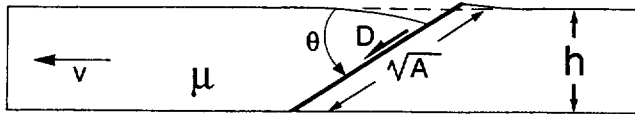


Figure 10. Diagram showing variables used to derive equations (2)–(6). See text for discussion.

constant rate of horizontal separation between hanging wall and footwall v , fewer earthquakes are required in a given time interval on shallow faults than on steep ones.

This relationship assumes, however, that strike length is free to expand with decreasing dip. The question arises as to whether the confinement of normal faults to relatively short segments [e.g., *Machette et al.*, 1992] would limit their lateral dimensions and therefore their ability to slip according to (3). As reviewed by *Jackson and White* [1989], the largest known normal fault earthquakes have strike lengths restricted to the range of a few tens of kilometers, about 1–2 times their down-dip rupture lengths. Thus a 15° normal fault would have a down-dip length of about 60 km and an along-strike length of 60–180 km. Shallow dip-slip ruptures have similar dimensions [e.g., *Scholz*, 1990, p. 297]. As mentioned above, the Sevier Desert detachment has been imaged as a single zone of reflections for a down-dip length of 60–70 km and for a strike length of at least 100 km [*Planke and Smith*, 1991]. Assuming it is indeed a normal fault, it seems to have an appropriately long strike dimension relative to its dip dimension and is substantially longer than the steep faults described by *Jackson and White* [1989].

A second consideration is the fact that for each earthquake a greater amount of slip is transferred into horizontal extension for shallow faults than for steep ones. Thus

$$v = D \cos \theta R'$$

where R' is the frequency of events per fault. This implies that for constant v ,

$$D \propto 1/(R' \cos \theta). \quad (4)$$

Equating (3) and (4) and solving for R ,

$$R' \propto \tan \theta. \quad (5)$$

Equation (5) allows comparison of earthquake frequency of two fault segments with contrasting θ but equal v , h , and μ . For example, a fault dipping 10°–15° would be expected to rupture about 7 times less frequently than a fault dipping 55°–60°.

A third consideration is that for a given total strike length of faults, there should be fewer faults in the case of low-angle versus high-angle faults. The frequency of events per unit length of fault is

$$R = R' / \sqrt{A} = R' \sin \theta,$$

where $1/\sqrt{A}$ is the number of faults per unit length of fault. Thus

$$R \propto \sin \theta \tan \theta. \quad (6)$$

For two rift zones of equal strike length with multiple fault segments, one characterized by 10°–15° faults and the other by 55°–60° faults, we would expect about 28 times more events

per unit time in the rift with steep faults than in the rift with low-angle faults.

The above reasoning suggests that low-angle faults should fail less often but with larger earthquakes. Since the moment of an earthquake is defined as

$$M_0 = \mu AD,$$

from (2) and (3) we have

$$M_0 \propto 1/\sin^3 \theta. \quad (7)$$

Again, given constant stress drop, rigidity modulus, thickness of the seismogenic layer, and extension velocity, low-angle faults will have substantially larger earthquakes than steep ones. In terms of moment magnitude M_w , faults dipping 10°–20° will produce earthquakes about one magnitude point stronger than faults dipping 50°–60°. Thus if 50° faults would typically yield magnitude 6.0–7.0 earthquakes, 10°–20° faults should produce magnitude 7.0–8.0 earthquakes.

Application to continental seismicity. Globally, earthquake stress drop and the presumed rigidity of the crust might not be expected to vary [e.g., *Kanamori and Anderson*, 1975], but the thickness of the seismogenic layer and the horizontal extension velocity probably vary from rift to rift. These and other factors would produce a wide range of maximum earthquake magnitudes in extensional provinces, with rapidly spreading areas producing more frequent earthquakes for a given fault dip. Of the five events studied by *Abers* [1991], the event with the shallowest nodal plane (~17°) was $M_w = 6.8$, while the other events were all between 5.5 and 6.0. In other words, 80% of the moment release occurred during the single low-angle event.

Equation (6) may be related to the global data set of dip-slip normal fault earthquakes (Figure 8), depending on the global distribution of fault dip over the total strike length of active faults. The simplest such distribution would be uniform, such that the same total length of fault plane would exist for each 10° increment of dip. This distribution would not agree well with the event frequency data (Figure 8a), because it predicts the vast majority of events would occur on planes dipping 60°–90°. In this case, consideration of both nodal planes would place a minimum number of events in the 30°–60° interval rather than the observed maximum (Figure 8a).

The simplest distribution that would explain the data in Figure 8a in terms of equation (6) is one that is even from 0° to 60°, greatly reduced from 60° to 70° (say, by an order of magnitude), and effectively zero from 70° to 90° (Figure 11a). According to Figure 8a, the ratio of events in the 0°–30° domain to that of the 30°–60° domain is about 0.1. Integrating the function $\sin \theta \tan \theta$ for these two domains also yields a ratio of shallow to steep events of about 0.1 (Figure 11b), in good agreement with the data. Adding the conjugate planes to such a model distribution doubles the number of events in the 30°–60° domain and adds whatever seismicity would exist in the 60°–90° domain to the 0°–30° domain, so the ratio of shallow to steep events is not appreciably different from the model without conjugate planes (Figure 11b). The principal difference between the model in Figure 11b and the data in Figure 8a is the ratio of events in the 30°–40° domain to events in the 40°–50° domain, which is about 1 in the model and 2 in the data. The discrepancy is perhaps mitigated by the fact that the uncertainty in dip is as large as the 10° bin size [e.g., *Thatcher and Hill*, 1991], and the total number of events is relatively

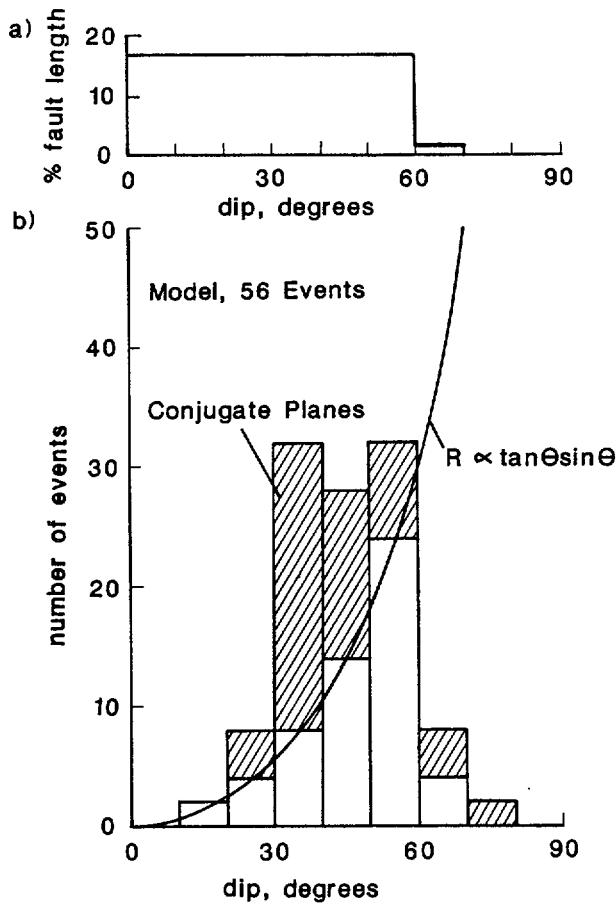


Figure 11. (a) Model for dip distribution of active normal faults that involve the entire seismogenic layer, discussed in text. (b) Number of earthquakes as a function of dip for 56 events (unpatterned areas) and conjugate planes (cross-hatching), according to equation (6).

small. The principal point is that the model predicts the correct overall proportions of low-angle and high-angle planes.

The 16-event sample with resolved fault planes (Figure 8b) is perhaps too small to make a meaningful comparison with the model, but nonetheless is in good agreement. It is clear, however, that a 16-event sample over a few decades is not necessarily sufficient to observe a large earthquake on a low-angle normal fault. Even if the large Papua New Guinea event occurred on the steep plane, the model predicts only one or two of the events would be less than 30° and none less than 20°. For the even smaller sample of events with $M_w > 6.5$, the same conclusion holds.

Of course, there are distributions other than the one shown in Figure 11a that could reconcile the data with equation (6). For example, an even distribution in the 30°–60° domain with a smaller fraction from 60° to 90°, with no faults from 0° to 30°, would also be consistent with the data. Unlike the distribution shown in Figure 11a, however, such a distribution is not successful in reconciling geological observations of brittle low-angle normal faults with the seismicity.

Mechanical implications. If distributions of the type shown in Figure 11a do indeed represent the global distribution of a “major” ctive normal faults in continents, how do they bear on Andersonian fault mechanics? The existence of low-angle normal faults suggests that Andersonian theory, which

predicts that normal faults form with a dip of 60°, would appear to be in need of substantial modification or abandonment.

One of its main assumptions, that the principal stress axes in the brittle crust are orthogonal to the Earth’s surface, is likely to be the major problem. Over the last 5 years, the problem has attracted the attention of fault mechanists, in the tradition of *Hafner* [1951]. Solutions to the problem have included rotation of stress trajectories through flexure [*Spencer and Chase*, 1989], igneous dilation at depth [*Parsons and Thompson*, 1993], viscous flow of deep crust against the seismogenic layer [*Yin*, 1989; *Melosh*, 1990], rotation of stress trajectories in the vicinity of the fault zone via high fluid pressure [*Axen*, 1992], and considerations of the energy efficiency of low-angle faults [*Forsyth*, 1992]. As yet, there is no consensus on which if any of these mechanisms are correct, but they do provide a framework for major progress in understanding fault mechanics and earthquakes. For example, the hypothesis that low-angle normal faults confine locally high fluid pressure and rotated stress trajectories [*Axen*, 1992] may be testable by moderate-depth drilling (5–6 km) into the Sevier Desert detachment of west central Utah [*Zoback and Emmermann*, 1994].

The fact that progressive extension tends to decrease the dip of fault planes reconciles Anderson theory with the preponderance of earthquakes on faults dipping much less than 60° with there being relatively few faults steeper than 60° [e.g., *Thatcher and Hill*, 1991]. To the extent that rotation of stress trajectories is common in continental rifts, this distribution may be substantially “smeared” well below 30° (the cutoff for frictional sliding if stress trajectories are not rotated), consistent with the model distribution in Figure 11a. In this case, 60° would represent the maximum initial dip, but lower initial dips and active slip not predicted by Anderson theory would be common.

Conclusions

Geologic reconstructions, thermochronology, paleomagnetism, and seismic reflection profiling indicate that initiation and slip on low-angle normal faults in the upper continental crust are common in the geologic record. The paradoxically low ratios of shallow and steep dipping focal planes to moderate ones in global seismicity may be resolved by a simple recurrence model, where the larger size and greater efficiency of shallow dip-slip faults cause them to fail much less frequently. This conclusion is perhaps not surprising when viewed in comparison with compressional dip-slip earthquakes. Approximately 80% of global seismic strain release over the last four decades occurred during two events, the 1960 Chilean earthquake and the 1964 Alaska earthquake, both of which occurred along shallowly dipping thrust faults.

The most probable reconciliation of this model with Andersonian fault mechanics lies in rotation of stress trajectories at depth in a significant fraction of active zones of continental extension.

The recognition of low-angle normal faults, and the prospect that they fail in large earthquakes, has significant implications for seismic hazard. Active low-angle normal faults may be difficult to detect on the basis of surface rupture patterns and paleoseismicity (e.g., the Sevier Desert detachment), as are low-angle thrust faults [e.g., *Hauksson et al.*, 1987]. Since many geophysicists have expressed doubt that large seismogenic low-angle normal faults even exist [e.g., *Jackson and McKenzie*, 1983; *Stein et al.*, 1988; *Buck*, 1988; *Jackson and White*, 1989;

King and Ellis, 1990], hazards in extending areas such as the Basin and Range province, western Turkey, and China may be seriously underestimated.

Acknowledgments. Discussions with D. L. Anderson and H. Kanamori helped clarify my thinking on seismological aspects of this paper. Reviews by G. A. Davis, R. K. Dokka, J. W. Geissman, T. A. Hauge, B. E. John, and JGR reviewers D. Davis, J. Oldow, and an anonymous referee contributed substantially toward improving the presentation. This research was supported by NSF grants EAR-9219939 and EAR-9316797.

References

- Abers, G. A., Possible seismogenic shallow-dipping normal faults in the Woodlark-D'Entrecasteaux extensional province, Papua New Guinea, *Geology*, *19*, 1205-1208, 1991.
- Allmendinger, R. W., Fold and thrust tectonics of the western United States exclusive of the accreted terranes, in *The Geology of North America*, vol. G-3, *The Cordilleran Orogen: Conterminous U.S.*, edited by B. C. Burchfiel, P. W. Lipman, and M. L. Zoback, pp. 583-607, Geol. Soc. of Am., Boulder, Colo., 1992.
- Allmendinger, R. W., and F. Royse, Jr., Comment on "Is the Sevier Desert reflection of west-central Utah a normal fault?" by M. Anders and N. Christie-Blick, *Geology*, *23*, 669-670, 1995.
- Allmendinger, R. W., J. W. Sharp, D. Von Tish, L. Serpa, L. Brown, S. Kaufman, J. Oliver, and R. B. Smith, Cenozoic and Mesozoic structure of the eastern Basin and Range province, Utah, from COCORP seismic-reflection data, *Geology*, *11*, 532-536, 1983.
- Allmendinger, R. W., H. Farmer, E. Hauser, J. Sharp, D. V. Tish, J. Oliver, and S. Kaufman, Phanerozoic tectonics of the Basin and Range-Colorado Plateau transition from COCORP data and geologic data: A review, in *Reflection Seismology: The Continental Crust*, *Geodyn. Ser.*, vol. 14, edited by M. Barazangi and L. Brown, pp. 257-267, AGU, Washington, D. C., 1986.
- Anders, M. H., and N. Christie-Blick, Is the Sevier Desert reflection of west-central Utah a normal fault?, *Geology*, *22*, 771-774, 1994.
- Anderson, E. M., *The Dynamics of Faulting*, 1st ed., 183 pp., Oliver and Boyd, Edinburgh, 1942.
- Anderson, R. E., Thin-skin distension in Tertiary rocks of southwestern Nevada, *Geol. Soc. Am. Bull.*, *82*, 43-58, 1971.
- Anderson, R. E., M. L. Zoback, and G. A. Thompson, Implications of selected subsurface data on the structural form and evolution of some basins in the northern Basin and Range province, Nevada and Utah, *Geol. Soc. Am. Bull.*, *94*, 1055-1072, 1983.
- Armstrong, R. L., Cordilleran metamorphic core complexes from Arizona to southern California, *Annu. Rev. Earth Planet. Sci.*, *10*, 129-154, 1982.
- Asmerom, Y., J. K. Snow, D. K. Holm, S. B. Jacobsen, B. Wernicke, and D. R. Lux, Rapid uplift and crustal growth in extensional environments: An isotopic study from the Death Valley region, California, *Geology*, *18*, 223-226, 1990.
- Axen, G. J., Pore pressure, stress increase, and fault weakening in low-angle normal faulting, *J. Geophys. Res.*, *97*, 8979-8991, 1992.
- Axen, G. J., Ramp-flat detachment faulting and low-angle normal reactivation of the Tule Springs thrust, southern Nevada, *Geol. Soc. Am. Bull.*, *105*, 1076-1090, 1993.
- Axen, G. J., and B. Wernicke, Comment on "Tertiary extension and contraction of lower-plate rocks in the Central Mojave metamorphic core complex, southern California" by J. M. Bartley, J. M. Fletcher, and A. F. Glazner, *Tectonics*, *10*, 1084-1086, 1991.
- Axen, G. J., B. Wernicke, M. J. Skelly, and W. J. Taylor, Mesozoic and Cenozoic tectonics of the Sevier thrust belt in the Virgin River Valley area, southern Nevada, in *Basin and Range Extensional Tectonics Near the Latitude of Las Vegas, Nevada*, edited by B. Wernicke, *Mem. Geol. Soc. Am.*, *176*, 123-153, 1990.
- Baldwin, S. L., G. S. Lister, E. J. Hill, D. A. Foster, and I. McDougall, Thermochronologic constraints on the tectonic evolution of active metamorphic core complexes, D'Entrecasteaux Islands, Papua New Guinea, *Tectonics*, *12*, 611-628, 1993.
- Bally, A. W., P. L. Gordy, and G. A. Stewart, Structure, seismic data, and orogenic evolution of the southern Canadian Rocky Mountains, *Bull. Can. Pe. Geol.*, *4*, 337-381, 1966.
- Bally, A. W., D. Bernoulli, G. A. Davis, and L. Montadert, Listric normal faults, *Oceanogr. Acta*, *SP*, 87-102, 1981.
- Bartley, J. M., J. M. Fletcher, and A. F. Glazner, Tertiary extension and contraction of lower-plate rocks in the central Mojave metamorphic core complex, southern California, *Tectonics*, *9*, 521-534, 1990.
- Bohannon, R. G., J. A. Grow, J. J. Miller, and R. H. Blank Jr., Seismic stratigraphy and tectonic development of Virgin River depression and associated basins, southeastern Nevada and northwestern Arizona, *Geol. Soc. Am. Bull.*, *105*, 501-520, 1993.
- Brewer, J. A., and D. K. Smythe, MOIST and the continuity of crustal reflector geometry along the Caledonian-Appalachian orogeny, *J. Geol. Soc. London*, *141*, 105-120, 1984.
- Brock, W. G., and T. Engelder, Deformation associated with the movement of the Muddy Mountain overthrust in the Buffington window, southeastern Nevada, *Geol. Soc. Am. Bull.*, *88*, 1667-1677, 1977.
- Brun, J. P., F. Wenzel, and ECORS-DEKORP Team, Crustal-scale structure of the southern Rhinegraben from ECORS-DEKORP seismic reflection data, *Geology*, *19*, 758-762, 1991.
- Buck, W. R., Flexural rotation of normal faults, *Tectonics*, *7*, 959-975, 1988.
- Burchfiel, B. C., K. V. Hodges, and L. H. Royden, Geology of the Panamint Valley-Saline Valley pull-apart system, California: Palinspastic evidence for low-angle geometry of a Neogene range-bounding fault, *J. Geophys. Res.*, *92*, 10,422-10,426, 1987.
- Burchfiel, B. C., D. S. Cowan, and G. A. Davis, Tectonic overview of the Cordilleran orogen in the western United States, in *The Geology of North America*, vol. G-3, *The Cordilleran Orogen: Conterminous U.S.*, edited by B. C. Burchfiel, P. W. Lipman, and M. L. Zoback, pp. 407-479, Geol. Soc. of Am., Boulder, Colo., 1992.
- Compton, R. R., V. R. Todd, R. E. Zartman, and C. W. Naeser, Oligocene and Miocene metamorphism, folding, and low-angle faulting in northwestern Utah, *Geol. Soc. Am. Bull.*, *88*, 1237-1250, 1977.
- Cook, F. A., J. L. Varsek, R. M. Clowes, E. R. Kanasewich, C. S. Spencer, R. R. Parrish, R. L. Brown, S. D. Carr, B. J. Johnson, and R. A. Price, Lithoprobe crustal reflection cross section of the southern Canadian Cordillera, 1, Foreland thrust and fold belt to Fraser River fault, *Tectonics*, *11*, 12-35, 1992.
- Crittenden, M. D., Jr., P. J. Coney, and G. H. Davis (Eds.), *Cordilleran Metamorphic Core Complexes*, *Mem. Geol. Soc. Am.*, *153*, 490 pp., 1980.
- Davis, G. A., and G. S. Lister, Detachment faulting in continental extension: Perspectives from the southwestern U. S. Cordillera, *Spec. Pap. Geol. Soc. Am.*, *218*, 133-159, 1988.
- Davis, G. A., J. L. Anderson, E. G. Frost, and T. S. Shackelford, Mylonitization and detachment faulting in the Whipple-Buckskin Rawhide Mountains terrane, southeastern California and western Arizona, in *Cordilleran Metamorphic Core Complexes*, edited by M. D. Crittenden Jr., P. J. Coney, and G. H. Davis, *Mem. Geol. Soc. Am.*, *153*, 79-130, 1980.
- Davis, G. A., G. S. Lister, and S. J. Reynolds, Structural evolution of the Whipple and South Mountains shear zones, southwestern United States, *Geology*, *14*, 7-10, 1986.
- Davis, G. H., Structural characteristics of metamorphic core complexes, in *Cordilleran Metamorphic Core Complexes*, edited by M. D. Crittenden Jr., P. J. Coney, and G. H. Davis, *Mem. Geol. Soc. Am.*, *153*, 35-77, 1980.
- Davis, G. H., and P. J. Coney, Geologic development of Cordilleran metamorphic core complexes, *Geology*, *7*, 120-124, 1979.
- Dibblee, T. W., Geologic map of the Daggett quadrangle, San Bernardino County, California, scale 1:62,500, *U.S. Geol. Surv. Map*, *I-592*, 1970.
- Dickinson, W. R., Tectonic setting of faulted Tertiary strata associated with the Catalina core complex in southern Arizona, *Spec. Pap. Geol. Soc. Am.*, *264*, 106 pp., 1991.
- Dokka, R. K., Patterns and modes of early Miocene crustal extension, central Mojave Desert, California, *Spec. Pap. Geol. Soc. Am.*, *208*, 75-95, 1986.
- Dokka, R. K., Original dip and subsequent modification of a Cordilleran detachment fault, Mojave extensional belt, California, *Geology*, *21*, 711-714, 1993.
- Doser, D. I., and R. B. Smith, An assessment of source parameters of earthquakes in the Cordillera of the western United States, *Bull. Seismol. Soc. Am.*, *79*, 1383-1409, 1989.
- Drewes, H., and C. H. Thorman, The Cordilleran orogenic belt be-

- tween Nevada and Chihuahua, *Geol. Soc. Am. Bull.*, 89, 641–657, 1978.
- Dumitru, T. A., P. B. Gans, D. A. Foster, and E. L. Miller, Refrigeration of the western Cordilleran lithosphere during Laramide shallow-angle subduction, *Geology*, 19, 1145–1148, 1991.
- Effimoff, I., and A. R. Pinezich, Tertiary structural development of selected basins: Basin and Range province, northeastern Nevada, *Spec. Pap. Geol. Soc. Am.*, 208, 31–42, 1986.
- Fitzgerald, P. G., J. E. Fryxell, and B. P. Wernicke, Miocene crustal extension and uplift in southeastern Nevada: Constraints from fission track analysis, *Geology*, 19, 1013–1016, 1991.
- Fitzgerald, P. G., et al., Thermochronologic evidence for timing of denudation and rate of crustal extension of the south mountains metamorphic core complex and sierra estrella, Arizona, *Nucl. Tracks Radiat. Meas.*, 21, 555–563, 1993.
- Forsyth, D. W., Finite extension and low-angle normal faulting, *Geology*, 20, 27–30, 1992.
- Foster, D. A., D. S. Miller, and C. F. Miller, Tertiary extension in the Old Woman Mountains area, California: Evidence from apatite fission track analysis, *Tectonics*, 10, 875–886, 1991.
- Fritz, W. H., Geologic map and sections of the southern Cherry Creek and northern Egan Ranges, White Pine County, Nevada, *Map 35*, Nev. Bur. of Mines and Geol., Reno, 1968.
- Fryxell, J. E., G. G. Salton, J. Selverstone, and B. Wernicke, Gold Butte crustal section, south Virgin Mountains, Nevada, *Tectonics*, 11, 1099–1120, 1992.
- Gans, P. B., G. A. Mahood, and E. Schermer, Synextensional magmatism in the Basin and Range province: A case study from the eastern Great Basin, *Spec. Pap. Geol. Soc. Am.*, 233, 1–53, 1989.
- Hafner, W., Stress distributions and faulting, *Geol. Soc. Am. Bull.*, 62, 373–398, 1951.
- Hamilton, W., Detachment faulting in the Death Valley region, California and Nevada, *U.S. Geol. Surv. Bull.*, 1790, 763–771, 1988.
- Harms, T. A., and R. A. Price, The Newport fault: Eocene listric normal faulting, mylonitization, and crustal extension in northeast Washington and northwest Idaho, *Geol. Soc. Am. Bull.*, 104, 745–761, 1992.
- Hauge, T. A., Kinematic model of a continuous Heart Mountain allochthon, *Geol. Soc. Am. Bull.*, 102, 1174–1181, 1990.
- Hauksson, E., et al., The Whittier Narrows earthquake in the Los Angeles metropolitan area, *Science*, 239, 1409–1412, 1987.
- Hill, E. J., S. L. Baldwin, and G. S. Lister, Unroofing of active metamorphic core complexes in the D'Entrecasteaux Islands, Papua New Guinea, *Geology*, 20, 907–910, 1992.
- Holm, D. K., and R. K. Dokka, Interpretation and tectonic implications of cooling histories: An example from the Black Mountains, Death Valley extended terrane, California, *Earth Planet. Sci. Lett.*, 116, 63–80, 1993.
- Holm, D. K., and B. Wernicke, Black Mountains crustal section, Death Valley extended terrain, California, *Geology*, 18, 520–523, 1990.
- Holm, D. K., J. K. Snow, and D. R. Lux, Thermal and barometric constraints on the intrusive and unroofing history of the Black Mountains: Implications for timing, initial dip, and kinematics of detachment faulting in the Death Valley region, California, *Tectonics*, 11, 507–522, 1992.
- Holm, D. K., J. W. Geissman, and B. Wernicke, Tilt and rotation of the footwall of a major normal fault system: Paleomagnetism of the Black Mountains, Death Valley extended terrane, California, *Geol. Soc. Am. Bull.*, 105, 1373–1387, 1993.
- Howard, K. A., and B. E. John, Crustal extension along a rooted system of imbricate low-angle faults: Colorado River extensional corridor, California and Arizona, in *Continental Extensional Tectonics*, edited by M. P. Coward, J. F. Dewey, and P. L. Hancock, *Geol. Soc. Spec. Publ. London*, 28, 299–311, 1987.
- Howard, K. A., P. Stone, M. A. Pernokas, and R. F. Marvin, Geologic and geochronologic reconnaissance of the Turtle Mountains area, California, west border of the Whipple Mountain detachment terrane, in *Mesozoic-Cenozoic Tectonic Evolution of the Colorado River Trough Region, California, Arizona and Nevada*, edited by E. G. Frost and D. L. Martin, pp. 341–354, Cordilleran Publ., San Diego, Calif., 1982.
- Jackson, J. A., Active normal faulting and crustal extension, in *Continental Extensional Tectonics*, edited by M. P. Coward, J. F. Dewey, and P. L. Hancock, *Geol. Soc. Spec. Publ. London*, 28, 3–17, 1987.
- Jackson, J. A., and D. McKenzie, The relationship between strain rates, crustal thickening, paleomagnetism, finite strain and fault movements within a deforming zone, *Earth Planet. Sci. Lett.*, 65, 182–202, 1983.
- Jackson, J. A., and N. J. White, Normal faulting in the upper continental crust: Observations from regions of active extension, *J. Struct. Geol.*, 11, 15–36, 1989.
- John, B. E., Geometry and evolution of a mid-crustal extensional fault system: Chemehuevi Mountains, southeastern California, in *Continental Extensional Tectonics*, edited by M. P. Coward, J. F. Dewey, and P. L. Hancock, *Geol. Soc. Spec. Publ. London*, 28, 313–335, 1987.
- John, B. E., and D. A. Foster, Structural and thermal constraints on the initiation angle of detachment faulting in the southern Basin and Range: The Chemehuevi Mountains case study, *Geol. Soc. Am. Bull.*, 105, 1091–1108, 1993.
- Johnson, R. A., and K. L. Loy, Seismic reflection evidence for seismogenic low-angle faulting in southeastern Arizona, *Geology*, 20, 597–600, 1992.
- Kanamori, H., The energy release in great earthquakes, *J. Geophys. Res.*, 82, 2981–2987, 1977.
- Kanamori, H., and D. Anderson, Theoretical basis of some empirical relations in seismology, *Seismol. Soc. Am. Bull.*, 65, 1073–1095, 1975.
- Kemnitzner, L. E., Structural studies in the Whipple Mountains, southeastern California, Ph.D. thesis, 150 pp., Calif. Inst. of Technol., Pasadena, 1937.
- King, G., and M. Ellis, The origin of large local uplift in extensional regions, *Nature*, 348, 689–692, 1990.
- Lachenbruch, A. H., and J. H. Sass, Models of an extending lithosphere and heat flow in the Basin and Range province, *Mem. Geol. Soc. Am.*, 152, 1978.
- Livaccari, R. F., J. W. Geissman, and S. J. Reynolds, Paleomagnetic evidence for large-magnitude, low-angle normal faulting in a metamorphic core complex, *Nature*, 361, 56–59, 1993.
- Livaccari, R. F., J. W. Geissman, and S. J. Reynolds, Large-magnitude extensional deformation in the South mountains metamorphic core complex, Arizona: Evaluation with paleomagnetism, *Geol. Soc. Am. Bull.*, 107, 877–894, 1995.
- Longwell, C. R., Low-angle normal faults in the Basin and Range province, *Eos Trans. AGU*, 26, 107–118, 1945.
- Machette, M. N., S. F. Personius, and A. R. Nelson, The Wasatch fault zone, *Ann. Tectonicae*, 6, suppl., 5–39, 1992.
- Malaveielle, J., Extensional shearing deformation and kilometer-scale “a”-type folds in a Cordilleran metamorphic core complex (Raft River Mountains, northwestern Utah), *Tectonics*, 6, 423–448, 1987.
- Mancktelow, N. S., and T. L. Pavlis, Fault-fold relationships in low-angle detachment systems, *Tectonics*, 13, 668–685, 1994.
- Mann, A., S. S. Hanna, and S. C. Nolan, The post-Campanian tectonic evolution of the Central Oman Mountains: Tertiary extension of the eastern Arabian margin, in *The Geology and Tectonics of the Oman Region*, edited by A. H. F. Robertson et al., *Geol. Soc. Spec. Publ. London*, 49, 549–563, 1990.
- Manning, A. H., and J. M. Bartley, Postmylonitic deformation in the Raft River metamorphic core complex, northwestern Utah: Evidence of a rolling hinge, *Tectonics*, 13, 596–612, 1994.
- McDonald, R. E., Tertiary tectonics and sedimentary rocks along the transition Basin and Range province to Plateau and Thrust belt province, Utah, in *Symposium on Geology of the Cordilleran Hinge-line*, edited by J. G. Hill, pp. 281–317, Rocky Mountain Assoc. of Geol., Denver, Colo., 1976.
- McGee, W. J., On the origin and hade of normal faults, *Am. J. Science*, 26, 294–298, 1883.
- McKenzie, D. P., Some remarks on the development of sedimentary basins, *Earth Planet. Sci. Lett.*, 40, 25–32, 1978a.
- McKenzie, D. P., Active tectonics of the Alpine-Himalayan belt: The Aegean Sea and surrounding regions, *Geophys. J. R. Astron. Soc.*, 55, 217–254, 1978b.
- Melosh, H. J., Mechanical basis for low-angle normal faulting in the Basin and Range province, *Nature*, 343, 331–335, 1990.
- Miller, E. L., P. B. Gans, and J. D. Garing, An exhumed brittle-ductile transition in the Snake Range, Nevada, *Tectonics*, 2, 239–263, 1983.
- Misch, P., Regional structural reconnaissance in central-northeast Nevada and some adjacent areas—Observations and interpretations, in *Guidebook to the Geology of East-Central Nevada: 11th Annual Field Conference*, pp. 17–42, Intermountain Assoc. of Pet. Geol. and East. Nev. Geol. Soc., Salt Lake City, Utah, 1960.
- Morton, W. H., and R. Black, Crustal attenuation in Afar, in *Afar Depression of Ethiopia, Proc. Sci. Rep. 14*, edited by A. Pilgar and

- A. Rosler, pp. 55–65, E. Schweizerbart'sche, Stuttgart, Germany, 1975.
- Mueller, K. J., and A. W. Snoke, Progressive overprinting of normal fault systems and their role in Tertiary exhumation of the East Humboldt–Wood Hills metamorphic complex northeast Nevada, *Tectonics*, *12*, 361–371, 1993.
- Mutter, J. C., and J. A. Karson, Structural processes at slow-spreading ridges, *Science*, *257*, 627–634, 1992.
- Noble, L. F., Structural features of the Virgin Spring area, Death Valley, California, *Geol. Soc. Am. Bull.*, *52*, 941–1000, 1941.
- Okaya, D. A., and G. A. Thompson, Geometry of Cenozoic extensional faulting: Dixie Valley, Nevada, *Tectonics*, *4*, 107–125, 1985.
- Otton, J. K., Western frontal fault of the Canyon Range: Is it the breakaway zone of the Sevier Desert detachment?, *Geology*, *23*, 547–550, 1995.
- Parsons, T., and G. A. Thompson, Does magmatism influence low-angle normal faulting? *Geology*, *21*, 247–250, 1993.
- Pierce, W. G., Heart Mountain and South Fork detachment thrusts of Wyoming, *Am. Assoc. Pet. Geol. Bull.*, *41*, 591–626, 1957.
- Planke, S., and R. B. Smith, Cenozoic extension and evolution of the Sevier Desert Basin, Utah, from seismic reflection, gravity, and well log data, *Tectonics*, *10*, 345–365, 1991.
- Price, R. A., The Cordilleran foreland fold and thrust belt in the southern Canadian Rock Mountains, in *Thrust and Nappe Tectonics*, edited by K. R. McClay and N. J. Price, pp. 427–448, Geol. Soc. of London, 1981.
- Proffett, J. M., Jr., Cenozoic geology of the Yerington district, Nevada, and implications for the nature and origin of Basin and Range faulting, *Geol. Soc. Am. Bull.*, *88*, 247–266, 1977.
- Ransome, F. L., W. H. Emmons, and W. H. Garrey, Geology and ore deposits of the Bullfrog district, Nevada, *U.S. Geol. Surv. Bull.*, *407*, 130 pp., 1910.
- Reynolds, S. J., Geology of the South Mountains, central Arizona, *Ariz. Bur. Geol. Miner. Technol. Bull.*, *195*, 61 pp., 1985.
- Richard, S. M., J. E. Fryxell, and J. F. Sutter, Tertiary structure and thermal history of the Harquahala and Buckskin Mountains, west central Arizona: Implications for denudation by a major detachment fault system, *J. Geophys. Res.*, *95*, 19,973–19,987, 1990.
- Royse, F., Jr., An overview of the geologic structure of the thrust belt in Wyoming, northern Utah, and eastern Idaho, in *Geology of Wyoming, Mem. 5*, edited by A. W. Snoke, J. R. Steidtmann, and S. M. Roberts, pp. 272–311, Geol. Surv. of Wyo., Laramie, 1993.
- Royse, F., Jr., M. A. Warner, and D. L. Reese, Thrust belt structural geometry and related stratigraphic problems, Wyoming-Idaho-northern Utah, in *Deep Drilling Frontiers in the Central Rocky Mountains*, pp. 41–54, Rocky Mountain Assoc. of Geol., Denver, Colo., 1975.
- Russell, L. R., and S. Snelson, Structural style and tectonic evolution of the Albuquerque Basin segment of the Rio Grande rift, in *The Potential of Deep Seismic Profiling for Hydrocarbon Exploration, Proceedings of the Fifth IFP Exploration and Production Research Conference, Publ. 165, Int. Lithosphere Program*, edited by B. Pinet and C. Bois, pp. 175–208, Editions Technip, Paris, 1990.
- Scholz, C. H., *The Mechanics of Earthquakes and Faulting*, 439 pp., Cambridge Univ. Press, New York, 1990.
- Scott, R. J., and G. S. Lister, Detachment faults: Evidence for a low-angle origin, *Geology*, *20*, 833–836, 1992.
- Selverstone, J., G. Axen, and J. Bartley, P-T conditions of successive fracturing events during unroofing of an extensional mylonite zone: Constraints from oriented fluid inclusion planes, *Geol. Soc. Am. Abstr. Programs*, *25*, A423, 1993.
- Selverstone, J., G. Axen, and J. M. Bartley, Fluid inclusion constraints on the kinematics of footwall uplift beneath the Brenner Line normal fault, eastern Alps, *Tectonics*, *14*, 264–278, 1995.
- Smith, R. B., and R. L. Bruhn, Intraplate extensional tectonics of the eastern Basin and Range; Inferences on the structural style from seismic reflection data, regional tectonics, and thermal-mechanical models of brittle-ductile deformation, *J. Geophys. Res.*, *89*, 5733–5762, 1984.
- Smith, R. B., W. C. Nagy, K. A. Julander, J. J. Viveiros, C. A. Barker, and D. G. Gants, Geophysical and tectonic framework of the eastern Basin and Range–Colorado Plateau–Rocky Mountain transition, *Mem. Geol. Soc. Am.*, *172*, 205–233, 1989.
- Spencer, J. E., Role of tectonic denudation in warping an uplift of low-angle normal faults, *Geology*, *12*, 95–98, 1984.
- Spencer, J. E., Miocene low-angle normal faulting and dike emplacement, Homer mountain and surrounding areas, southeastern California and southernmost Nevada, *Geol. Soc. Am. Bull.*, *9*, 1140–1155, 1985.
- Spencer, J. E., and C. G. Chase, Role of crustal flexure in initiation of low-angle normal faults and implications for structural evolution of the Basin and Range province, *J. Geophys. Res.*, *94*, 1765–1775, 1989.
- Spencer, J. E., and S. J. Reynolds, Tectonics of mid-Tertiary extension along a transect through west central Arizona, *Tectonics*, *10*, 1204–1221, 1991.
- Stein, R. S., G. C. P. King, and J. B. Rundle, The growth of geological structures by repeated earthquakes, 2, Field examples of continental dip-slip faults, *J. Geophys. Res.*, *93*, 13,319–13,331, 1988.
- Thatcher, W., and D. P. Hill, Fault orientations in extensional and conjugate strike-slip environments and their implications, *Geology*, *19*, 1116–1120, 1991.
- Tse, S. T., and J. R. Rice, Crustal earthquake instability in relation to the depth variation of frictional slip properties, *J. Geophys. Res.*, *91*, 9452–9472, 1986.
- Wernicke, B., Low-angle normal faults in the Basin and Range province: Nappe tectonics in an extending orogen, *Nature*, *291*, 645–648, 1981.
- Wernicke, B., Uniform-sense normal simple shear of the continental lithosphere, *Can. J. Earth Sci.*, *22*, 108–125, 1985.
- Wernicke, B., Cenozoic extensional tectonics of the U.S. Cordillera, in *The Geology of North America*, vol. G3, *The Cordilleran Orogen: Conterminous U.S.*, edited by B. C. Burchfiel, P. W. Lipman, and M. L. Zoback, pp. 553–582, Geol. Soc. of Am., Boulder, Colo., 1992.
- Wernicke, B., and G. J. Axen, On the role of isostasy in the evolution of normal fault systems, *Geology*, *16*, 848–851, 1988.
- Wernicke, B., and B. C. Burchfiel, Modes of extensional tectonics, *J. Struct. Geol.*, *4*, 105–115, 1982.
- Wernicke, B., J. D. Walker, and M. S. Beaufait, Structural discordance between Neogene detachments and frontal Sevier thrusts, central Mormon Mountains, southern Nevada, *Tectonics*, *4*, 213–246, 1985.
- White, R. S., and D. A. Ross, Tectonics of the western Gulf of Oman, *J. Geophys. Res.*, *84*, 3479–3489, 1979.
- Worral, D. M., and S. Snelson, Evolution of the northern Gulf of Mexico, with emphasis on Cenozoic growth faulting and the role of salt, in *The Geology of North America: An Overview*, edited by A. W. Bally and A. R. Palmer, pp. 97–138, Geol. Soc. of Am., Boulder, Colo., 1989.
- Wright, L. A., and B. W. Troxel, Shallow-fault interpretation of Basin and Range structure, southwestern Great Basin, in *Gravity and Tectonics*, edited by K. A. DeJong and R. Scholten, pp. 397–407, John Wiley, New York, 1973.
- Wright, L. A., and B. W. Troxel, Geology of the northern half of the Confidence Hills 15' quadrangle, Death Valley region, eastern California: The area of the Amargosa chaos, map sheet 34, Calif. Div. of Mines and Geol., Sacramento, 1984.
- Xiao, H. B., F. A. Dahlen, and J. Suppe, Mechanics of extensional wedges, *J. Geophys. Res.*, *96*, 10,301–10,318, 1991.
- Yin, A., Origin of regional rooted low-angle normal faults: A mechanical model and its tectonic implications, *Tectonics*, *8*, 469–482, 1989.
- Yin, A., and J. F. Dunn, Structural and stratigraphic development of the Whipple–Chemehuevi detachment fault system, southeastern California: Implications for the geometrical evolution of domal and basinal low-angle normal faults, *Geol. Soc. Am. Bull.*, *104*, 659–674, 1992.
- Zhang, Y. K., Mechanics of extensional wedges and geometry of normal faults, *J. Struct. Geol.*, *16*, 725–732, 1994.
- Zoback, M. D., and R. Emmermann, Scientific rationale for establishment of an international program of continental scientific drilling, in *Report of the International Meeting on Continental Scientific Drilling*, 194 pp., GeoForschungs Zentrum, Potsdam, Germany, 1994.

B. Wernicke, Division of Geological and Planetary Sciences, 170-25, California Institute of Technology, Pasadena, CA 91125. (e-mail: brian@legs.gps.caltech.edu)

(Received August 26, 1994; revised June 13, 1995; accepted June 20, 1995.)

Precarious Rocks and Seismic Events at Yucca Mountain, Nevada

James Brune
John Whitney

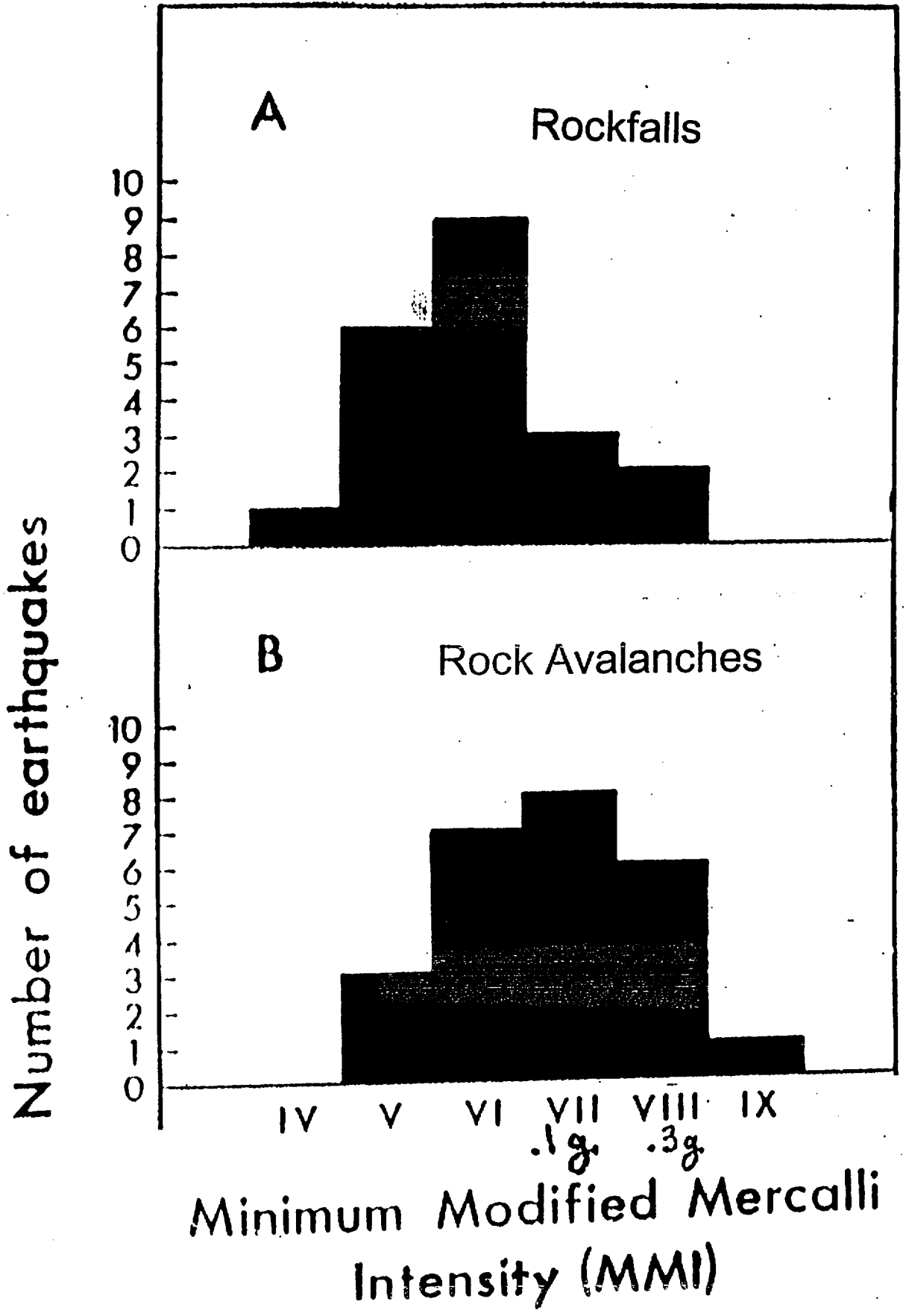
Presented at Salt Lake City

PSHA Conference

January 6, 1997

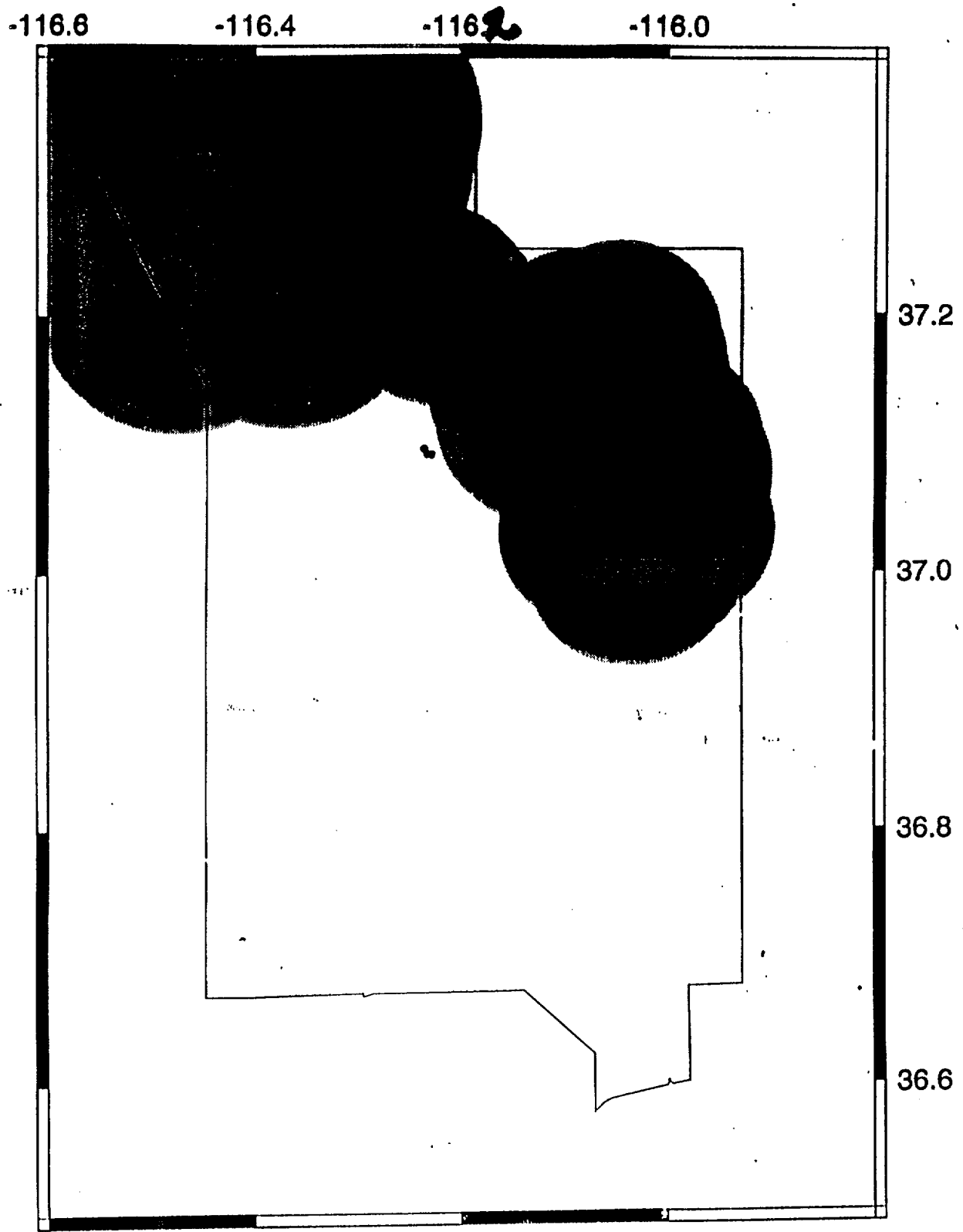
CONCLUSION

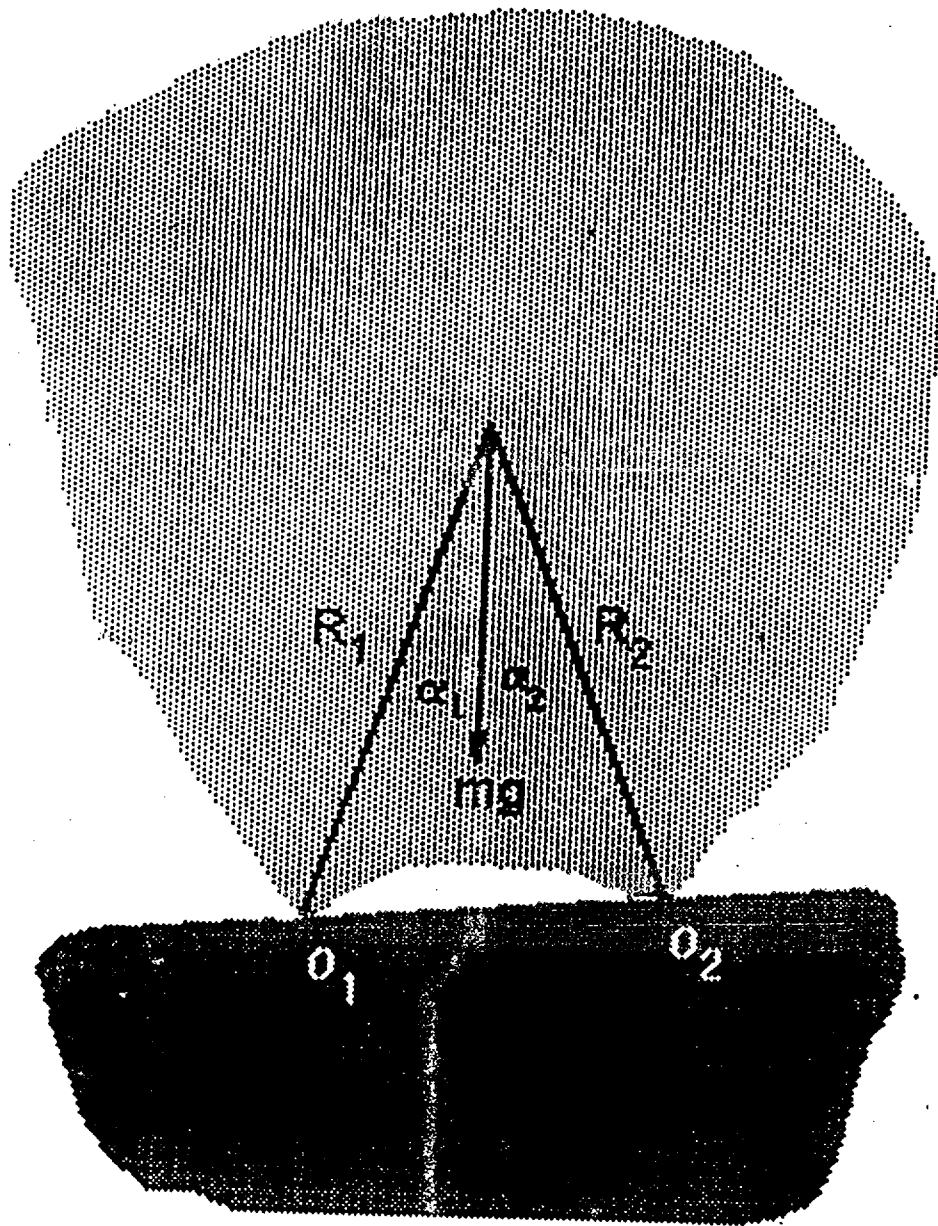
1. In some types of terrain groups of precariously balanced rocks evolve naturally unless shaken down by earthquakes.
2. Groups of precariously balanced rocks are effectively strong motion seismoscopes that have been operating on solid rock outcrops for thousands of years. They provide direct evidence about past ground shaking (fault paleoslip studies only provide indirect evidence).
3. Study of precarious rocks can provide important information about seismic hazard.
4. The assumption of large randomly distributed earthquakes is not valid for some areas of S. California.
5. There has not been severe shaking at Yucca Mtn., Nev., in several thousand years.

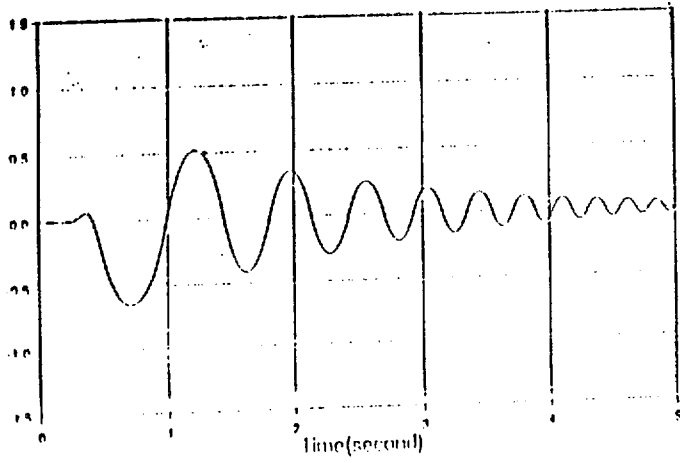


≥ 0.2 g Acceleration

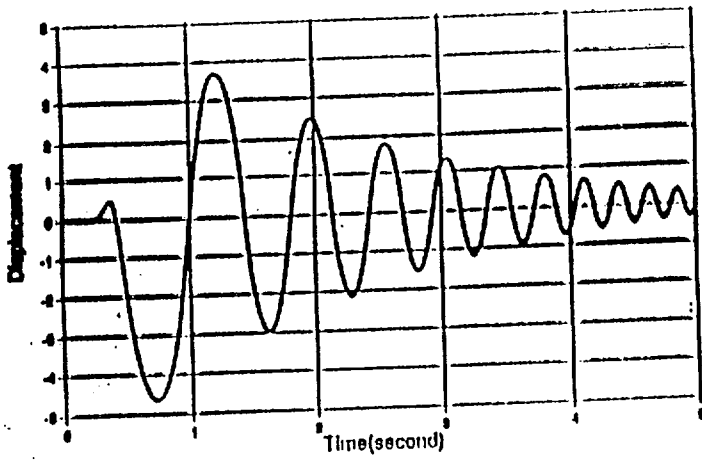
Assuming Maximum Value of Announced Yield



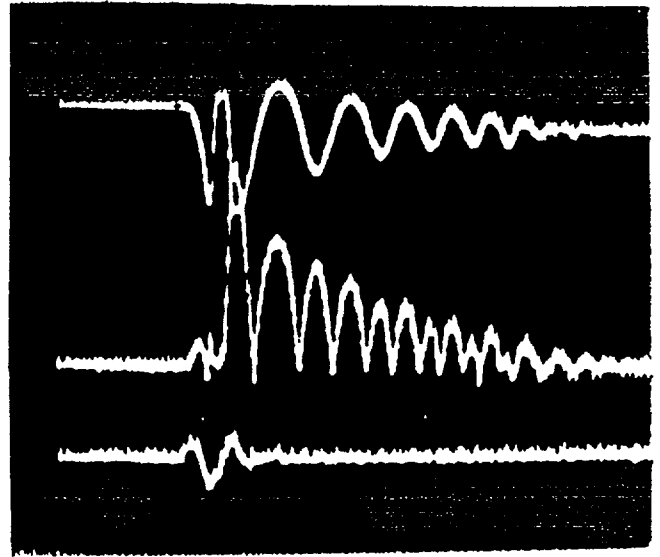
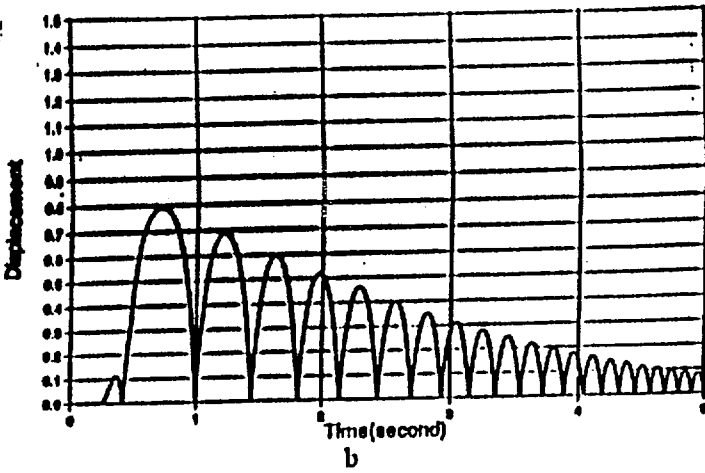




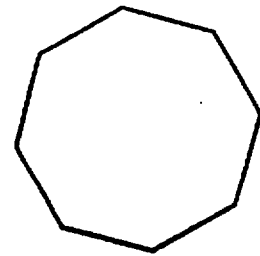
Horizontal Displ



Vertical Displ



a



Figure(10)

Octagon Model Free Rocking:

a. Experimental Result

b. Numerical Simulation

EL CENTRO ACCELEROGRAM

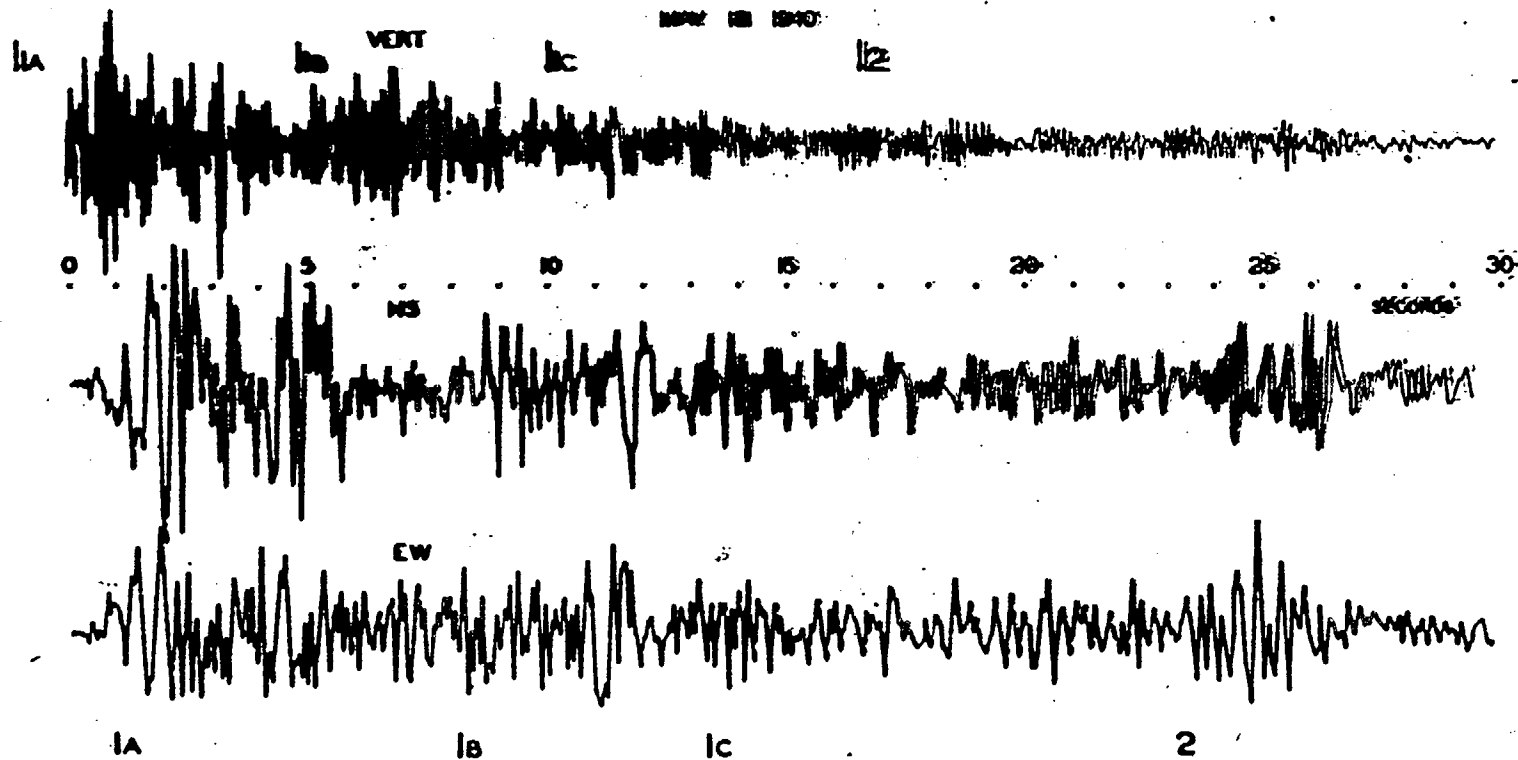
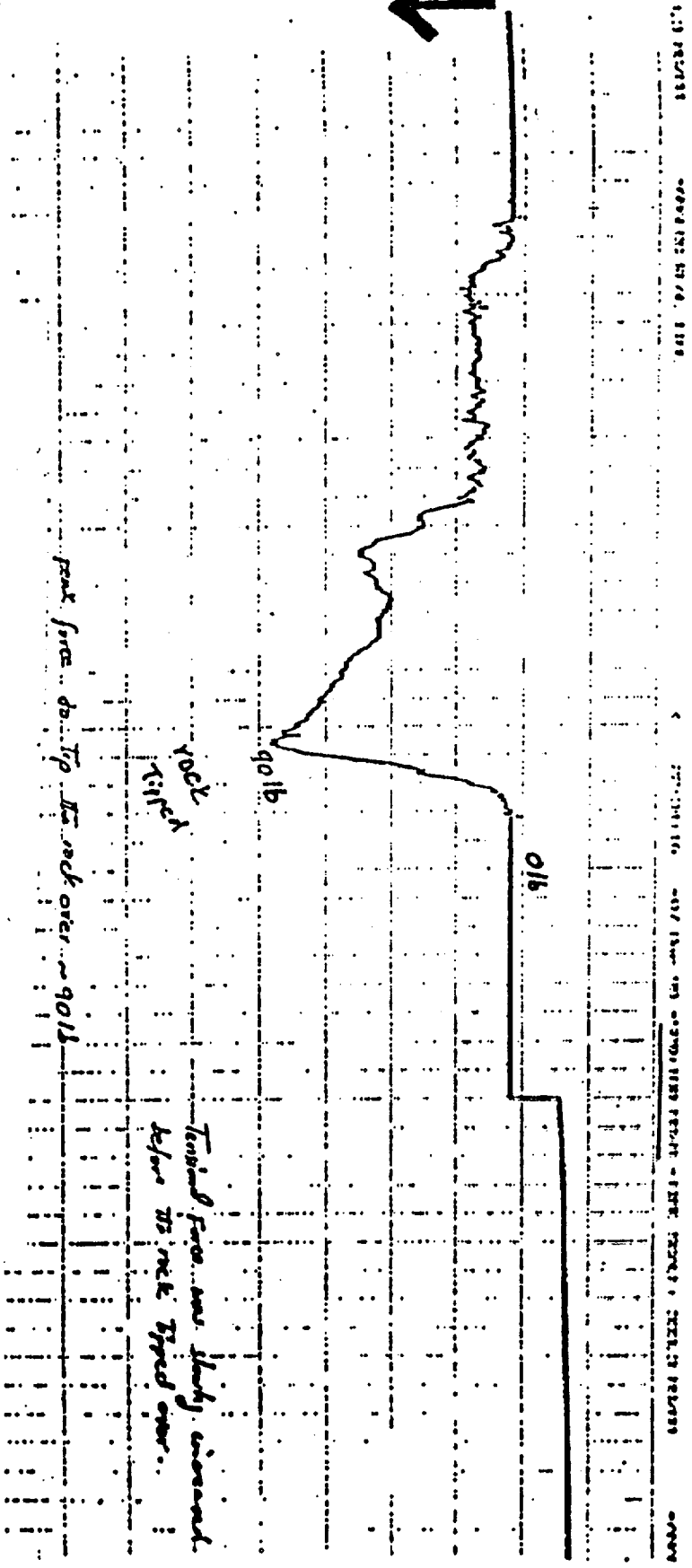


FIG. 2a. El Centro strong motion accelerograph record for events 1A, 1B, 1C and 2. The time is given in seconds.

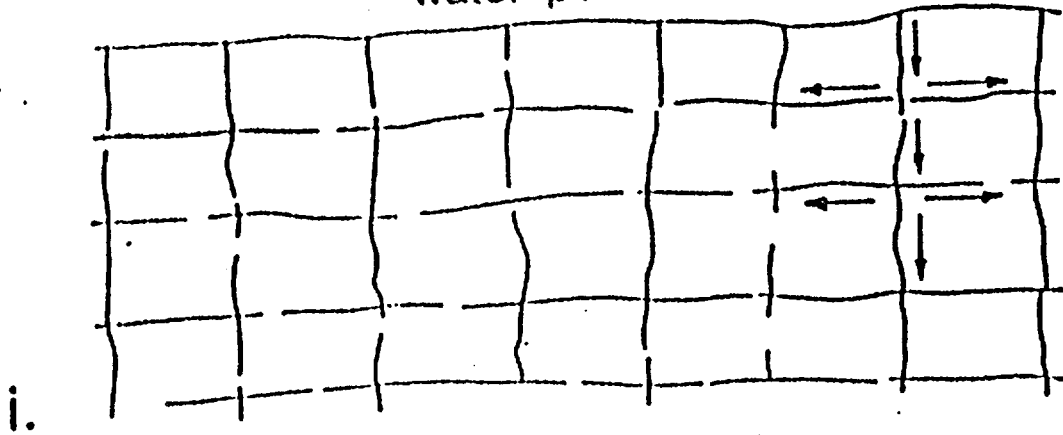
FIG. 2b. Replotted El Centro strong motion accelerograph record for events 1A, 1B, 1C, and 2. For better readability of the record the gain is reduced by the factor of 2.10.

Force

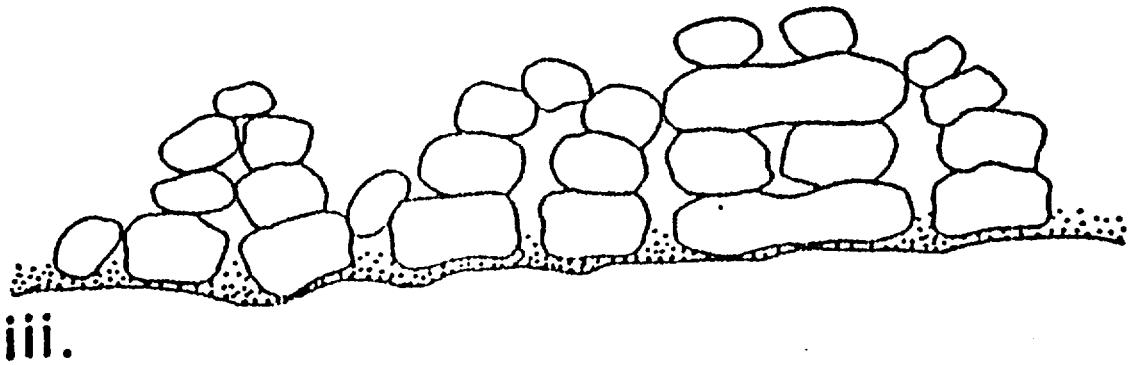
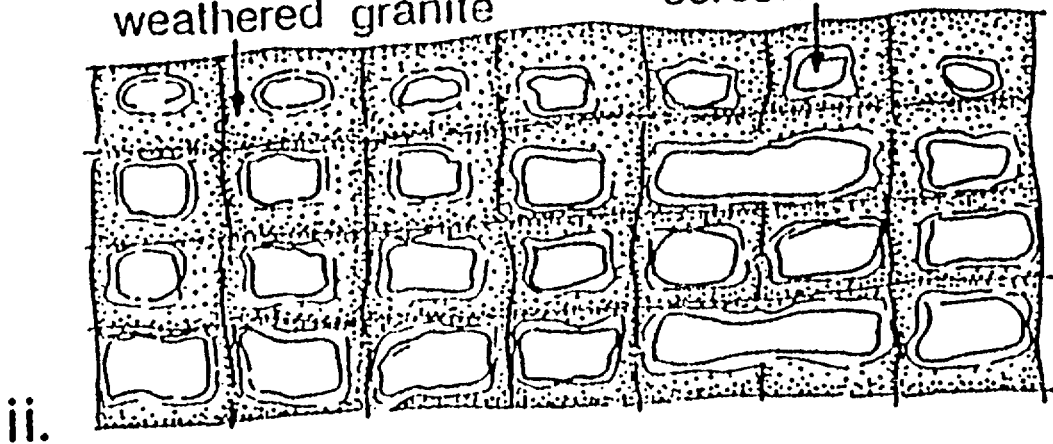


Quasi-static field test

water penetrates down joints



weathered granite corestone or kernel



Two-stage development of boulders by differential fracture-controlled surface weathering and subsequent exposure of corestones by evacuation of friable weathered debris (Twidale, 1982).

³⁶Cl sample

Sample E

Sample D
VL > 10.5

Sample C

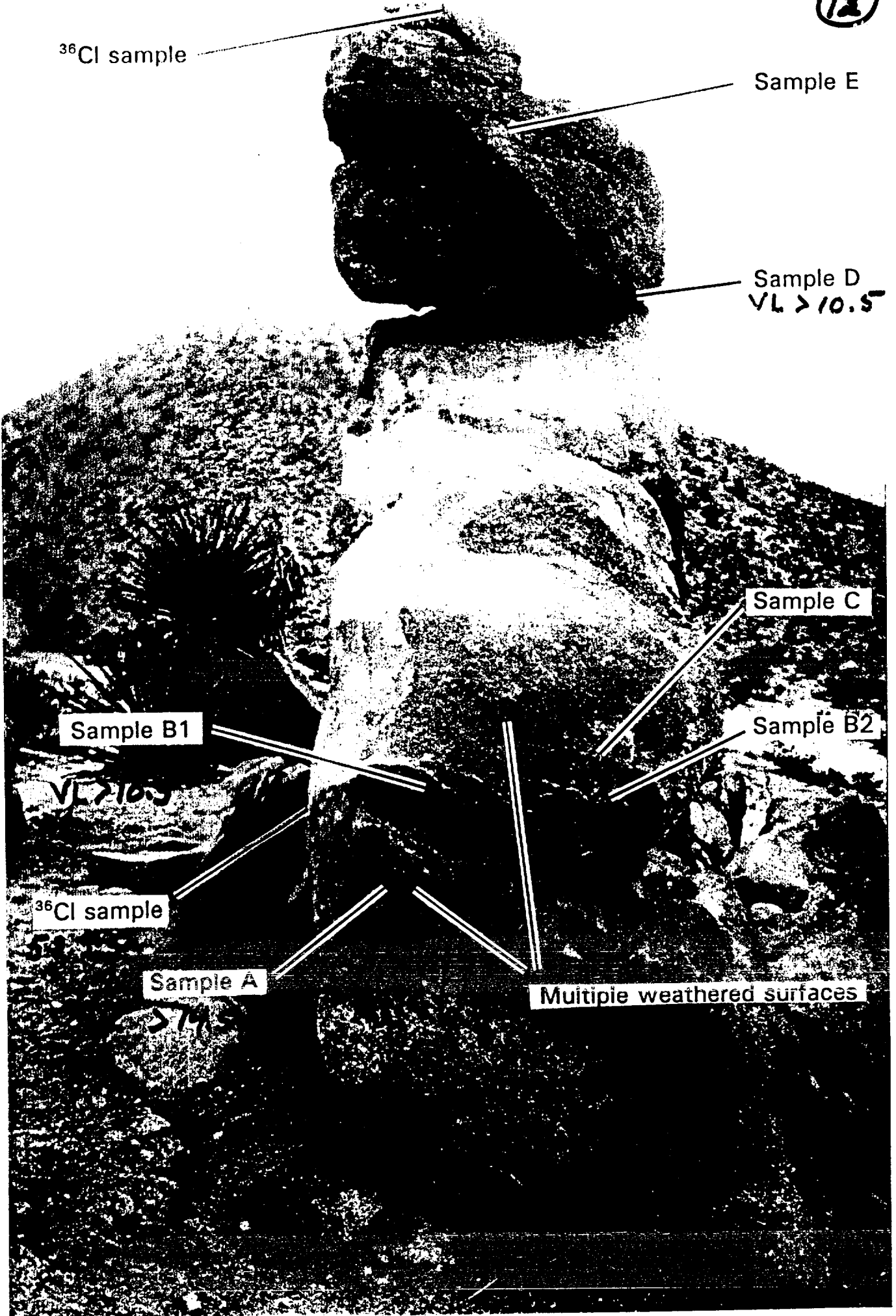
Sample B1

Sample B2

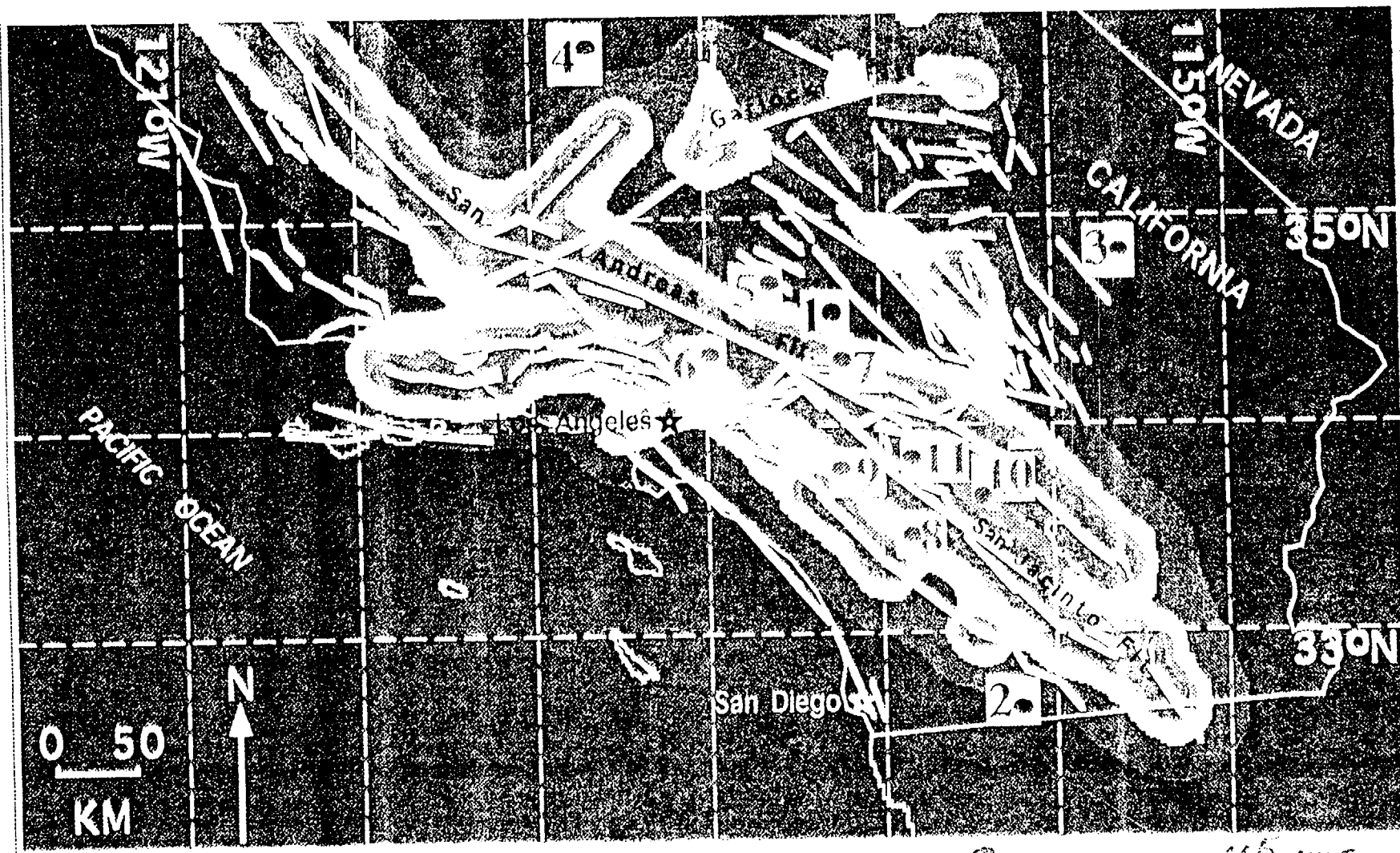
³⁶Cl sample

Sample A

Multiple weathered surfaces



5-2



SOUTHERN CALIFORNIA FAULTS: Peak Ground Accelerations; 90% probability in 1000 years

Dark Blue: $\leq 0.1g$

Light Blue: 0.1-0.2g

Orange: 0.3-0.4g

Red: $> 0.4g$

PGA map supplied by S.G.Wesnousky, M.W.Stirling & C.H.Willoughby

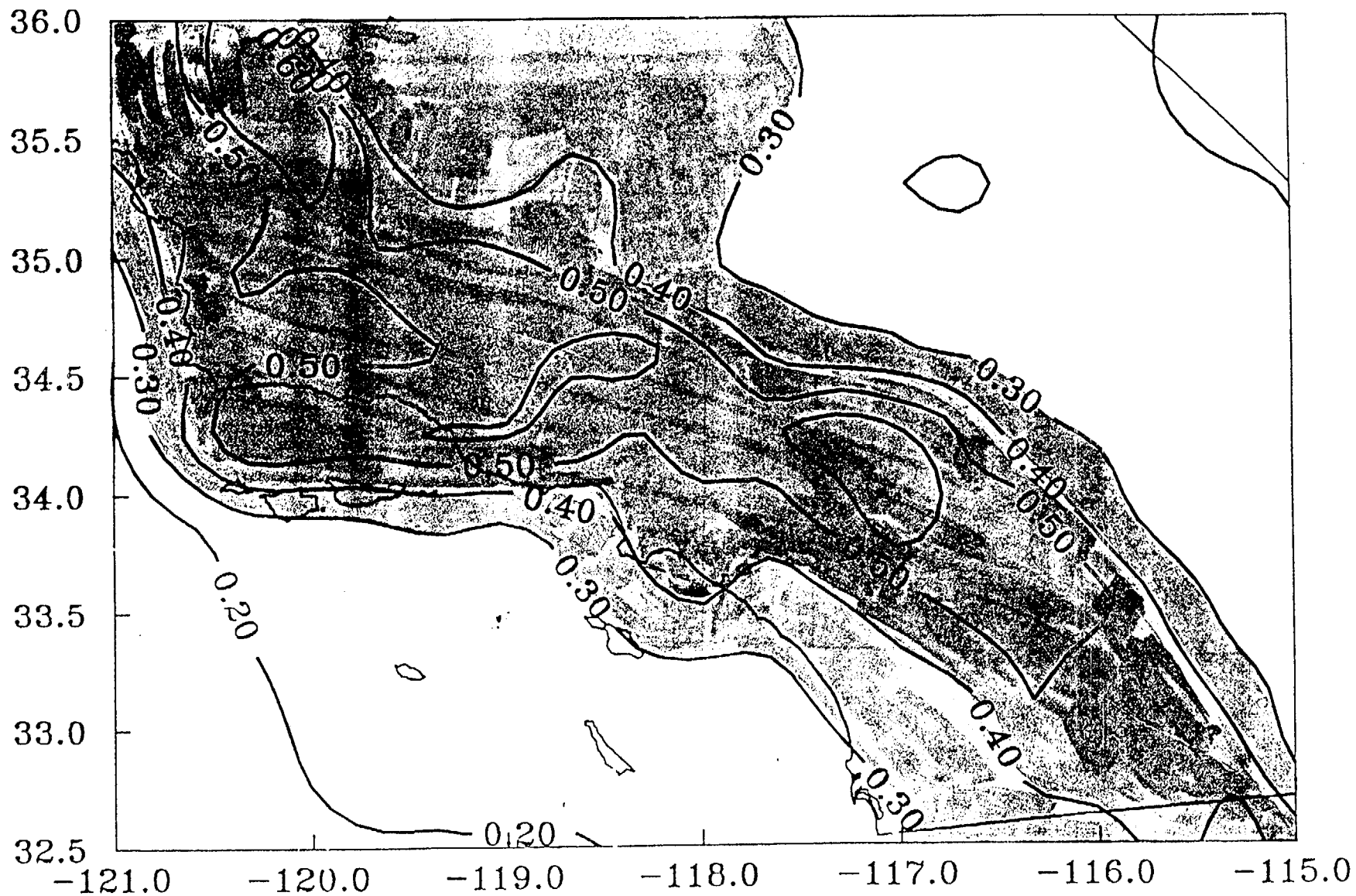
①

SCEC Working Group

10

45

PGA with 90% Probability of Exceedance in 1000 Years



NEVADA

90% 1000-yr and 5000-yr PROBABILITIES

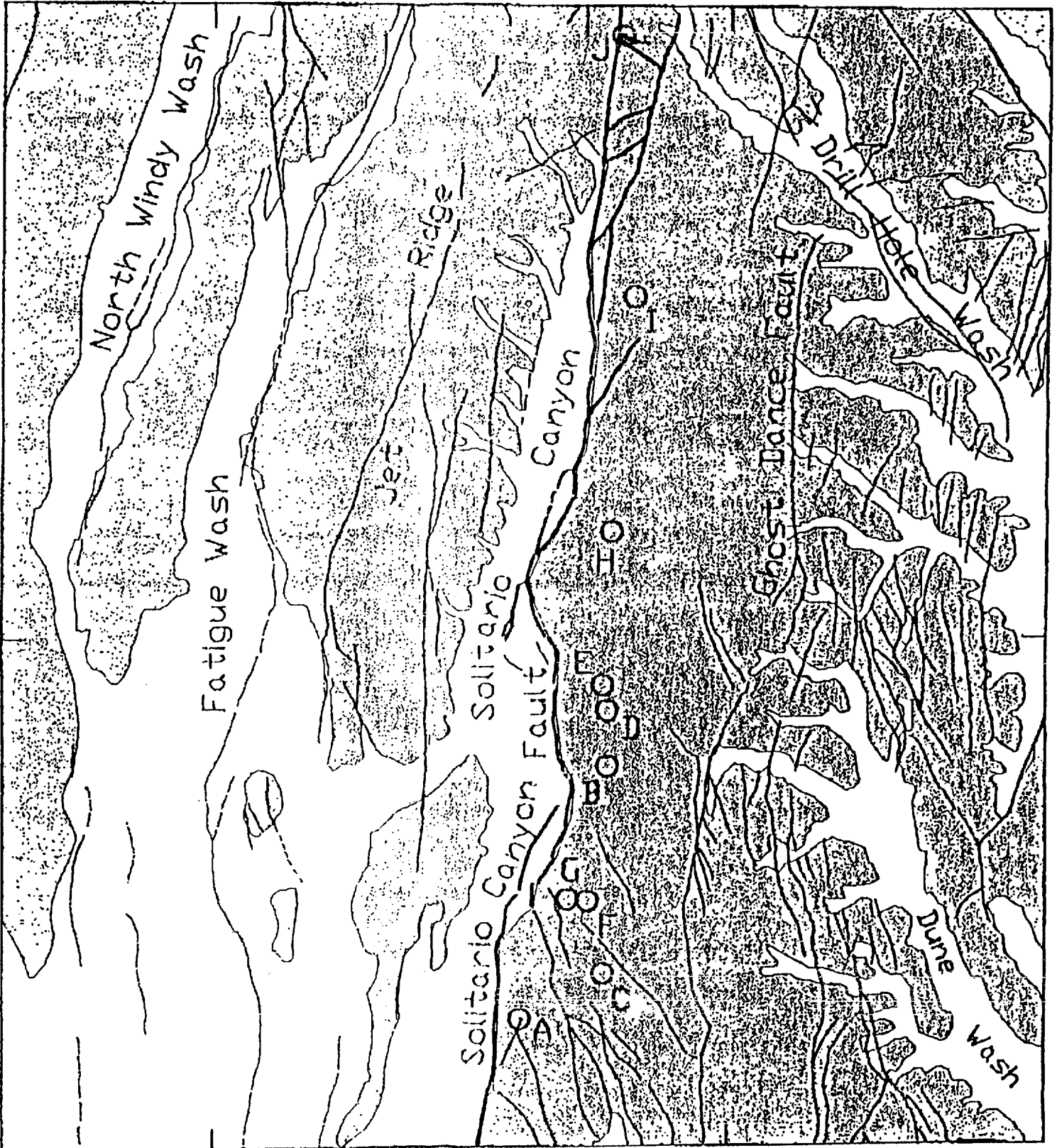
Site	Without Diffuse		With Diffuse		Det.
	10 ⁻¹ 1000 yr	10 ⁻² 5000 yr	10 ⁻¹ 1000 yr	10 ⁻² 5000 yr	
Contact	.01	.04	.08	.28	.70+
Owyhee	.01	.04	.08	.28	.60*
Jarbridge	.01	.04	.08	.28	<.40
Sand	.033	.14	.50*	.90	.70*
So. Lake Tahoe	.01	.04	.04	.16	.70
Beatty	.04	.16	.25	.50	.45
So. Crater Flat	.04	.16	.4 *	.8 *	.70
Tarantula Canyon	.04	.16	.4 *	.8 *	.70 [#]
Red Rock	.04	.32*	.32*	.63*	>.70*
Austin Sum.	.02	.10	.40*	.80*	.70 [#]
Palmetto Wash	.01	.25	.12	.25	.55*
Ash Springs	.01	.06	.025	.35*	.60*
Nelson Landing	.01	.04	.025	.06	<.40
W of Wabuska	.04	.19	.32	.68	.70*
Wilson Canyon	.04	.20	.32	.68	.70*
Winn. Ranch	.04	.40	.32	.70	.70*

*Exceeds precarious rock estimate

[#]Semi-precarious

116°30'00"

116°27'30"



Modified from Scott (1990)

EXPLANATION

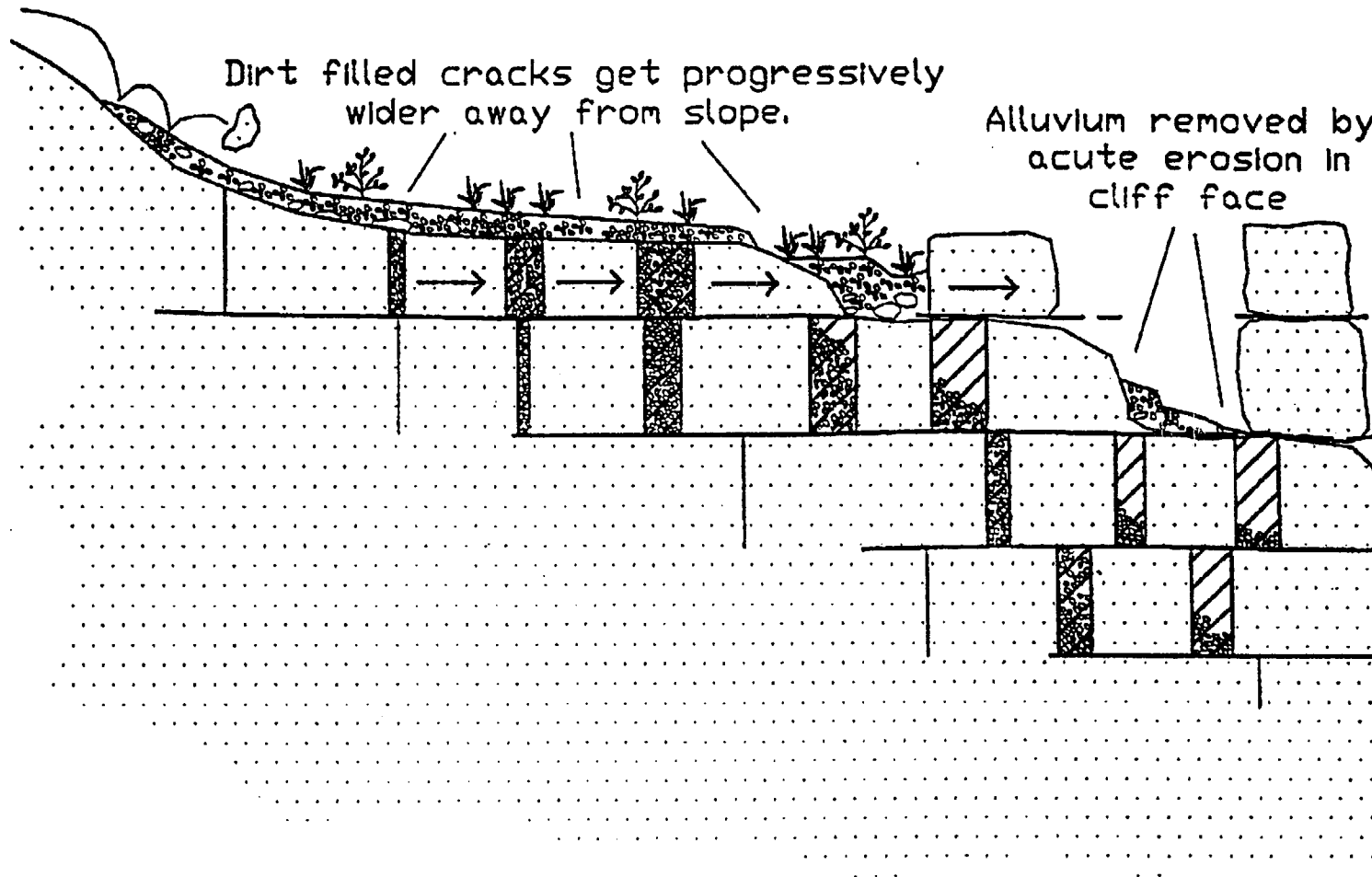
- Location of a precariously balanced rock



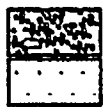
SCALE



Creation of a balanced rock by erosion.
 A schematic cross section through welded tuff
 of the western face of Yucca Mountain



EXPLANATION



Alluvium
 Bedrock



Joint



Open fracture

**SUMMARY OF
YUCCA MOUNTAIN
QUATERNARY GEOLOGY RESEARCH**

**Prepared for NAS Committee for Yucca Mountain
Peer Review Field Trip**

JOHN W. BELL

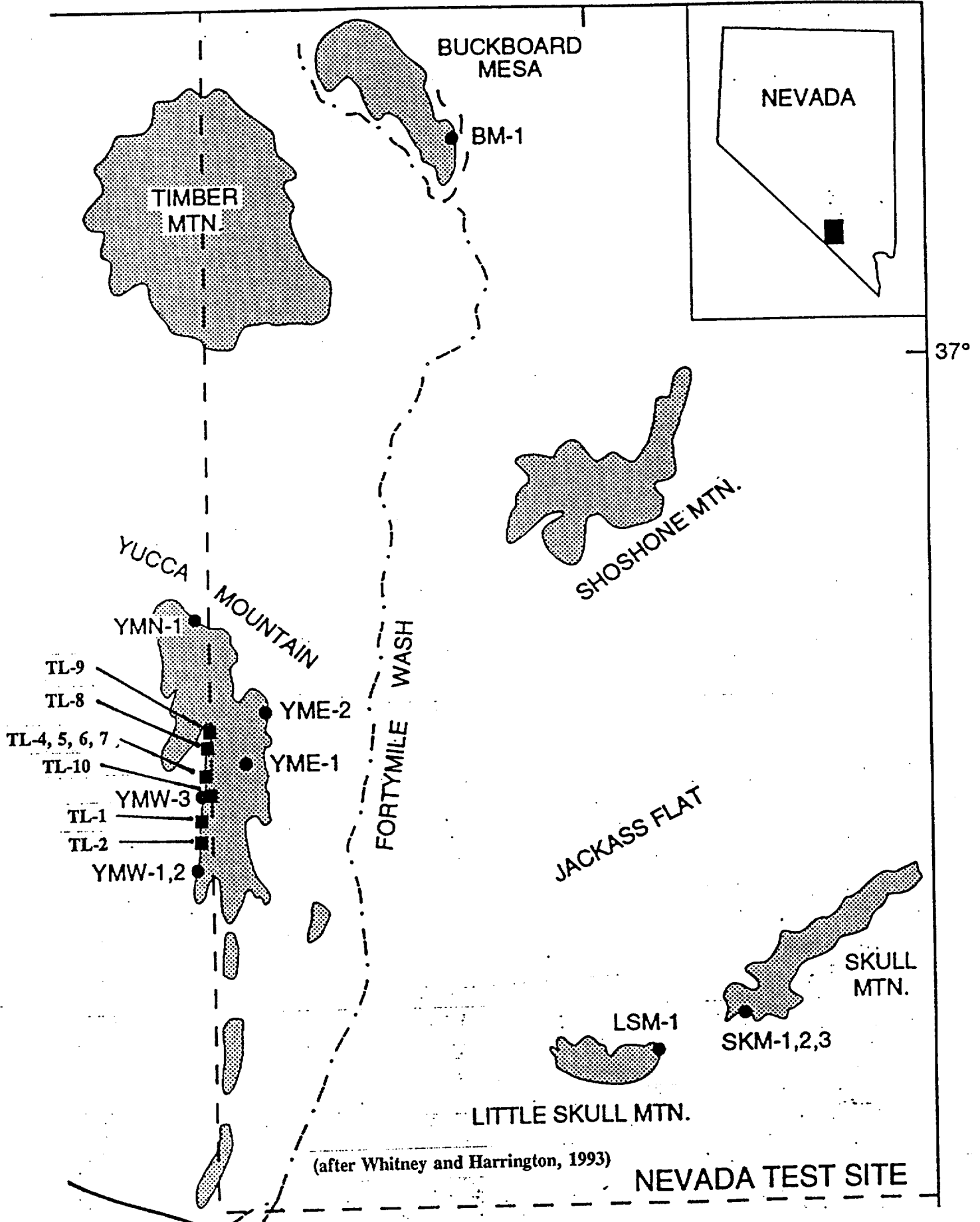
**NEVADA BUREAU OF MINES AND GEOLOGY
MACKAY SCHOOL OF MINES
UNIVERSITY OF NEVADA, RENO**

**Nevada Bureau of Mines and Geology
Is Non-Regulatory
Research and Public Service Department**

**As the State Geological Survey
NBMG conducts research on all aspects of Nevada geology**

Varnish Microlamination Sites

116°15'



(after Whitney and Harrington, 1993)

Preliminary Varnish Microlamination Ages

(Additional microlamination studies are in progress)

Tanzhuo Liu
Lamont-Doherty Earth Observatory

Yucca Mountain Bedrock Cliffs

Age (ka)

TL-1	>10.5 <27
TL-2	>14.5 <21
TL-4	>10.5 <14.5
TL-5	>10.5 <14.5
TL-6	>10.5 <14.5
TL-7	>10.5 <14.5
TL-8	>10.5 <14.5
TL-9	>10.5 <14.5

Yucca Mountain Stone Stripe

Whitney and Harrington (1993)
colluvial boulder site YMW-3

710

TL-10

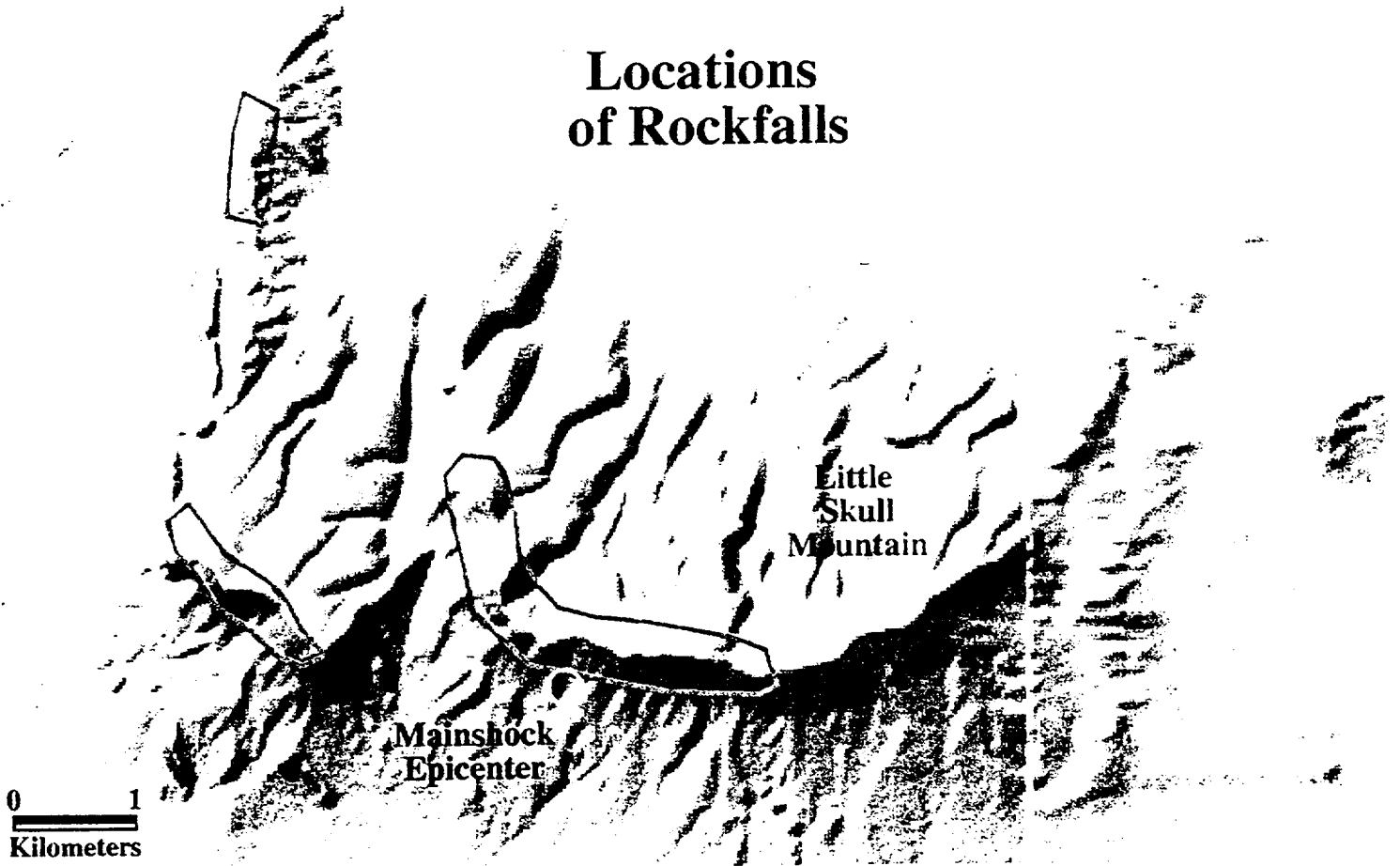
21-27 (<70)

Precarious Rocks and Ground Motion from the Little Skull Mountain Earthquake

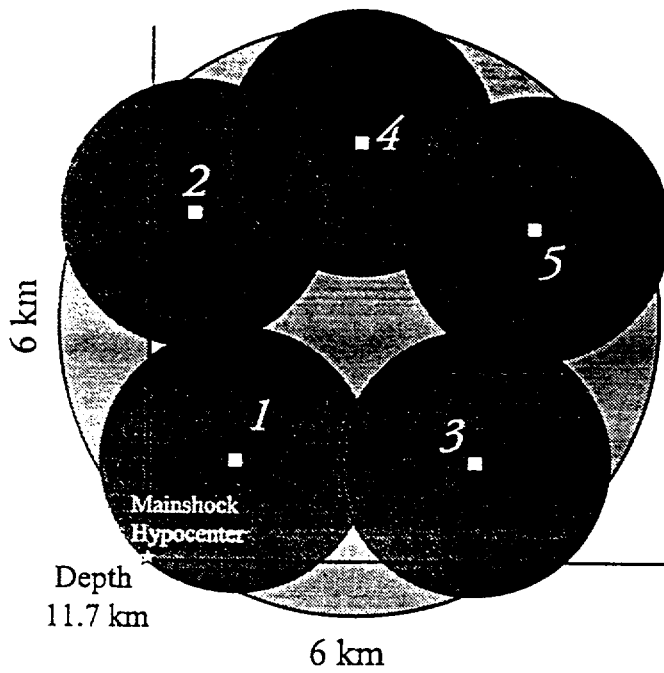
James Brune and Kenneth Smith

1. The shape of predicted ground motion maps agrees with the distribution of rockfalls and precarious rocks.
2. There are a number of precarious rocks of old age still standing along the eastern 2/3 of Little Skull Mountain, indicating the region is not very active and that there have not been any much larger events nearby in the last 10 ka. This may be consistent with LSM being a rare triggered event, triggered by the Landers earthquake.
3. There is evidence of moderate shaking at the east end of LSM several thousand years ago.
4. The technique shows promise for future studies of ground motion and seismic risk.

Locations of Rockfalls

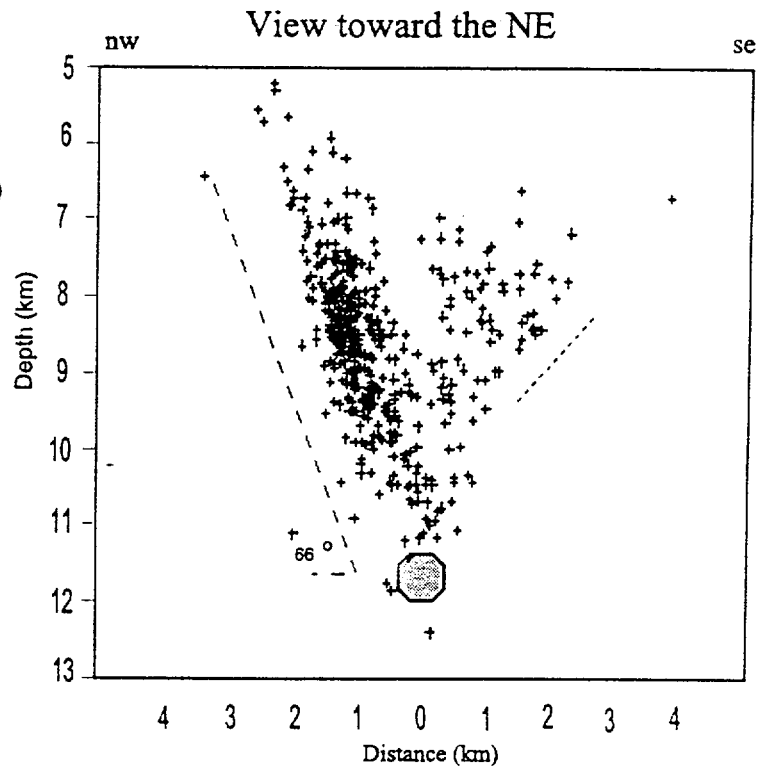
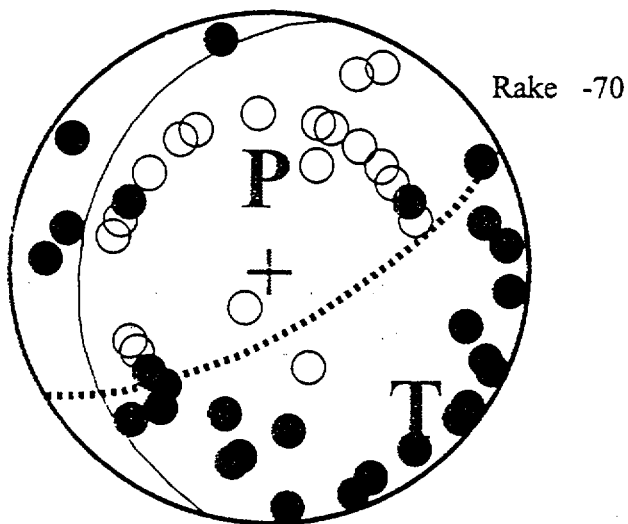


Source Model Geometry

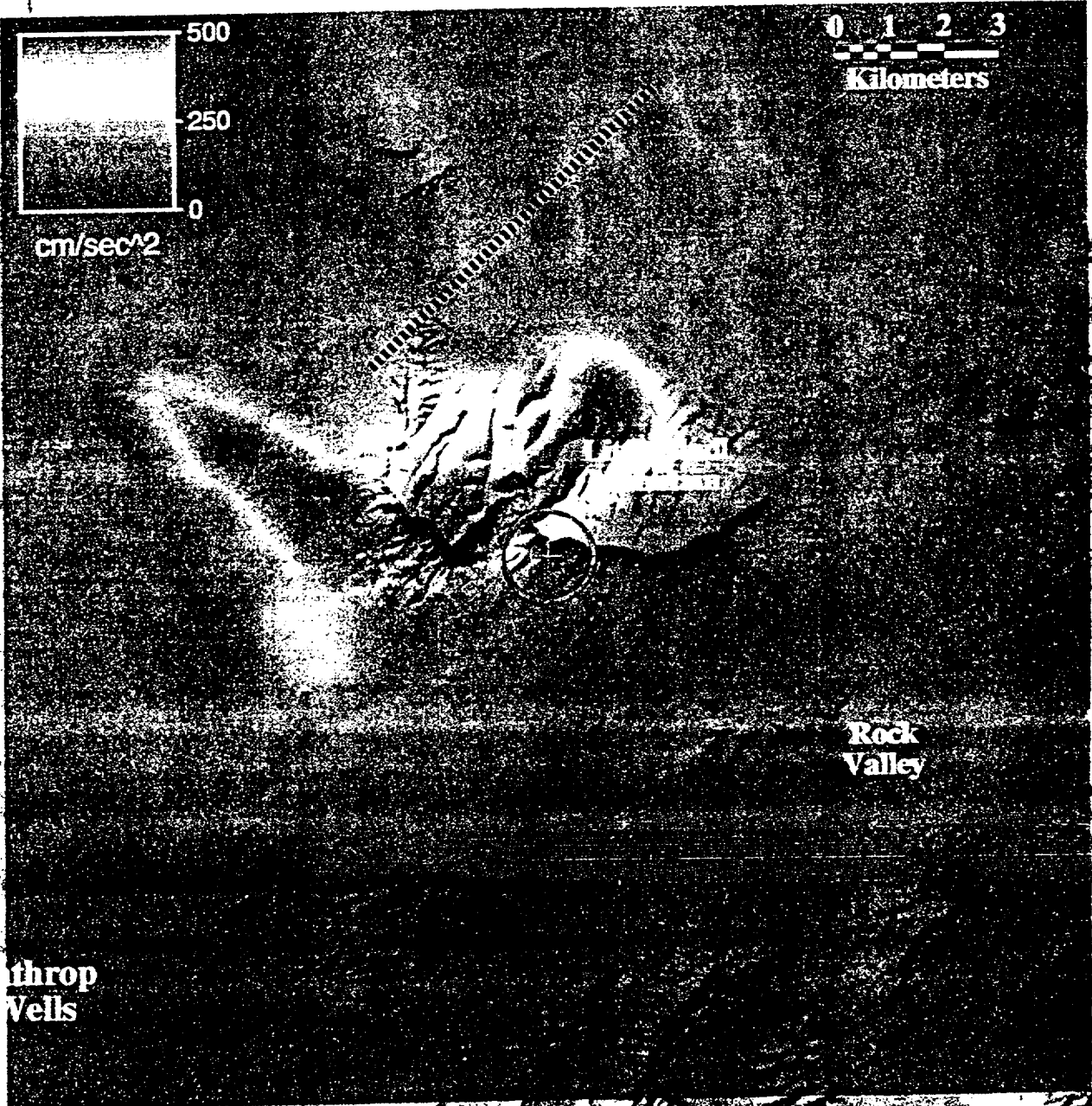


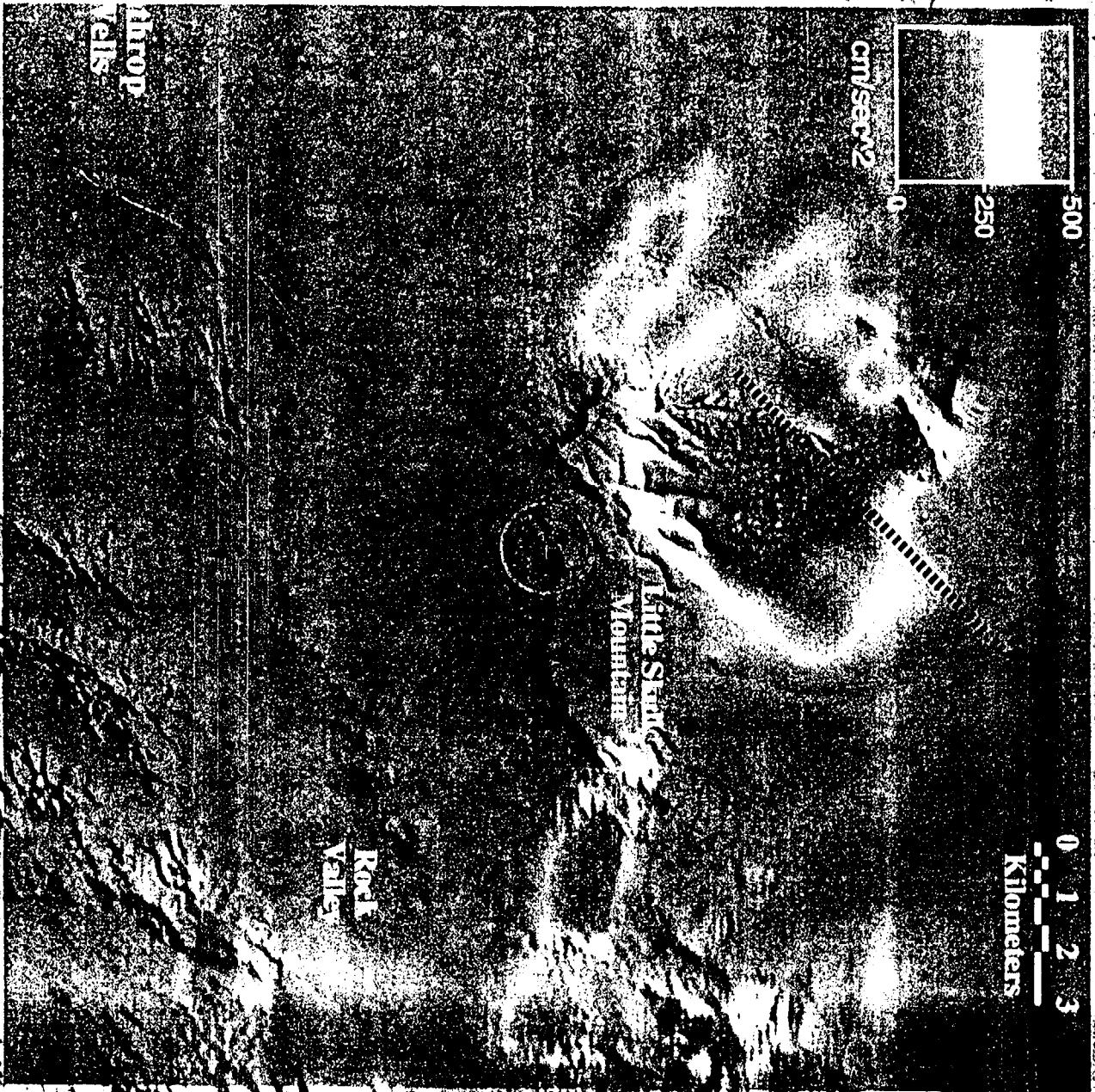
Strike N48E
 Dip 65SE
 Displacement 40 cm
 Subevent Risetime ..1 sec

Mainshock Short Period Mechanism



 Mainshock





TECTONIC MODELS--A COMPARISON

Team= Jon Ake, Jim McCalpin, Burt Slemmons
Jan. 6, 1997

1. CALDERA MODEL (includes caldera-detachment model of Carr)

1A. Passive Model (crustal blocks sliding into a "hole" beneath Crater Flat; hole made by Tertiary caldera collapse or by westward detachment faulting)

STRENGTHS:

1) The caldera complex is centered on a deep N-S trough or rift (Amargosa Desert rift); however, it is not clear whether the calderas are a result of the rift, or the reverse.

2) Crater Flat/Yucca Mountain faults make a distributed fault system that mirrors the faults north of the caldera complex. This symmetry about the calderas suggests a causal connection.

WEAKNESSES:(from p. 8-61)

1) Calderas have been inactive since 14 Ma, so how could they affect current faulting?

2) Calderas don't explain the change from rhyolitic to basaltic eruptions in Crater Flat in past 3 Ma.

3) Doesn't explain vertical axis rotations.

4) Doesn't explain post-10 Ma uplift of Bare Mountain block.

Probability= 0%

2. VOLCANIC-TECTONIC MODEL (surface-rupturing earthquakes are accompanied by dike injection)

STRENGTHS:

1) With continuing Quaternary eruptions in Crater Flat and south, some connection between volcanic and tectonic processes is likely.

2) Yucca Mtn faulting is widely distributed, like faulting in other volcanotectonic areas such as Mammoth Lakes. If USGS "Scenario earthquakes" are single events, then such distributed rupture is also characteristic of volcanic-tectonic events.

3) The "ash event" at 70 ka appears to be connected with basaltic eruptions.

WEAKNESSES:

1) Most of the 12 large (or 35 total) paleoearthquakes in the past 500 ka at Yucca Mountain are not associated with the episodes of volcanic eruption.

2) There is no direct evidence that the rift beneath Crater Flat was formed by volcanic action. Other possible origins: 1) a deep graben created by east-west tectonic extension, 2) a more northerly trending part of a Amargosa Desert rift, that happened to thin the crust until subcrustal magma was tapped, or 3) a northerly jog in the N50W-trending Amargosa River-Pahump-Stewart Valley strike-slip fault zone.

Probability: 10% (only to indicate that a volcanic-tectonic connection may operate some of the time, and not that the calderas are active or control faulting).

3. DETACHMENT MODEL (SIMPLE SHEAR)

STRENGTHS:

- 1) Explains the many narrow, parallel fault blocks as dominos above a detachment.
- 2) Tertiary detachment faults do exist in the region surrounding Yucca Mountain.
- 3) Normal faults may be utilizing parts of old detachments, as in the Overthrust Belt (Smith and Arabasz).

WEAKNESSES: (from p.8-74)

General:

- 1) Historic EQs show planar faulting (L. Skull Mtn.); no evidence of low-angle seismicity.
- 2) The known detachments to the E and W are old (>6 Ma).
- 3) Basaltic volcanism requires deeply penetrating structures.

Applies to Shallow Detachments:

- 4) No shallow (<5-6 km) detachment is seen on the seismic line.
- 5) Elsewhere in the region, there is no detachment at the T/Pal boundary (it's an unconformity).
- 6) Movement on the Bare Mtn. Fault would have truncated the detachment.

Applies to Deep Detachments:

- 7) A deep (6-15 km) detachment could not produce the observed dip rollovers and opposed slip on some faults.
- 8) Deep detachment requires tensile behavior at the base of the dominos=unlikely.

Probability: 20%; deep detachment cannot be ruled out by geophysics.

4. PLANAR FAULT BLOCKS MODEL (PURE SHEAR)

4.1 E-W Basin & Range-type extension, with some influence of dextral shear in S. part of area

STRENGTHS:

- 1) Amargosa Desert rift and all N-S trending parallel faults suggest E-W horst and graben system.
- 2) Largest historic EQs (e.g., Little Skull Mtn.) show planar faulting to depth.
- 3) Seismic lines show there are no detachments within the upper 5-6 km.
- 4) Rifting can explain basaltic volcanism.
- 5) Boundary element modeling can replicate the seismic section using planar faults.
- 6) Explains increasing vertical axis rotation of fault blocks in southern Crater Flat.

WEAKNESSES:

- 1) Pure horizontal extension does not explain vertical axis rotations.
- 2) Net slip (and slip rate) on the Bare Mtn. fault (=master fault) must be greater than the sum of all the slips (and slip rates) on all the antithetic (Yucca Mtn) faults; **THIS IS NOT THE CASE.** (However, some of the faults in the Bare Mtn. fault zone may be buried by Holocene and late Quaternary alluvium up to 150k yr old).
- 3) Boundary element model predicts that, to get a slip event on antithetic faults, you need multiple slip events on the main (Bare Mtn.) fault; **THIS IS NOT THE CASE.**
- 4) Doesn't explain the "ash event".

Probability: 35%

4.2 Crater Flat is a transtensional rhombochasm (pull-apart) due to a right step in the Walker Lane

STRENGTHS:

- 1) Explains inferred oblique component of normal faulting in/near Yucca Mountain.
- 2) Explains oblique nature of instrumental seismicity.
- 3) Could possibly explain why fault behavior in past 500 ka does not match the results of boundary element models.
- 4) The extreme northern limit on the main Yucca Mountain faults is at or near the linear northwest-trending Yucca Wash on the north. The faults have displacements that decrease toward this geophysical lineament, that has no known fault origin in the shallower units, and it does not appear to be a seismic source. [Only one fault, the Paintbrush Canyon fault clearly crosses this feature and it may change in character across Yucca Wash.] The extreme southern limit to Crater Flat and Yucca Mountain faults is near the linear northeast-trending inferred fault shown by Fridrich and Price (199x). The orientation of N45W suggests that it may be a right-lateral oblique fault. **THUS, THESE NW-TRENDING FAULTS MAY BOUND A RHOMBOCHASM.**

WEAKNESSES:

- 1) Ambiguity about the existence of the required dextral faults at the N and S ends of the rhomboid.

Probability: 35%

5. LATERAL SHEAR MODELS

5.1 Transtensional nappe model (Hardyman).

STRENGTHS:

- 1) Explains how Walker Lane shear could produce observed fault blocks.
- 2) Cedar Mtns. EQ of 1932 displayed distributed faulting with a high oblique component.

WEAKNESSES: (from p. 8-80)

1) "none of the criteria or geometry required for Hardyman's model exist at >Yucca Mtn." [Hardyman originally proposed this model for the Gillis Range-Cedar Mountain area, for a well-bedded pyroclastic sequence, above a sheared unconformity with Mesozoic rocks that is cut by a lateral fault. I don't think there is any evidence for this type of mechanism at YM-DBS].

Probability: <1%.

5.2 Buried, 250 km-Long Strike-Slip Fault beneath YM (Schweickert)

STRENGTHS:

1) Explains vertical axis rotations.

WEAKNESSES: (from p. 8-84)

1) There is no surface evidence of strike-slip faults at YM/Crater Flat, nor of any single, continuous strike-slip fault southeast of Crater Flat along the State line.

2) Vertical axis rotations in the area are variable in time and space, not uniform as expected if there was only one long SS fault.

3) No evidence for 25 km dextral offset of volcanics in Crater Flat.

Probability: <1% (unless mappers have missed a big SS fault nearby).

OUR PREFERRED COMPOSITE TECTONIC MODEL.

This model is based primarily on the Planar Fault Model:

1. Generally, the fault azimuth may be a first order control on the type of fault, with conjugate relationships (a la Wright, 1976). Regionally northwest-trending faults are right-lateral, northerly-trending faults are normal, and northeast-trending are left-lateral. By far the most active faults are the strike-slip faults; normal faults have slip rates of 1%-10% of the SS faults. Most of the surface expressed faults at Yucca Mountain are northerly trending, and are mainly normal faults.
2. Faults are planar (or weakly curved) to seismogenic depths.
3. Most Yucca Mountain faults do not appear to merge above seismogenic depths. For those that are so closely spaced that they may merge above 15 km, we still calculate Maximum Magnitude as if they were entirely separate faults.
4. Fault slip is dominantly dip slip in the northern part of the area; southwards, the horizontal component increases by a vertical axis rotation. Currently it is not known whether this is do to local effect at the southerneastern edge of Crater Flat, or to a subordinate tectonic rotation induced by a right-lateral fault zone in Amargosa Valley.

From the Lateral Shear Model:

5. The oblique component of slip on Yucca Mtn. faults, and the clockwise vertical axis rotation are related to dextral strain (bending) transmitted from the Walker Lane. However, it is unclear whether discrete NW-striking dextral faults exist N and S of Yucca Mtn. (defining a rhombochasm), or whether lateral strain is diffuse.

From the Volcanic-Tectonic Model: [Note: This model does not require a caldera source, but depends on the simultaneous basaltic volcanic eruption and the extensive tectonic, seismogenic rupturing of several faults that fan out (radiate) northward from a Lathrop Cone volcanic source.

6. Some surface-rupturing paleoearthquakes (e.g., Scenario U) have probably accompanied episodes of basalt eruption and dike injection.

IMPLICATIONS OF OUR PREFERRED MODEL TO SEISMIC HAZARDS

1. Fault plane areas will be computed as if each fault individually extends to seismogenic depths (ca. 15 km).
2. Due to (1), for multi-fault-rupture Scenarios we assume that fault area is the sum of areas for all faults that ruptured. [Note, however, that unless the separate faults ruptured simultaneously (i.e., within about 12 seconds of each other), we will assume that these Scenario earthquakes are separate earthquakes spaced a few hours to decades apart, with correspondingly lower magnitudes than a large simultaneous rupture.]
3. The magnitudes of volcanic-tectonic earthquakes (e.g., Scenario U) cannot always be estimated from data sets such as Wells and Coppersmith (1994), which contain only tectonic earthquakes. [Note that the some of the Mammoth Lakes, New Zealand, Hawaii, and Iceland events from volcanic areas have $M > 7.2$ and fit the W&C curves. Other events have very low magnitudes associated with long rupture lengths or large displacements.]
4. Behavioral aspects such as distributed, multi-fault earthquake "scenarios" could occur in any of the Tectonic Models. However, simultaneous faulting on parallel normal faults may be more easily explained by the Volcanic-Tectonic Model (which we have weighted at only 5%) than by the Lateral Shear Model (a variant of which we weight at 20%), and least by the Planar Block Model (which we weight the highest at 60%). Thus, our weighting of Tectonic Models implies that, in our opinion, simultaneous multi-fault ruptures (i.e., within a 12-15 second time span) have a low probability.

CALDERA MODEL - 1

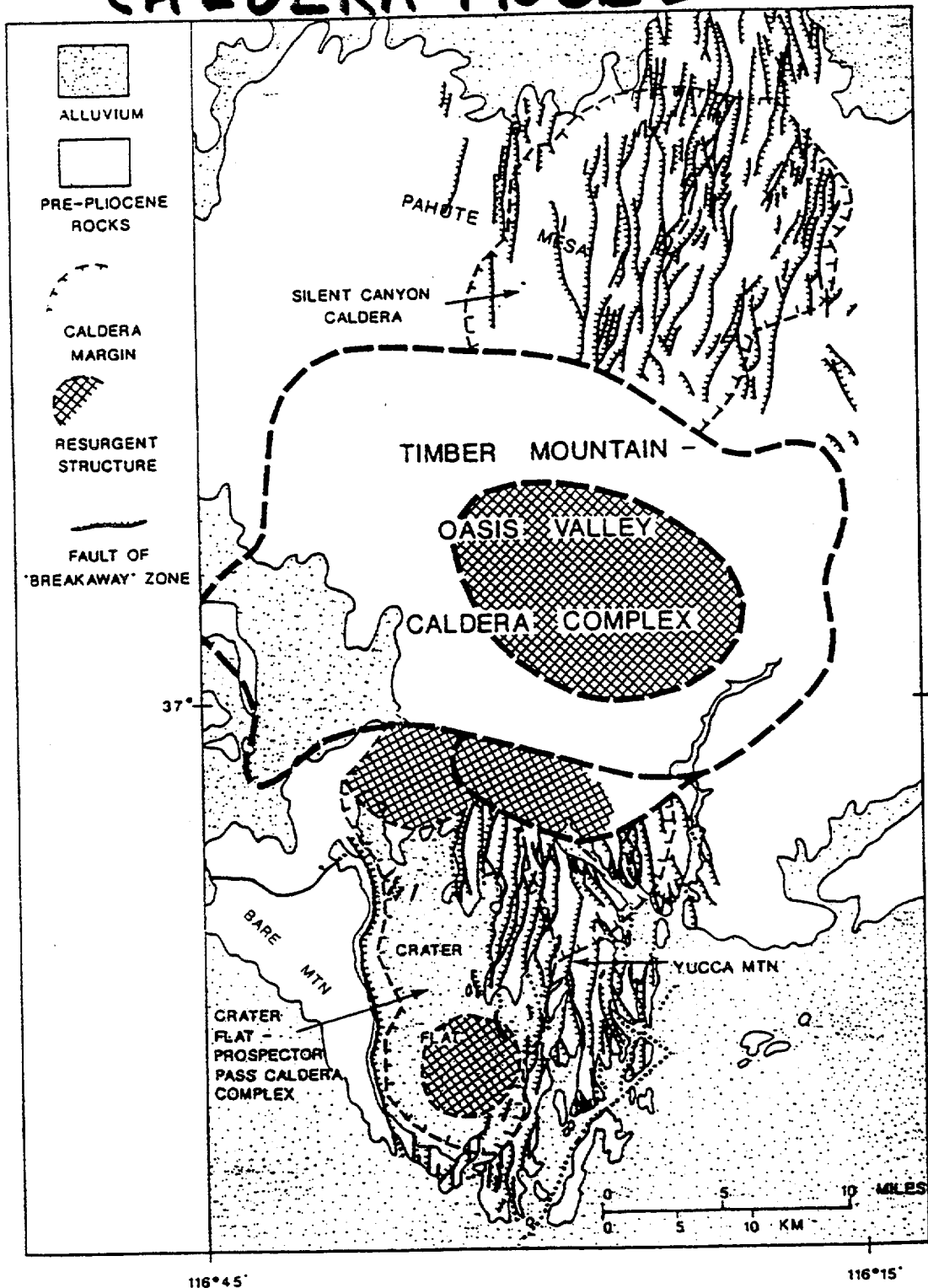


Figure 8.14. Coaxial fault sets of Yucca Mountain and Pahute Mesa separated by caldera complex (from Carr, 1990, p. 293). Carr related these faults to the Kawich-Greenwater rift. "Breakaway zone" refers to the idea that the rift, and the fault sets, form a structural boundary for detachment faults west of the Bare Mountain fault.

CALDERA MODEL-2

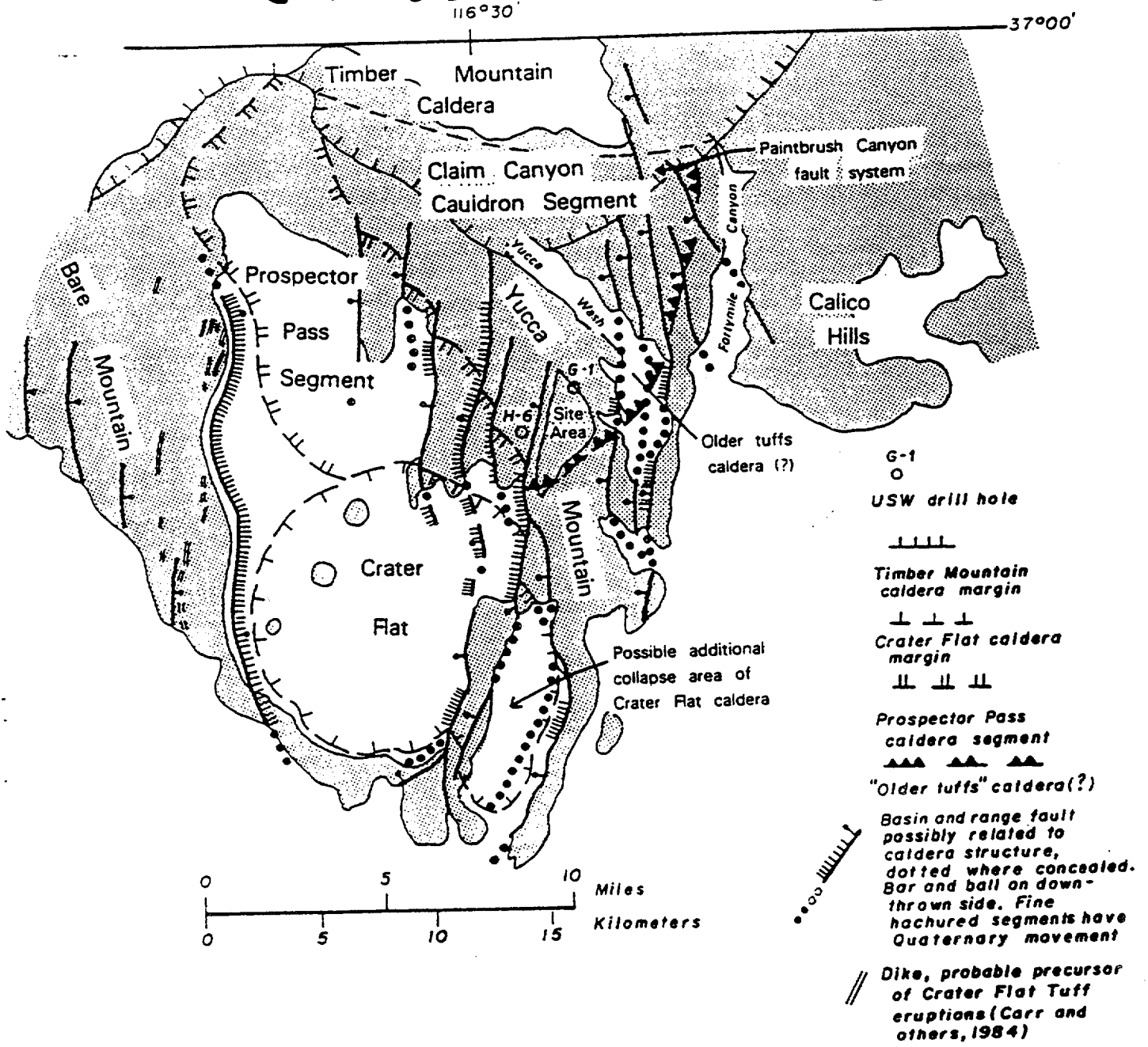


Figure 8.16. Size and extent of inferred calderas beneath Crater Flat and Yucca Mountain (from Carr, 1984, p. 67) revised from Carr (1982). Note that some faults cut across or offset the inferred caldera rims.

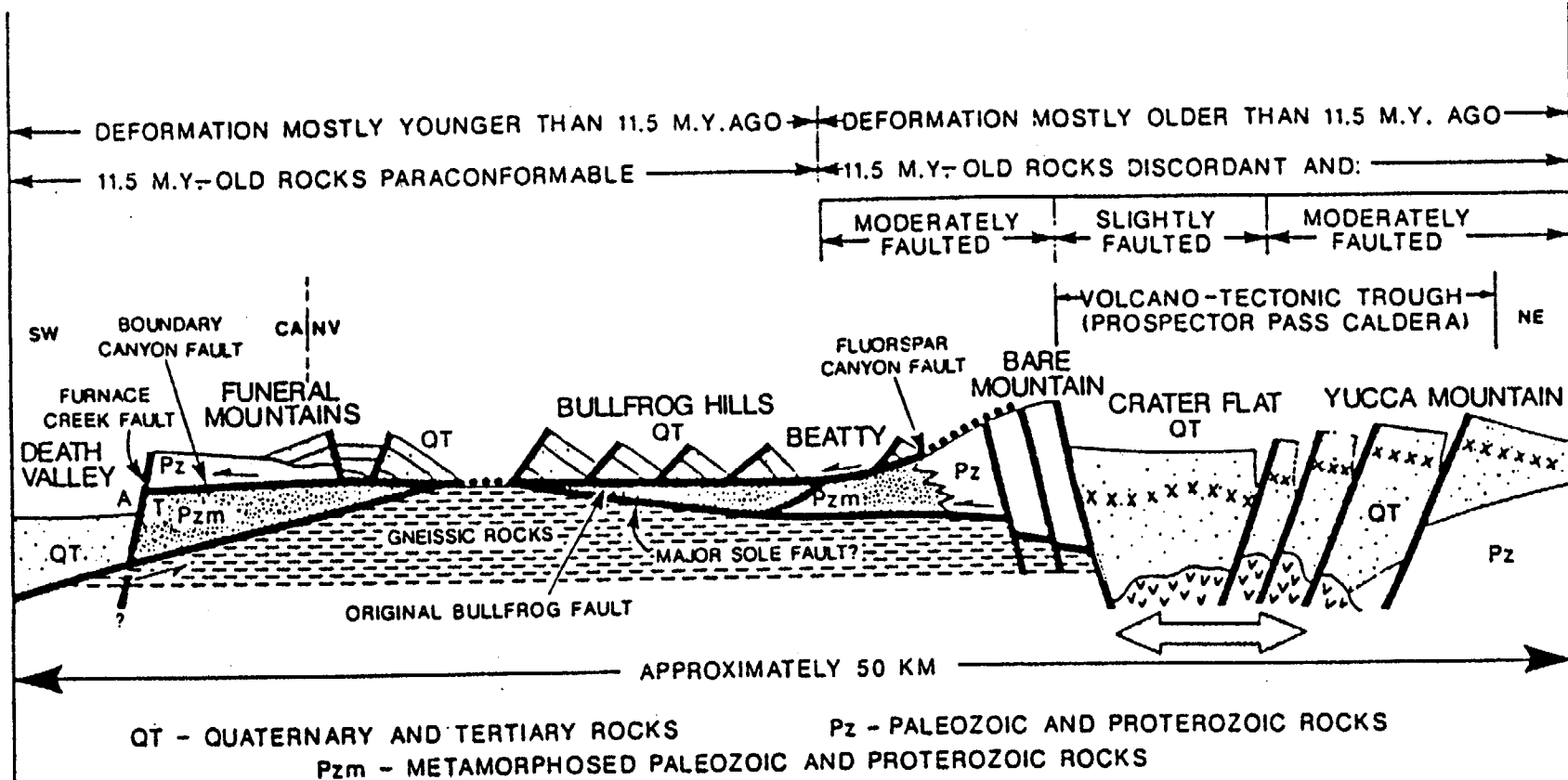


Figure 11. Model of crustal extension across detachment and volcano-tectonic terrain in the region between Death Valley and Yucca Mountain, showing lateral changes in style and fault chronology with respect to the Timber Mountain Tuff. The Crater Flat area is represented as a volcano-tectonic rift resulting from pull apart (arrow) and collapse at the headwall of the detachment system to the west.

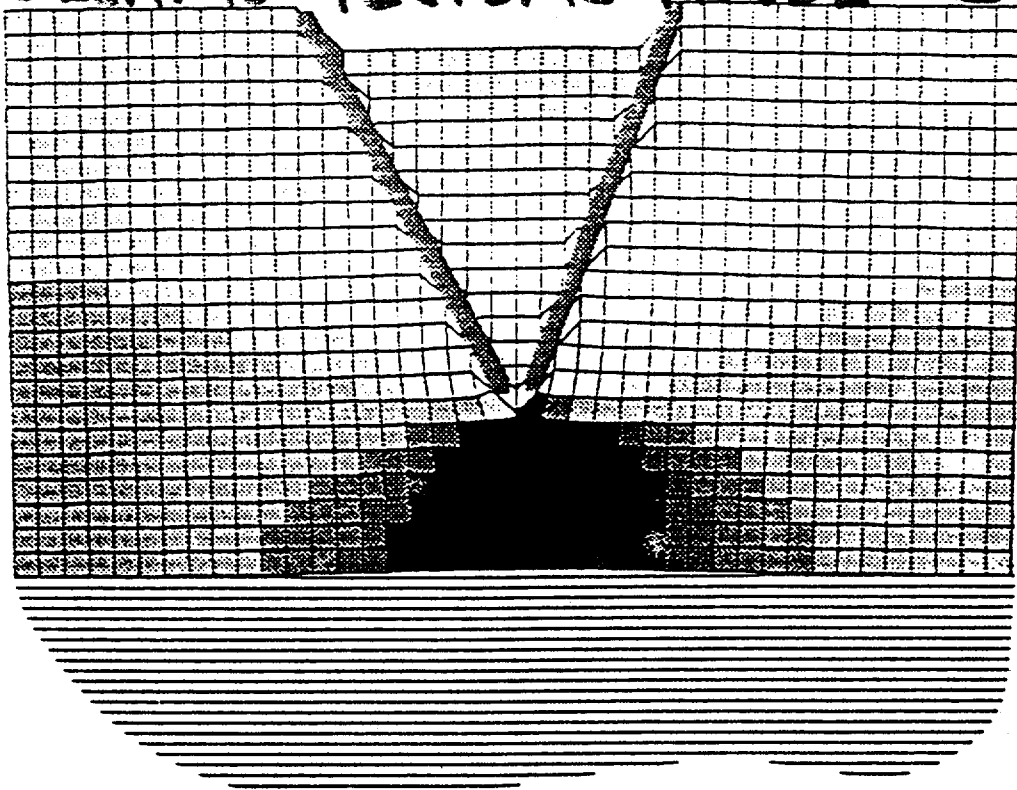
Mountain-Oasis Valley caldera complex (Fig. 4). The scallop-like pattern of the Fluorspar Canyon fault and several low-angle faults on the north end of Bare Mountain (Carr and Mosen, 1988, Fig. 2) suggests large gravity-glide blocks that slid toward the caldera but at the same time were dragged off to the northwest on some deeper-seated structure. I suggest that, rather than

The structure within the Kawich-Greenwater Rift (Fig. 6) is related, I believe, to the presence of a major steep-sided deep trough in the basement rock. The en echelon fault system (Fig. 6) in the Paintbrush Tuff at Yucca Mountain could have formed by reactivation of properly oriented segments of buried caldera or sector graben structure (Carr, 1984a). The faults are interpreted as a response to weakening of lateral support by rapid withdrawal

CALDERA-DETACHMENT MODEL - 1

VOLCANIC-TECTONIC MODEL - I

a)



b)

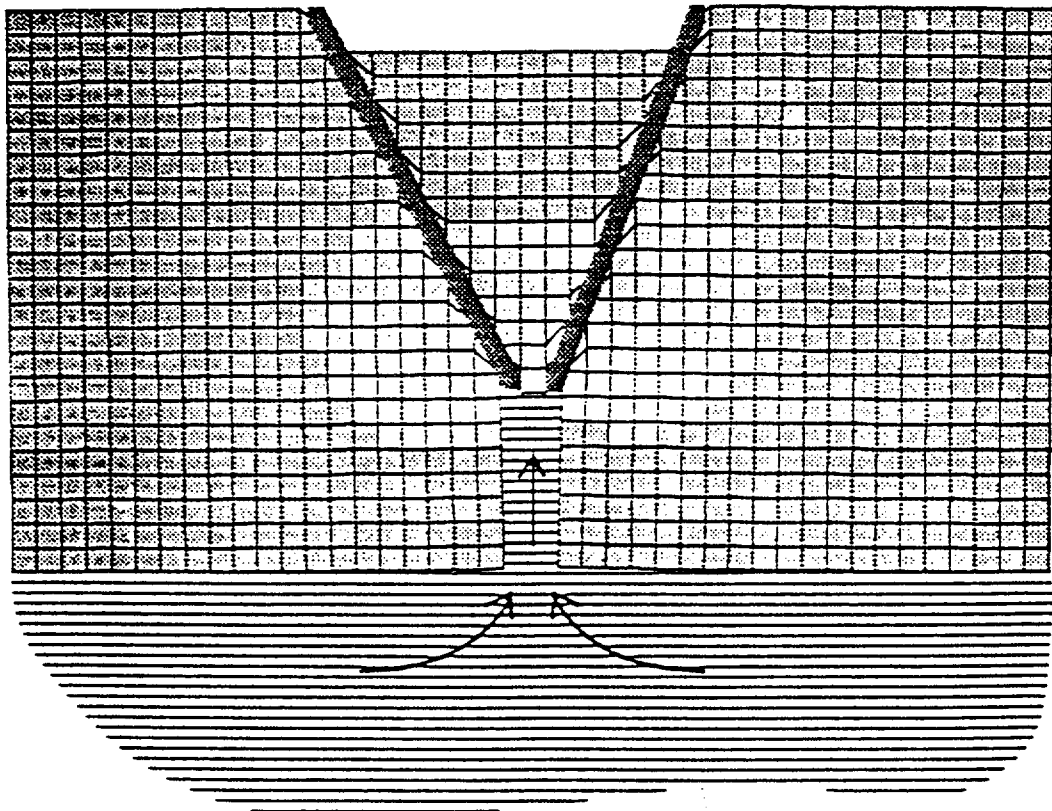


Figure 8.30. Faults that converge near the base of the brittle crust can create zones of dilation (dark area in a). This phenomenon can lead to structural guidance of magma into the upper crust (b); faults are not necessarily utilized as ascent paths.

(1984), and Wernicke and others (1988a) have described the geometry of extensional structures in the area west of a break-away fault zone in the Sheep Range (Fig. 1). Between the Pint-water Range and Bare Mountain, evidence of the nature of extensional structures is less clear.

For the area of Yucca Mountain itself, several extensional tectonic settings have been suggested. These settings include (1) a volcano-tectonic origin (W. J. Carr and others, 1986; Carr, 1984; Snyder and Carr, 1984), (2) tilting of a detachment surface related to tectonic unloading in the Bare Mountain-Bullfrog Hills

area (F. M. Byers, Jr., oral communication, 1985) indicates that thick, more mafic-rich, late-stage magmas expected within a caldera are not present (Lipman and others, 1966) and that members of the Crater Flat Tuff are not thicker than in surrounding areas.

Geologic evidence cited by W. J. Carr and others (1986) to support the proposed caldera is also equivocal. Rhyodacite dikes are parallel to the Bare Mountain fault rather than parallel to the proposed caldera in southern Crater Flat (compare Figs. 9 and 18 of W. J. Carr and others, 1986). The monolithologic breccias

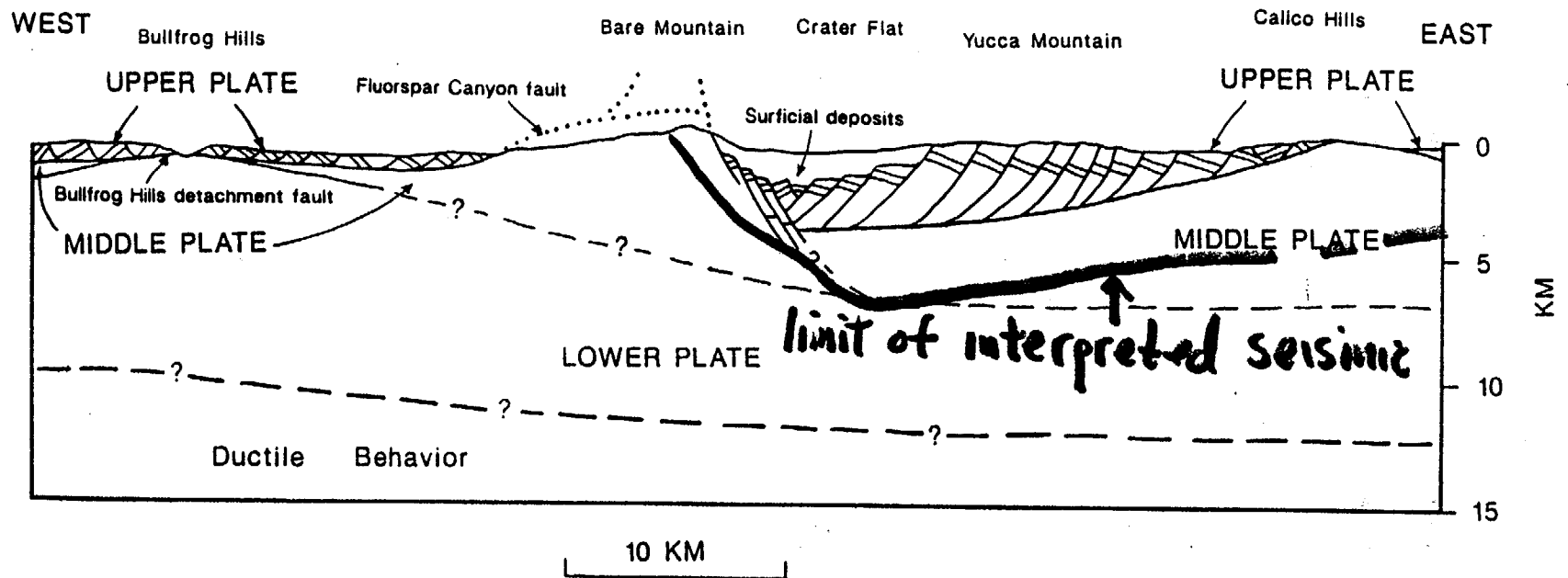
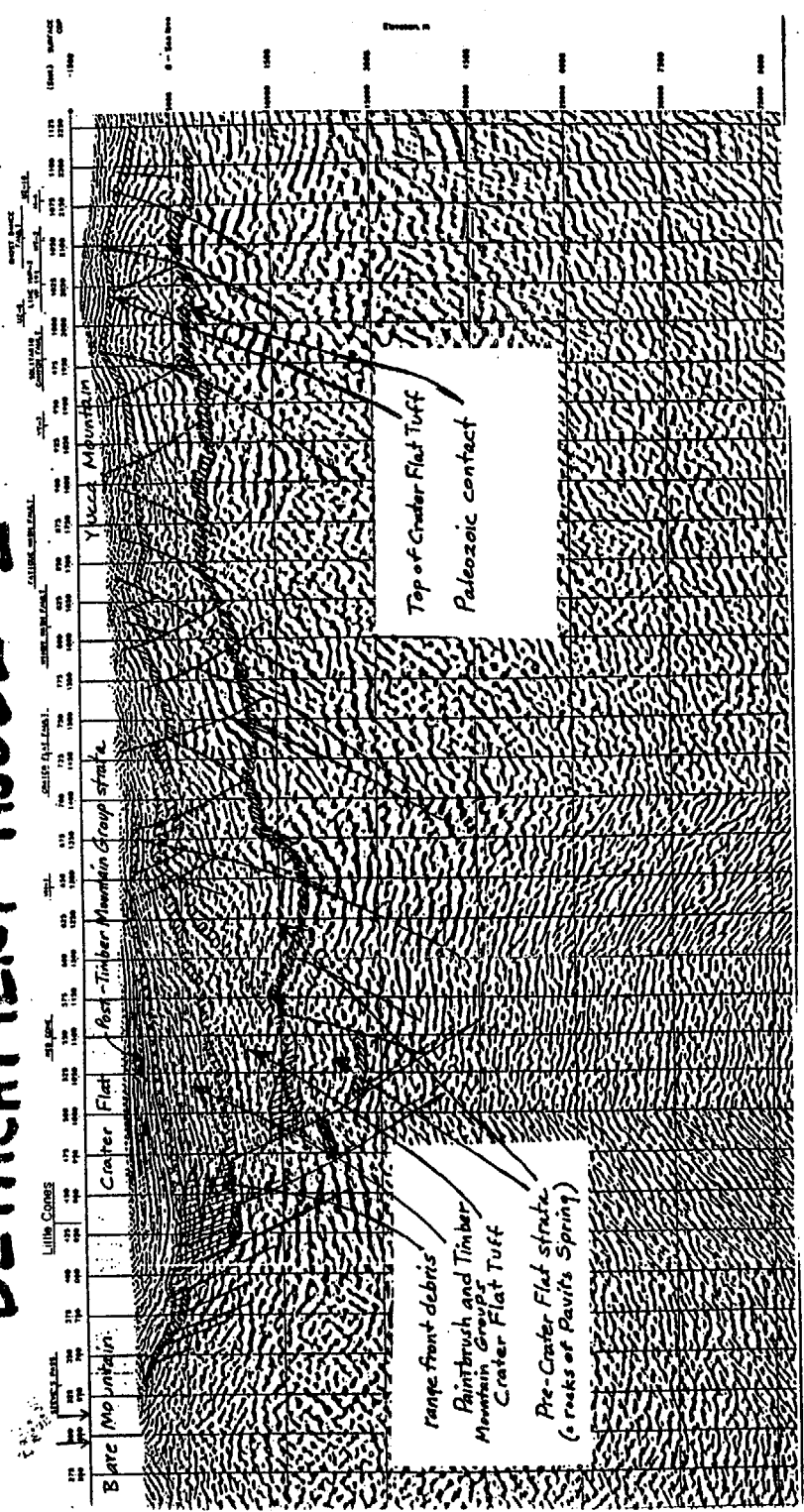


Figure 15. Conceptual cross section from Calico Hills to the metamorphic core complex in the Bullfrog Hills (McKee, 1983). No vertical exaggeration. Depths and configuration of detachment faults are speculative where dashed and queried. Generalized dips of strata are shown conceptually in the upper plate. Although listric faults under Yucca Mountain are shown to sole into the uppermost detachment, some may extend to a lower level. Steep normal faults, not shown here, probably translate extension from the lowest detachment upward to shallower low-angle faults and to the surface. The middle low-angle fault may surface near the metamorphic core complex in the Bullfrog Hills (Maldonado, 1985b), south of Mercury at Point of Rocks (Burchfiel, 1965) and possibly in the Funeral Mountains. The lowest detachment surface, between 10 and 15 km, is probably the modern shear between deeper, relatively ductile crust and shallower, relatively brittle crust.

DETACHMENT MODEL - 1

DETACHMENT MODEL - 2

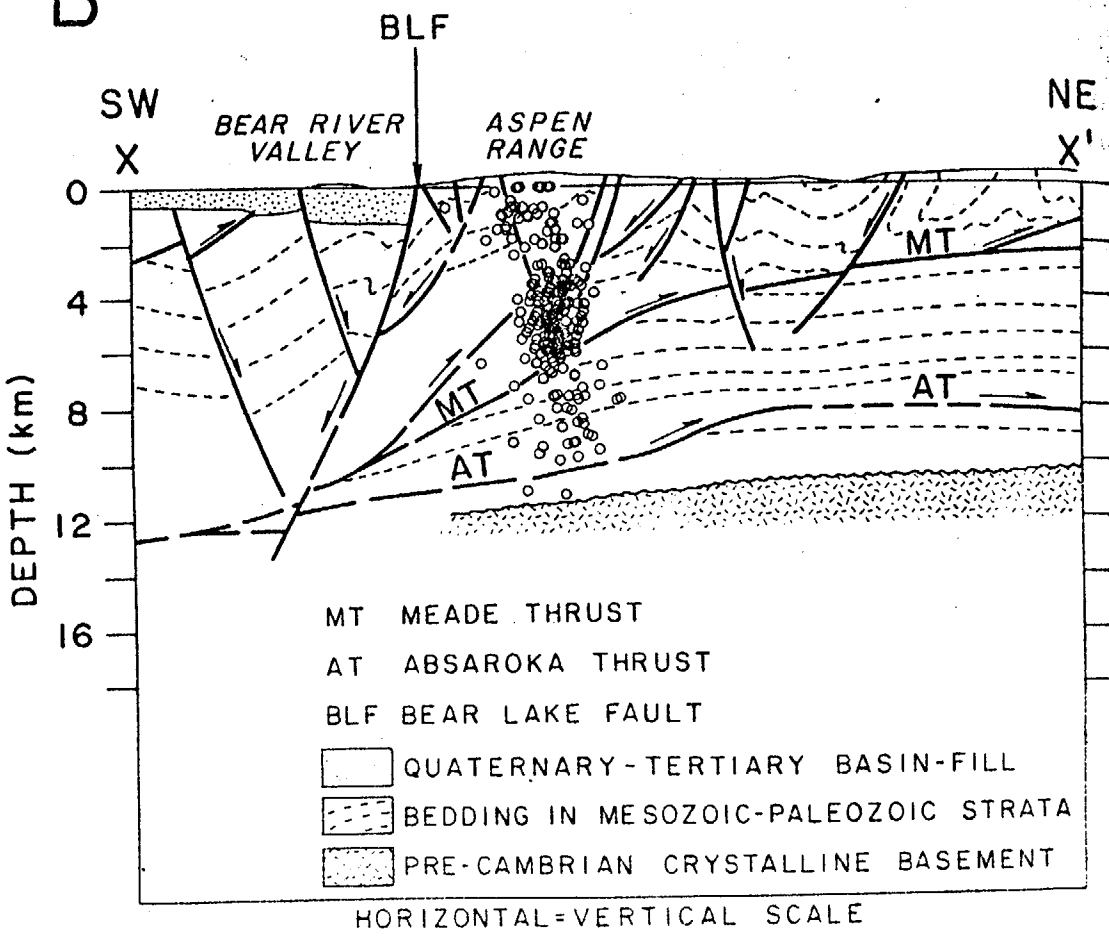
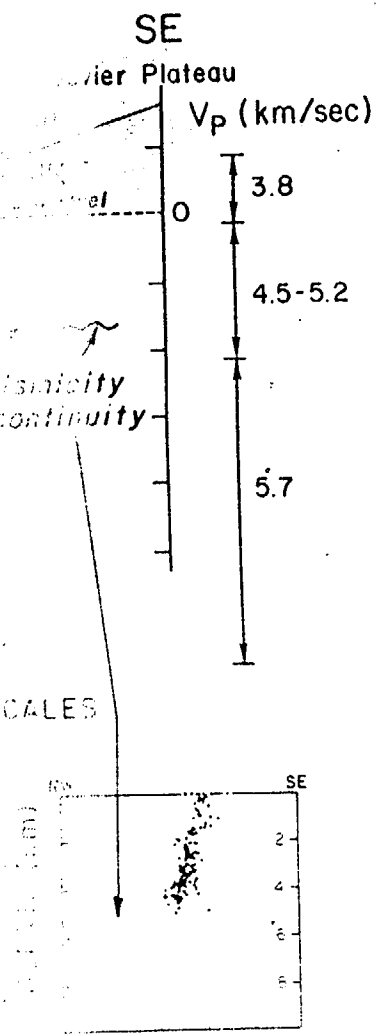


segment of Crater Flat seismic reflection profile (Brocher and others, 1966). See figure 8.6 for location. Subvertical solid lines indicate faults.

5-34

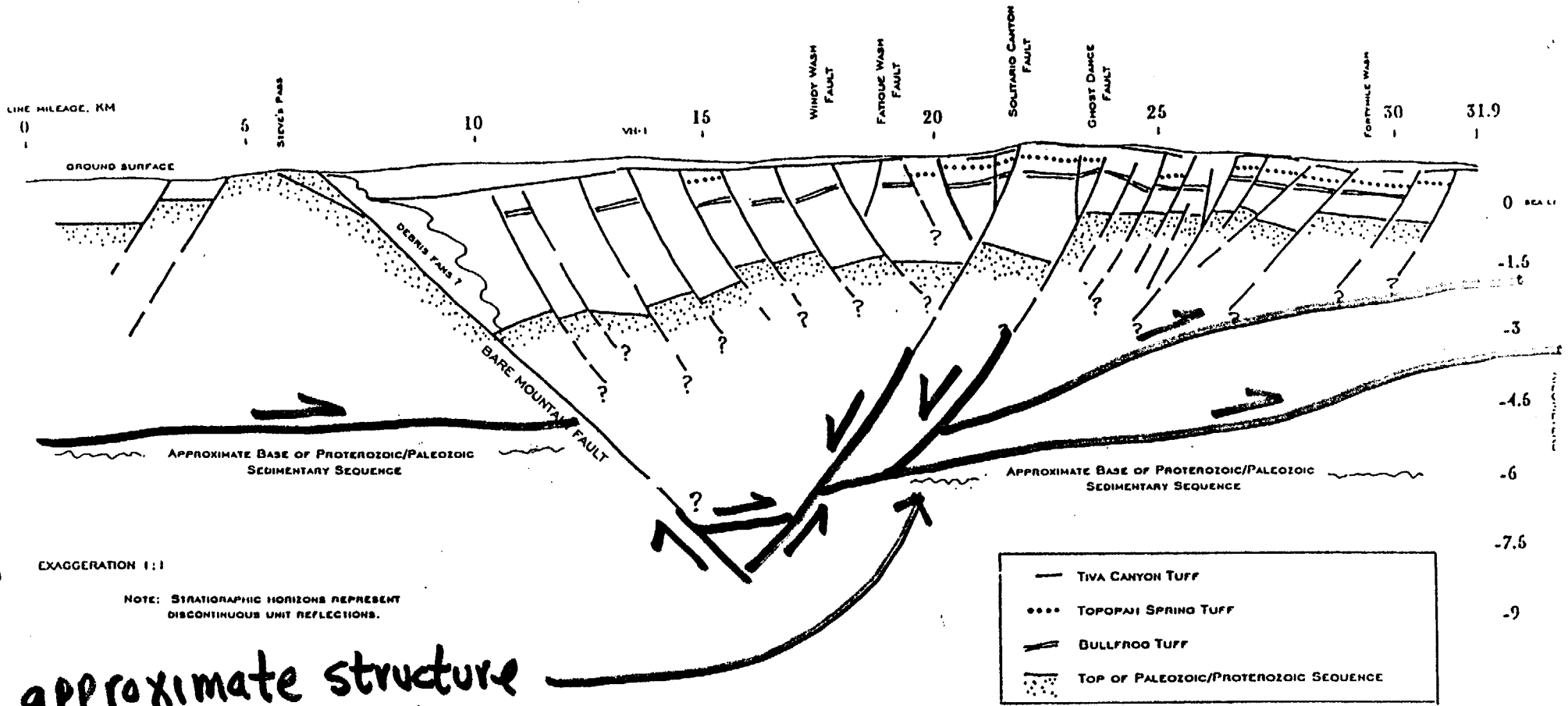
PLANAR FAULT BLOCKS MODEL-2

B



arcuate pattern of earthquakes has deviatoric stress. Yellowstone hot beneath the Yellowstone preparation; And seismogenic potential to be affected our for example, no increase in seismic transverse to the Using Figure wise circuit of border region (between the southern Utah border to northeast-trending Cenozoic normal locations verified Arabasz, 1985)

selected earthquake field studies carried out by the University of Utah of low-angle structural discontinuities on seismicity, from Arabasz and Julander geologic cross section across the Sevier Valley near Richfield, Utah, showing seismicity with depth coincident with the location of a low-angle detachment reflection data. V_p = P-wave velocity; T_v = Tertiary volcanic rocks; other abbreviations are given in the text. B, Cross section showing the association of swarm seismicity in the Aspen Range, Idaho, with geologic structure; earthquake data from Richins and others



9-36

approximate structure
from ISB X-section

PRELIMINARY INTERPRETED REGIONAL SEISMIC REFLECTION PROFILE,
YUCCA MOUNTAIN, NEVADA

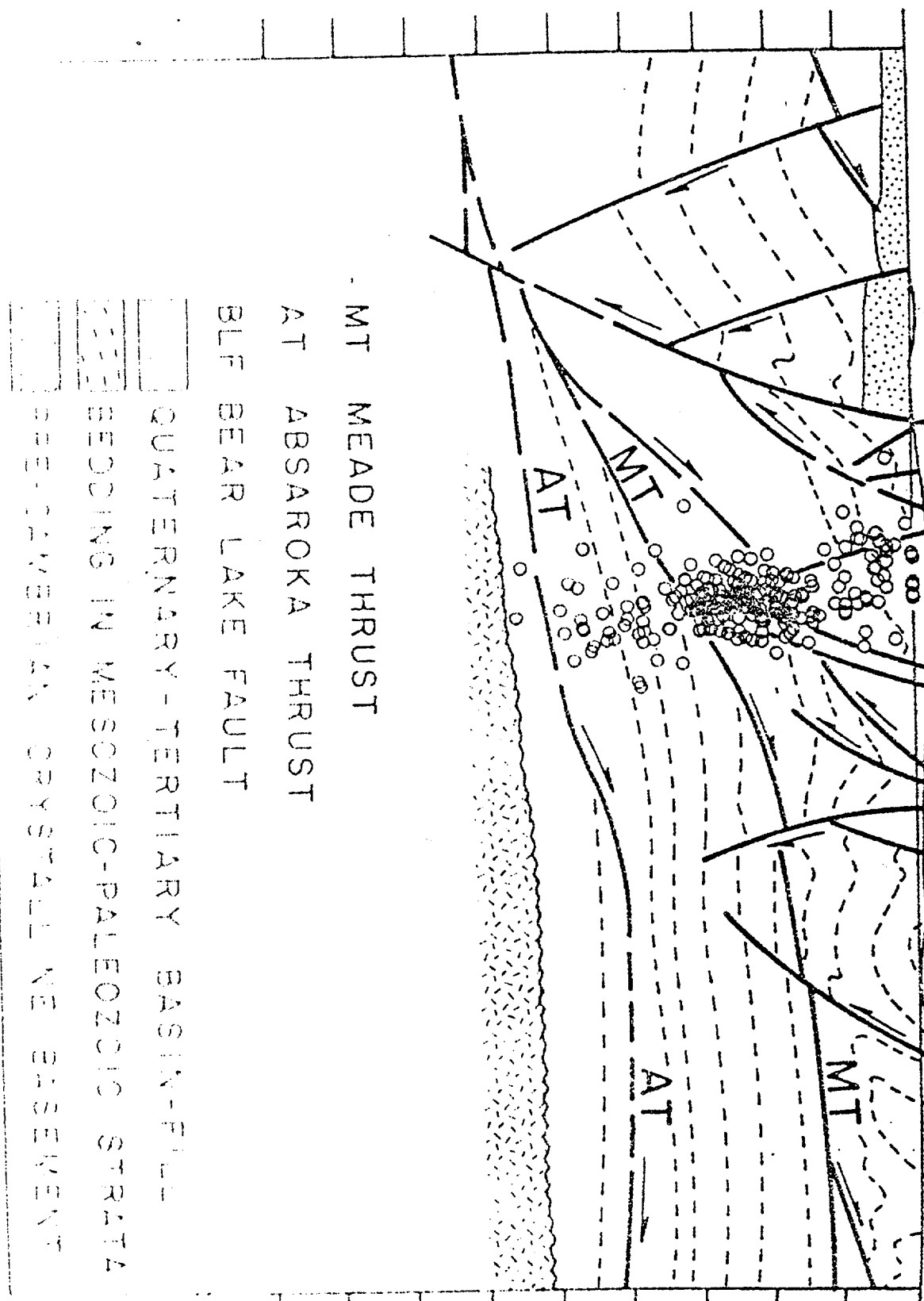
July
Brocher, Hunter, and others, U.S. Geological Survey, June 1996
UNREVIEWED NOT FOR DISTRIBUTION

Figure 8.12. Crater Flat seismic reflection profile interpreted by Brocher and Hunter (written commun., 1966).

DEPTH (km)

0
4
8
12
16

X' X' BEAR RIVER VALLEY ASPEN RANGE



MT MEADE THRUST

AT ABSAROKA THRUST

BLF BEAR LAKE FAULT

QUATERNARY-TERTIARY BASIN-FILL

BEDDING IN MESOZOIC-PALEOZOIC STRATA

PRECAMBRIAN CRYSTALLINE BASEMENT

SECTION ALONG X-X'

PLANAR FAULT BLOCKS MODEL-4

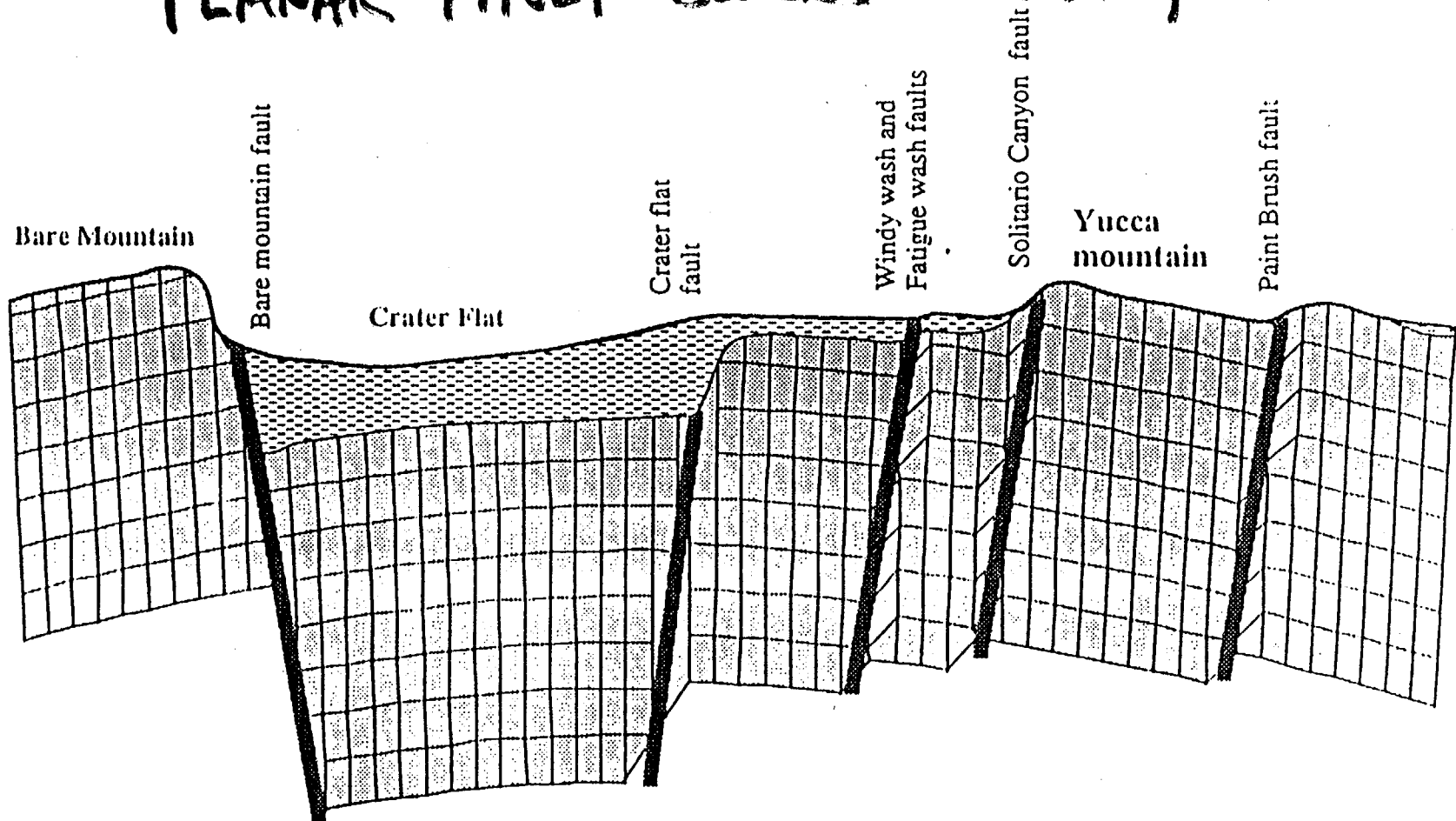
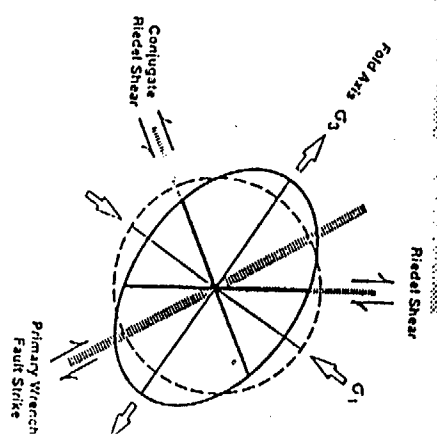
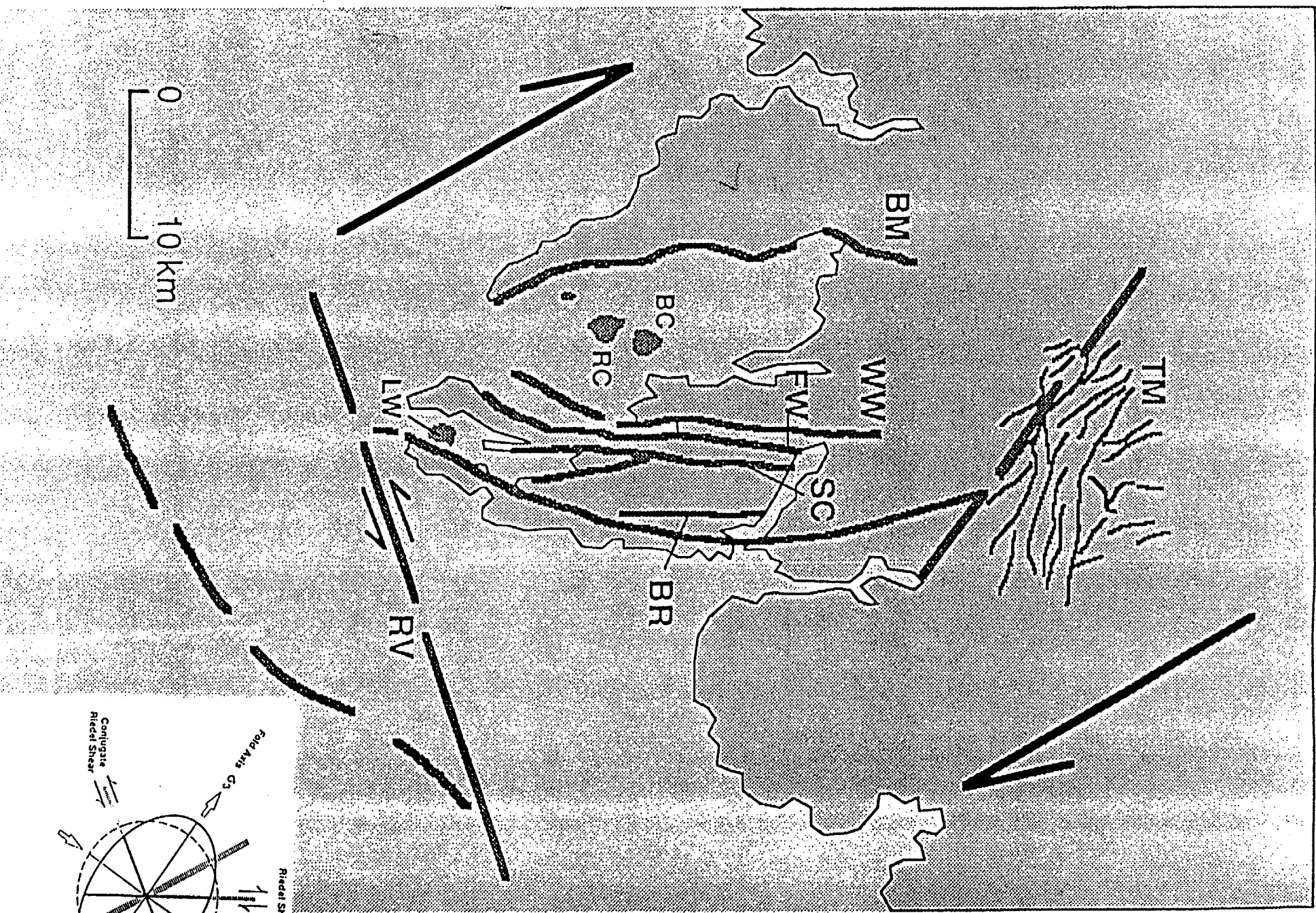


Figure 8.29. Modeled cross section of Yucca Mountain with alluvium added and erosion simulated to arrive at a Yucca Mountain-Crater Flat-Bare Mountain structural configuration.

PLANNED FAULT BLOCKS MODEL-5



PLANAR FAULT BLOCKS MODEL-G

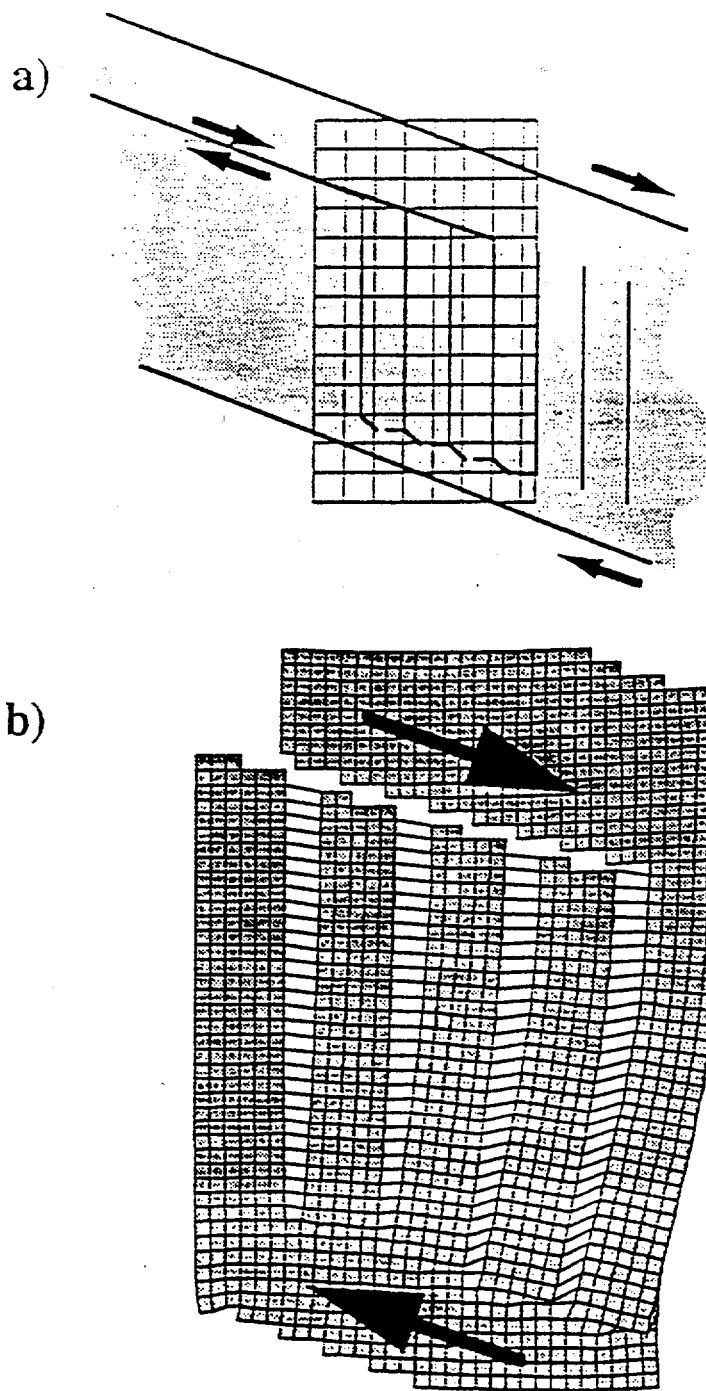
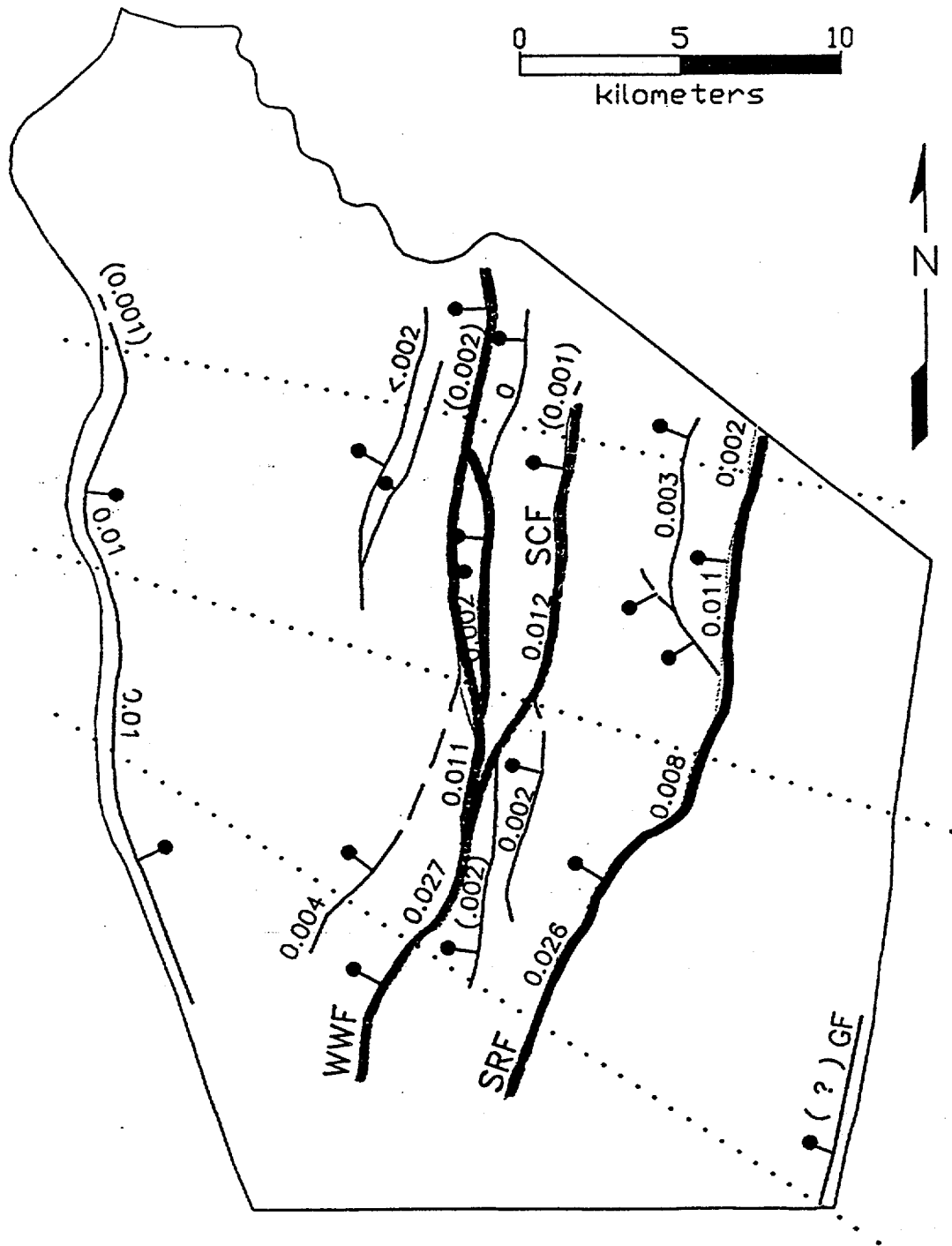


Figure 8.32. Adjustments made to the planimetric model to achieve oroclinal bending of fault blocks at south end of Yucca Mountain: a) faults at the south end are pinned and shear is allowed to enter the modeled space only from the northwest, b) although a shear couple is imposed across the modeled area, results of slip are seen only along the northern end of the fault tract.

PLANAR FAULT BLOCKS MODEL-7



Calculated and estimated () slip rates on faults in the Yucca Mountain area.

LATERAL SHEAR MODEL - 5.1

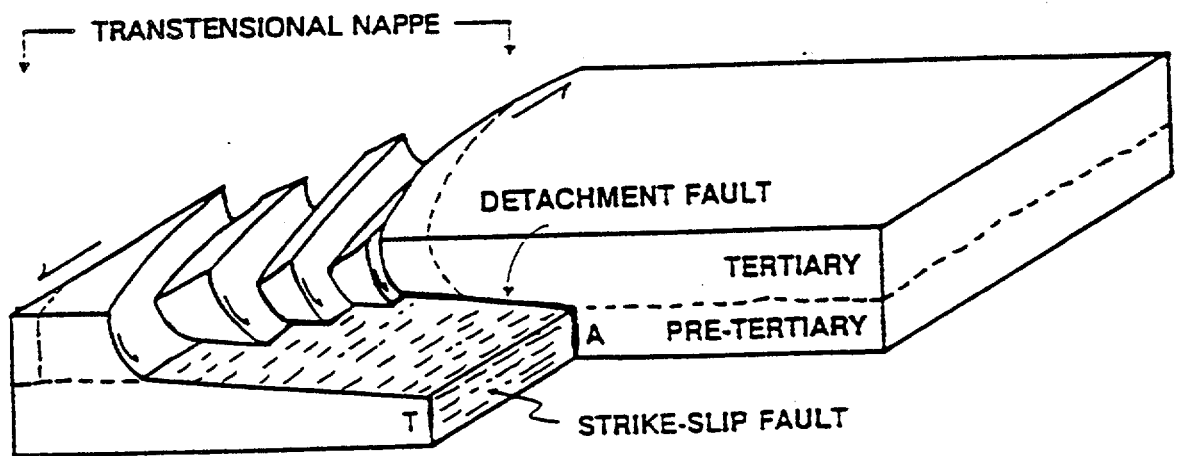


Figure 8.23 Diagrammatic model of detachment faults controlled by a deeper, hidden strike-slip fault. From Hardyman and Oldow (1991, p. 295).

LATERAL SHEAR MODEL - 5.2

SCHMATIC CONCEPTUAL
2D MODEL OF FAULTS

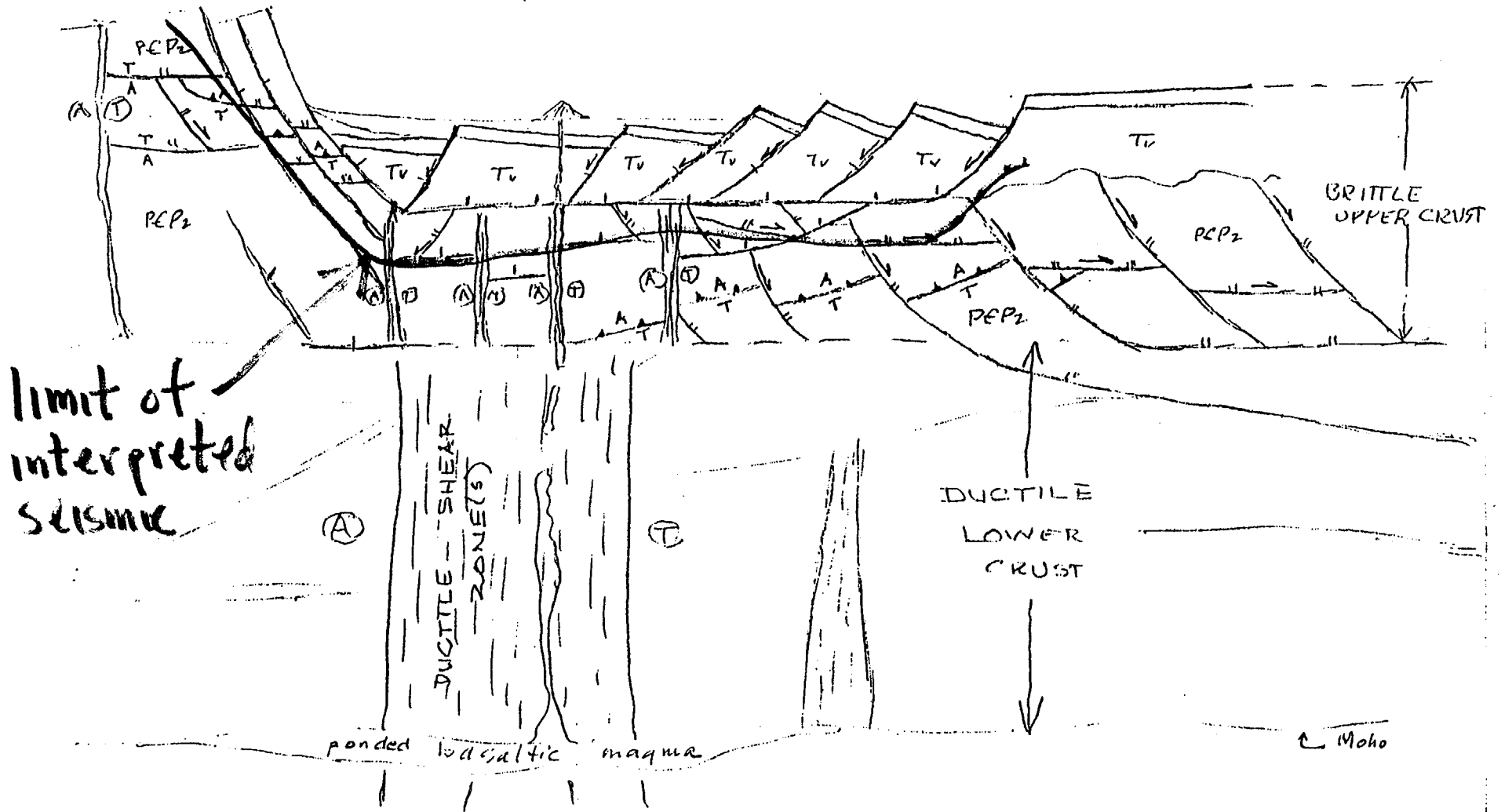
AT YUCCA MTN.
(NOT TO SCALE)

RICH SCHWEICKERT CNS/UNR
11/96

post-14 Ma
half or half

pre-mid Miocene
half or half

Mz thrust



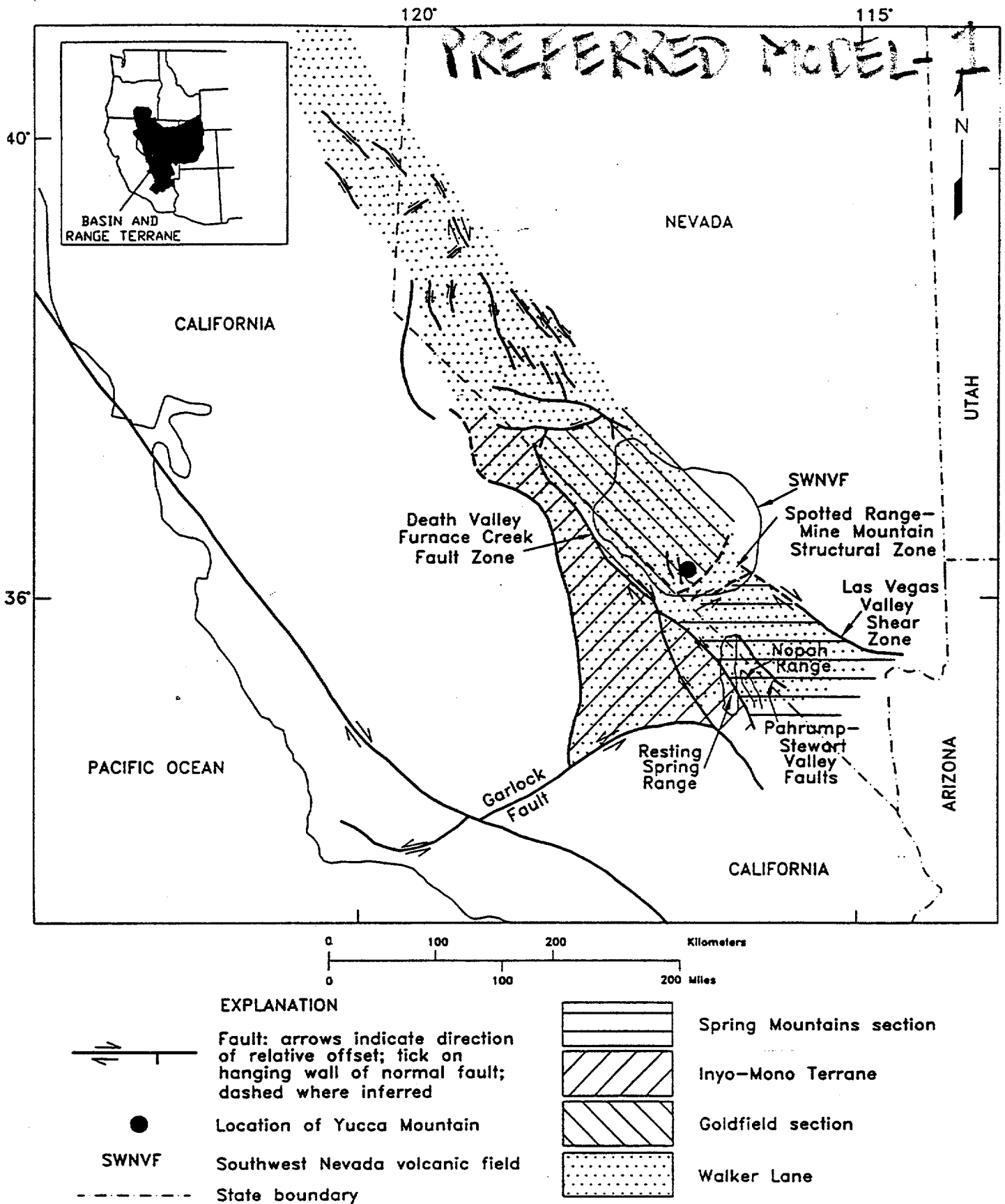


Figure 8.2 The Walker Lane, its regional setting and tectonic components

PREFERRED MODEL - 2

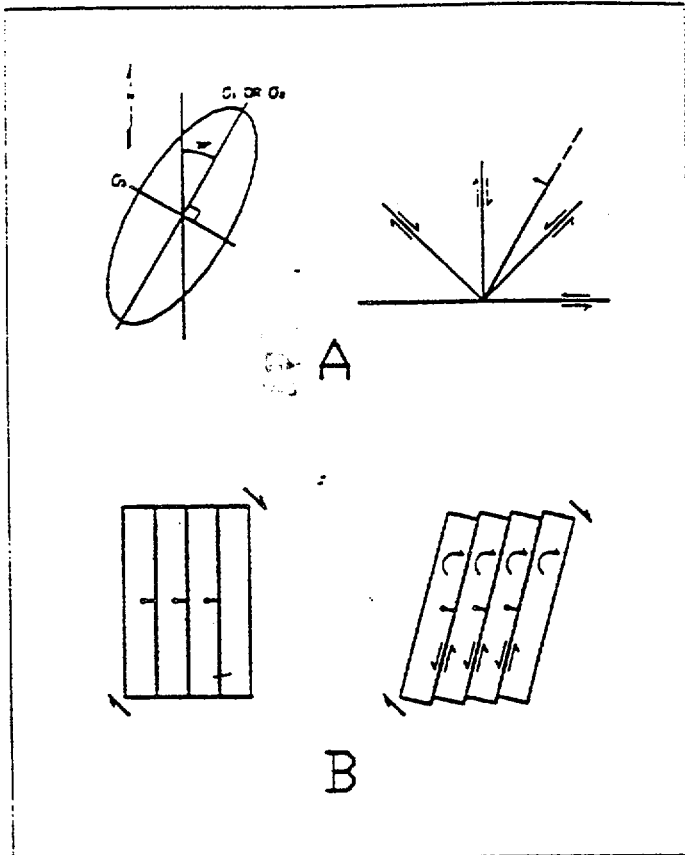


Figure 2-4 Schematic illustrations of (A) resolved sense of strike-slip shear on faults having a range of orientations, given a representational stress ellipsoid for the western Great Basin, and (B) illustration showing the dynamic sense of strike-slip shear along originally north-striking faults when the same stress regime results in vertical axis rotation concurrent with extension.

Depolo, Merges, Smith

Team

Prokinney
Toctonic
Kodler

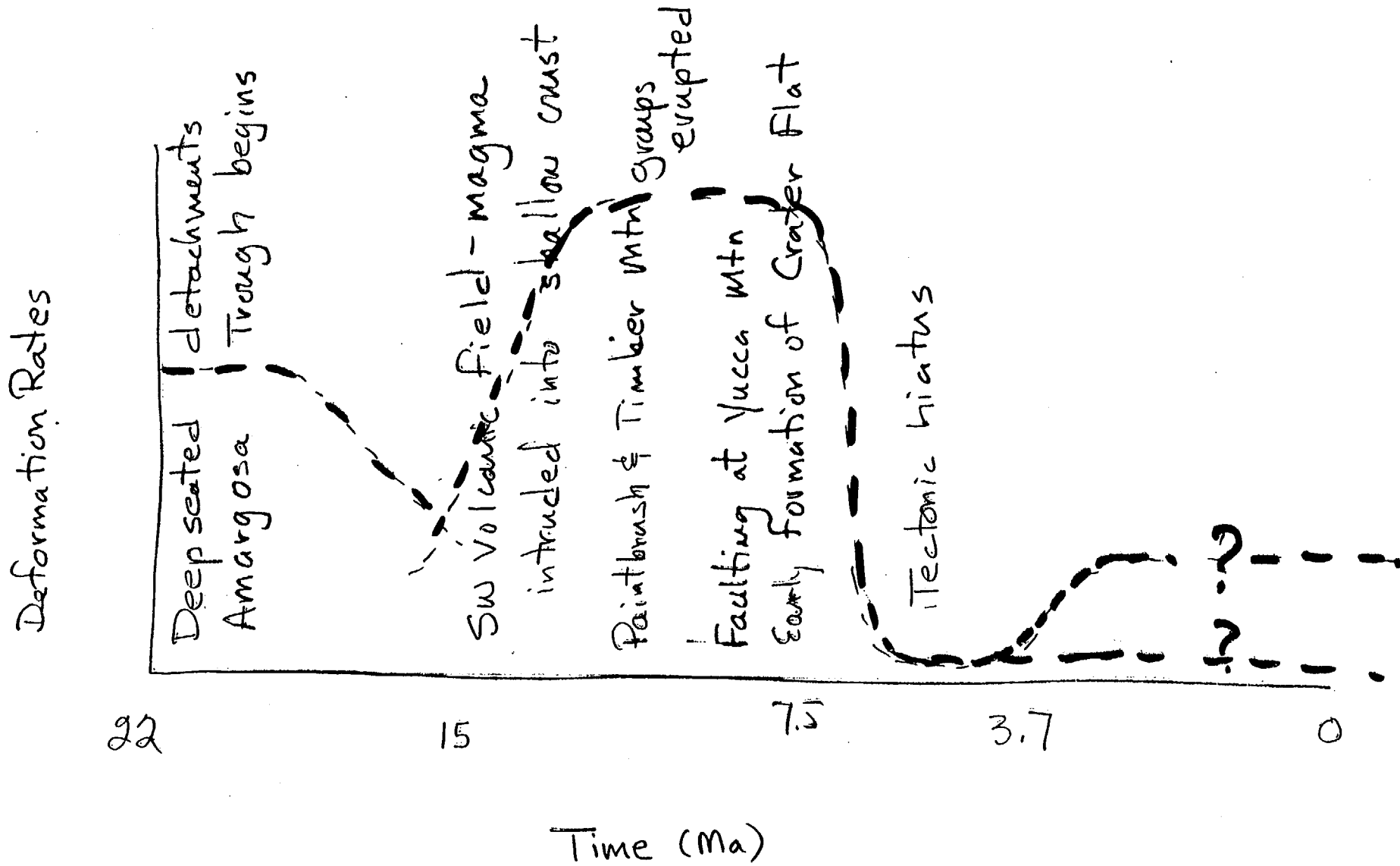
Some Important Information We Need From Tectonics

- We need to understand the physical crustal setting.
- We need to understand the contemporary tectonic setting and potential transient tectonics.

this leads us to the geometry of faults, potentially important to defining the dimensions of potential earthquakes.

the nature and rates of tectonic activity can further help constrain the rates of earthquakes.

Time-Dependent Stress Fields



Tertiary (Paleotectonic) Setting

- large caldera complex
- regional (and local??). detachment
- oblique half-graben
- translation / transtension
- possible hiatus in activity (8? - 3.7? Ma)
- stress rotation -

- half-graben
 - planar
 - curved
- detachment
 - shallow
 - deep
- volcanism
- strike slip

Seismotectonic Models

- low extension rate (driving planar to curvilinear faults)
- transient tectonics
 - Walker Lane belt incursion
 - extensional pulse (with or w/o volcanism)
 - triggered activity (wild card; distant earthquake)
- other models
 - detachment (may or may not exist)
 - volcanism (not contemporary; tectonic b -value)
 - focussed strike-slip fault (not evident to N.)

Contemporary Setting

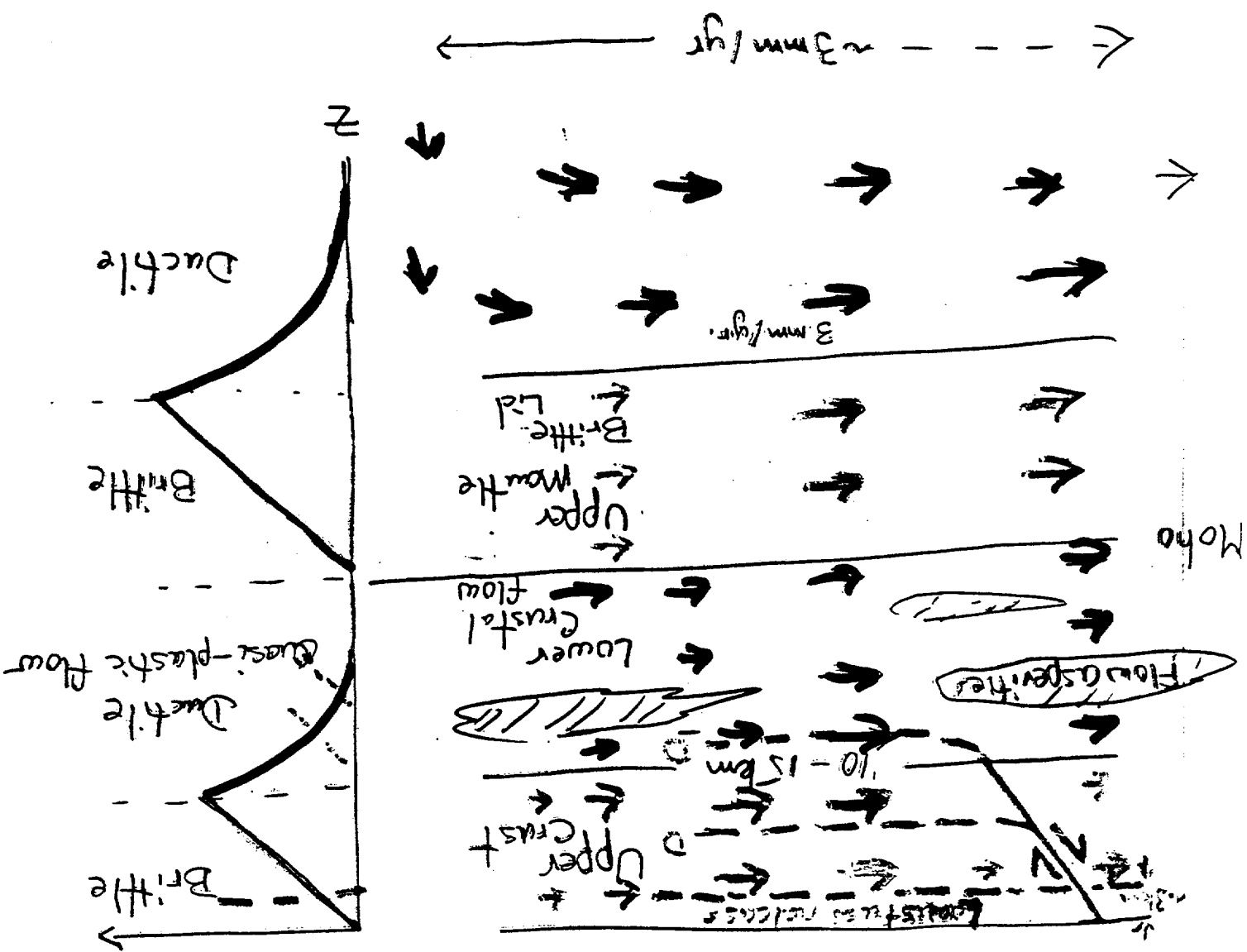
Geophysical Setting

- low strain rates (geodesy, seismicity) $10^{-17}/s$
- least-horizontal principal stress direction $\sim N50^{\circ}W$
- seismogenic depth 12-16 km (80th percentile f.d.)
- effective elastic thickness 5-15 km.
- seismicity
 - focal mechanisms normal & SS ^{roughly equal}
 - b-value -0.87 (tectonic)
 - moment rate

Structural Setting

- faults have small cross-strike distances (1-3 km) & anastomosing nature; likely merge at depth.
- detailed mapping and reflection data do not support shallow detachment.
- Bare Mountain fault may limit the depths of some of the western Yucca Mountain faults.

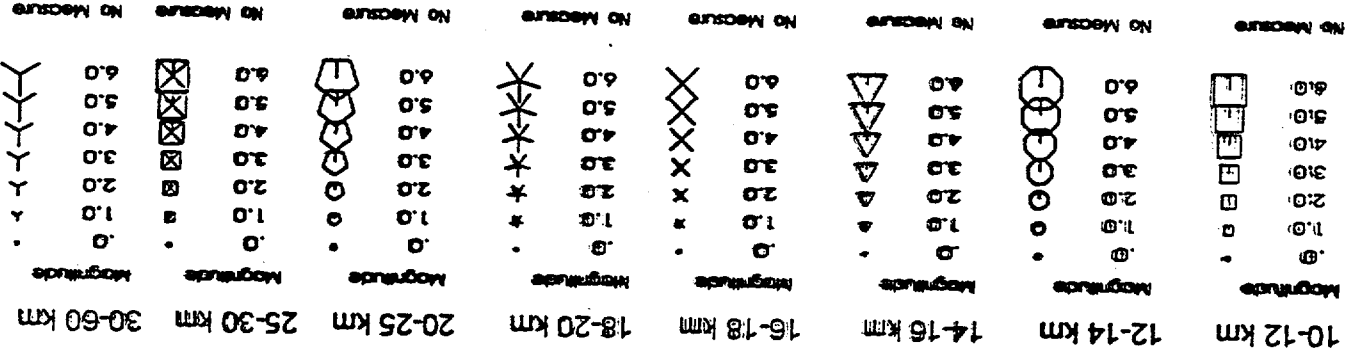
Leads to transient loading rates



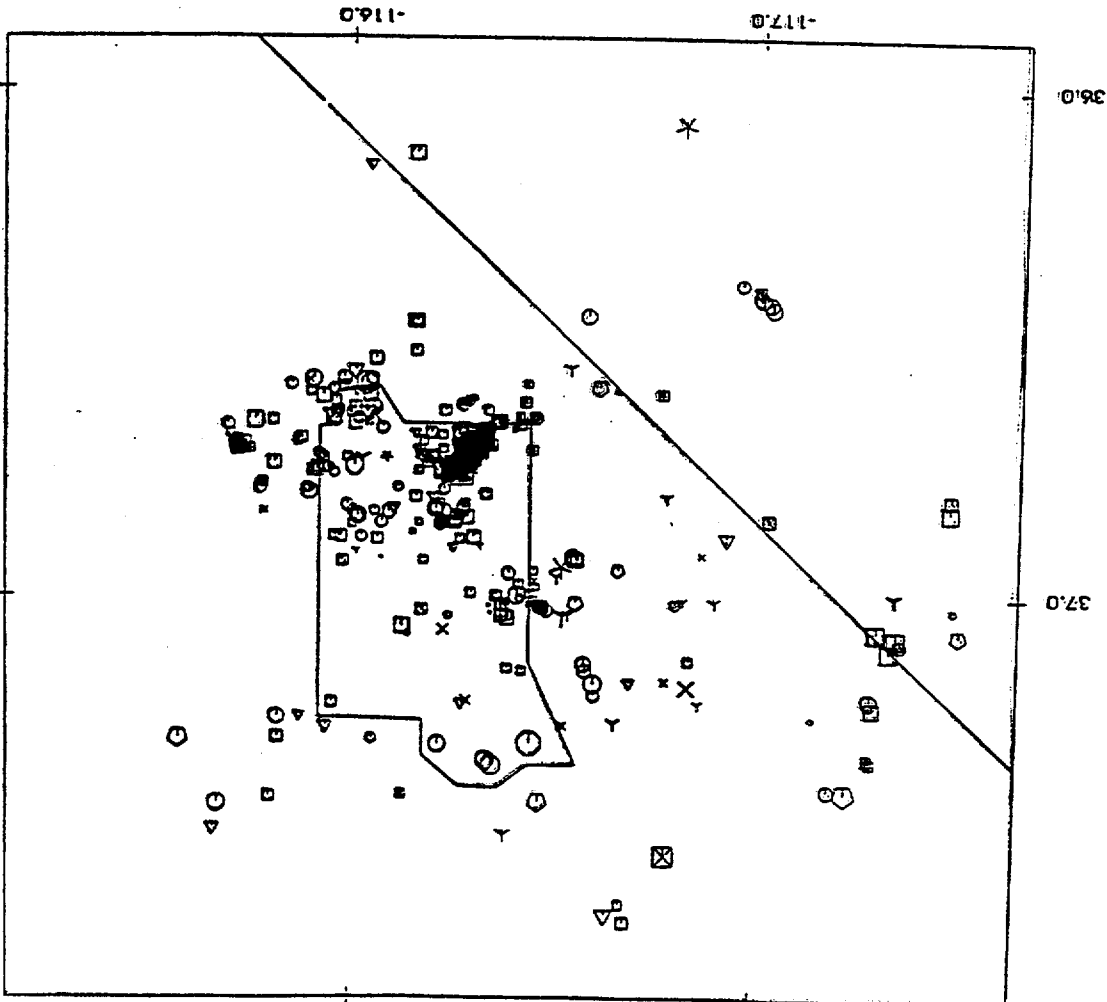
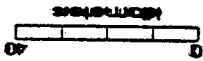
Strength
z

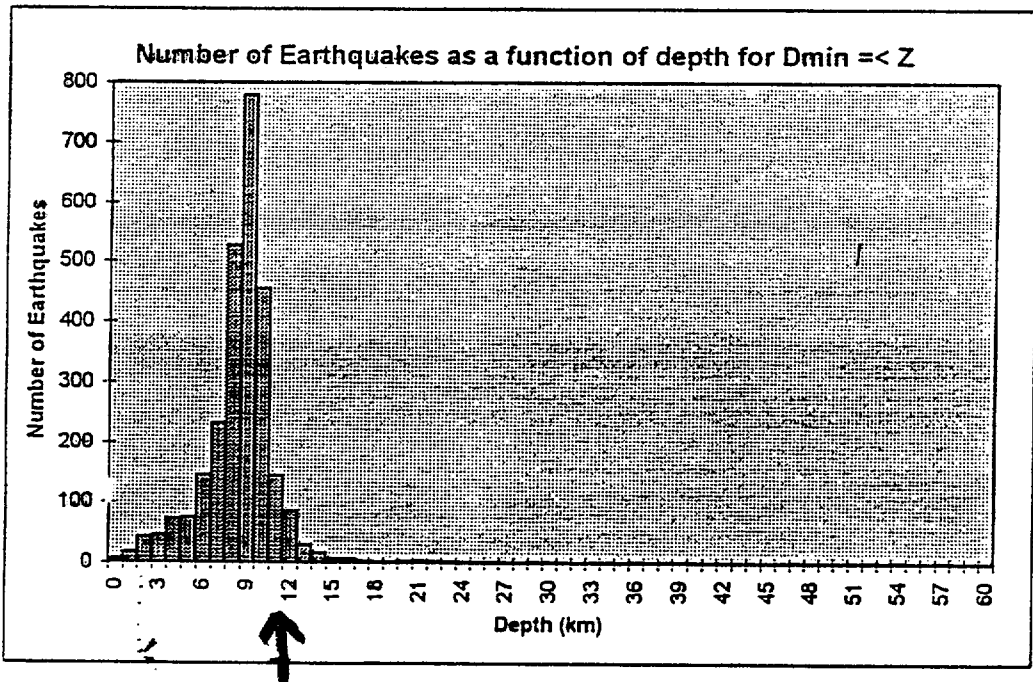
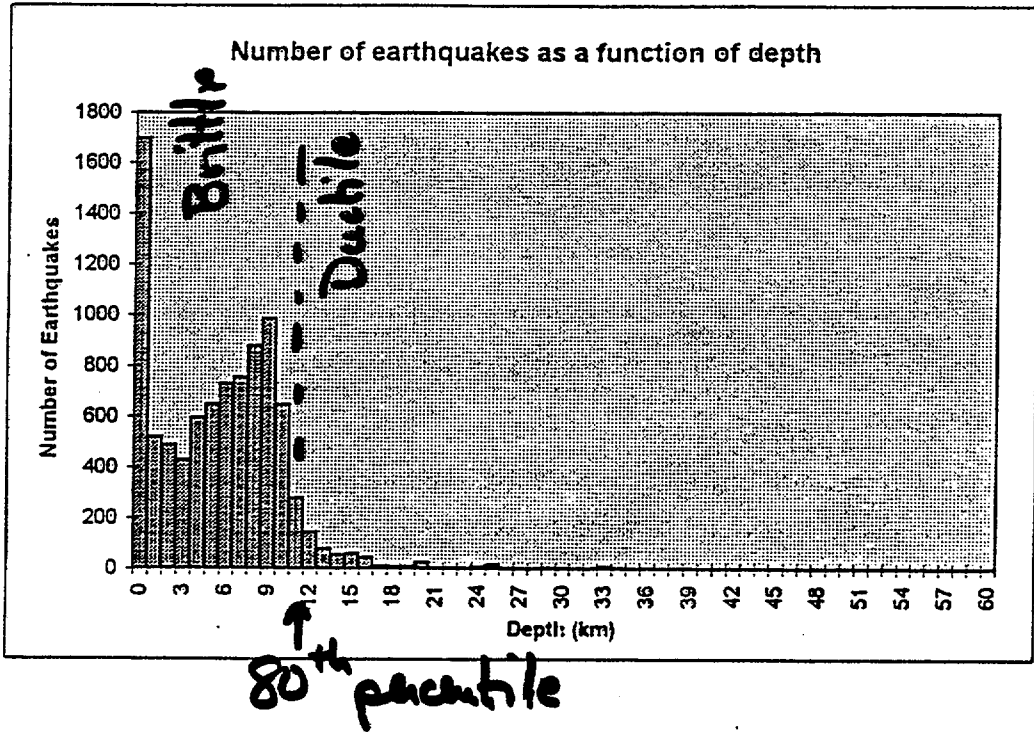
WELL-LOCATED EARTHQUAKES (DMIN > Z)
AS A FUNCTION OF DEPTH

Figure



Depth Ranges





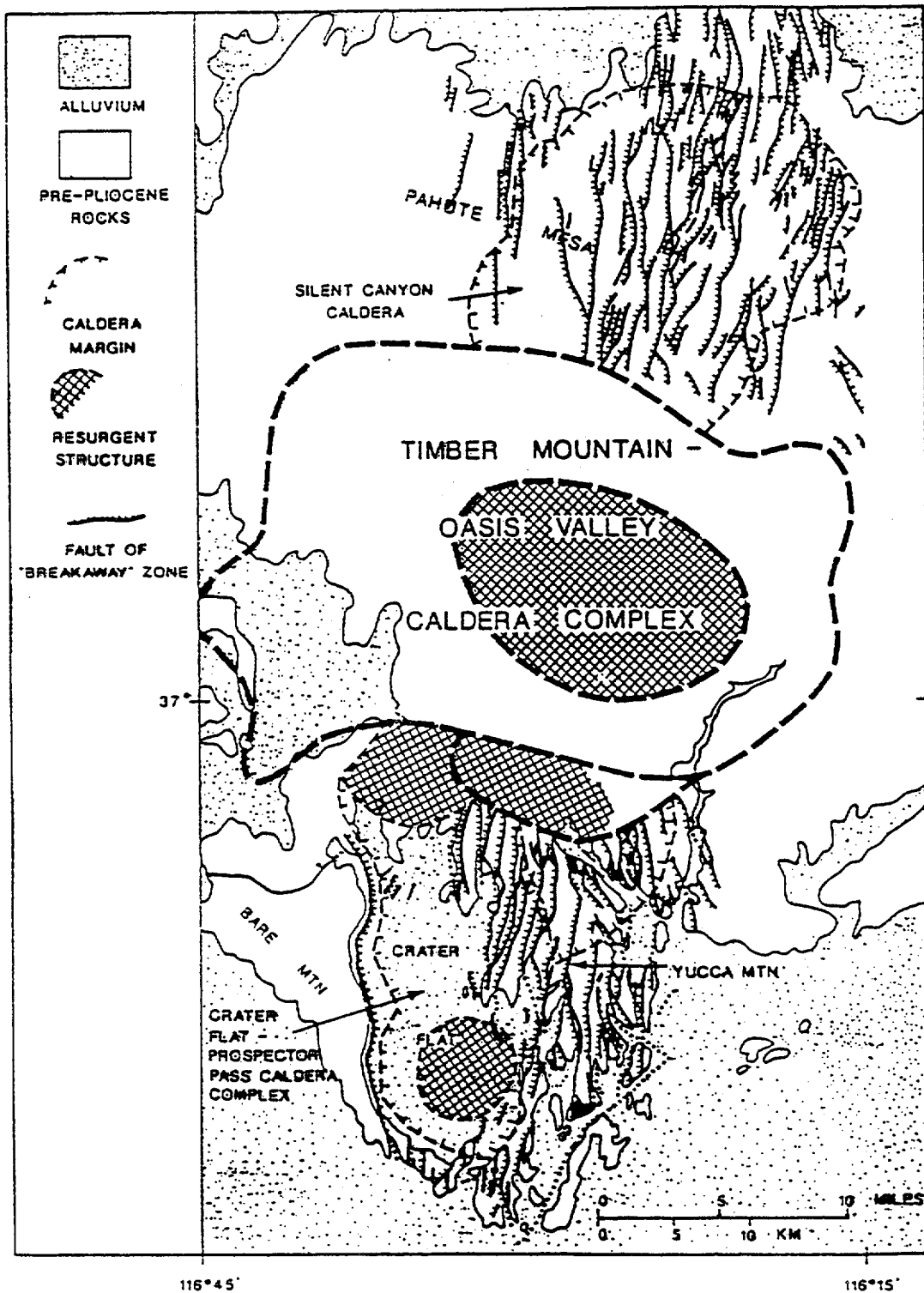
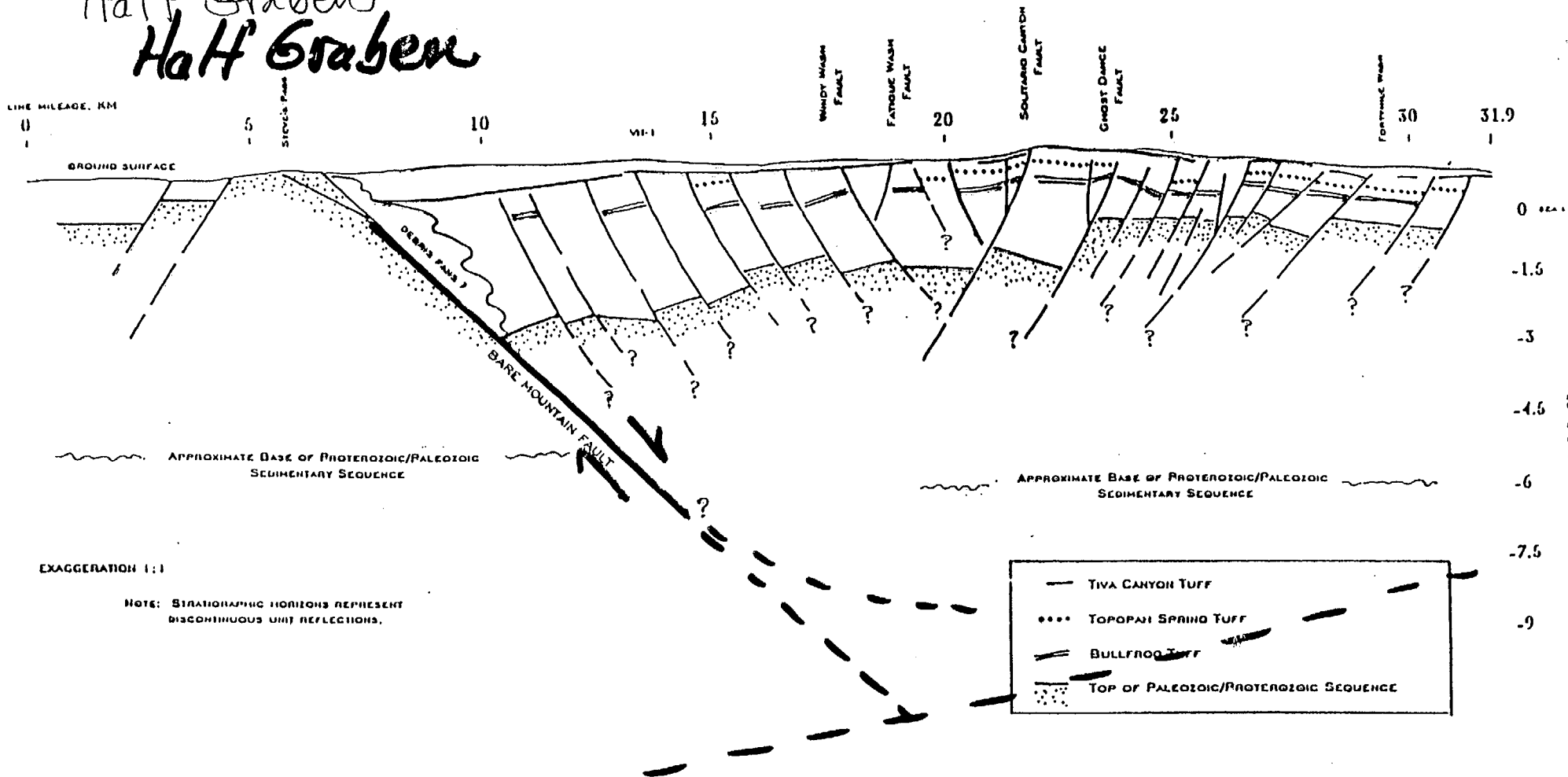


Figure 8.14. Coaxial fault sets of Yucca Mountain and Pahute Mesa separated by caldera complex (from Carr, 1990, p. 293). Carr related these faults to the Kawich-Greenwater rift. "Breakaway zone" refers to the idea that the rift, and the fault sets, form a structural boundary for detachment faults west of the Bare Mountain fault.

Half Graben Half Graben



PRELIMINARY INTERPRETED REGIONAL SEISMIC REFLECTION PROFILE,
YUCCA MOUNTAIN, NEVADA

July
Brocher, Hunter, and others, U.S. Geological Survey, June 1996
UNREVIEWED NOT FOR DISTRIBUTION

Figure 8.12. Crater Flat seismic reflection profile interpreted by Brocher and Hunter (written commun., 1966).

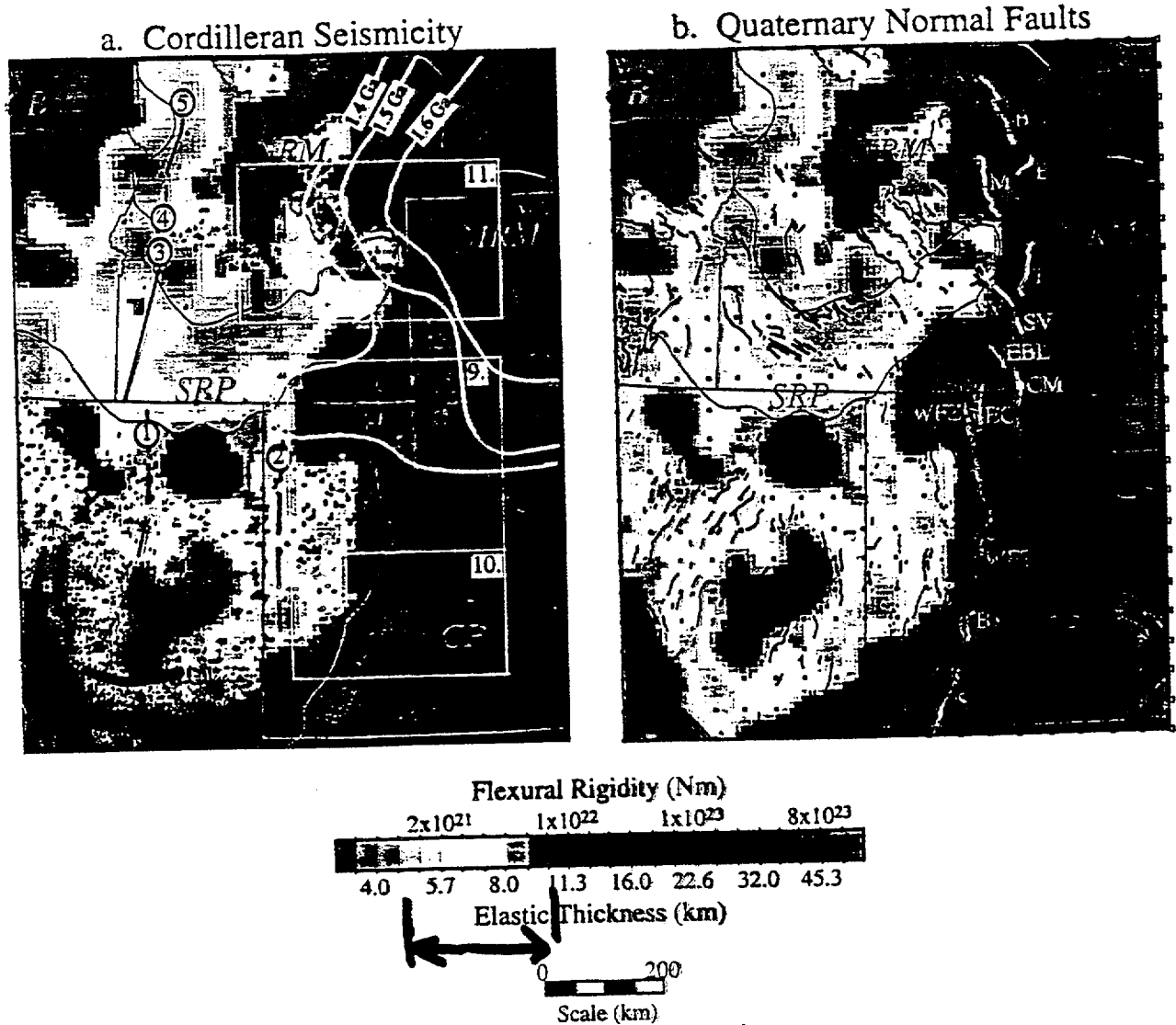


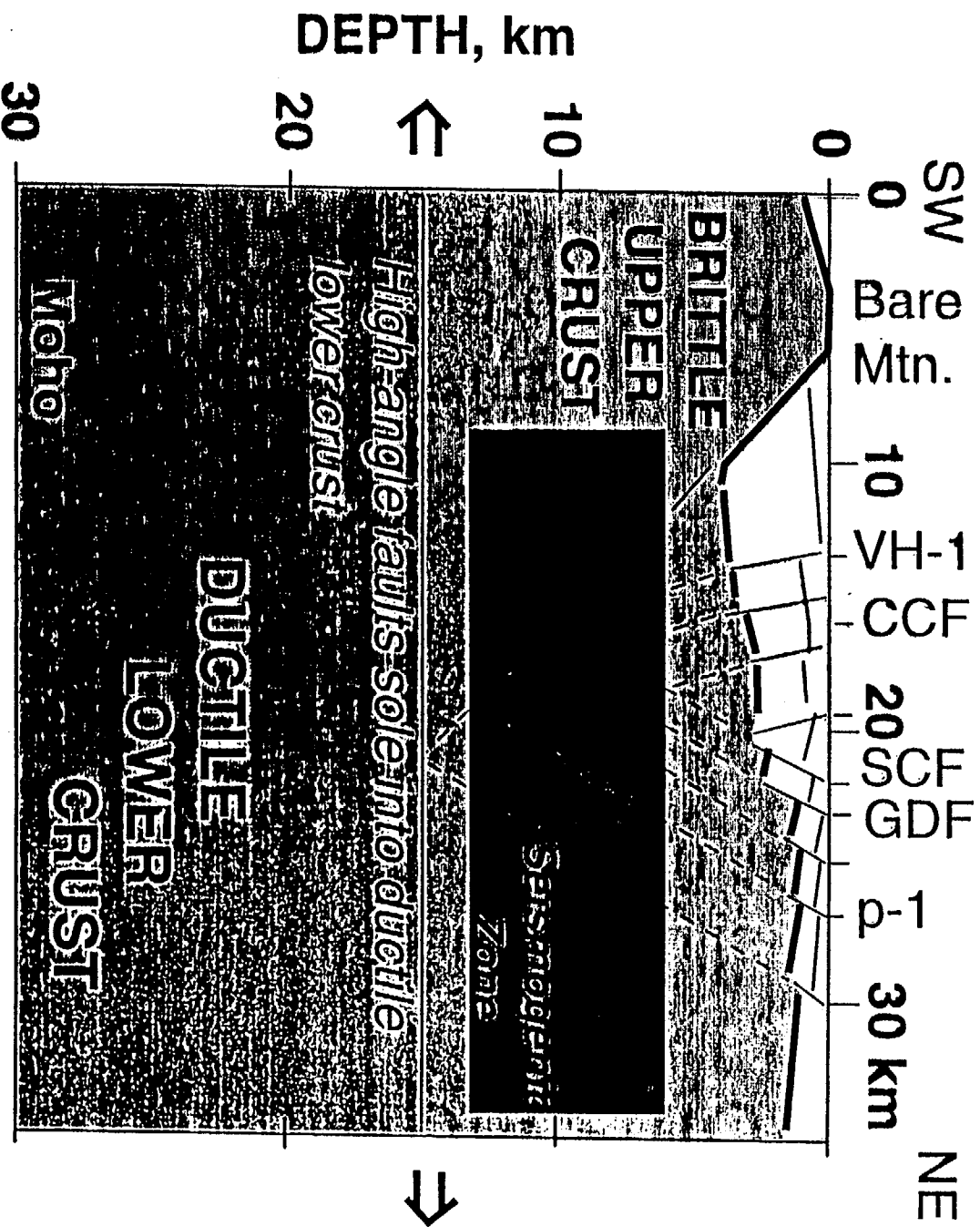
Plate 1. Elastic thickness of the western U.S. Cordillera, with historic seismicity and Cenozoic normal faults. (a) Earthquake epicenters, $M_L > 1$, recorded by University of Utah, University of Nevada-Reno, and U.S. Geological Survey seismograph networks. The white boxes locate ISB seismicity examined in detail in Figures 9, 10, and 11. Light grey lines are K/Ar isotopic ages of the Archean Wyoming craton [Condie, 1981]. Darker grey lines are boundaries between genetically distinct lithospheric blocks located via geochemistry of magmas, from (1) and (2) Farmer and DePaolo [1983], (3) Leeman *et al.* [1992], (4) Manduca *et al.* [1992], and (5) Fleck and Criss [1985]. (b) Surface traces of normal faults exhibiting late Quaternary (<500 ka) surface rupture [after Hecker, 1993; Smith and Arabasz, 1991]. Thick white lines are the eastern-most faults with significant, > 1 km, offset. Faults are B, Bozeman; BV, Beaver; CM, Crawford Mtns; E, Emigrant; EBL, East Bear Lake; EC, East Cache; GV, Grand Valley; M, Madison; S, Sevier; SV, Star Valley; T, Teton; WFZ, Wasatch Fault Zone. Boxes indicate locations of T_e estimates (larger boxes are 400 km by 400 km windows; smaller are 200 km by 200 km windows of data). Physiographic provinces are BR, Basin-Range; CB, Columbia Basin; CP, Colorado Plateau; MRM, middle Rocky Mountains; NRM, northern Rocky Mountains; SRP, Snake River Plain.

for extension, where μ is the coefficient of static friction, ρ is density of overburden, g is acceleration of gravity, z is depth, $\lambda = P/\rho gz$, and P is pore pressure [e.g., Sibson, 1974]. Power law creep is described by

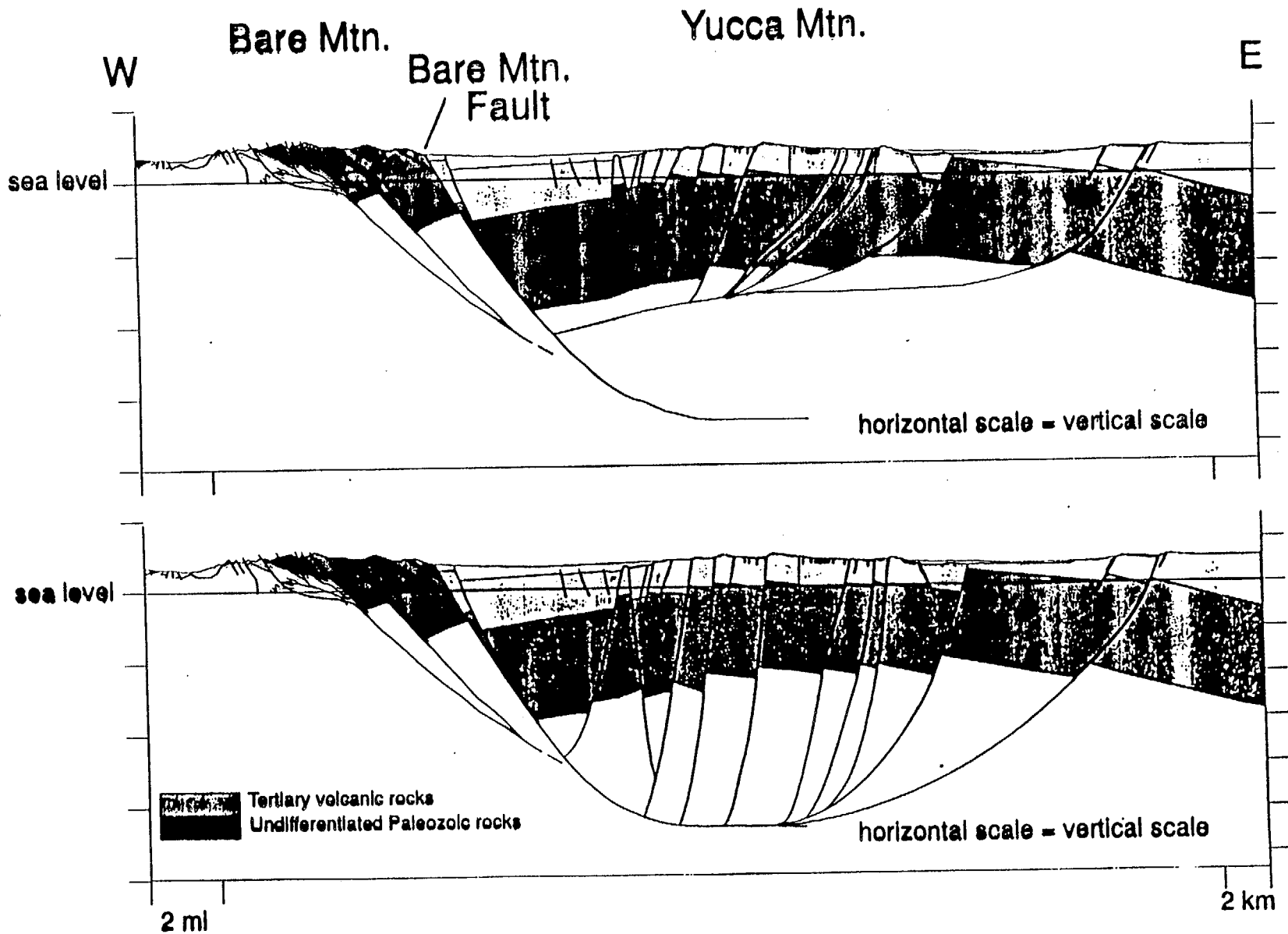
$$\Delta\sigma = \left(\frac{\dot{\epsilon}}{A}\right)^{1/n} \exp\left(\frac{H^*}{nRT}\right) \quad (4)$$

where $\dot{\epsilon}$ is strain rate, A and n are empirically derived material constants, R is the gas constant, T is temperature, and H^* is the activation energy of the material [e.g., Goetze and Evans, 1979]. A more sophisticated estimate of yield strength might also incorporate contributions from the low-temperature ductile and semibrittle rheological regimes, but frictional slip and ductile creep are generally sufficient for flexural analysis [McNutt and Menard, 1982].

PRESENT DAY TECTONIC MODEL



ALTERNATIVE MODELS FOR YUCCA MOUNTAIN FAULTS



across the entire Great Basin along three profiles (B-B', B-B'' and C-C', Fig. 9). The components of the deformation along the profiles were summed to give the integrated opening rate of the Great Basin.

Profile B-B', a line across northern California, Nevada, and northern Utah had a

The deformation rate in the northern Basin is more than twice as high as the s Great Basin (without including the Ower earthquake). This pattern implies far opening of the Great Basin similar to a that was deduced from Cenozoic fault by Wernicke *et al.* (1982).

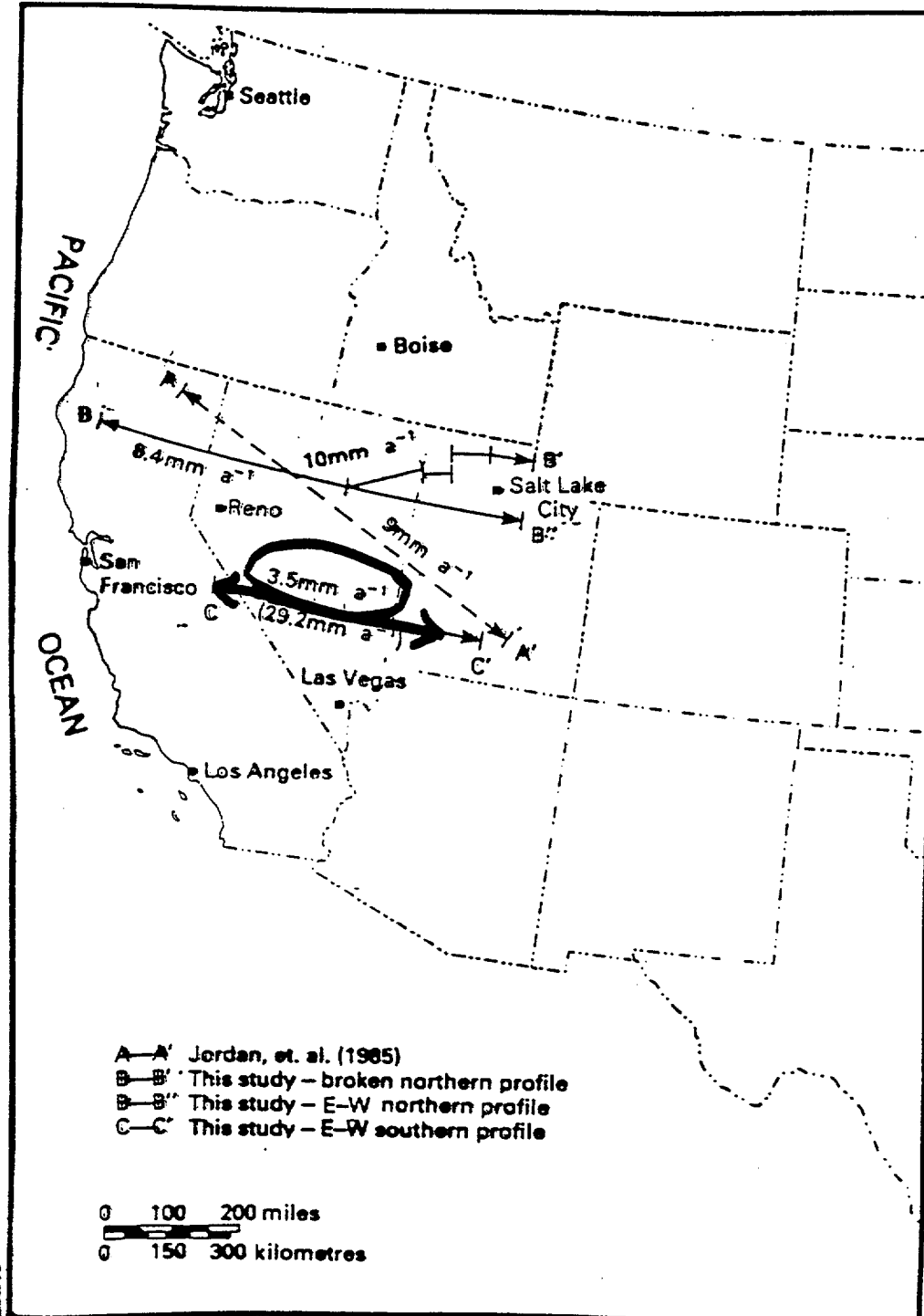
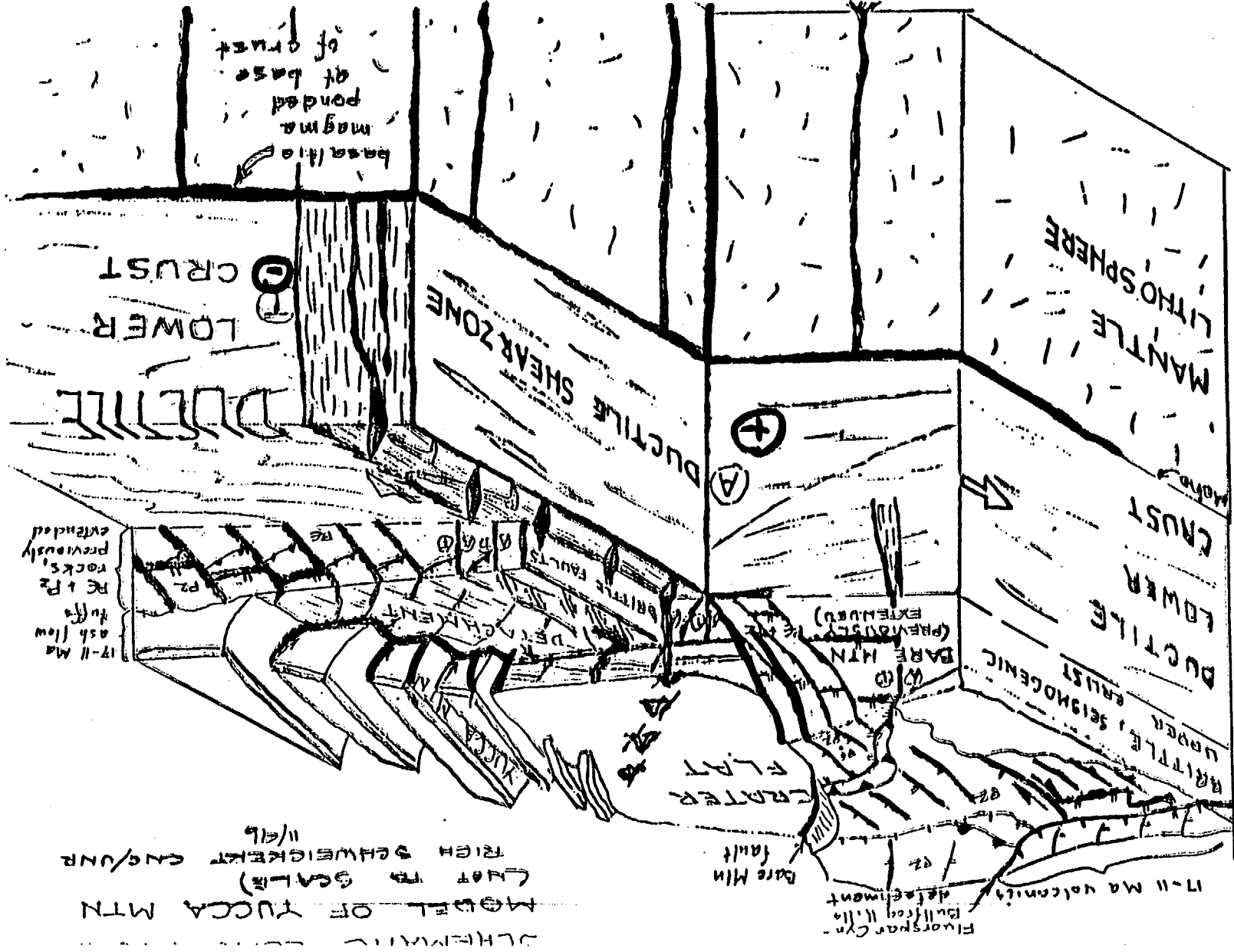


FIG. 9. Great Basin regional tension. A-A' is from Jordan *et al.*'s (in press) intraplate kinematic model of motion between North American and Pacific Plates constrained by satellite ranging data; B-B', B-B'', C-C' from this study. Values in parentheses below C-C' is deformation from the Owens Valley, California, 1872 to present.

Strike-slip



17-11 Ma ash flow tuffs
R1 & R2 rocks, previously extended

basaltic magma ponded at base of crust

LOWER CRUST

DUCTILE

DUCTILE SHEAR ZONE

(A) (+)

MANTLE LITHOSPHERE

CRUST

LOWER DUCTILE

UPPER CRUST
BRITTLE, SEISMOGENIC

(W) (BARE MTN (PREVIOUSLY EXTENDED))

CRATER FLAT

Bare Min fault

Fluorspar Cyn - Bullfrog Mts - detachment

17-11 MA volcanicly detachment
MODEL OF YUCCA MTN (NOT TO SCALE) (LEFT TO RIGHT SHWRIGHT CNG/UNR 11/96)

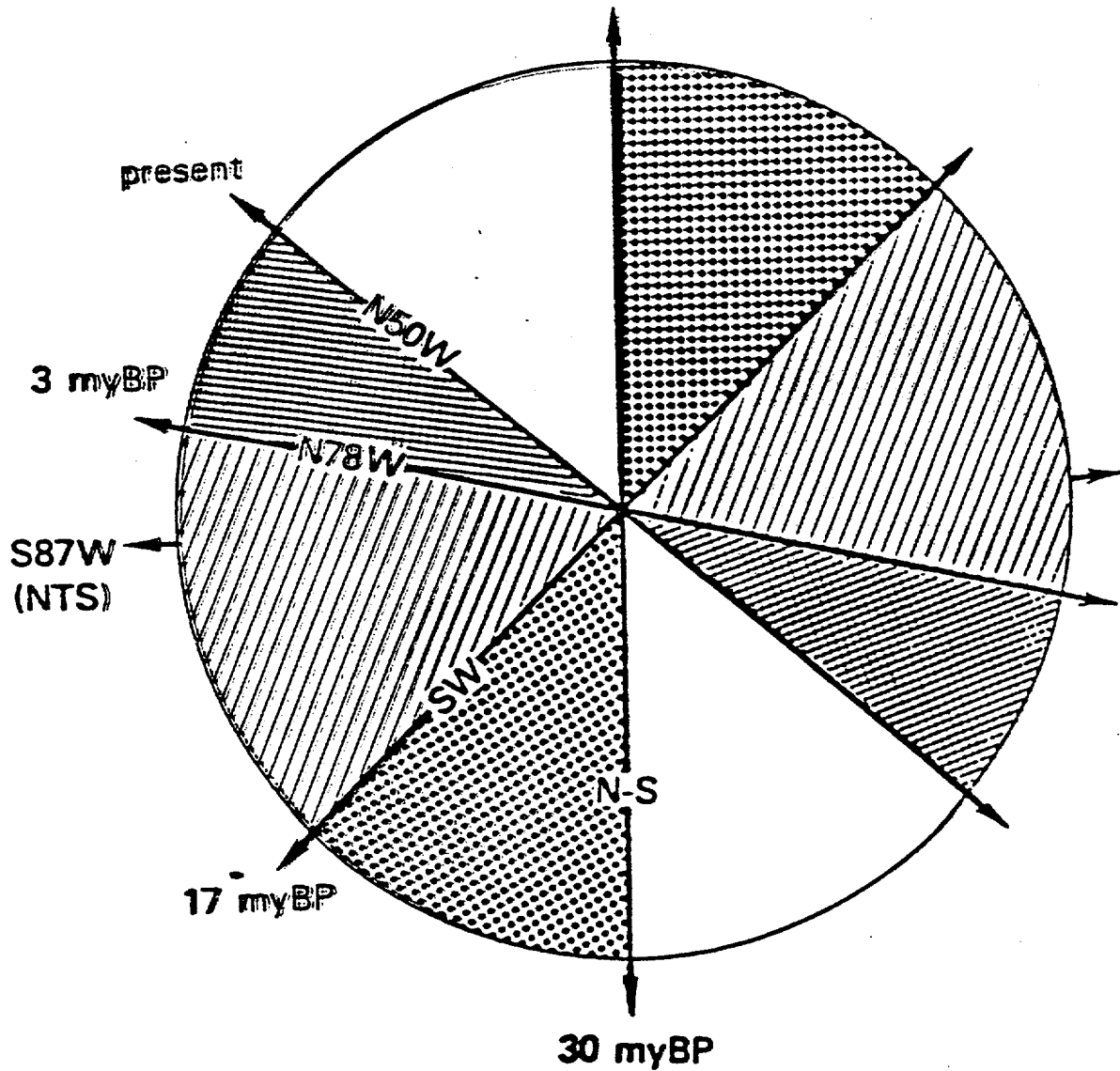
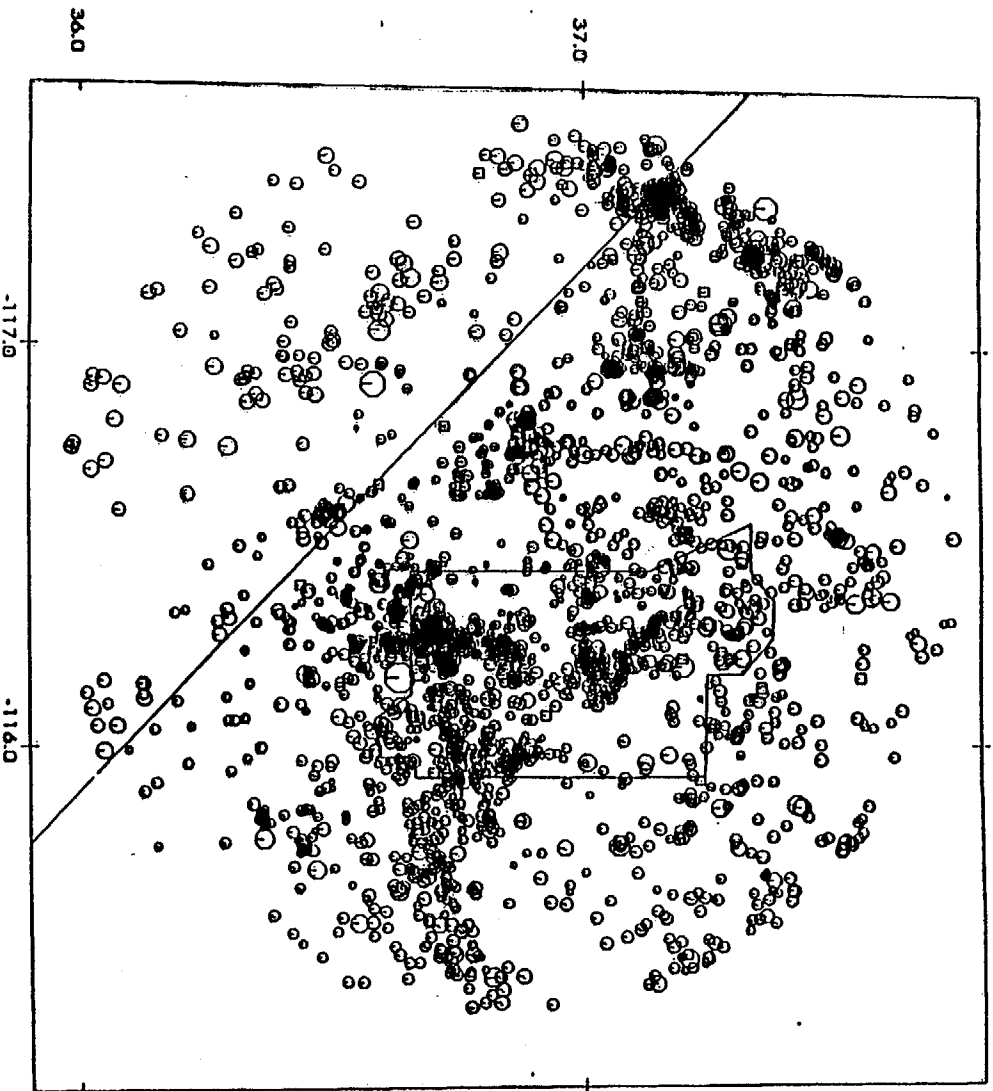


Figure 20. Postulated rotation of extensional stress directions and associated time periods generalized from regional studies. Measurement in west-southwesterly field indicates value from slickensides at NTS.

Auder, 1984



Magnitudes:

- 0.0
- 1.0
- 2.0
- 3.0
- 4.0
- 5.0
- 6.0

No Measure ◻



Project No.
5001A

YUCCA MOUNTAIN WMS

Woodward-Clyde Federal Services

INDEPENDENT EARTHQUAKES
BETWEEN AUG. 1978 AND SEPT. 1992

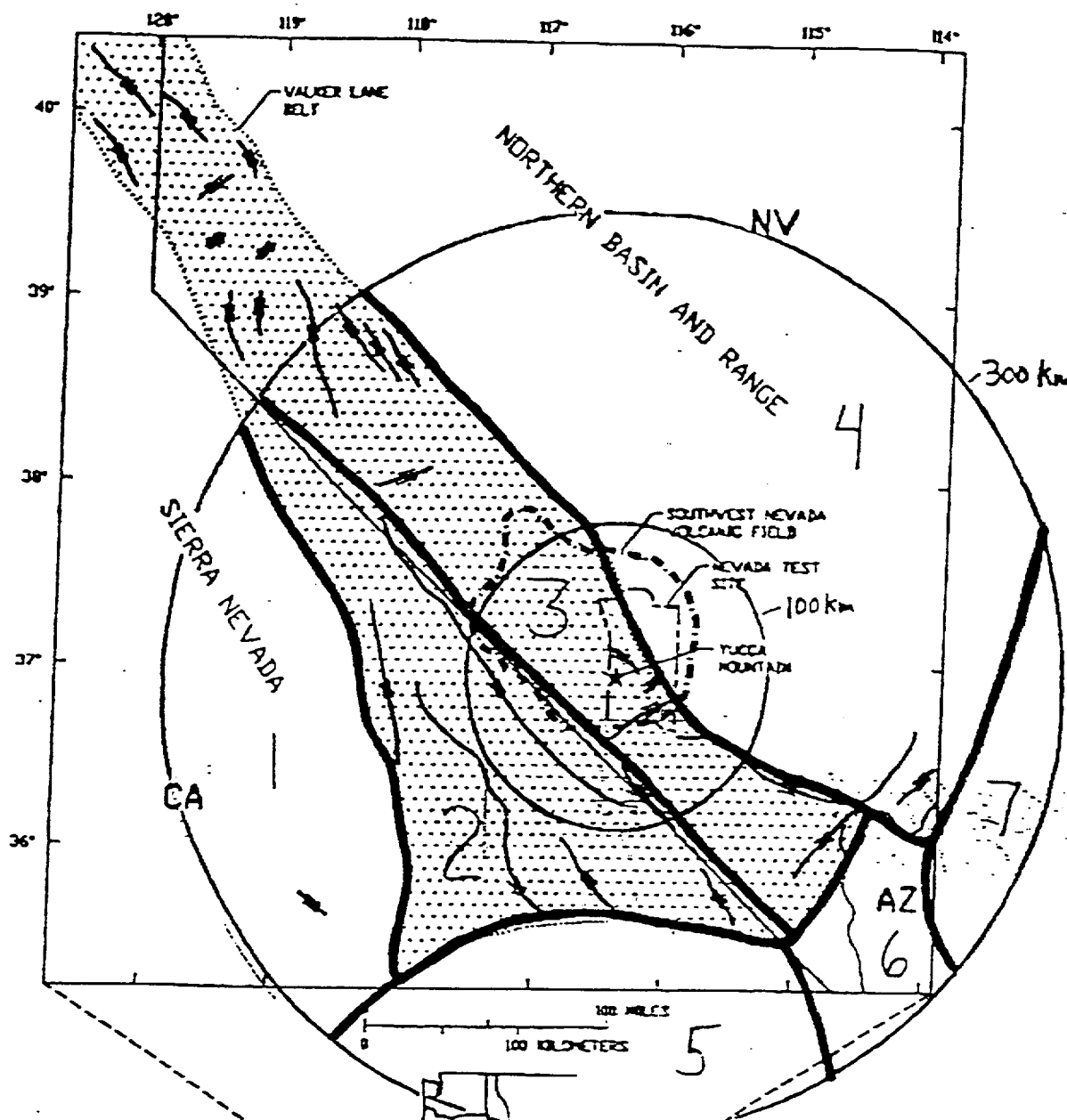
Figure

POTENTIAL SEISMIC SOURCES:

PRESENTATION OF TEAM INTERPRETATION

FRIDRICH, SWAN, DOSER

PSHA MEETING OF JANUARY 7, 1997

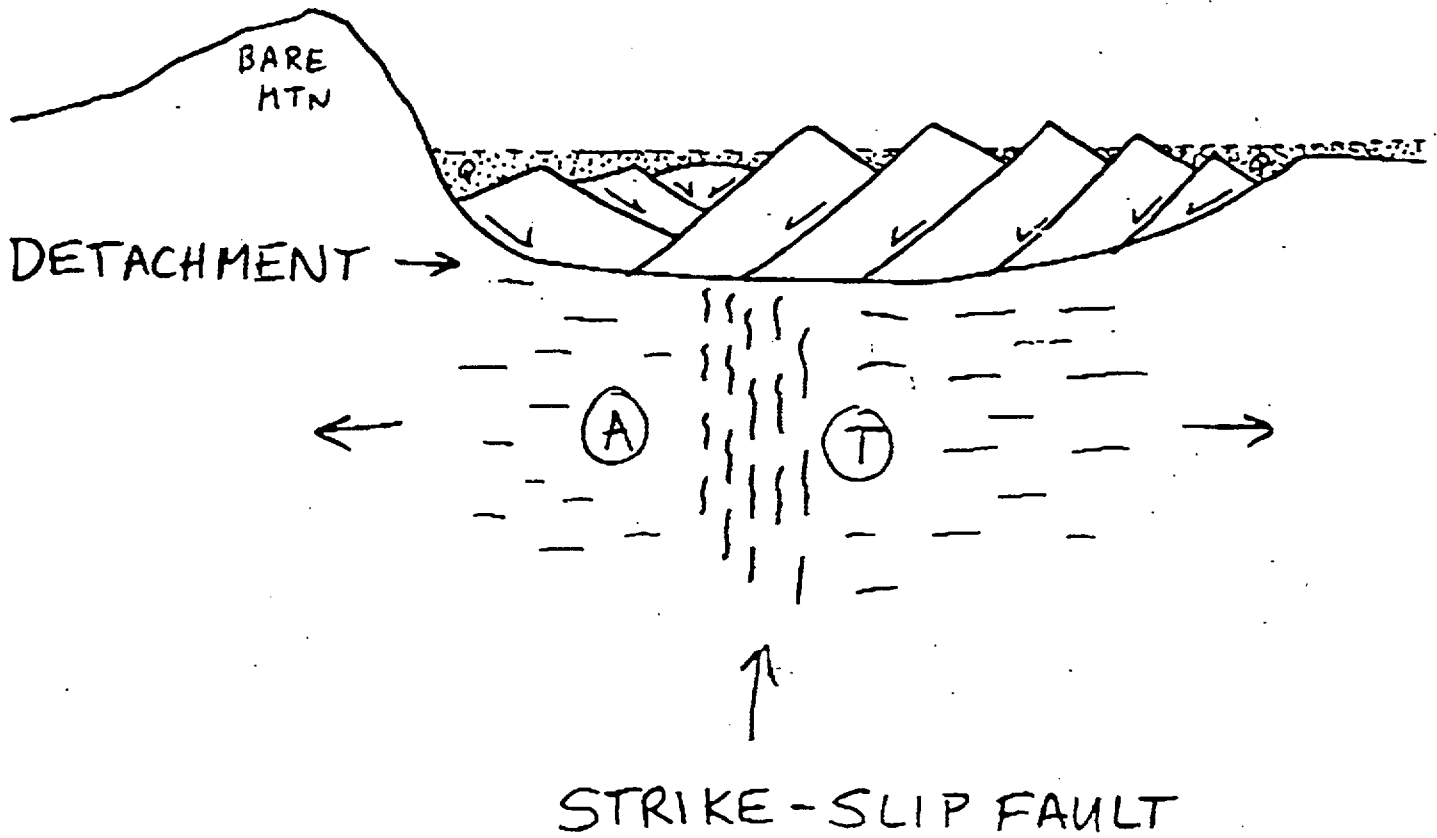


- 1 SIERRA NEVADA
- 2 SW WALKER LANE
- 3 NE WALKER LANE
- 4 N. BASIN-RANGE
- 5 MOHAVE
- 6 S. BASIN-RANGE
- 7 COLO PLATEAU

DOMAINS OF THE SOUTHERN GREAT BASIN AND VICINITY:

<u>DOMAIN</u>	<u>CHARACTERISTICS</u>
1 SIERRA NEVADA	LARGE UPLIFTED TILTED RANGE
2 SOUTHWEST WALKER LANE BELT	TRANSTENSIONAL W/ RELATIVELY LONG STRIKE-SLIP FAULTS
3 NORTHEAST WALKER LANE BELT	TRANSTENSIONAL W/ DISCONTINUOUS AND DISTRIBUTED S-S DEFORMATION
4 NORTHERN BASIN & RANGE	EXTENSIONAL - N20°E FAULTS
5 MOHAVE DESERT	TRANSTENSIONAL SOUTH OF GARLOCK FAULT
6 SOUTHERN BASIN & RANGE	EXTENSIONAL, LARGELY INACTIVE
7 COLORADO PLATEAU	UNEXTENDED UPLIFTED PLATEAU

CROSS SECTION THRU CRATER FLAT BASIN, LOOKING NNW



Seismic Sources and Recurrence

Salt Lake City January 5-9, 1997

Larry Anderson, Al Rogers, Jim Yount

SEISMIC SOURCES

- **Fault Sources**
- **Hidden/Background Sources**
- **Volcanic (Ash Event) Sources**

Criteria for Considering a Fault System a Potential Seismic Source

(Not all criteria are necessarily present for each fault considered
a potential source.):

1. Evidence of Quaternary displacement
2. Evidence that at least 10 km of fault system has ruptured at approximately the same time
3. Evidence of at least 10 cm of slip (total, horizontal, or vertical) at some place on the fault system.
4. Associated seismicity.
5. Proximity to repository.

Preferred Fault Sources

Death Valley-Furnace Creek

Largest, longest, youngest system in region.

No associated seismicity.

$p=.99$

Rock Valley

40 km length, 1m vertical slip and perhaps 2m horizontal slip
in largest event.

Late Pleistocene event involving all parts of fault zone.

Weak association of seismicity.

$p=.95$

Bare Mountain

20-40km length depending on whether confined to mountain front or extended south along gravity gradient.

1m vertical displacement 20-40 Ka.

No associated seismicity.

($p=.9$)

Solitario Canyon-Windy Wash

20 km length, small (10 cm) last event but previous events around 70-80 cm at 70Ka (Ash event).

No associated seismicity

Hard to see how it could act independently of Windy Wash system. $p=.8$ for both systems acting together

Windy Wash on its own: $p=.5$

Paintbrush-Bow Ridge

20 km length. Most events small ($<.5\text{m}$), old ($>100\text{ Ka}$).

No associated seismicity.

Probably involves both faults: $p=.8$

Bow Ridge event independent of Paintbrush: $p=.5$

May also involve Stagecoach Road

Ash Meadows-West Spring Mountains

Quaternary scarps and some trench data to support old events.

West Spring Mountain faults as independent sources may have too low a rate to be significant.

No associated seismicity.

$p=.2$

Stagecoach Road

Very short (8 km) as independent fault, but moderate (.4 to .6m) and young displacements.

May be associated with Paintbrush. Timing from trenches doesn't support much Paintbrush association, however.

No associated seismicity.

$p=.1$ as an independent source

Crater Flat

Short, discontinuous, old small events.

No associated seismicity.

$p=.1$

Amargosa Valley-Pahrump-Stateline:

Biggest scarps may be old (Pliocene) fault line scarps.

Many linears may be nontectonic.

No associated seismicity.

$p=.01$ that whole system acts as single source.

Volcano-Seismic Source

From Crowe and others, 1995:

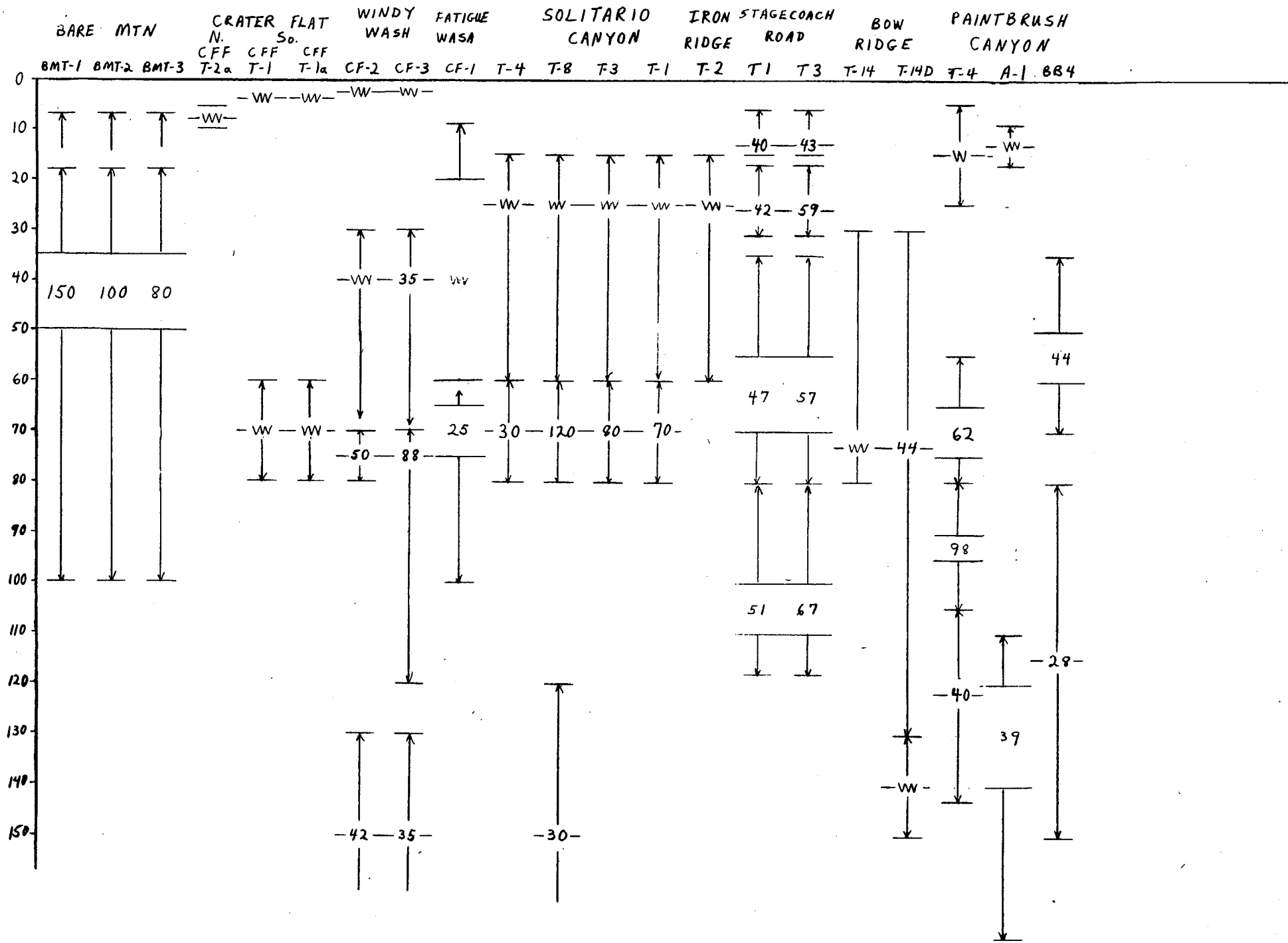
“Quaternary basalt sites, “”, do not appear to be controlled by or follow prevailing surface structural features.”

“Some structures may be preferential sites for ascent of basalt magma but there is not a causative relationship between structure and volcanism.”

(Both citations from page 3-39)

Are these assertions true?

If so, does a seismic source, driven by volcanism need to be considered?



All events on all eight Yucca Mtn Faults:

23 events in last 170 ka

Ave = 7.4 ka

All events (disp \geq 20 cm) on all Yucca Mtn Faults:

14 events in last 170 ka

Ave = 12 ka

EARTHQUAKE RECURRENCE

EVENT	FAULTS	AGE (ka)
Z (cracking)	WW,CF	6 ± 4
Y	SCR, PC	13 ± 3
X	SCR, SC, IR	25 ± 7
W ¹	WW, FW, BM?	40 ± 20
V ²	SCR, PC?	59 ± 24
U ²	CF, WW, SC, BR, PC?, SCR?,	75 ± 10
T	PC, SCR?	100 ± 20
S	PC, SCR?	125 ± 20
R	WW, SC	150 ± 20

¹ W could be a Bare Mountain fault event.

² U and V are likely the same event.

8 events in 170 ka

Ave Recur = 21 ka

$$M \geq 6 \frac{1}{4} \pm \frac{1}{4}$$

Events V and U could be the same event

Event W could be a Bare Mountain fault event

That would leave 6 events in 170 ka;

3 on east side,

2 on west side, and

1 on all

or

28 ka ave rec

Issues 2 and 4: Earthquake Sources and Recurrence

Preliminary Team Interpretation

A. Rogers

J. Yount

L. Anderson

Two Models: Seismicity or Slip Rate Based

Common Elements

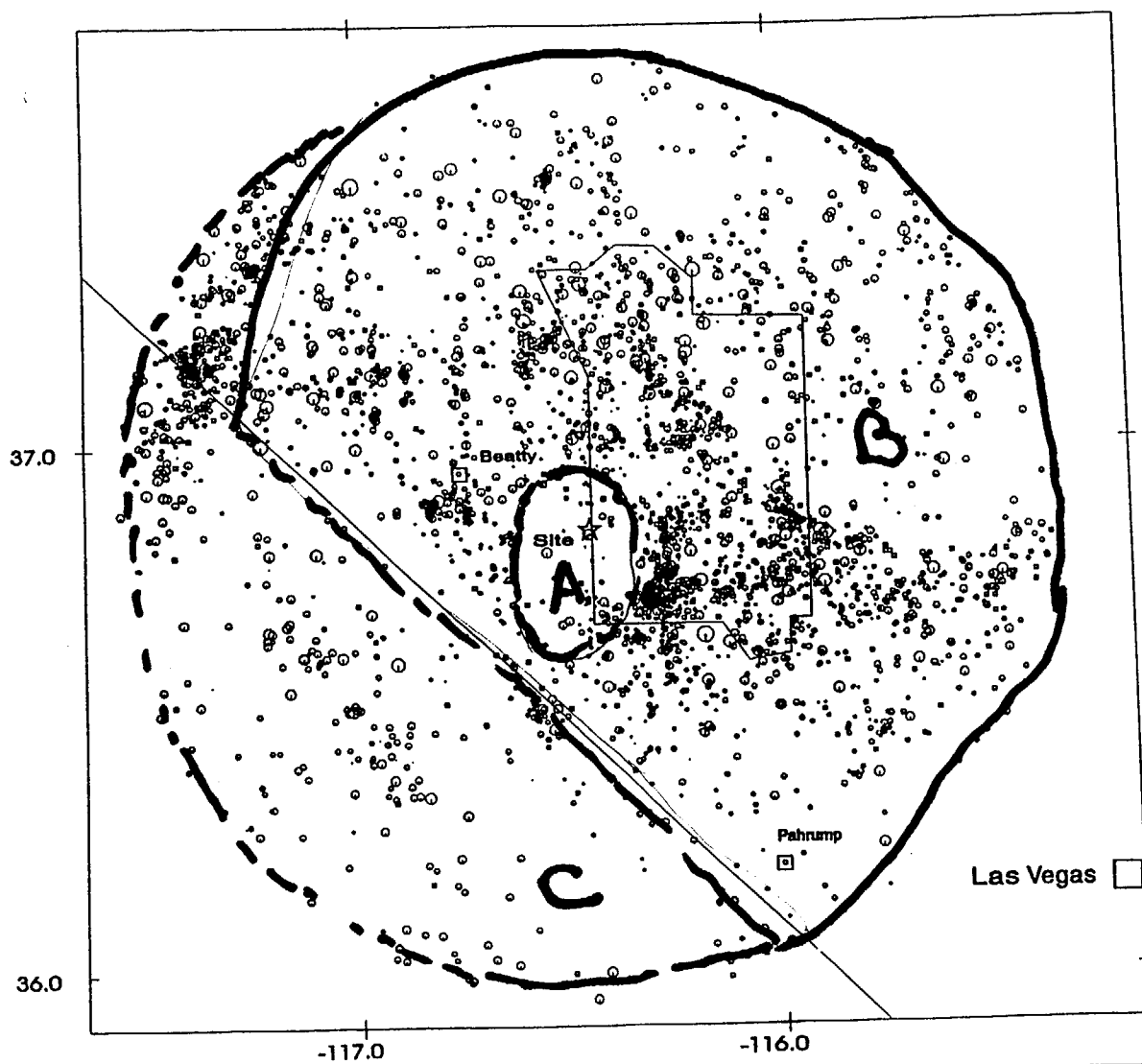
- Three Background Zones
 - > Zone A
 - Yucca Mt.
 - Crater Flat and Bare Mountain
 - Western Portions of Jackass Flat
 - > Zone B
 - Remaining 100 km minus Death Valley-Furnace Creek
 - > Zone C
 - Death Valley-Furnace Creek
- Varying Combinations of Mapped and Background Faults
- All Faults Steeply Dipping, Surface to Mid-Crust
- Discrete Statistical Distributions on Recurrence Rates and M_{\max}

Earthquake Recurrence

- Decluster Catalog
 - > Veneziano's Method
 - > Reasenberg's Method
 - > Young's Method
- Remove UNE's and UNE Aftershocks
 - > Use Distance Decay Observations to Set Limits
- Determine Completeness Intervals
 - > Compute Annual Rates for M_{bins} During Completeness Intervals
- Compute Regional (100 km radius) b-value and a-value
 - > Truncated Exponential Recurrence Relationship
 - > $M_{\text{max}} = 6.5$
- Allocate Total Seismic Rate Among Individual Zones

Model 1: Recurrence: Seismicity Based

- Uniformly Distributed Background Faults: All Zones
- Truncated Exponential Model w/Zone Dependent Recurrence Based on Seismicity
- Orientation Parallel to Structural Grain or Significant Faults, Lengths Based on M_{\max}
- Zone A: $M_{\max} = 6.8$ and Background Faults that are Coincident with
 - > Solitario Canyon
 - > Paintbrush Canyon-Stage Coach Road
 - > Windy Wash-Fatique Wash
 - > Bare Mountain
- Zone B: $M_{\max} = 7.2$ and One Background Fault Coincident with RV Fault
- Zone C: $M_{\max} = 7.9$ and One Background Fault Coincident with DV-FC



Magnitude

.0 ·

1.0 ·

2.0 ·

3.0 ○

4.0 ○

5.0 ○

6.0 ○

No Measure ·



Project No. 5001A	YUCCA MOUNTAIN WHB	HISTORICAL SEISMICITY (1904-1994) WITHIN 100 KM OF THE YUCCA MOUNTAIN SITE USED IN RECURRENCE	Figure
Woodward-Clyde Federal Services			

Model 2: Recurrence: Slip Rate Based

- Use Mapped Faults In All Zones
 - > Zone A, DV-FC, and RV
 - Recurrence from Slip Rates with Characteristic Model
 - > Zones B & C: Seismic Rate for Faults With No Slip Rate
 - Subtract out Equivalent Recurrence Rates for RV and DV-FC
 - Fault Length Dependent M_{\max} and Rate
- M_{\max} as in Model 1

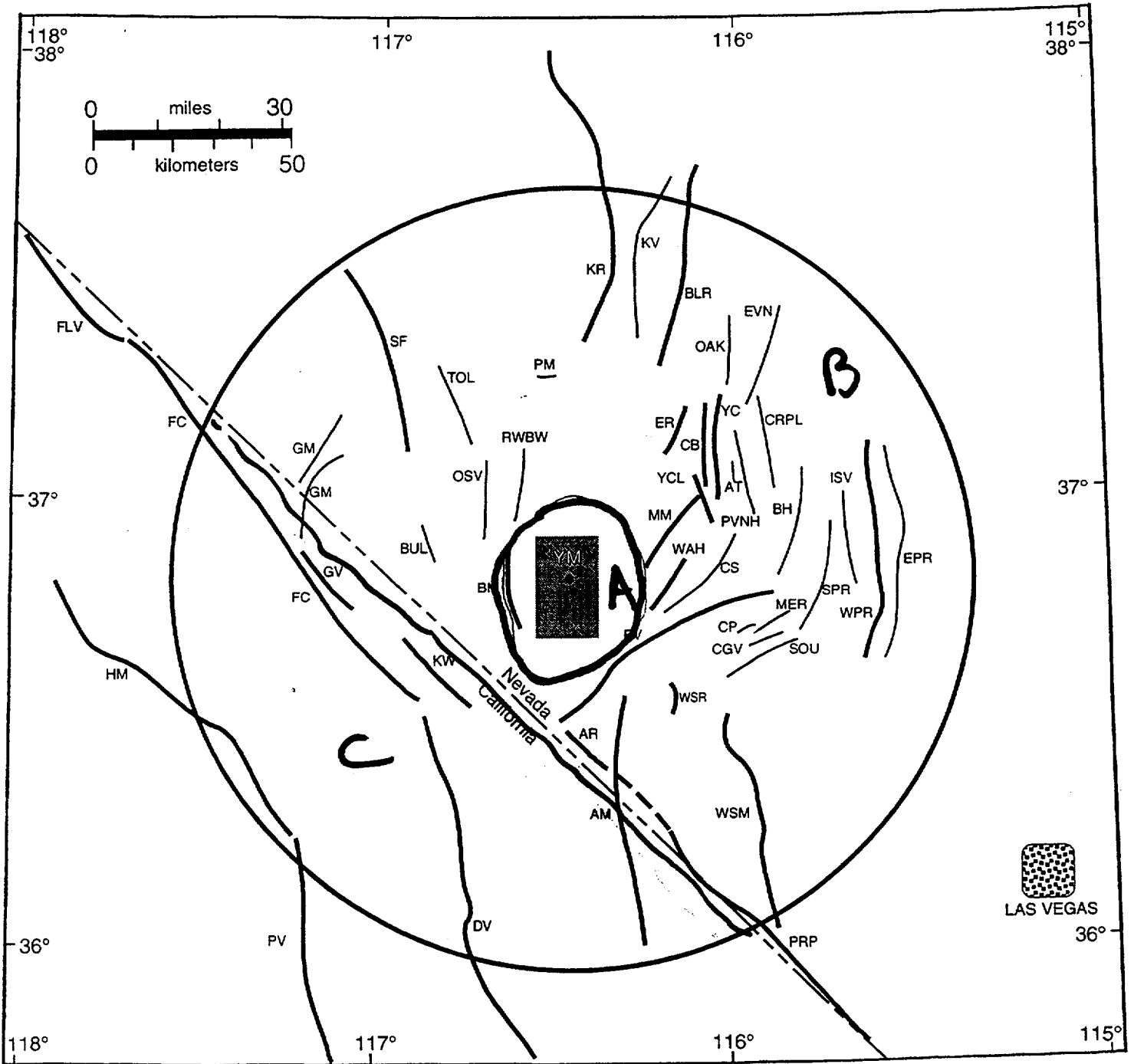


Figure 3-1. Index map showing location of relevant (bold line) and potentially relevant faults capable of generating average median and 84th percentile peak accelerations that equal or exceed 0.1 g at the potential radioactive waste repository at Yucca Mountain (YM). Faults in the immediate site area (shaded rectangle) are shown on Figure 3-2. Large circle is 100 km radius from the site. Abbreviations of faults are as follows:

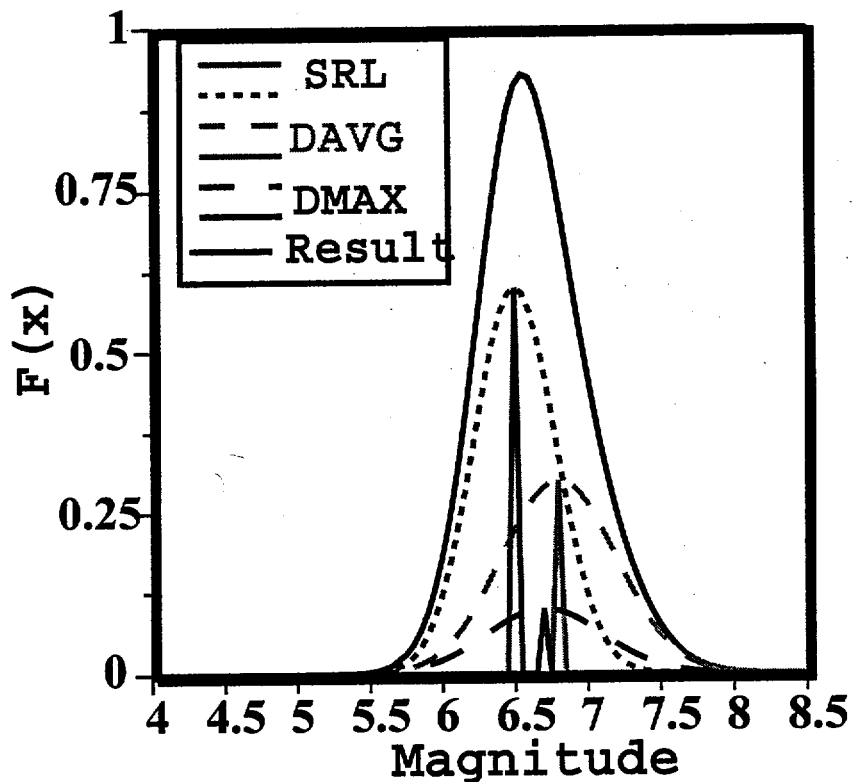
AM	Ash Meadows	CS	Cane Spring	KR	Kawich Range	RV	Rock Valley
AR	Amargosa River	DV	Death Valley	KV	Kawich Valley	RWBW	Rocket Wash-Beatty Wash
AT	Area Three	EPR	East Pintwater Range	KW	Keane Wonder	SF	Sarcobatus Flat
BH	Buried Hills	ER	Eleana Range	MER	Mercury Ridge	SOU	South Ridge
BLR	Belted Range	EVN	Emigrant Valley North	MM	Mine Mountain	SPR	Spotted Range
BM	Bare Mountain	FC	Fumace Creek	OAK	Oak Spring Butte	TOL	Tolicha Peak
BUL	Bullfrog Hills	FLV	Fish Lake Valley	OSV	Oasis Valley	WAH	Wahmonie
CB	Carpetbag	GM	Grapevine Mountains	PM	Pahute Mesa	WPR	West Pintwater Range
CGV	Crossgrain Valley	GV	Grapevine	PRP	Pahrump	WSM	West Springs Mountain
CP	Checkpoint Pass	HM	Hunter Mountain	PV	Panamint Valley	WSR	West Specter Range
CRPL	Cockeyed Ridge-Papoose Lake	ISV	Indian Springs Valley	PVNH	Plutonium Valley-N Halfpint Range	YC	Yucca
						YCL	Yucca Lake

Maximum Magnitudes in the Yucca Mountain Area: A Preliminary Interpretation

Team Members: Jim McCalpin, Burt Slemmons and Jon Ake

Seismic Source Characterization Workshop #4
Salt Lake City, UT
January 6-8, 1996

Fault Magnitude Functions



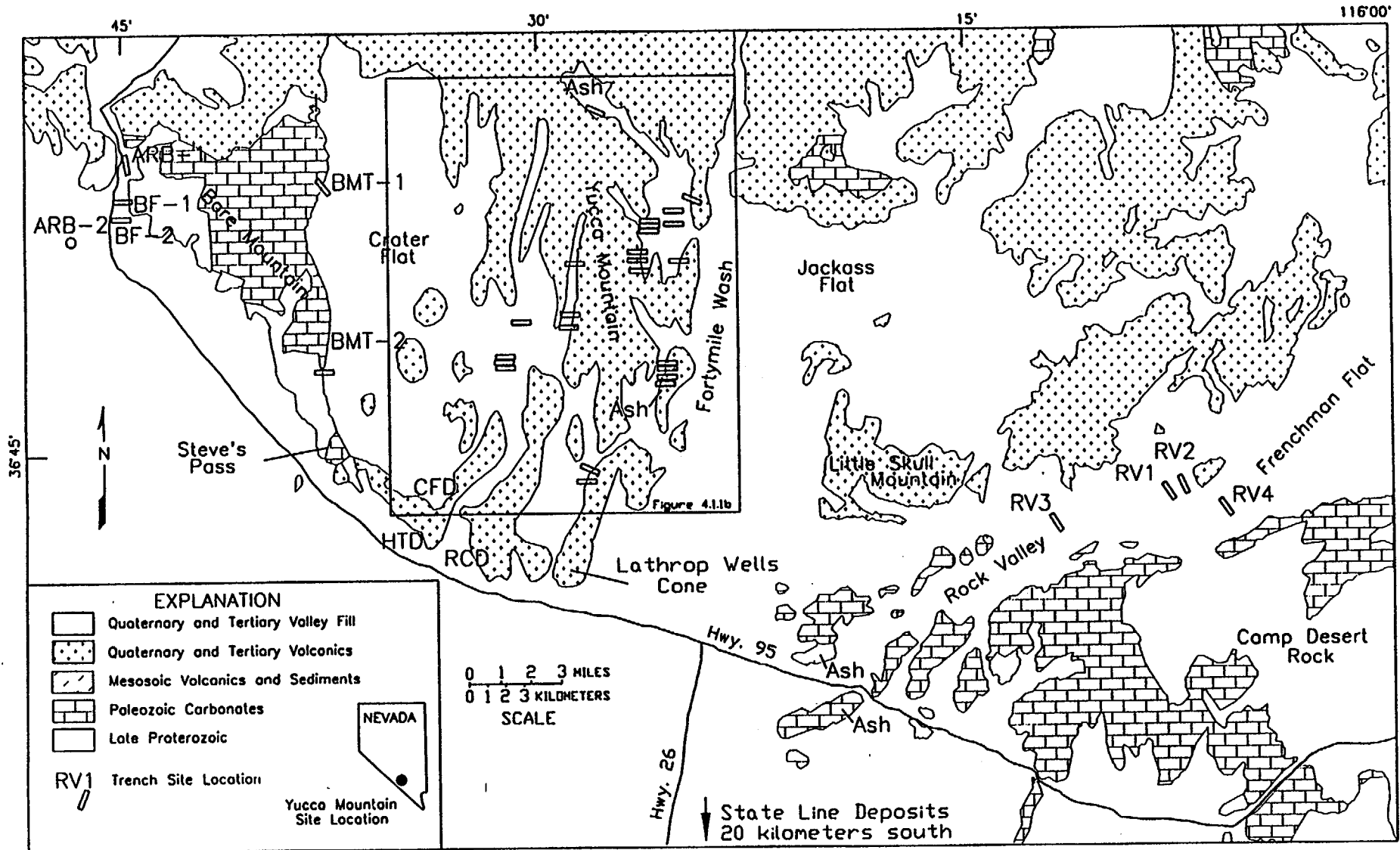


Figure 4.1.1a Map of Yucca Mountain area showing major faults and locations of sites from which samples have been dated

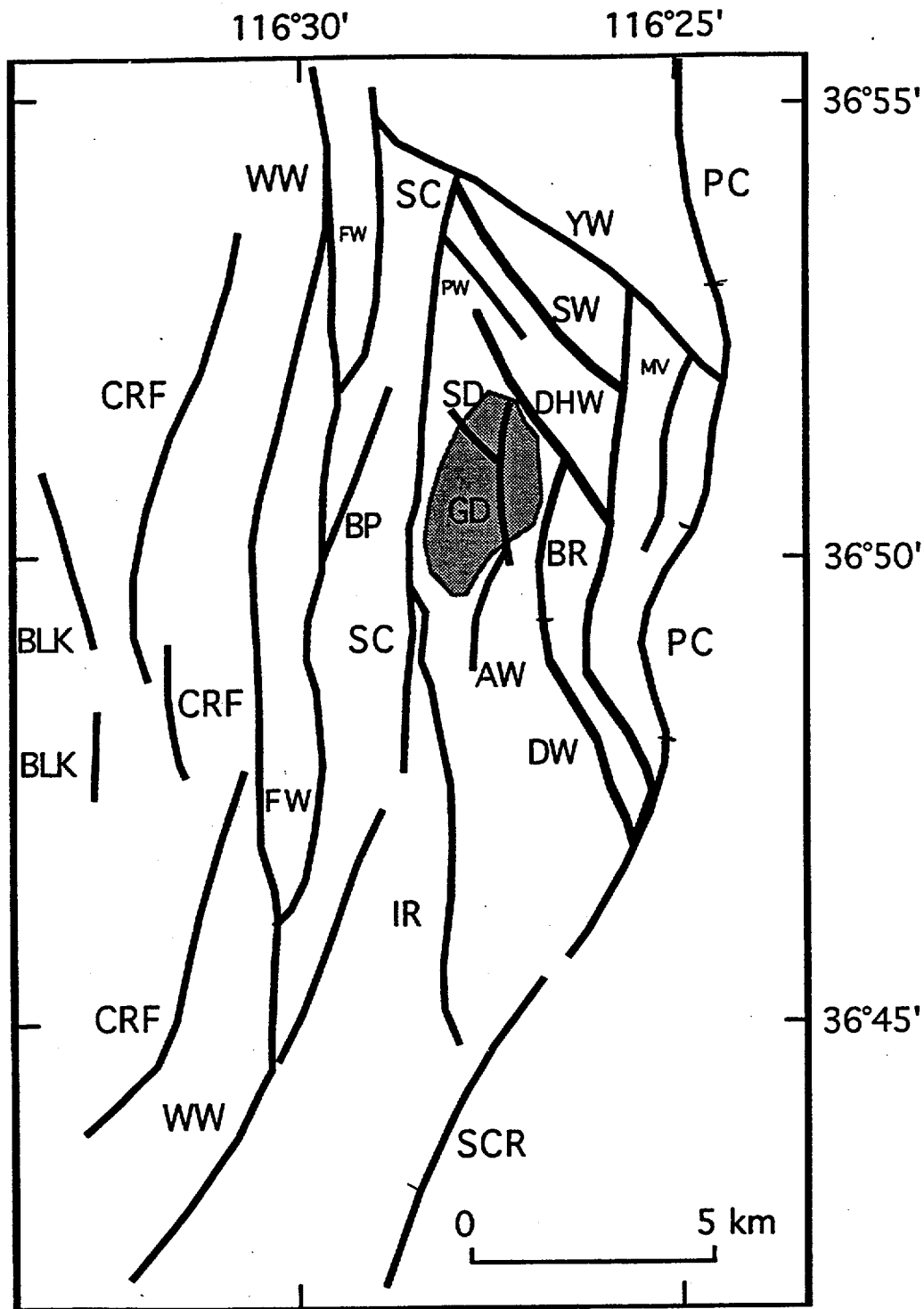
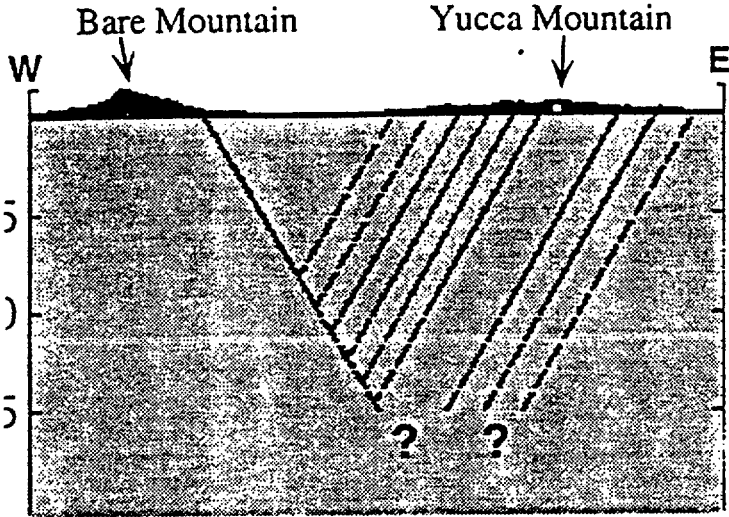
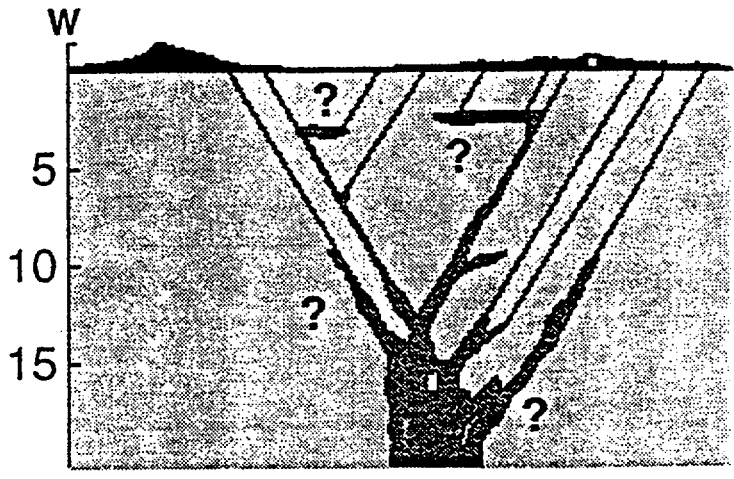
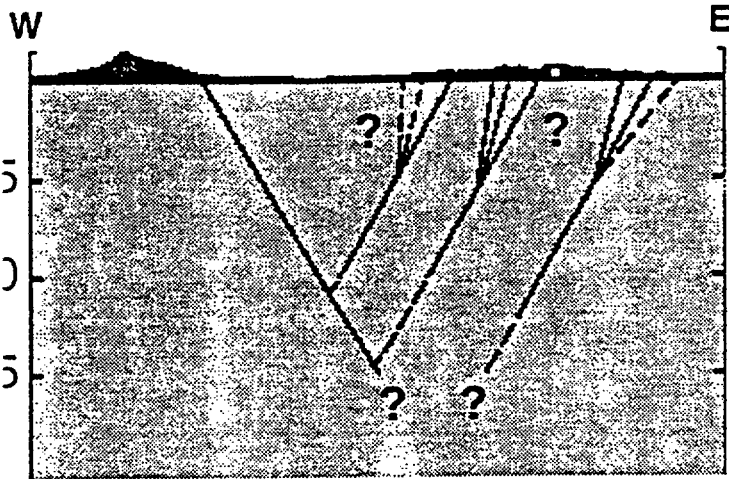
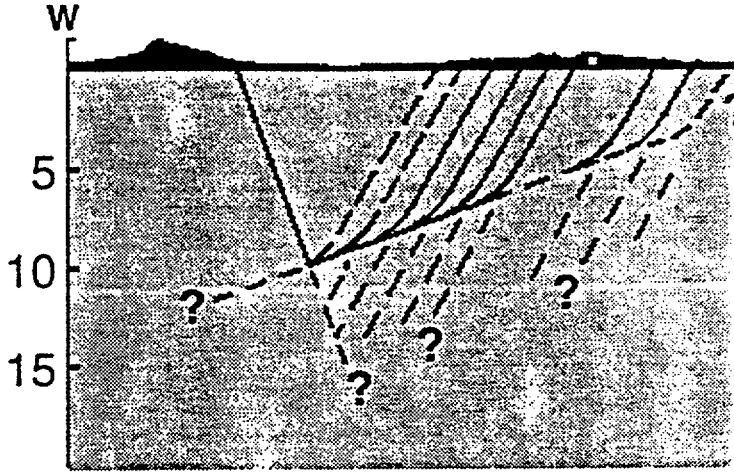


Figure 3-2. Index map of faults in and near Yucca Mountain. Fault abbreviations are: AW - Abandoned Wash; BLK - Black Cone; BP - Boomerang Point; BR - Bow Ridge; CRF - Crater Flat; DHW - Drill Hole Wash; DW - Dune Wash; FW - Fatigue Wash; GD; Ghost Dance; IR - Iron Ridge; MV - Midway Valley; PC - Paintbrush Canyon; PW - Pagan Wash; SC - Solitario Canyon; SCR - Stagecoach Road; SD -

SOME HYPOTHETICAL STRUCTURAL MODELS



True Scale



Yucca Mountain Maximum Magnitudes

Basic Data:

Mapped Fault Lengths

Displacement Data from Trenches

**Maximum Displacement from maximum reported displacement from
Trench(es) on each fault**

Average Displacement from average preferred values

**Surface Rupture Length from measured length of individual faults (no
linkage)**

Link Between Data and Magnitudes

Wells and Coppersmith (1994)

(all slip types relationships)

Assumptions and Prejudices

Mapped Fault Lengths a Proxy for Surface Rupture Lengths in W&C'94

Nucleation depths of 9-15 km, moderate-high angle fault dips, consistent w/ tectonic model

Independent:

We use this in a ground motion estimation sense, i.e. fault ruptures that are separated by more than 15-30 seconds are INDEPENDENT. Alternative hypotheses may need to be investigated for fault rupture hazard.

Hierarchy:

Surface Rupture Length is a more stable estimator of Magnitude than any surface displacement measure.

Average Displacement is more representative of moment (and hence magnitude) than is maximum displacement.

SRL, AD, MD

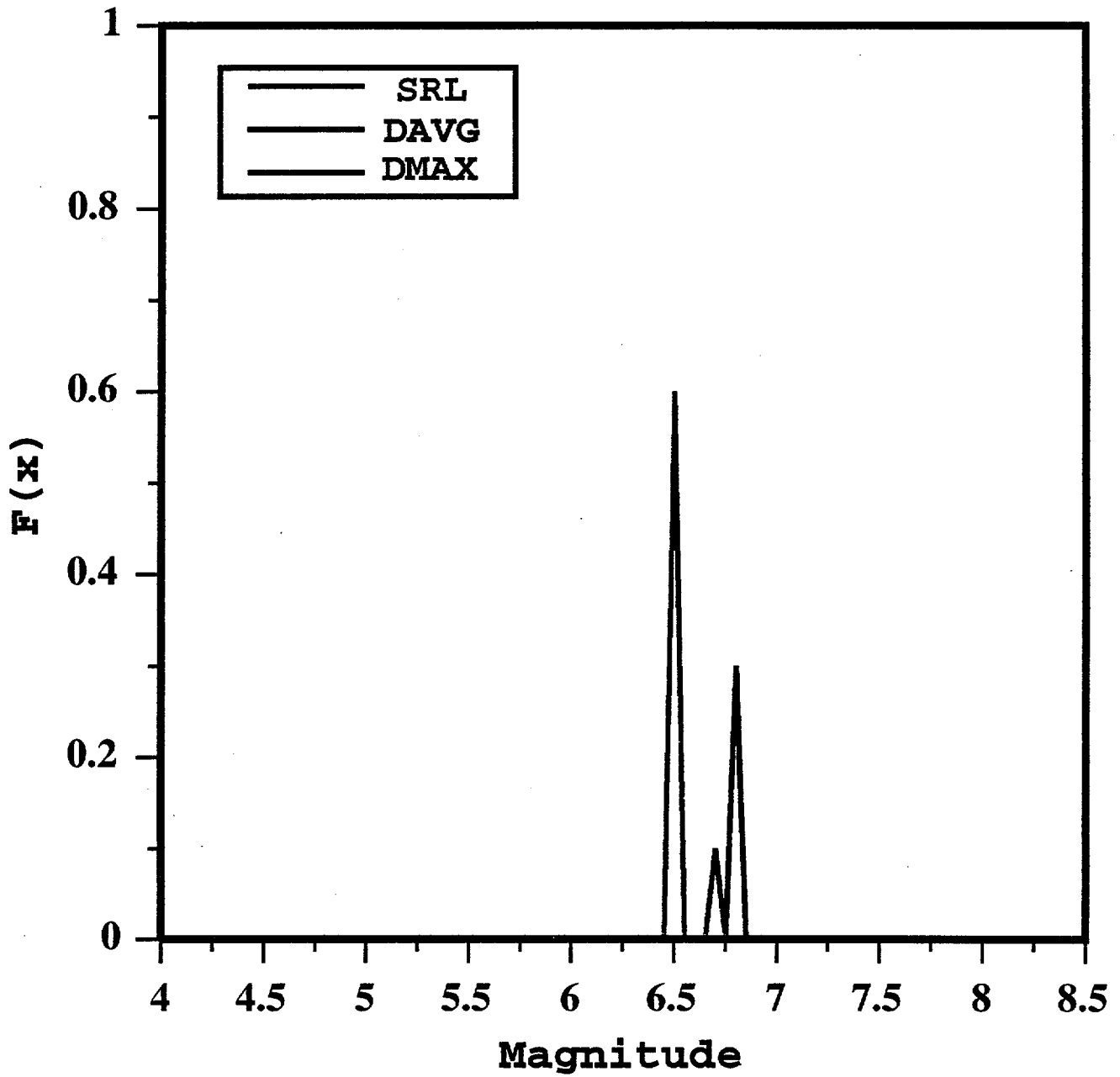
Shortcomings

**Short Fault lengths lead to question of applicability in W&C'94
(limited data in this range)**

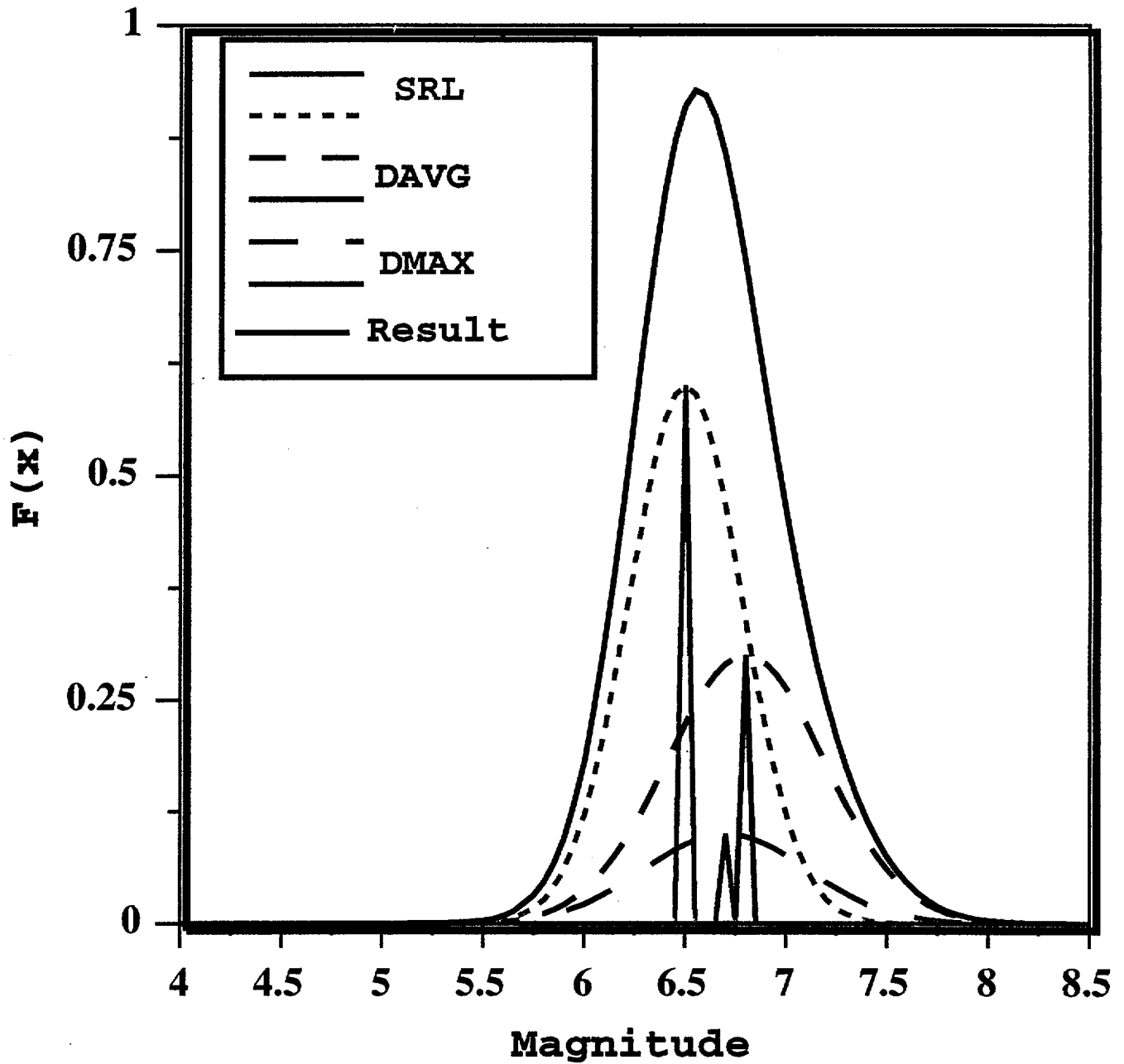
**Slip rate relationship to magnitudes, could lead to slightly different
answer
(Mason, Anderson)**

**Difficult to project some of the short, closely-spaced faults to
depth, leads to questions r.e. seismogenic potential.**

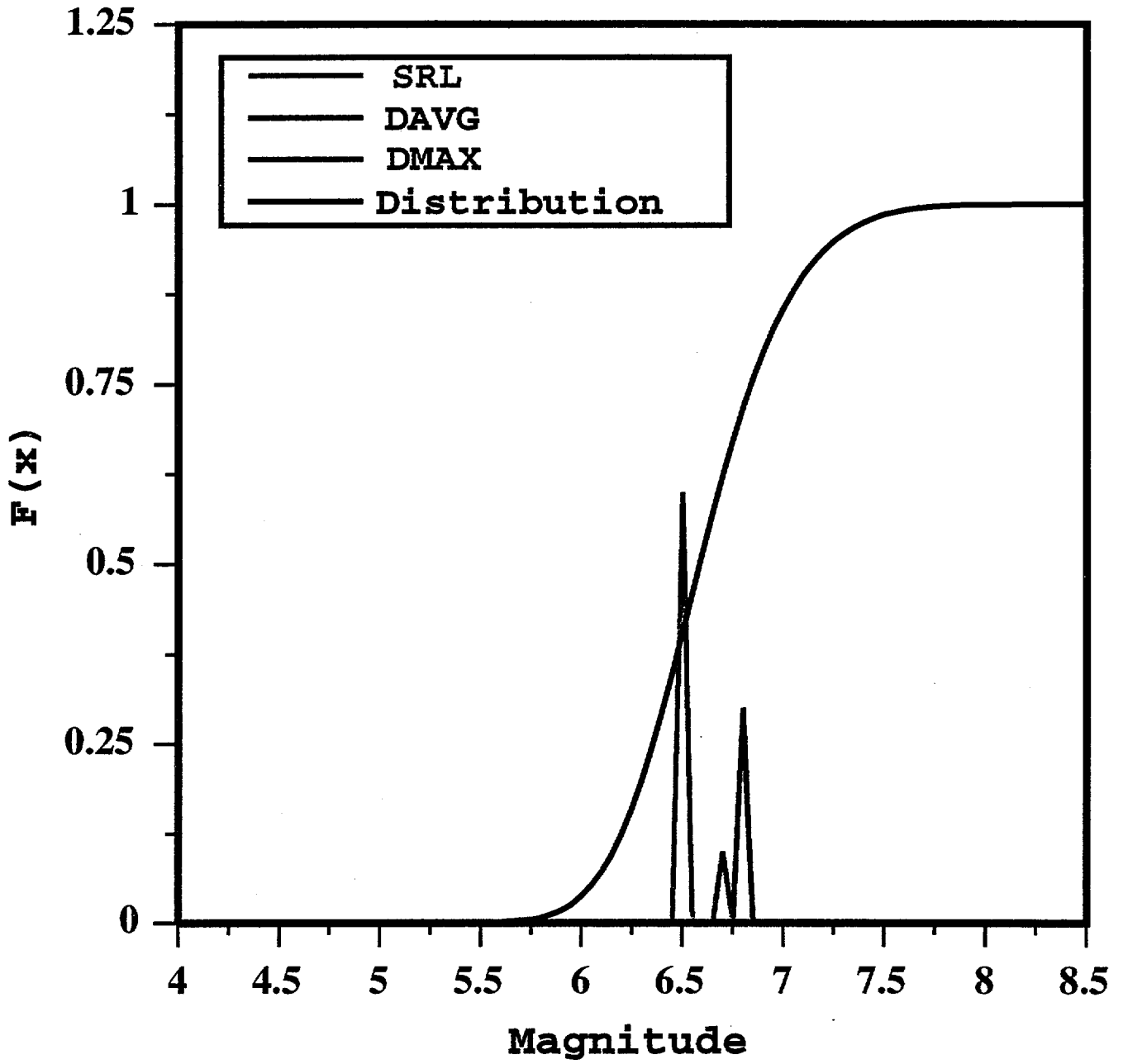
Magnitude Estimates



Fault Magnitude Functions



Magnitude Distribution



Consistency - Reality Check

Iron Ridge Fault -

Srl ~ 9 km ($M_w^{srl} \sim 6.19$)

Max displacement - 130 cm (M_w 6.78)

Avg surface displ. - 61 cm (M_w 6.75)

Assume 60° dip ; 15 km seismogenic depth

Notes - unusual aspect ratio

To produce M 6.76 requires ~ 3.3 m
of slip (avg) over fault surface
or $\Delta\sigma$ of ~ 540 bars.

Assume aspect ratio ≈ 1 ; 10 km depth
and 60° dip for 75 bar $\Delta\sigma$
result is M_w 6.1

Assume AD of 61 cm is avg slip on
fault - M_w 6.2.

Fundamental question of which date set to place most weight on.

$$D_{avg} \sim 1.0 \sigma$$

$$D_{max} \sim 1.1 \sigma$$

For 9km SRL -

of 61 cm?

• what is probability of D_{max} of 130 cm and/or D_{avg}

rapture.

• Large displacement events are related/due to compound

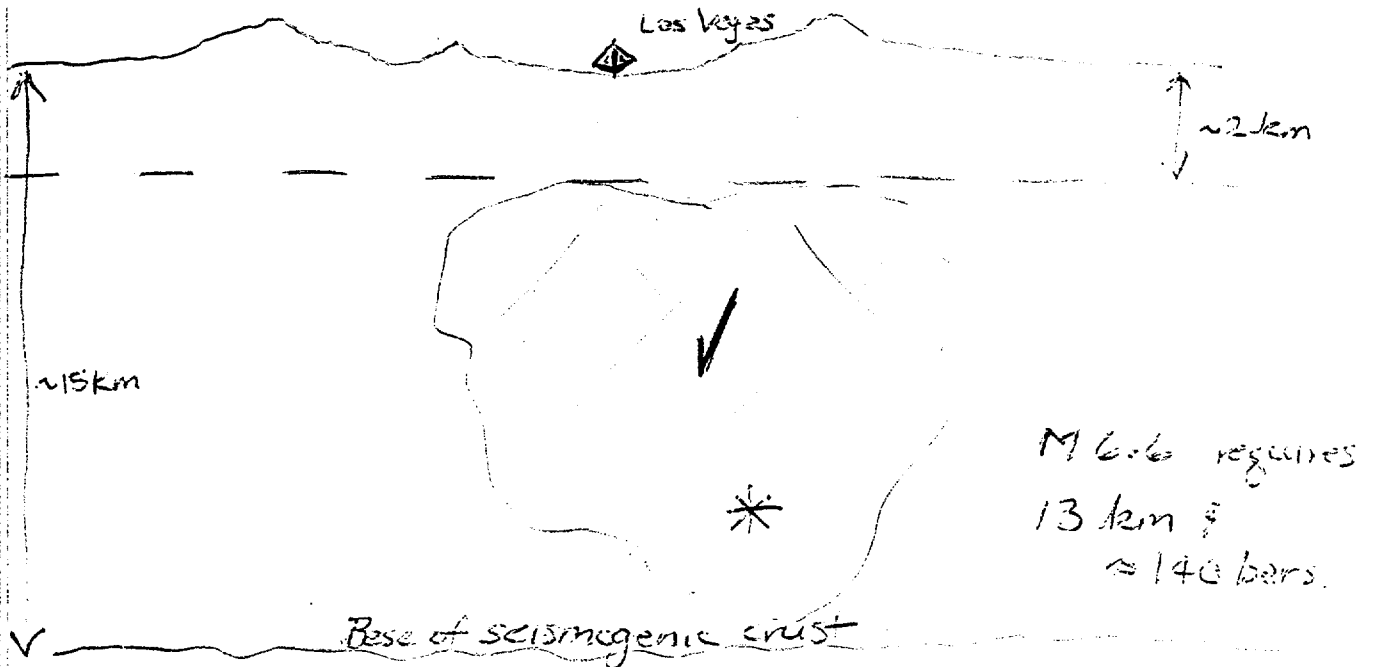
Possible explanations:

Maximum Background Earthquake

Preliminary Estimate - based
primarily on work by DePolo
and others

$M_w 6.3$ ($S = \pm 0.3$)

Does it make sense?
crustal fault model



For $M_w 6.3$ and 75 bar stress drop
we estimate rupture area of $\approx 102 \text{ km}^2$ ($r \approx 5.7 \text{ km}$)
consistent w/ slip (avg) of 1.1 m.

Table 1: Maximum Magnitudes-Yucca Mountain

Fault/Source	Independent Rupture Probability	SRL (km) M_w^{srl}	Max Disp (cm) M_w^{Dmax}	Avg. Preferred Disp (cm) M_w^{Dbar}	M_{max}, Prob., sigma
Bare Mountain	Yes P=0.95	21 6.62	300 7.04	127 7.02	M=7.0, P=0.5, S=0.4 M=6.6, P=0.5, S=0.28
	No P=0.05				
Northern Crater Flat	Yes P=0.90	11 6.3	50 6.47	29.6 6.50	M=6.5, P=0.4, S=0.4 M=6.3, P=0.6, S=0.28
	No P=0.10	21 6.61			
Southern Crater Flat	Yes P=0.90	8.5 6.16	32 6.32	13.2 6.21	M=6.3, P=0.20, S=0.4 M=6.2, P=0.80, S=0.28
	No P=0.10				
Windy Wash	Yes P=0.80	23 6.66	98 6.69	36.5 6.57	M=6.7, P=0.80, S=0.28 M=6.6, P=0.20, S=0.39
	No P=0.20				
(w/Fatigue Wash?)	No P=0.20				

Table 2: Maximum Magnitudes-Yucca Mountain

Fault	Independent Rupture Probability	SRL (km) M_w^{srl}	Max Disp (cm) M_w^{Dmax}	Avg. Preferred Disp (cm) M_w^{Dbar}	M_{max} , Prob., sigma
Fatigue Wash	Yes P=0.80	17 6.51	105 6.71	61.3 6.76	M=6.8, P=0.30, S=0.39 M=6.7, P=0.10, S=0.4 M=6.5, P=0.60, S=0.28
(w/Windy Wash?)	No P=0.20				
Solitario Canyon	Yes P=	18.5 6.55	140 6.78	37.5 6.58	M=6.8, P=0.20, S=0.4 M=6.6, P=0.80, S=0.28
	No P=0.				
Iron Ridge	Yes P=0.	9 6.19	130 6.78	61 6.75	M=6.8, P=0.40, S=0.39 M=6.2, P=0.60, S=0.28
	No P=0.				
Paintbrush Canyon	Yes P=0.80	21 6.61	205 6.92	64 6.77	M=6.9, P=0.15, S=0.40 M=6.8, P=0.25, S=0.39 M=6.6, P=0.60, S=0.28
(w/Sagecoach Road?)	No P=0.20				

Table 3: Maximum Magnitudes-Yucca Mountain

Fault	Independent Rupture Probability	SRL (km) M_w^{srl}	Max Disp (cm) M_w^{Dmax}	Avg. Preferred Disp (cm) M_w^{Dbar}	M_{max} , Prob., sigma
Stagecoach Road	Yes P=0.80	7.5 6.10	99 6.69	49 6.68	M=6.7, P=0.40, S=0.39 M=6.1, P=0.60, S=0.28
(w/Paintbrush Canyon?)	No P=0.20				
Bow Ridge	Yes P=0.	8.5 6.20	80 6.62	23.7 6.42	M=6.6, P=0.10, S=0.40 M=6.4, P=0.30, S=0.39 M=6.2, P=0.60, S=0.28
	No P=0.				
Ghost Dance	Yes P=0.98	6 5.9	----	---	M=5.9, P=1.0, S=0.28
(w/Abandon Wash?)	No P=0.02	8 6.1	----	----	M=6.1, P=1.0, S=0.28
Rock Valley	Yes P=0.	32 6.83	451 7.17	244 7.25	M=7.3, P=0.25, S=0.39 M=7.2, P=0.40, S=0.40, M=6.8, P=0.35, S=0.28
	No P=0.	65 7.18			

Table 4: Maximum Magnitudes-Yucca Mountain

Fault	Independent Rupture Probability	SRL (km) M_w^{srl}	Max Disp (cm) M_w^{Dmax}	Avg. Preferred Disp (cm) M_w^{Dbar}	M_{max} , Prob., sigma
Death Valley	Yes P=0.60	100 7.4	-----	240(?) 7.24	M=7.4, P=0.60, S=0.28 M=7.2, P=0.40, S=0.39
(w/Furnace Creek)	No P=0.40	205 7.76	-----	470(?) 7.48	M=7.8, P=0.60, S=0.28 M=7.5, P=0.40, S=0.39
Furnace Creek	Yes P=0.60	145 7.59	-----	470(?) 7.48	M=7.6, P=0.60, S=0.28 M=7.5, P=0.40, S=0.39
(w/Death Valley?)	No P=40	205 7.76	-----	470(?) 7.48	M=7.8, P=0.60, S=0.28 M=7.5, P=0.40, S=0.39
Background Earthquake	Yes P=1.0(?)				M=6.3, P=1.0, S=0.3

Maximum Magnitudes in the Yucca Mountain Area

Team Tectonic: Jim McCalpin, Burt Slemmons and Jon Ake

Assumptions and Prejudices-

There are three basic data sets we have chosen to use to estimate maximum magnitudes for faults in the Yucca Mountain area: maximum displacement, surface rupture length and preferred displacement. The data considered was that available from the synthesis report. Because it is a descriptor of the fault as a whole, surface rupture length (SRL) is felt to be a more stable estimator of maximum magnitude than is maximum displacement (D_{\max}) (If one needs additional confirmation-look at plots in Wells and Coppersmith (1994) for this parameter). We do not concur with the synthesis report that maximum surface displacements have necessarily been captured in the limited number of trenches.

The maximum fault lengths described in the synthesis report are almost always based on linking different faults, an example is the Northern and Southern Crater Flat faults in Table 5-1. We have remeasured fault lengths from the maps for individual faults. These are the values that appear in this note. The *all slip-type*, surface rupture length relationship of Wells and Coppersmith (1994) was then used to compute magnitude estimates (M_w^{SRL}). The *all fault-slip-types* relationship was used for all of the estimates (average displacement, surface rupture length, and maximum displacement). We feel this is appropriate given the probable oblique motion on many of the faults and is consistent with the inferred tectonic model.

To compute a magnitude from maximum displacement data, the largest reported displacement value on each individual fault was used with the maximum displacement relationship of Wells and Coppersmith (1994) (hereafter referred to as W&C'94) to compute an M_w^{Dmax} .

Looking at the displacement data for faults with several ruptures (Solitario Canyon for example) there appears to be large differences in displacement from event-to-event at certain sites, i.e. "Noisy data". A possible method to "quiet" the noise in this data is to construct the arithmetic mean of the preferred displacement values for each fault, this is an estimate of an average or "characteristic" displacement (AD). We have used this value with W&C'94 average displacement relationship (all events) to estimate an M_w^{Dbar} value.

Given several estimates of M_{\max} , we need to establish a likelihood (or probability in an ad hoc sense) for each. Given the prejudice for SRL described above, we have given the highest weight to that estimate, the next highest weight was given to the estimate from average preferred displacement, and the least to maximum displacement. This is the scheme if the three estimates are different.

If SRL and AD give consistent estimates of M_{\max} , give that estimate a very high weight.

If D_{\max} and SRL give consistent estimates of M_{\max} , give that estimate a moderately high weight.

If the estimate of M_{\max} from D_{\max} is considerably larger than that from SRL, then look at possibility of linkage with other faults, is this a scenario where other faults are important? Is this maximum displacement value an outlier or within reason given other displacement values at this trench and along strike? The same questions are asked when M_{\max} from AD and D_{\max} both suggest larger magnitudes than SRL does. In general when this situation occurs, I have less faith in the estimate from displacement. From a big-picture, physics standpoint we asking for a large-slip event to ~14km depth on short faults with extremely small cumulative displacement over ~12M yrs. This suggests a consistently strange aspect ratio to the fault surface. A large magnitude with these geometries requires unreasonably large average stress drops. This may fail the physical plausibility test for independent rupture.

Questions of simultaneous/"scenario" earthquakes. I think the synthesis report went off in the wrong direction with magnitude estimates for "scenarios". I think it is best to estimate magnitudes for individual faults and then estimate the FREQUENCY that fault may link with other faults in a **SIMULTANEOUS** rupture. From a strong ground motion estimation perspective, it only makes sense to sum rupture lengths and/or displacements (and implicitly rupture areas) if the rupture on one fault occurs during the slip event for another. Slip durations for the size faults we have here would be ~12-15secs, duration of strong shaking no more than 30 secs. I maintain that the separation in time of the scenario events described by Silvio could be minutes, hours, days, weeks or even months. These would be inappropriate situations to sum rupture parameters to estimate magnitudes.

So with all that having been said, I have estimated several maximum magnitudes for each fault source, I have estimated a probability for each. I have relied on the relationships of Wells and Coppersmith '94. However, the results are then a discrete series of delta functions (spikes) whose height is proportional to the assigned probability to each magnitude. These values however are merely median estimates and 50% of the values could lie above and 50% below this estimate. There are sigma values for each type of relationship (dmax, average displacement, rupture area, SRL) in W&C'94. What I propose is to superimpose a Gaussian (with amplitude scaled to the weight of the probability assigned to that magnitude estimate and sigma value from appropriate relationship) on each spike and then sum the result to develop a probability density function (PDF) for maximum magnitude for each fault. I think this is the best way to incorporate uncertainty from the range of estimates that arise from different data sets, i.e. D_{\max} vs SRL vs AD, as well as uncertainty from each type of estimate, i.e. sigma=0.28 magnitude units for SRL magnitude vs sigma=0.4 for D_{\max} . One advantage of this is we will have a cumulative distribution from which we can identify 16-%tile, median, and 84-%tile magnitudes.

Fault by fault synopsis:

Bare Mountain Fault:

Does not appear to show any along strike surface relationships with other faults, scenario W suggests there may be some relationship to other faults in the area (i.e. when Bare Mountain ruptures other faults may exhibit smaller displacements). This inference is consistent with

structural interpretations which suggest linkage between Bare Mountain and faults west of Yucca Mtn at depth.

This fault wins the coveted "Fault Most Likely to Extend to the Base of the Seismogenic Crust" award.

Fault length- 21 km, hence, $M_w(\text{SRL}) \sim 6.62$

Maximum reported displacement-300 cm, hence $M_w(D_{\text{max}}) \sim 7.04$

Average of preferred displacements-127 cm, hence $M_w(D_{\text{bar}}) \sim 7.02$

results:

$M_{\text{max}} = 7.0$ Prob=0.5 $\sigma = 0.4$

$M_{\text{max}} = 6.6$ Prob=0.5 $\sigma = 0.28$

Northern Crater Flat Fault:

Surface fault length=10.5 to 12 km, hence, $M_w(\text{SRL}) \sim 6.26-6.33$

Maximum reported displacement-50 cm, hence, $M_w(D_{\text{max}}) \sim 6.47$

Average of preferred displacements-29.6 cm, hence, $M_w(D_{\text{bar}}) \sim 6.50$

This fault appears to rupture infrequently. Consistency between D_{bar} and D_{max} values suggests may have dependent behavior on at least some occasions. Because of geometry may be related to Southern Crater Flat (see below).

$M_{\text{max}} = 6.5$ Prob=0.4 ($\sigma = 0.4$)

$M_{\text{max}} = 6.3$ Prob=0.6 ($\sigma = 0.28$)

Southern Crater Flat

Surface fault length-8.5km, hence, $M_w(\text{SRL}) \sim 6.16$

Maximum reported displacement-32 cm, hence, $M_w(D_{\text{max}}) \sim 6.32$

Average of preferred displacement values-13.2 cm, hence, $M_w(D_{\text{bar}}) \sim 6.21$

Most likely for Northern and Southern Crater Flat faults to operate independently, however, these two faults have ruptured "together" at least once (scenario event Z), the combined rupture length is 21 km for this possibility.

Hence, $M_w(\text{SRL}) \sim 6.61$

$M_{\text{max}} = 6.3$ Prob=0.20 ($\sigma = 0.4$)

$M_{\text{max}} = 6.2$ Prob=0.80 ($\sigma = 0.28$)

Windy Wash Fault

Surface fault length-23 km, hence, $M_w(\text{SRL}) \sim 6.66$

Maximum reported displacement-98 cm, hence, $M_w(D_{\text{max}}) \sim 6.69$

The average of preferred displacement-36.5 cm, hence, $M_w(D_{\text{bar}}) \sim 6.57$

No obvious along strike relationship to other faults but in several scenarios Windy Wash has been implicated with other faults. However, the consistency between magnitudes suggested by D_{\max} and SRL data suggests events larger than M 6.7 are rare. Average preferred displacement values suggest at least some events may be smaller.

$M_{\max}=6.7$ Prob=0.80 (sigma=0.28)

$M_{\max}=6.6$ Prob=0.20 (sigma=0.39)

Fatigue Wash Fault

Surface fault length-17 km, hence, $M_w(\text{SRL})\sim 6.51$

(possibly segmented)

Maximum reported displacement-105 cm, hence, $M_w(D_{\max})\sim 6.71$

Average of preferred displacement-61.3 cm, hence, $M_w(D_{\text{bar}})\sim 6.76$

Based on map patterns and seismic reflection interpretations it seems plausible that Fatigue Wash and Windy Wash are linked at depth.

$M_{\max}=6.8$ Prob=0.30 (sigma=0.39)

$M_{\max}=6.7$ Prob=0.10 (sigma=0.4)

$M_{\max}=6.6$ Prob=0.60 (sigma=0.28)

Solitario Canyon Fault

Surface fault length-18.5 km, hence, $M_w(\text{SRL})\sim 6.55$

(possibly segmented)

Maximum reported displacement-140 cm, hence, $M_w(D_{\max})\sim 6.78$

Average of preferred displacement values-37.5 cm, hence, $M_w(D_{\text{bar}})\sim 6.58$

This fault appears to have some relationship with the Iron ridge Fault based on several rupture scenarios (X and Y for example). There may be a small probability of simultaneous rupture for these two faults, length becomes 27km for this case, and $M_w(\text{SRL})\sim 6.75$ then. The 140 cm displacement event is estimated from fracture dimensions.

Results:

$M_{\max}=6.8$ Prob=0.20 (sigma=0.4)

$M_{\max}=6.6$ Prob=0.80 (sigma=0.28)

Iron Ridge Fault

Surface fault length-9 km, hence, $M_w(\text{SRL})\sim 6.19$

(does not appear segmented)

Maximum reported displacement-130 cm, hence, $M_w(D_{\max})\sim 6.78$

Average of preferred displacement-61 cm, hence, $M_w(D_{\text{bar}})\sim 6.75$

As noted above this fault may be linked to Solitario Canyon and could give rise to thoroughgoing rupture.

Results:

$M_{\max}=6.8$ Prob=0.40 (sigma=0.4)

$M_{\max}=6.2$ Prob=0.60 (sigma=0.28)

Ghost Dance Fault

Surface fault length-5-8 km, hence, $M_w(\text{SRL})\sim 5.9$ to 6.1

(uncertainty in length)

No reported displacement data

The lack of young events suggests very little linkage/influence from neighboring faults.

Results:

$M_w=6.1$ Prob=0.4 (sigma=0.28)

$M_w=5.9$ Prob=0.6 (sigma=0.28)

Paintbrush Canyon Fault

Surface fault length-21 km, hence, $M_w(\text{SRL})\sim 6.61$

(appears segmented)

Maximum reported displacement-205 cm, hence, $M_w(D_{\max})\sim 6.92$

(I have disregarded events older than 740,000 kyrs)

Average of preferred displacement-64 cm, hence, $M_w(D_{\text{bar}})\sim 6.77$

Several proposed rupture scenarios suggest Paintbrush Canyon has earthquakes related to those on other faults (usually Stagecoach Road Fault). For rupture on Paintbrush as well as Stagecoach, the rupture length becomes 28.5 km, and hence, $M_w(\text{SRL})\sim 6.77$.

Results:

$M_{\max}=6.9$ Prob=0.15 (sigma=0.4)

$M_{\max}=6.8$ Prob=0.25 (sigma=0.39)

$M_{\max}=6.6$ Prob=0.60 (sigma=0.28)

Stagecoach Road Fault

Surface fault length-7.5 km, hence, $M_w(\text{SRL})\sim 6.10$

(does not appear segmented, but may be related to Paintbrush Canyon, see above, in that case, SRL=28.5 km and $M_w(\text{SRL})\sim 6.77$)

Maximum reported displacement-99 cm, hence, $M_w(D_{\max})\sim 6.69$

Average of preferred displacements-49 cm, hence $M_w(D_{\text{bar}})\sim 6.68$

The large values for both D_{\max} and D_{bar} and short surface fault length suggest this may be connected at depth to other faults.

Results:

$M_{\max}=6.7$ Prob=0.40 (sigma=0.39)

$M_{\max}=6.1$ Prob=0.60 (sigma=0.28)

Bow Ridge Fault

Surface fault length-8.5 km, hence, $M_w(\text{SRL}) \sim 6.20$

Maximum reported displacement-80 cm, hence, $M_w(D_{\text{max}}) \sim 6.62$

Average of preferred displacements-23.7 cm, hence $M_w(D_{\text{bar}}) \sim 6.42$

Appears to be structurally related to adjacent faults. Winner of the also coveted "Least Likely to Extend to Base of Seismogenic Crust" award.

Results:

$M_{\text{max}}=6.6$ Prob=0.10 (sigma=0.4)

$M_{\text{max}}=6.4$ Prob=0.30 (sigma=0.39)

$M_{\text{max}}=6.2$ Prob=0.60 (sigma=0.28)

Rock Valley Fault

Favored surface fault length-32 km, hence, $M_w(\text{SRL}) \sim 6.83$

Maximum reported displacement-451 cm, hence, $M_w(D_{\text{max}}) \sim 7.17$

Average of preferred displacements-244 cm, hence $M_w(D_{\text{bar}}) \sim 7.25$

Maximum interpreted fault length-65 km, hence, $M_w(\text{SRL}) \sim 7.18$

Results:

$M_{\text{max}}=7.3$ Prob=0.25 (sigma=0.39)

$M_{\text{max}}=7.2$ Prob=0.40 (sigma=0.4)

$M_{\text{max}}=6.8$ Prob=0.35 (sigma=0.28)

Death Valley Fault

Surface fault length-100 km, hence, hence, $M_w(\text{SRL}) \sim 7.4$

Preferred displacement-240 cm, hence $M_w(D_{\text{bar}}) \sim 7.25$

Suggestion of linkage w/ Furnace Creek, Surface rupture length-205 km, and hence, $M_w(\text{SRL}) \sim 7.76$

Results:

$M_{\text{max}}=7.4$, Prob=0.60 (sigma=0.28)

$M_{\text{max}}=7.2$, Prob=0.40 (sigma=0.39)

Furnace Creek Fault

Surface fault length-145 km, hence, hence, $M_w(\text{SRL}) \sim 7.59$

Preferred displacement-470 cm, hence $M_w(D_{\text{bar}}) \sim 7.48$

Suggestion of linkage w/ Furnace Creek, Surface rupture length-205 km, and hence, $M_w(\text{SRL}) \sim 7.76$

Results:

$M_{\max}=7.6$, Prob=0.60 (sigma=0.28)

$M_{\max}=7.5$, Prob=0.40 (sigma=0.39)

Background Earthquake

Based on work by dePolo and others and physical constraints, we make a very preliminary estimate of:

$M_{\max}=6.3$, Prob=1.0 (sigma=0.3)

Maximum Magnitude Estimation Approaches

Magnitude vs. Length
 Magnitude vs. Maximum Displacement
 Magnitude vs. Average Displacement
 Magnitude vs. Area
 Magnitude vs. Length \times Displacement
 Magnitude vs. Length $\&$ Slip Rate
 Magnitude vs. Moment
 Relative Earthquake

poss. use Magnitude vs. Subsurface Length

Fault	length		displacement		Width	Slip rate
	surface	subsurface	Max.	Ave.		
Fault A	X					
Fault B	X		X			
Fault C	X					X
Fault D	X			X	X	

Regressions

applicability

- extensional areas
 - normal components included
 - mod. to low slip rates
 - Basin and Range Province

Earthquake Size Scaling Techniques (Regressions)

Mag. vs. length

Wells & Coppersmith
Mason
dePolo + ?

Mag. vs. subsurface length
Mag. vs. displacement (Max.)

Wells & Coppersmith
Wells & Coppersmith
Mason
dePolo + ?

(Ave)

Wells & Coppersmith
Mason

Mag. vs. area

Wells & Coppersmith
Wyss

Mag. vs. length x displacement

Mason

Mag. vs. length & slip

Anderson +

Mag. vs. moment

Doser & Smith

Hanks & Kanamori

Relative Earthquake

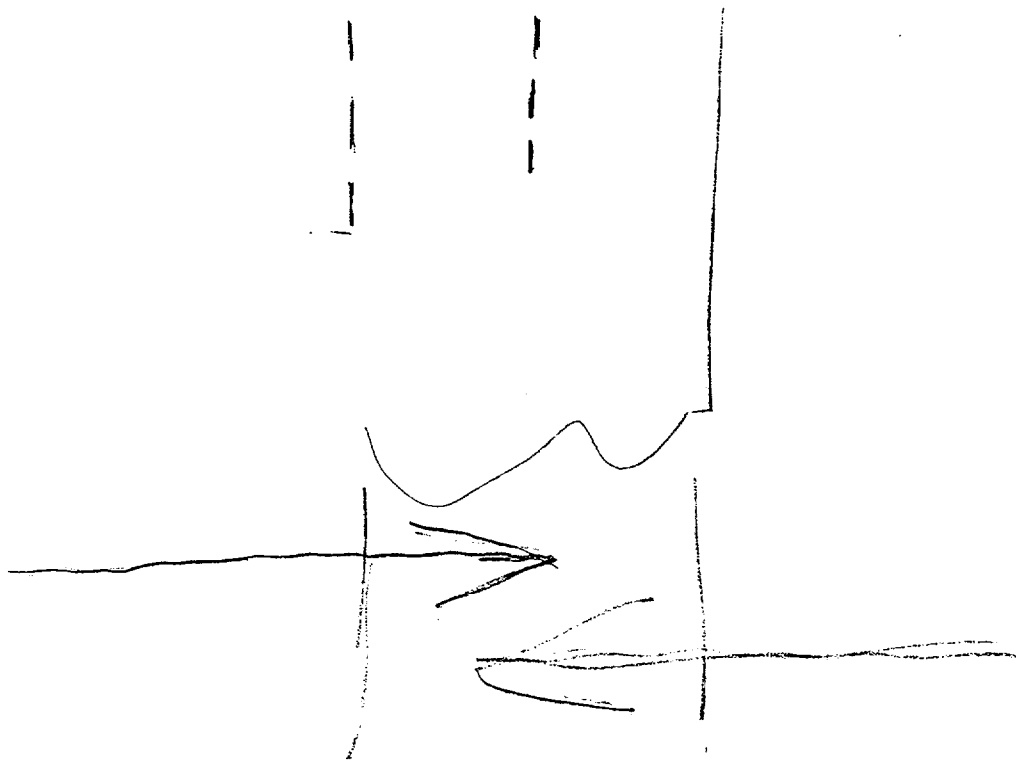
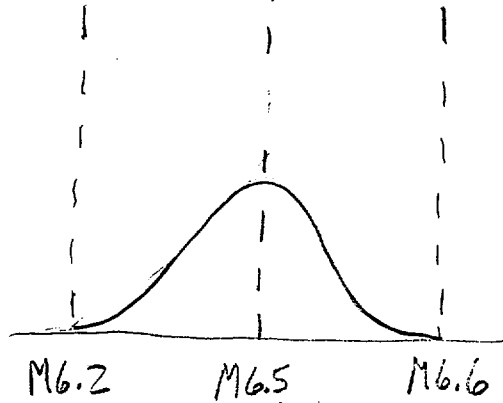
Background
eqs.

fuzzy features

Significant
Surface faulting
events

seismicity
data

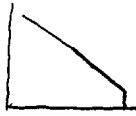
faults $M6.2+$
(unless limited by area)



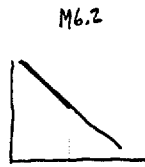
fault A



fault B



background eqs



use fault distribution data
for earthquakes $M_{6.2}$ to M_{max}

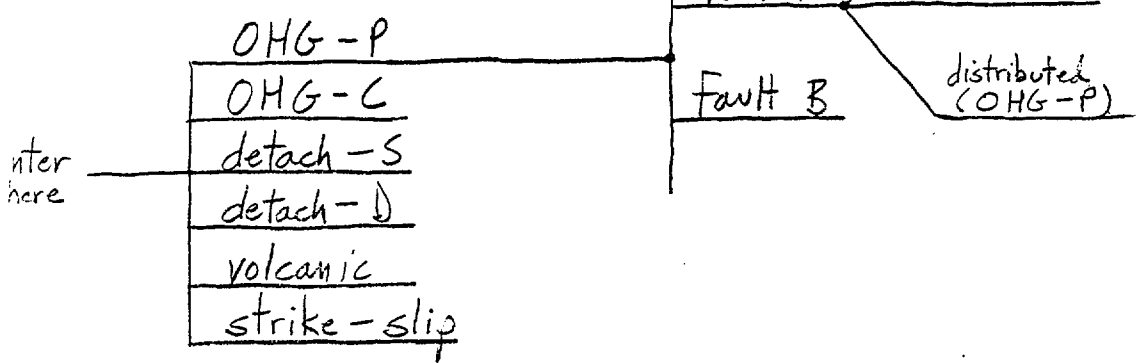
use background earthquakes
for earthquakes M_{min} to $M_{6.1}$

one way not to double count

Seismo-Tectonic Models

Faults

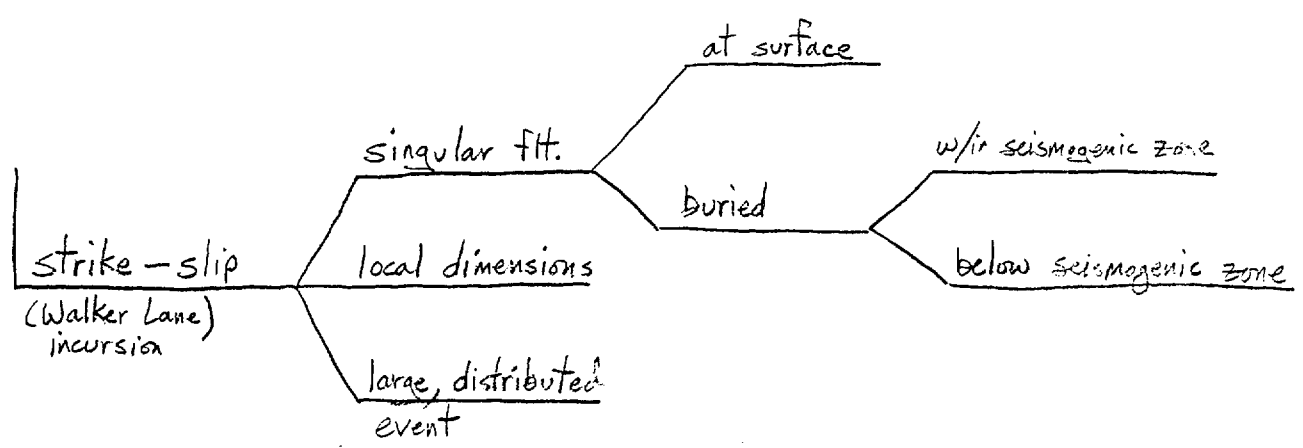
behavioral dependence



↑
weighted
for confidence in

↑
individually
weighted
for existence

↑
weighted
against
each other



Concern of Using Only Converted M_w Magnitudes
Not Appropriate for Extension

Staudach (Kawanami & Hanks, 1979)

Dominantly strike-slip regimes

$$M_w = 0.66 M_0 - 10.71$$

Extensional Regimes

• Utah (Doser and Smith, 1984)

• Long Valley, Mammoth sequence

Arbuckle, et al. (1980)

• Borah Peak aftershocks

Shenota & Pederson (1993)

Use original magnitude determinations for scaling M_L , M_S , M_w

Seismicity (Rates & Magnitudes)

— Magnitude scale conversions

$M_u, M_L, M_s, \dots \rightarrow M_w$

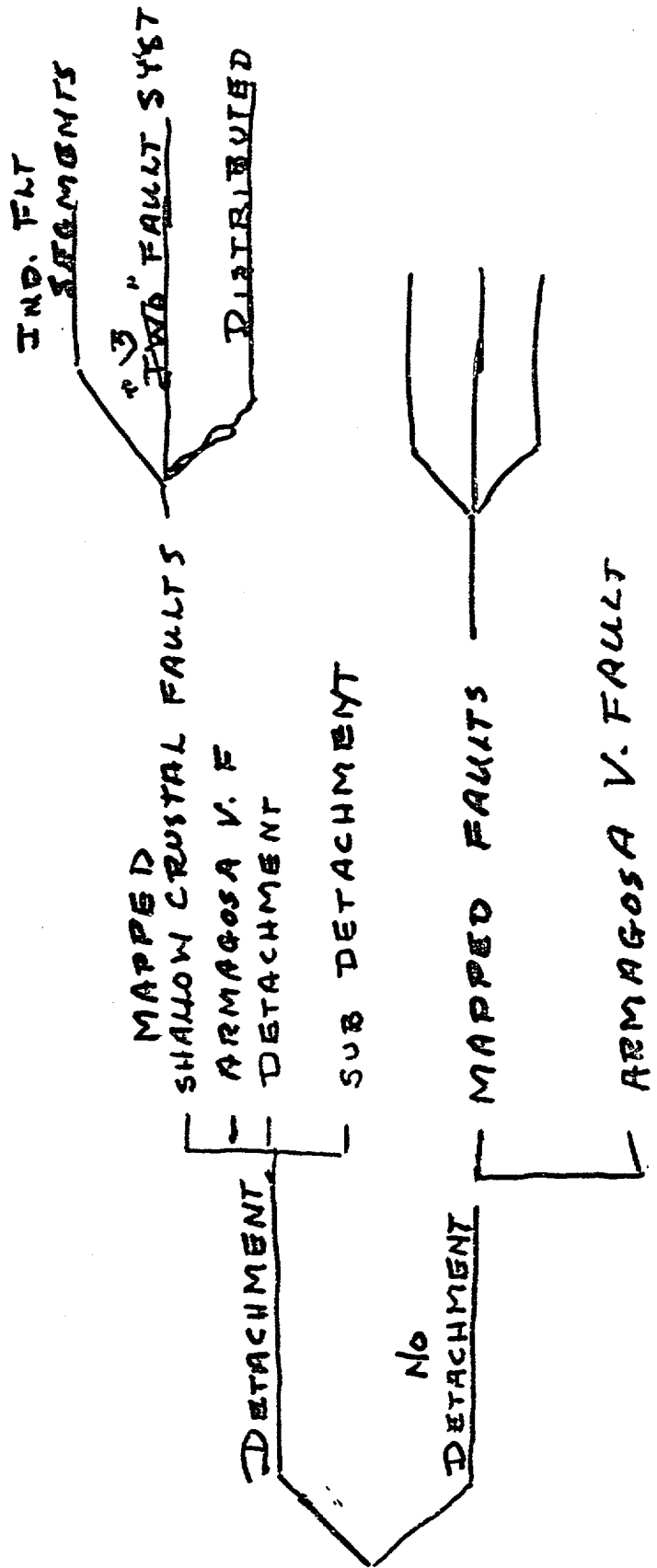
Various models for extensional domains

— Declustering

Removing moment \rightarrow removing tectonic deformation.

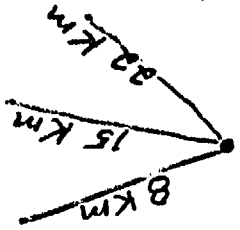
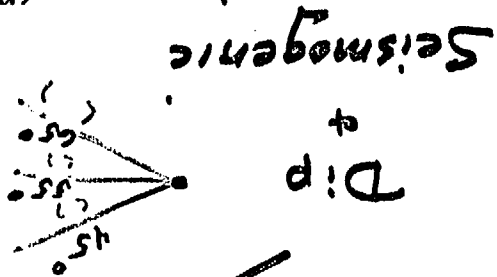
\rightarrow changes b-values and frequency of occurrence

SITE VICINITY STRUCTURAL MODELS



SEISMIC MOMENT RATE:

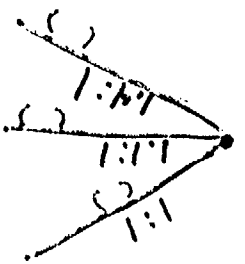
Length x Down Dip Width x Slip Rate x Rigidity Factor



Vertical Rates
Adjusted for
possible horizontal
component

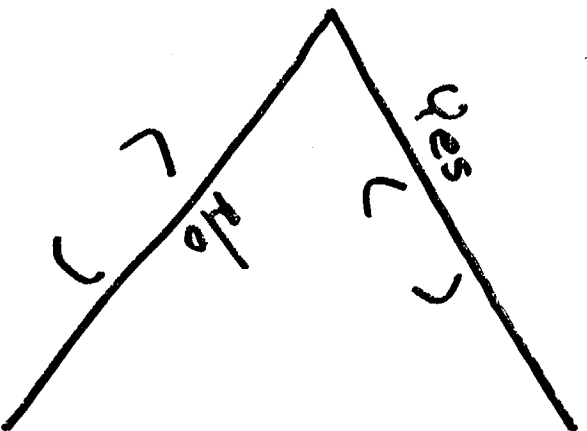
Horiz: Vert

1.1 : 1
1.4 : 1



Activity

Degree of belief that the modeled feature represents a seismicogenic source.



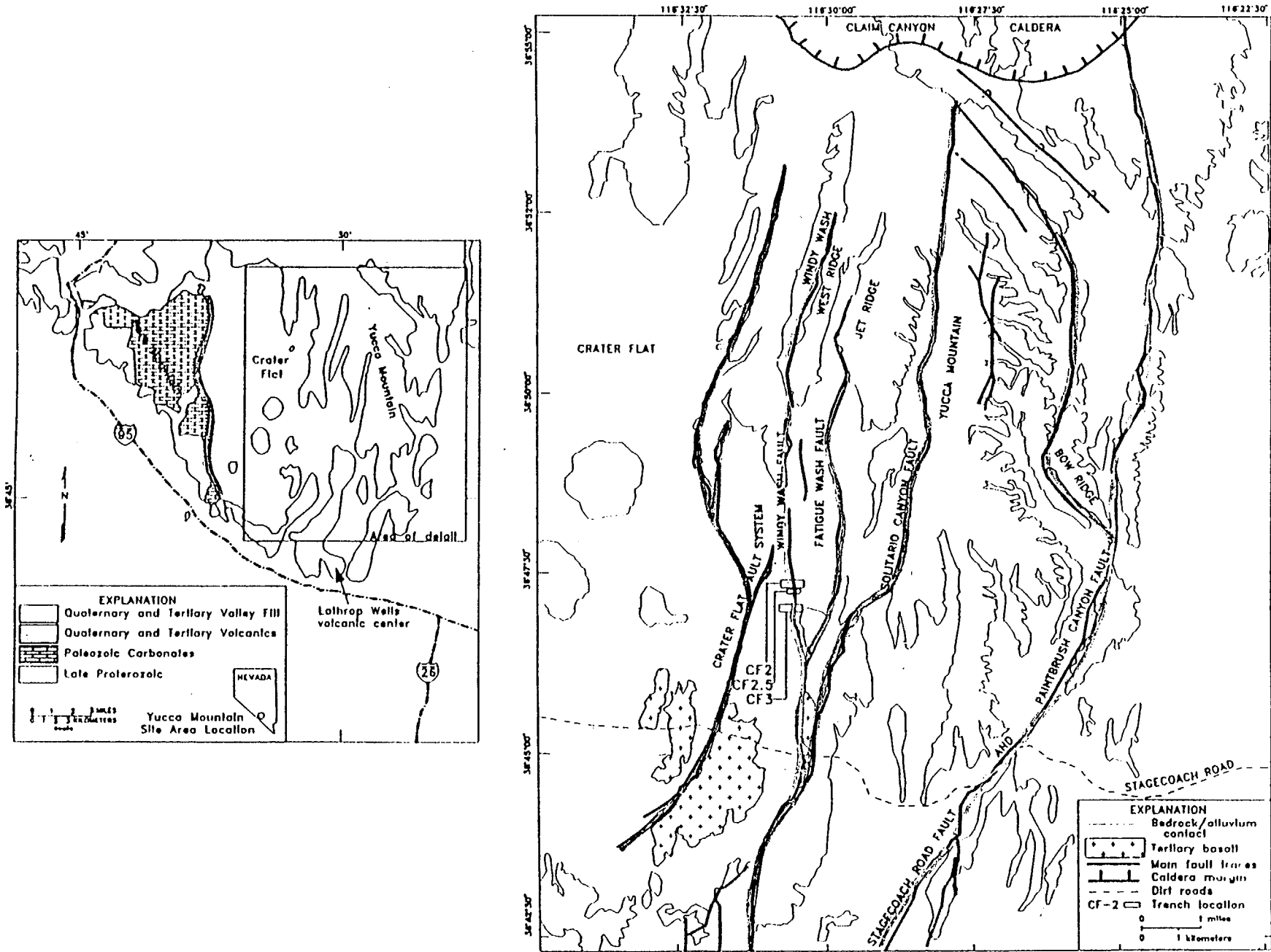


Figure 4.9.1. Location of the Windy Wash fault and trenches CF-2, CF-2.5, and CF-3, in Crater Flat, west of Yucca Mountain, Nye County, Nevada

UNCLASSIFIED

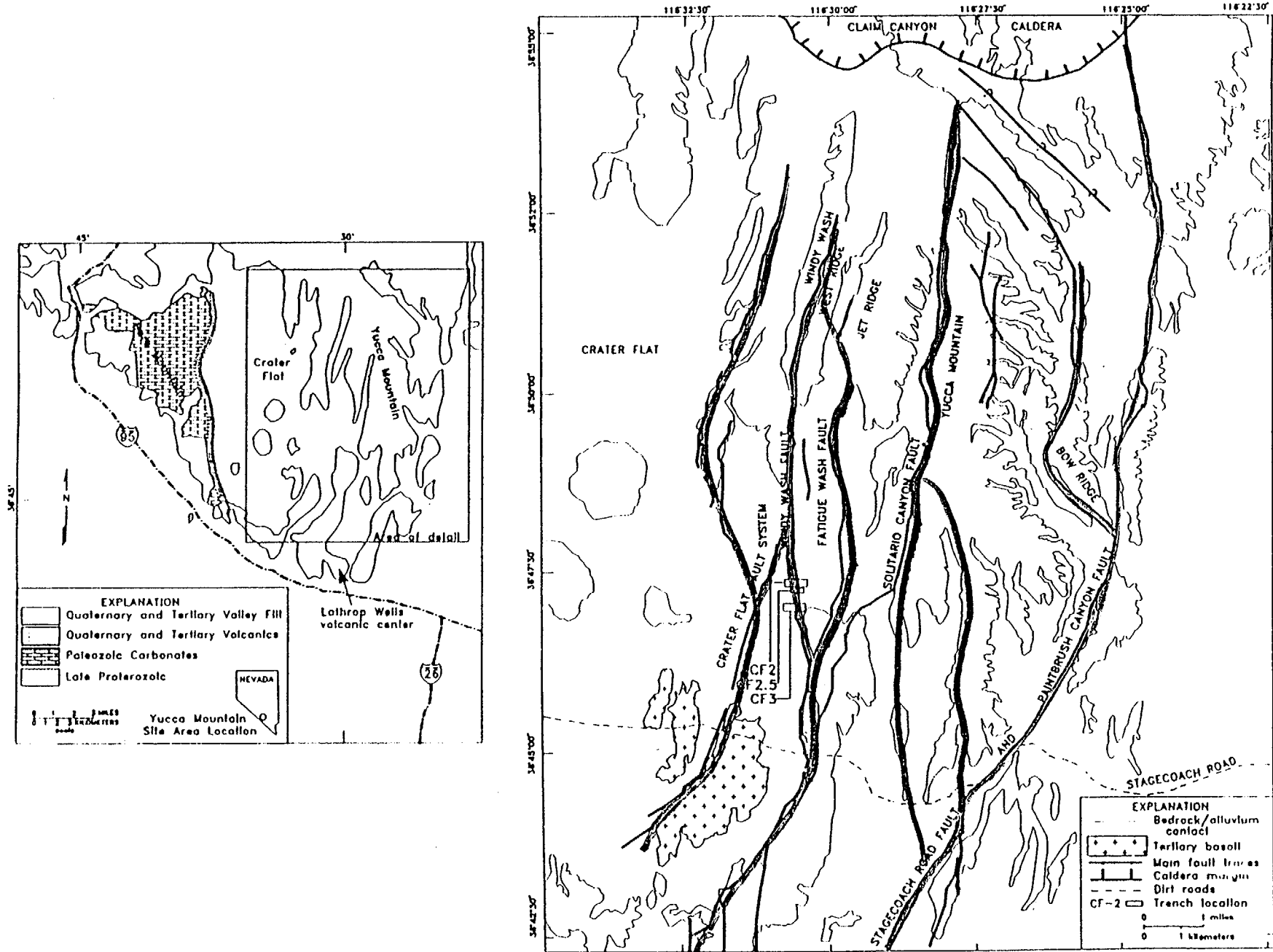


Figure 4.9.1. Location of the Windy Wash fault and trenches CF-2, CF-2.5, and CF-3, in Crater Flat, west of Yucca Mountain, Nye County, Nevada

INDEPENDENT FAULT SEGMENT MODEL



Figure 4.9.1. Location of the Windy Wash fault and trenches CF-2, CF-2.5, and CF-3, in Crater Flat, west of Yucca Mountain, Nye County, Nevada

Fault Patterns Generalized From Simonds et al., 1995

FAULT	Activity	Length	Dip		Down-Dip Width 8 / 15 / 22 (wt)	Vertical Slip Rate (mm/yr)			Net Slip Vert.:Horiz.
			(I)	Range 50 / 65 / 85 (wt)		Preferred	Maximum	Minimum	
Independent Fault-Segment Model:									
1 Paintbrush Canyon					71 W				
Northern segment	?					0.002	0.004	0.001	
Central segment	Q					0.017	0.025	0.013	
Southern segment	Q					0.01	0.016	0.004	
2 Stagecoach Road	Q				73 W	0.04	0.07	0.01	
3 Iron Ridge					68 W	0.04	0.05	0.01	
4 Bow Ridge	Q				75 W	0.003	0.007	0.002	
5 Solitario Canyon	Q				72 W	0.011	0.02	0.002	
6 Fatigue Wash	Q				73 W	0.002	0.015	0.001	
7 Northern Windy Wash	Q				63 W		0.03	0.001	
8 Southern Windy Wash	Q				63 W	0.11	0.027	0.009	
9 Northern Crater Flat	Q				70 W		0.002	0.001	
10 Southern Crater Flat	Q				70 W		0.002	0.001	
11 Bare Mountain	Q				50-70E	0.01	0.02	0.005?	
12 Amargosa Valley	hypothetical				90	rate of extension south end of YMFS			
13 Subhorizontal Detachment	hypothetical				0	?			
14 Subdetachment SS Faulting	hypothetical				90	background seismicity extrapolated to Mmax??			

EARTHQUAKE

REFERENCE MODELS

FAULT SPECIFIC SOURCES:

CHARACTERISTIC
Wernowsky et al. 1983

Uchowitz + Coppersmith, 1984

Exponential

e.g. Gutenberg Richter, 1944

SANITY CHECKS

- PSEUDOSEISMIC RECURRENCE
- HISTORICAL SEISMICITY